frontiers | Research Topics

Cross-disciplinary approaches to characterize gait and posture disturbances in aging and related diseases, volume II

Edited by
Simone Tassani, Claudio Belvedere and Juan Ramírez

Coordinated by
Giorgio Davico

Published in
Frontiers in Bioengineering and Biotechnology
Frontiers in Neurology

ISSN 1664-8714
ISBN 978-2-8325-5010-6
DOI 10.3389/978-2-8325-5010-6

About Frontiers

Frontiers is more than just an open access publisher of scholarly articles: it is a pioneering approach to the world of academia, radically improving the way scholarly research is managed. The grand vision of Frontiers is a world where all people have an equal opportunity to seek, share and generate knowledge. Frontiers provides immediate and permanent online open access to all its publications, but this alone is not enough to realize our grand goals.

Frontiers journal series

The Frontiers journal series is a multi-tier and interdisciplinary set of open-access, online journals, promising a paradigm shift from the current review, selection and dissemination processes in academic publishing. All Frontiers journals are driven by researchers for researchers; therefore, they constitute a service to the scholarly community. At the same time, the *Frontiers journal series* operates on a revolutionary invention, the tiered publishing system, initially addressing specific communities of scholars, and gradually climbing up to broader public understanding, thus serving the interests of the lay society, too.

Dedication to quality

Each Frontiers article is a landmark of the highest quality, thanks to genuinely collaborative interactions between authors and review editors, who include some of the world's best academicians. Research must be certified by peers before entering a stream of knowledge that may eventually reach the public - and shape society; therefore, Frontiers only applies the most rigorous and unbiased reviews. Frontiers revolutionizes research publishing by freely delivering the most outstanding research, evaluated with no bias from both the academic and social point of view. By applying the most advanced information technologies, Frontiers is catapulting scholarly publishing into a new generation.

What are Frontiers Research Topics?

Frontiers Research Topics are very popular trademarks of the *Frontiers journals series*: they are collections of at least ten articles, all centered on a particular subject. With their unique mix of varied contributions from Original Research to Review Articles, Frontiers Research Topics unify the most influential researchers, the latest key findings and historical advances in a hot research area.

Find out more on how to host your own Frontiers Research Topic or contribute to one as an author by contacting the Frontiers editorial office: frontiersin.org/about/contact

Cross-disciplinary approaches to characterize gait and posture disturbances in aging and related diseases, volume II

Topic editors

Simone Tassani — Pompeu Fabra University, Spain

Claudio Belvedere — Laboratory of Movement Analysis, Rizzoli Orthopedic Institute (IRCCS), Italy

Juan Ramírez — National University of Colombia, Medellin, Colombia

Topic coordinator

Giorgio Davico — Alma Mater Studiorum - University of Bologna, Italy

Citation

Tassani, S., Belvedere, C., Ramírez, J., Davico, G., eds. (2024). *Cross-disciplinary approaches to characterize gait and posture disturbances in aging and related diseases, volume II*. Lausanne: Frontiers Media SA. doi: 10.3389/978-2-8325-5010-6

Table of contents

frontiers | Frontiers in Bioengineering and Biotechnology

TYPE Editorial
PUBLISHED 30 May 2024
DOI 10.3389/fbioe.2024.1422815

OPEN ACCESS

EDITED AND REVIEWED BY
Markus O. Heller,
University of Southampton, United Kingdom

*CORRESPONDENCE
Simone Tassani,
simone.tassani@upf.edu

RECEIVED 24 April 2024
ACCEPTED 21 May 2024
PUBLISHED 30 May 2024

CITATION
Tassani S, Belvedere C, Ramírez J and Davico G (2024), Editorial: Cross-disciplinary approaches to characterize gait and posture disturbances in aging and related diseases, Volume II. *Front. Bioeng. Biotechnol.* 12:1422815. doi: 10.3389/fbioe.2024.1422815

Editorial: Cross-disciplinary approaches to characterize gait and posture disturbances in aging and related diseases, Volume II

Simone Tassani[1]*, Claudio Belvedere[2], Juan Ramírez[3] and Giorgio Davico[4]

[1]Department of Engineering, Universitat Pompeu Fabra, Barcelona, Spain, [2]Movement Analysis Laboratory, IRCCS Istituto Ortopedico Rizzoli, Bologna, Italy, [3]National University of Colombia, Medellin, Colombia, [4]Alma Mater Studiorum, University of Bologna, Bologna, Italy

KEYWORDS

gait, posture, multi-factorial analysis, cross-disciplinary, repeatability, aging

Editorial on the Research Topic
Cross-disciplinary approaches to characterize gait and posture disturbances in aging and related diseases, Volume II

Cross-disciplinary research is the space where different disciplines meet and generate new knowledge. However, publishing multidisciplinary research can be difficult since the advances presented in the single disciplines might be small or negligible if considered independently, and the organization of the work can be extremely challenging, starting from the development of a common language and knowledge base and dealing proactively with misunderstandings (Domino et al., 2007; Daniel et al., 2022). Nonetheless, the union of the different areas can be knowledge itself (Priaulx and Weinel, 2018). For these reasons, this Research Topic: "*Cross-Disciplinary Approaches to Characterize Gait and Posture Disturbances in Aging and Related Diseases, Volume II*" gives once again space to multidisciplinary research in gait and posture to help increase the body of evidence at the intersection between the various scientific disciplines and research fields that focus and/or impact on gait and posture.

Great global challenges require cross-disciplinary spaces where science, humanities, and culture can meet and develop solutions for great global problems. For instance, the planetary wellbeing initiative (Antó et al., 2021; Kortetmäki et al., 2021) is considering the loop of changes made by humans to our lifestyle, which in turn affect human health. Situations of high emotional distress, created by the society we have developed, have been seen to promote musculoskeletal disorders, already at a young age (Diepenmaat et al., 2006). In this framework Tassani et al. evaluated the relationship among posture, breathing, and anxiety, therefore exploring the interaction between physical and emotional spheres in University students. Similarly, Kong et al. explored the influence of cognitive load on the trajectory of the center of pressure during gait initiation in young males with excess weight. Cognitive and emotional burdens are often ignored in the study of gait and posture until they reach major relevance (Canales et al., 2017) when any approach to revert the dynamic of the pathology is likely very difficult. For this reason, working on prevention is paramount and even if the focus of the Research Topic is on aging-related diseases, we found it relevant to give space to studies performed on healthy subjects (De Blasiis et al., Peiffer et al.), or

where the aging process was simulated in young volunteers (Ma et al.). The mentioned studies are all presenting balances and stability assessments related to fall prediction and fall-related injuries, which again, for a long time was mainly related to the elderly, but is becoming a common problem also in the younger population. It is also very important to develop studies on children (Jiang et al.) and on how posture variations can affect sensitive subjects during development, with changes that can disturb their adulthood.

The first volume of this Research Topic gave space to age-related functionality reduction and the combination of imaging techniques for the study of gait. The relation between gait and imaging technique is probably one of the most common cross-disciplinary approaches in motion analysis (Bohnen and Jahn, 2013). These Research Topic are covered in the work by Ricciardi et al. The study presents how the influence of soft-tissue composition on gait can be evaluated on a large cohort using imaging techniques.

Osteoarthritis is also a common aging disorder, that has negative consequences as disability and societal costs (Hunter and Bierma-Zeinstra, 2019). In the optics of prevention, kinetic and kinematic studies have been developed (Stief et al., 2018). Drongelen et al. have studied the effect of Total Hip Replacement, an end-stage treatment for this pathology, over a bipedal stance. Even if the therapy was found to have a positive effect on the standing position and load distribution of the patients, preventive therapy directed at the disproportionate load distribution might have reduced the progression of the disease.

Another typical problem in multifactorial and multivariate motion studies is the large number of features to be considered in the analysis (Benedetti et al., 1998). For this reason, dimensionality reduction and feature selection of the most appropriate and representative features is an important matter that again finds space in this Research Topic (Ulrich et al., Sato et al.). For example, when evaluating the construct validity of the trunk impairment scale in patients with serious physical problems, like stroke and Parkinson's disease, correlations and multiple regression analysis showed that this scale may evaluate the trunk function related to balance function, disease severity, activities of daily living function, lower limb strength, but the relevant factors were constructed with three different aspects, and this differs from other factors that included many other aspects. Similarly, in the evaluation of medial knee osteoarthritis, several parameters related to knee moments are considered, which differ with the severity of osteoarthritis, but if properly combined can provide the possibility of developing a severity index. Considering a larger number of parameters helps improve the description of a specific issue, but in turn, is likely to increase the overall complexity of the study design. The possibility to reduce and combine parameters is often desirable and therefore does not surprise that advanced multivariate analysis and machine learning techniques are more and more integrated into movement analysis (Phinyomark et al., 2018) making feature reduction approaches another discipline that nowadays crosses gait biomechanics.

Through this Research Topic and the related articles collected therein, we hope to offer the reader new insights into a more comprehensive approach to the study of human motion and its use in research as well as in clinics, again addressing the interaction of gait with cognitive conditions and the integration of multiple techniques for gait analysis. Working with multivariate approach and considering high dimensionality is becoming mandatory for a holistic vision of gait analysis. Nonetheless, with this Research Topic we wanted to give more space especially to the effect that cognitive and emotional loads can have over gait and posture. Unfortunately, the study of the disease risks to shadow the understanding of the patient, forgetting that his daily life and personal feelings can have deep effect over the development of many musculoskeletal conditions, especially in their germinal state. In this scenario, the inclusion of humanities to the pool of multidisciplinary teams devoted to the study of gait and posture might be an important step.

In conclusion, in the age of the Anthropocene, in which humans are changing the world, which in turn is changing humans, working synergistically and multidisciplinarily on the prevention of musculoskeletal diseases seems mandatory. Looking at the human condition not only technically and medically, but promoting studies that explore the cognitive, emotional, philosophical, and also artistical expression of human motion, can be a way to turn a deep introspective gaze at our lifestyle and change it before it changes us.

Author contributions

ST: Conceptualization, Writing–original draft, Writing–review and editing. CB: Writing–original draft, Writing–review and editing. Juan Ramirez: Writing–original draft, Writing–review and editing. GD: Writing–original draft, Writing–review and editing.

Conflict of interest

The authors declare that the research was conducted in the absence of any commercial or financial relationships that could be construed as a potential conflict of interest.

Publisher's note

References

Antó, J. M., Martí, J. L., Casals, J., Bou-Habib, P., Casal, P., Fleurbaey, M., et al. (2021). The planetary wellbeing initiative: pursuing the sustainable development goals in higher education. *Sustain. Switz.* 13, 3372. doi:10.3390/su13063372

Benedetti, M., Catani, F., Leardini, A., Pignotti, E., and Giannini, S. (1998). Data management in gait analysis for clinical applications. *Clin. Biomech. (Bristol, Avon)* 13, 204–215. doi:10.1016/s0268-0033(97)00041-7

Bohnen, N. I., and Jahn, K. (2013). Imaging: what can it tell us about parkinsonian gait? *Mov. Disord.* 28, 1492–1500. doi:10.1002/mds.25534

Canales, J. Z., Fiquer, J. T., Campos, R. N., Soeiro-de-Souza, M. G., and Moreno, R. A. (2017). Investigation of associations between recurrence of major depressive disorder and spinal posture alignment: a quantitative cross-sectional study. *Gait Posture* 52, 258–264. doi:10.1016/J.GAITPOST.2016.12.011

Daniel, K. L., McConnell, M., Schuchardt, A., and Peffer, M. E. (2022). Challenges facing interdisciplinary researchers: findings from a professional development workshop. *PLoS One* 17, e0267234. doi:10.1371/journal.pone.0267234

Diepenmaat, A. C. M., Van Der Wal, M. F., De Vet, H. C. W., and Hirasing, R. A. (2006). Neck/shoulder, low back, and arm pain in relation to computer use, physical activity, stress, and depression among Dutch adolescents. *Pediatrics* 117, 412–416. doi:10.1542/peds.2004-2766

Domino, S. E., Smith, Y. R., and Johnson, T. R. B. (2007). Opportunities and challenges of interdisciplinary research career development: implementation of a women's health research training program. *J. Womens Health* 16, 256–261. doi:10.1089/jwh.2006.0129

Hunter, D. J., and Bierma-Zeinstra, S. (2019). Osteoarthritis. *Lancet* 393, 1745–1759. doi:10.1016/S0140-6736(19)30417-9

Kortetmäki, T., Puurtinen, M., Salo, M., Aro, R., Baumeister, S., Duflot, R., et al. (2021). Planetary well-being. *Humanit Soc. Sci. Commun.* 8, 258. doi:10.1057/s41599-021-00899-3

Phinyomark, A., Petri, G., Ibáñez-Marcelo, E., Osis, S. T., and Ferber, R. (2018). Analysis of big data in gait biomechanics: current trends and future directions. *J. Med. Biol. Eng.* 38, 244–260. doi:10.1007/s40846-017-0297-2

Priaulx, N., and Weinel, M. (2018). Connective knowledge: what we need to know about other fields to 'envision' cross-disciplinary collaboration. *Eur. J. Futur. Res.* 6, 21. doi:10.1186/s40309-018-0150-z

Stief, F., Schmidt, A., van Drongelen, S., Lenarz, K., Froemel, D., Tarhan, T., et al. (2018). Abnormal loading of the hip and knee joints in unilateral hip osteoarthritis persists two years after total hip replacement. *J. Orthop. Res.* 36, 2167–2177. doi:10.1002/jor.23886

frontiers | Frontiers in Bioengineering and Biotechnology

TYPE Original Research
PUBLISHED 13 June 2023
DOI 10.3389/fbioe.2023.1176471

OPEN ACCESS

EDITED BY
Simone Tassani,
Pompeu Fabra University, Spain

REVIEWED BY
Jonathan Rylander,
Baylor University, United States
Xiaolong Zeng,
Second Affiliated Hospital of Guangzhou Medical University, China

*CORRESPONDENCE
Baptiste Ulrich,
baptiste.ulrich@chuv.ch

†These authors share last authorship

RECEIVED 28 February 2023
ACCEPTED 31 May 2023
PUBLISHED 13 June 2023

CITATION
Ulrich B, Erhart-Hledik JC, Asay JL, Omoumi P, Andriacchi TP, Jolles BM and Favre J (2023), Diverse parameters of ambulatory knee moments differ with medial knee osteoarthritis severity and are combinable into a severity index. *Front. Bioeng. Biotechnol.* 11:1176471. doi: 10.3389/fbioe.2023.1176471

Diverse parameters of ambulatory knee moments differ with medial knee osteoarthritis severity and are combinable into a severity index

Baptiste Ulrich[1]*, Jennifer C. Erhart-Hledik[2,3], Jessica L. Asay[3,4], Patrick Omoumi[5], Thomas P. Andriacchi[4†], Brigitte M. Jolles[1,6†] and Julien Favre[1,7†]

[1]Swiss BioMotion Lab, Department of Musculoskeletal Medicine, Lausanne University Hospital and University of Lausanne (CHUV-UNIL), Lausanne, Switzerland, [2]Department of Orthopaedic Surgery, Stanford University, Stanford, CA, United States, [3]Veterans Affairs Palo Alto Health Care System, Palo Alto, CA, United States, [4]Department of Mechanical Engineering, Stanford University, Stanford, CA, United States, [5]Department of Diagnostic and Interventional Radiology, Lausanne University Hospital and University of Lausanne (CHUV-UNIL), Lausanne, Switzerland, [6]Institute of Microengineering, Ecole Polytechnique Fédérale de Lausanne (EPFL), Lausanne, Switzerland, [7]The Sense Innovation and Research Center, Lausanne, Switzerland

Objective: To characterize ambulatory knee moments with respect to medial knee osteoarthritis (OA) severity comprehensively and to assess the possibility of developing a severity index combining knee moment parameters.

Methods: Nine parameters (peak amplitudes) commonly used to quantify three-dimensional knee moments during walking were analyzed for 98 individuals (58.7 ± 9.2 years old, 1.69 ± 0.09 m, 76.9 ± 14.5 kg, 56% female), corresponding to three medial knee osteoarthritis severity groups: non-osteoarthritis (n = 22), mild osteoarthritis (n = 38) and severe osteoarthritis (n = 38). Multinomial logistic regression was used to create a severity index. Comparison and regression analyses were performed with respect to disease severity.

Results: Six of the nine moment parameters differed statistically significantly among severity groups ($p \leq 0.039$) and five reported statistically significant correlation with disease severity ($0.23 \leq |r| \leq 0.59$). The proposed severity index was highly reliable (ICC = 0.96) and statistically significantly different between the three groups ($p < 0.001$) as well as correlated with disease severity ($r = 0.70$).

Conclusion: While medial knee osteoarthritis research has mostly focused on a few knee moment parameters, this study showed that other parameters differ with disease severity. In particular, it shed light on three parameters frequently disregarded in prior works. Another important finding is the possibility of combining the parameters into a severity index, which opens promising perspectives based on a single figure assessing the knee moments in their entirety. Although the proposed index was shown to be reliable and associated with disease severity, further research will be necessary particularly to assess its validity.

KEYWORDS

gait analysis, kinetics, knee adduction moment, knee flexion moment, biomechanics, machine learning

1 Introduction

Knee osteoarthritis (OA) is a painful and disabling disease affecting hundreds of millions of people worldwide and this number is expected to grow in the decades to come, notably due to the aging of the population (Wallace et al., 2017; Safari et al., 2020). No cure exists for knee OA and the disease end-stage often leads to major surgery through total knee replacement (Ringdahl and Pandit, 2011), highlighting the need to better understand the pathogenesis of the disease and find ways to slow down its progression.

The repetitive mechanical loading at the knee associated with walking has been shown to play an important role in knee OA (Andriacchi et al., 2004). This contribution was particularly well highlighted in a recent report introducing the term "Mechanokine" to stress the unique property of mechanical signals to transcend scales from the external forces acting on the whole-body to the mechanical environment of the cell in a manner that can influence joint heath associated to knee OA (Andriacchi et al., 2020). For instance, the maximum values (peaks) of the knee adduction (KAM_{first}) and flexion (KFM_{first}) moments during the first half of stance have been related to medial knee OA severity and progression (Kean et al., 2012; Chehab et al., 2014; Erhart-Hledik et al., 2015) and gait modifications based on these parameters showed improvement in clinical outcomes (Cheung et al., 2018; Richards et al., 2018). However, the large majority of previous research on medial knee OA, the most frequent form of the disease (Ahlbäck, 1968), focused on these two parameters and little is known about the seven others usual parameters of knee moments during walking (Figure 1) (Benedetti et al., 1998; Chehab et al., 2017). While analyzing KAM_{first} and KFM_{first} was well motivated in prior works, the disregard of the other parameters was rarely justified. This is even more intriguing that there are evidences scattered across a few specific publications that the other parameters vary with medial knee OA (Thorp et al., 2006; Astephen et al., 2008; Huang et al., 2008; Baert et al., 2013; Mills et al., 2013). Given the possibility that each of the nine parameters illustrated in Figure 1 could influence joint health in different ways and at different stages of the disease, there is a need for comprehensive studies analyzing all nine parameters over the full range of medial knee OA severity.

While considering more parameters will enhance the description of knee moments, having a larger number of parameters to deal with could render the analysis and use of knee kinetics more complex. For example, assessing the effect of a treatment could become difficult when the results diverge among parameters. The situation could be even more arduous with personalized interventions, such as insoles or gait retraining (Reeves and Bowling, 2011), where it could be impossible to find solutions fulfilling modifications on several parameters (Edd et al., 2020; Ulrich et al., 2020). In fact, the increase in complexity when describing knee moments with a higher number of parameters could well be the main reason why most of prior works focused on KAM_{first} and KFM_{first}. Therefore, to benefit from a more complete characterization of knee moment without increasing the complexity-of-use, there is a need to combine the parameters into indices associated with specific features of the disease, such as severity. Prior works have already shown the relevance of combining knee moment parameters. For instance, the total joint moment (TJM) combination was introduced to assess the relative contributions of the KAM and KFM (Zabala et al., 2013) and the medial contact force (MCF_{first}) parameter to estimate the peak force applied on the medial tibial plateau during the first half of stance (Walter et al., 2010; Manal et al., 2015).

This study first aimed at characterizing all nine usual parameters of knee moments during walking with respect to medial knee OA severity, through comparison and correlation analyses. A second objective was to assess the possibility of developing a severity index combining all nine parameters.

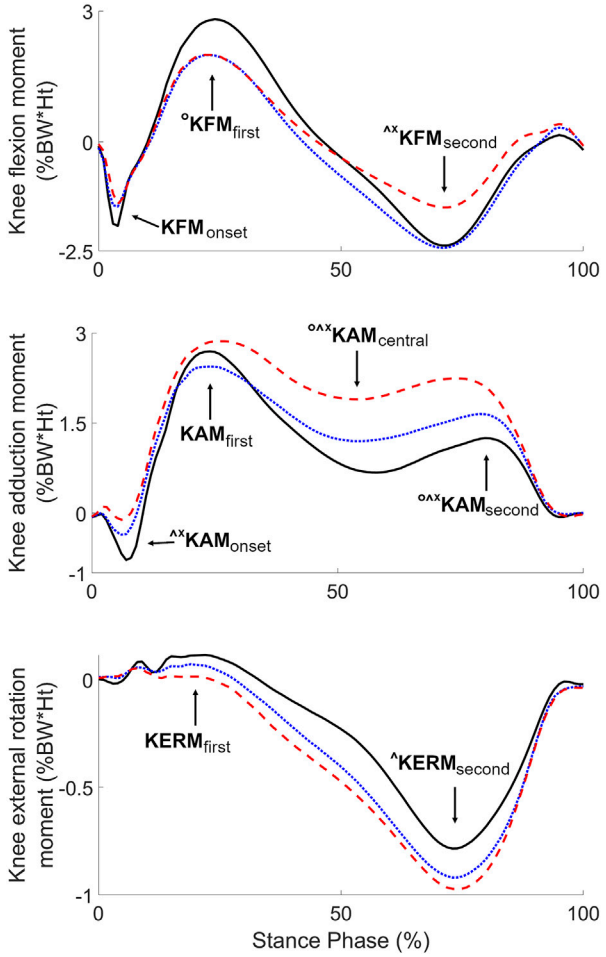

FIGURE 1
Average knee moments of the three severity groups (black solid lines: non-OA, blue dotted lines: mild OA, red dashed lines: severe OA), with indication of the nine usual parameters. Symbols indicate significant differences between groups (°: non-OA different from mild OA, ^: non-OA different from severe OA, *: mild OA different from severe OA) ($p < 0.017$).

2 Methods

2.1 Study population

For this study, the database of the Stanford BioMotion lab was screened for individuals aged 40 years old or older, with a body mass index (BMI) lower than 35 kg/m^2, and who got their gait analyzed following a standard procedure (see below) at the same time they were evaluated for symptoms and imaging signs of knee OA. From those, non-OA individuals, defined as individuals without self-reported pain or significant injury in the lower limb or lower back and without evidence of cartilage loss, osteophytes, subchondral bone marrow lesions, bone attrition, or meniscal pathology (subluxation, maceration, degeneration) in any knees, were selected for the present study (Hunter et al., 2011). Structural alterations of the knees were determined based on magnetic resonance imaging exams, including a three-dimensional fat-suppressed spoiled-gradient recalled echo sequence (3D SPGR; plane = sagittal, TR = 50 ms, TE = 7 ms, flip angle = 30°, field of view = 140 × 140 mm^2, slice thickness = 1.5 mm, number of slices = 60, acquisition matrix = 256 × 256) and a fat-suppressed proton density fast spin echo sequence (PDFSE; plane = sagittal, TR = 4,000 ms, TE = 13 ms, flip angle = 90°, field of view = 140 × 140 mm^2, slice thickness = 2.5 mm, number of slices = 33, acquisition matrix = 256 × 256), using a 1.5T machine (GE Medical Systems, Milwaukee, WI). Individuals with medial compartment knee OA were also selected for the present study. These persons were characterized by persistent self-reported pain and radiographic confirmation of the presence of primarily medial compartment OA in at least one knee, no primarily lateral or trochlea OA or arthroplasty in any knees, Kellgren and Lawrence (K/L) grading of both knees (Kellgren and Lawrence, 1957), no diagnosis or symptoms of OA in other lower extremity joints, no serious ankle, hip or back injury or surgery, no gout or recurrent pseudogout, and no use of ambulatory aids. All individuals selected for the present study got their data recorded in the framework of researches approved by the internal review board of Stanford University and gave their consent for further analysis of their data. Data from the most recent testing were used for individuals with multiple records in the database.

In total, 98 individuals (43 males) were available for this study. They were of mean (± standard deviation) age, height and weight of 58.7 ± 9.2 years old, 1.69 ± 0.09 m, and 76.9 ± 14.5 kg, respectively. One knee per individual was analyzed. For non-OA individuals, the study knee was randomly chosen, while the knee with the highest K/L grade was analyzed for OA individuals. In case of equal K/L grade for both knees, the study knee was randomly chosen. For comparison analyses, knees with K/L grade of I or II were considered mild OA and knees with K/L grade of III or IV severe OA, resulting in three severity groups of 22–38 knees each (Table 1). There was no statistically significant demographic difference among the severity groups, except for age, with younger individuals in the non-OA group compared to the two other groups ($p < 0.001$). A *post hoc* power analysis showed that effect sizes of at least 0.8 are detectable with groups of 22–38 knees each (Table 1) considering a power of 80% and a Bonferroni-corrected alpha level of 5% (G*Power, DE). These detectable effect sizes are appropriate, considering the large to strong effect sizes reported in prior studies comparing ambulatory knee moments with respect to OA severity (Cohen's d between 0.8 and 1.2) (Astephen et al., 2008; Mills et al., 2013).

2.2 Gait analysis

All knees in this study were tested following the same standardized procedure including the recording of three 10 m-long straight-line trials at self-selected normal gait speed with personal walking shoes across a walkway instrumented with an optoelectronic motion capture system (Qualisys Medical, Gothenburg, SE) and a force plate (Bertec, Columbs, OH) operating synchronously at 120 Hz. Multiple operators from the same laboratory collected the data. Only trials with a clear step of the foot below the knee of interest on the force plate were recorded. Before recording the gait trials, clusters of reflective markers were fixed on the individuals and a calibration based on anatomical landmarks was performed, following a common protocol (Chehab et al., 2017). During the gait trials, the position and orientation of the lower-limb segments were calculated using the cluster marker trajectories and the calibration information (Andriacchi et al., 1998; Favre et al., 2009). The flexion, adduction and external rotation moments at the knee during the stance phases with the foot of interest on the force plate were calculated following a standard inverse dynamics approach (Zabala et al., 2013). The three moments were time-normalized to 0%–100% during stance and expressed as external moments in percentage of bodyweight and height (%BW × Ht). During each stance phase, the nine characteristic parameters of the moment curves were extracted for analysis (Table 2; Figure 1) (Benedetti et al., 1998; Chehab et al., 2017). Finally, each of the nine parameters was averaged over the three trials to have one value per parameter and knee. All biomechanical processing was done using the software application BioMove (Stanford, CA).

2.3 Severity index

The severity index was computed by multinomial logistic regression with the severity groups as nominal response and the nine knee moment parameters as predictors (McCullagh and Nelder, 2019). The parameters were standardized using a z-score transformation before performing the regression and a sigmoid transformation was applied to the regressed data to have indices ranging between 0 and 100. The regression was calculated by bootstrapping which allowed determining confidence intervals for the regression coefficients and assessing the reliability of the index (Efron and Tibshirani, 1994). Reliability was characterized using the intraclass correlation coefficient (ICC) and the standard error of measurement (SEM) (Weir, 2005).

For completeness with literature, two previously proposed combinations of knee moment parameters, the total knee joint moment (Zabala et al., 2013) and the medial contact force (Walter et al., 2010; Manal et al., 2015), were also computed. For the total knee joint moment, the square root of the sum of the squared knee flexion, adduction and external rotation moments was calculated for each time point of each stance (Zabala et al., 2013). Then, the maximal values during the first and second halves of each

TABLE 1 Characteristics of the three severity groups.

	Non-OA	Mild OA	Severe OA
	n = 22	*n* = 38	*n* = 38
Gender (number)	W: 13, M: 9	W: 20, M: 18	W: 22, M: 16
KL grade (number)		I: 26, II: 12	III: 19, IV: 19
Age (years)*	50.5 ± 5.5	59.3 ± 8.6	62.8 ± 8.6
Height (m)	1.70 ± 0.09	1.70 ± 0.10	1.70 ± 0.09
Weight (kg)	74.3 ± 14.7	74.5 ± 14.4	81.0 ± 13.8
Walking speed (m/s)[#]	1.41 ± 0.22	1.28 ± 0.19	1.22 ± 0.19

Data are presented as mean ± SD or as numbers. *Non-OA individuals were statistically significantly younger than mild and severe OA individuals ($p < 0.001$). [#]Walking speed was statistically significantly faster in non-OA than severe OA individuals ($p < 0.001$).

TABLE 2 Values of the knee moment parameters for the three severity groups, as well as Spearman correlation between the parameters and disease severity.

Parameter	Definition	Values per severity group: median (1st quartile; 3rd quartile)			Correlation with disease severity, *n* = 98			
		Non-OA, *n* = 22	Mild OA, *n* = 38	Severe OA, *n* = 38	Spearman correlation		Partial spearman correlation[Δ]	
					r_s (95% CI)	*p*-value	r_s (95% CI)	*p*-value
$KAM_{central}$	Minimum adduction moment between KAM_{first} and KAM_{second}	0.61 (0.30; 0.86)[#$]	0.98 (0.77; 1.56)*[$]	1.69 (1.17; 2.55)*[#]	0.59 (0.43; 0.71)	<0.001	0.52 (0.35; 0.66)	<0.001
KFM_{second}	Minimum flexion moment during second half of stance	−2.34 (−2.92; −1.87)[$]	−2.58 (−3.15; −1.87)[$]	−1.56 (−2.38; −0.79)*[#]	0.35 (0.16; 0.52)	<0.001	0.21 (0.01; 0.40)	0.037
KAM_{first}	Maximum adduction moment during first half of stance	3.01 (2.34; 3.24)	2.49 (2.16; 3.22)	3.16 (2.50; 3.82)	0.13 (−0.07; 0.32)	0.189	0.31 (0.11; 0.48)	0.002
$KERM_{second}$	Minimum external rotation moment during second half of stance	−0.79 (−1.00; −0.70)[$]	−0.94 (−1.07; −0.74)	−0.96 (−1.19; −0.76)*	−0.24 (−0.42; −0.04)	0.016	−0.36 (−0.53; −0.17)	<0.001
KFM_{first}	Maximum flexion moment during first half of stance	3.00 (2.21; 3.61)[#]	2.06 (1.47; 2.52)*	2.05 (0.85; 3.43)	−0.17 (−0.36; 0.03)	0.095	−0.01 (−0.21; 0.18)	0.893
KAM_{onset}	Minimum adduction moment before KAM_{first}	−0.87 (−0.55; −1.19)[$]	−0.83 (−0.40; −0.94)[$]	−0.37 (−0.13; −0.54)*[#]	0.48 (0.30; 0.63)	<0.001	0.46 (0.28; 0.61)	<0.001
KAM_{second}	Maximum adduction moment during second half of stance	1.32 (0.91; 1.69)[#$]	1.62 (1.40; 2.05)*[$]	2.40 (1.64; 2.89)*[#]	0.49 (0.31; 0.63)	<0.001	0.53 (0.35; 0.66)	<0.001
$KERM_{first}$	Maximum external rotation moment during first half of stance	0.19 (0.11; 0.26)	0.16 (0.11; 0.22)	0.12 (0.07; 0.19)	−0.23 (−0.42; −0.03)	0.021	−0.11 (−0.31; 0.09)	0.273
KFM_{onset}	Minimum flexion moment before KFM_{first}	−2.42 (−2.93; −1.68)	−2.08 (−2.49; −1.60)	−1.88 (−2.33; −1.64]	0.18 (−0.02; 0.37)	0.077	0.04 (−0.16; 0.23)	0.711

All parameters are reported in %BW*Ht. See Figure 1 for an illustration of the parameters and their differences with disease severity. To facilitate reading across tables, parameters are reported following the order in Table 4. [Δ]Partial correlation between knee moment parameters and disease severity while controlling for age and walking speed. *significantly different compared to the non-OA group ($p < 0.017$). [#]significantly different compared to the mild OA group ($p < 0.017$). [$]significantly different compared to the severe OA group ($p < 0.017$).

stance were extracted (TJM_{first} and TJM_{second}, respectively). Regarding the medial contact force, the maximum value during the first half of each stance (MCF_{first}) was estimated based on KAM_{first} and KFM_{first} using a formula determined with instrumented knee prostheses (Walter et al., 2010; Manal et al., 2015; Uhlrich et al., 2018). Similar to the other moment parameters, TJM_{first}, TJM_{second} and MCF_{first} were averaged over the three trials recoded for each knee.

2.4 Statistical analysis

Since the data were not normally distributed (Kolmogorov-Smirnov tests), they were analyzed using non-parametric statistics. Specifically, comparisons of the nine knee moment parameters, the proposed severity index, the three prior combination parameters and the walking speed among the severity groups were performed using Kruskal-Wallis tests with *post hoc* ranksum tests. Associations with disease severity, for the knee moment parameters, the severity index and the prior combination parameters, were assessed using Spearman correlations across severity groups. Since walking speed and age have been shown to influence knee moment parameters (Lelas et al., 2003; Chehab et al., 2017), partial Spearman correlations were also calculated to describe the relationship with disease severity while controlling for walking speed and age. Finally, Spearman correlations were performed to quantify the associations among parameters. Significance level was set *a priori* at $p < 0.05$, with Bonferroni corrections for multiple comparisons during *post hoc* analyses (effective $p < 0.017$).

3 Results

Six of the nine knee moment parameters showed statistically significant effect of disease severity (KFM_{first}, $p = 0.034$; $KERM_{second}$, $p = 0.039$; $KAM_{central}$, KFM_{second}, KAM_{onset}, and KAM_{second}, all $p < 0.001$). Post-hoc testing indicated significant incremental differences in $KAM_{central}$ and KAM_{second} from non-OA to mild OA, to severe OA, with larger values in more severely affected knees (Table 2; Figure 1). KAM_{onset} was significantly larger in the severe OA group compared to both the non-OA and the mild OA groups. KFM_{second} was significantly larger in severe OA knees compared to both the non-OA and the mild OA knees, while KFM_{first} was significantly smaller in mild OA than in non-OA knees. Finally, $KERM_{second}$ was significantly smaller in the severe OA than in the non-OA group.

Statistically significant correlations with disease severity were found for five of the nine moment parameters: $KAM_{central}$ ($r_s = 0.59$, $p < 0.001$), KAM_{second} ($r_s = 0.49$, $p < 0.001$), KAM_{onset} ($r_s = 0.48$, $p < 0.001$), KFM_{second} ($r_s = 0.35$, $p < 0.001$), $KERM_{second}$ ($r_s = -0.24$, $p = 0.016$) and $KERM_{first}$ ($r_s = -0.23$, $p = 0.021$) (Table 2). Controlling for age and walking speed resulted in the same statistically significant correlations, except for KAM_{first} which became significant ($r_s = 0.31$, $p = 0.002$) and $KERM_{first}$ which exceeded the significance level ($r_s = -0.11$, $p = 0.273$). Correlations among the nine moment parameters are reported in Supplementary Table S1.

The proposed regression method allowed compiling a severity index showing an excellent reliability, with ICC of 0.96 and SEM of 6.78 units (Koo and Li, 2016). Moreover, Kruskal-Wallis test showed statistically significant differences among severity groups ($p < 0.001$), with *post hoc* analyses indicating significant difference between the three groups. Indeed, the non-OA group had significantly lower severity indices than the mild OA and severe OA groups, and the mild OA group had significantly lower severity indices than the severe OA groups (Table 3). Additionally, a significant correlation was found between the severity index and disease severity ($r_s = 0.70$, $p < 0.001$). The correlation remained significant when controlling for age and walking speed ($r_s = 0.63$, $p < 0.001$).

Since the moment parameters were standardized before calculating the severity index, the coefficients of the regression leading to the severity index can be analyzed to compare the contribution of the nine moment parameters to the severity index. Doing so, indicated that $KAM_{central}$ had the biggest effect on the index with a coefficient of −1.52, contributing 27.0% to the severity index, followed by KFM_{second} and KAM_{first} with coefficients of −1.00 and 0.98 and contributing for 17.7% and 17.4% of the severity index, respectively (Table 4; Figure 2). On the opposite, KFM_{onset}, $KERM_{first}$ and KAM_{second} had the least impact on the index, with coefficients of 0.095, −0.178, and −0.304 and contributions of 1.7%, 3.2% and 5.4% to the severity index, respectively.

Additionally, Kruskal-Wallis tests showed no statistically significant difference among severity groups for any of the three prior combinations parameters (TJM_{first}, $p = 0.079$; TJM_{second}, $p = 0.168$; MCF_{first}, $p = 0.061$). When controlling for age and walking speed, statistically significant correlations with disease severity were observed for all three combinations: TJM_{first} ($r_s = 0.31$, $p = 0.002$), TJM_{second} ($r_s = 0.25$, $p = 0.014$), and MCF_{first} ($r_s = 0.29$, $p = 0.004$). The correlations were non-significant when no control for age and walking speed was applied ($r_s \leq 0.13$, $p \geq 0.188$).

4 Discussion

This study confirmed that diverse knee moment parameters differ with respect to the severity of medial knee OA. Compared to prior works, the present study, testing all usual parameters over the entire spectrum of disease severity, provided a basis to assemble the pieces disseminated in literature. Various factors, including participants' characteristics or analysis protocols, could influence knee moments and lead to diverging results among studies (Messier et al., 2005; Chehab et al., 2017; Schrijvers et al., 2021). Nevertheless, even with such possible methodological variations among studies, strong consensuses could be identified for four parameters. These included smaller KFM_{first} in mild OA compared to non-OA (asymptomatic) knees and in severe OA compared to mild OA knees, although the severe-mild difference was not observed in the present study (Weidow et al., 2006; Astephen et al., 2008; Huang et al., 2008). Consistent observations also existed for larger KFM_{second} in severe OA than in non-OA (asymptomatic) and mild OA knees (Astephen et al., 2008; Baert et al., 2013), as well as larger $KAM_{central}$ and KAM_{second} in mild OA than in non-OA (asymptomatic) and in severe OA than in mild OA (Thorp et al., 2006; Astephen et al., 2008; Huang et al., 2008). No consensus existed for KAM_{first}, which was already shown to have highly inconsistent results among studies (Mills et al., 2013), and no consolidation could be attempted for the other parameters due to lacking data in literature. Altogether, the present study shed light on three parameters, $KAM_{central}$, KAM_{second}, and KFM_{second}, which were frequently disregarded in prior works. This suggests that future research should not limit the analysis to KAM_{first} and KFM_{first}. This suggestion is particularly well supported by two recent studies relating $KAM_{central}$ with disease progression and symptoms (Astephen Wilson et al., 2017; Costello et al., 2020).

TABLE 3 Values of the severity index and of three prior moment combination parameters for the three severity groups, as well as Spearman correlation between these measures and disease severity.

Combination parameter	Definition; unit	Values per severity group: median (1st quartile; 3rd quartile)			Correlation with disease severity, $n = 98$			
		Non-OA, $n = 22$	Mild OA, $n = 38$	Severe OA, $n = 38$	Spearman correlation		Partial spearman correlation$^{\Delta}$	
					r_s (95% CI)	*p*-value	r_s (95% CI)	*p*-value
Severity index	Severity index; -	10.0 (3.7; 21.0)$^{\#\$}$	42.9 (25.3; 58.2)$^{*\$}$	84.2 (62.5; 94.4)$^{*\#}$	0.70 (0.57; 0.80)	<0.001	0.63 (0.48; 0.75)	<0.001
TJM_{first}	Maximum total knee joint moment during first half of stance; %BW*Ht	4.11 (3.53; 4.75)	3.29 (2.90; 4.25)	3.95 (3.20; 4.95)	0.01 (−0.19; 0.21)	0.893	0.31 (0.11; 0.48)	0.002
TJM_{second}	Maximum total knee joint moment during second half of stance; % BW*Ht	2.72 (2.27; 3.01)	3.27 (2.42; 3.82)	3.06 (2.72; 3.46)	0.11 (−0.09; 0.30)	0.277	0.25 (0.05; 0.43)	0.014
MCF_{first}	Maximum medial contact force during first half of stance; BW	2.07 (1.90; 2.27)	1.87 (1.72; 2.08)	2.12 (1.79; 2.25)	0.03 (−0.16; 0.23)	0.734	0.63 (0.48; 0.75)	0.004

$^{\Delta}$partial correlation between knee moment parameters and disease severity while controlling for age and walking speed. *significantly different compared to the non-OA group ($p < 0.017$). $^{\#}$significantly different compared to the mild OA group ($p < 0.017$). $^{\$}$significantly different compared to the severe OA group ($p < 0.017$).

TABLE 4 Coefficient of the nine moment parameters in the severity index regression.

Parameter	Regression coefficient (95% CI)
$KAM_{central}$	−1.52 (−1.58; −1.47)
KFM_{second}	−1.00 (−1.03; −0.97)
KAM_{first}	0.98 (0.94; 1.02)
$KERM_{second}$	0.69 (0.65; 0.74)
KFM_{first}	0.54 (0.51; 0.57)
KAM_{onset}	−0.33 (−0.37; −0.28)
KAM_{second}	−0.30 (−0.37; −0.24)
$KERM_{first}$	−0.18 (−0.21; −0.15)
KFM_{onset}	0.09 (0.07; 0.12)

Parameters are ordered according to the magnitude of the regression coefficients. Please refer to Table 2 and Figure 1 for a definition and an illustration of the parameters, respectively.

With the consideration of more than two parameters appearing wise for the characterization of the knee moments, the possibility to combine the parameters into an index reflecting disease severity constitutes another important finding of the present study. Indeed, while considering a larger number of parameters will contribute to better descriptions, having a larger number of parameters to manage could increase study design complexity and make gait interventions more complex (Edd et al., 2020). Therefore, the possibility of combining the parameters, as demonstrated in this study, is interesting practically. However, beyond practical considerations, indices could be especially relevant for the global assessments of the knee moments they allow. For example, in personalized interventions, such as gait retraining (Cheung et al., 2018; Richards et al., 2018; Ulrich et al., 2020), it could become possible to aim for a global change, instead of aiming for changes in one or two moment parameters, without consideration for the others.

The second objective of assessing the possibility of developing a severity index was fully achieved, with the design of an index reliable, significantly different among the three severity groups and showing a large correlation with disease severity. Further research will now be necessary to assess the validity of the proposed index. The techniques to record and calculate knee moments differ among institutions (Benedetti et al., 2013; Schrijvers et al., 2021). Therefore, the sensitivity of the severity index to variations in gait analysis protocols will need to be determined. It is well possible that the index will be little sensitive to such methodological differences, as it is an aggregate of standardized parameters. It will also be necessary evaluating the index longitudinally and characterizing its relationships with key features of knee OA, such as pain or disease progression (Felson, 2009).

It is interesting to note that KAM_{first} accounted for 17% of the severity index (third most important contributor to the index), although it was not significantly different among severity groups. While such an important role in the severity index could appear peculiar in view of its relationship with disease severity, this role well agrees with medial knee OA literature, where KAM_{first} is a prevalent parameter and the primary focus of gait interventions (Reeves and Bowling, 2011; Mills et al., 2013; Favre and Jolles, 2016). Thus, it is possible that the severity index actually captured the global essence of disease severity. Three combination parameters were already proposed in literature, TJM_{first}, TJM_{second}, and MCF_{first} (Walter et al., 2010; Zabala et al., 2013; Manal et al., 2015), but the severity index in this study is the first to have been designed to reflect disease severity.

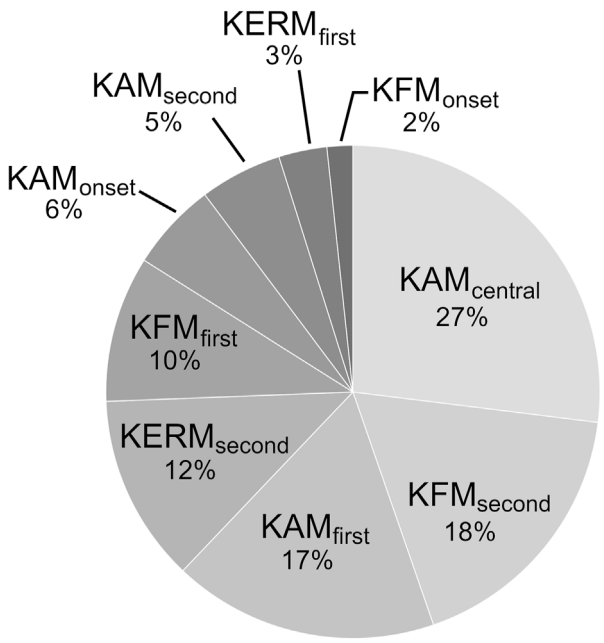

FIGURE 2
Contribution of the nine moment parameters to the severity index.

The present study brought new insights into the relationship between knee moment parameters and disease severity that could reveal particularly useful in the evaluation and rehabilitation of medial knee OA gait (Favre and Jolles, 2016). Nevertheless, further research will be necessary to determine the mechanisms behind these relationships. Walking speed and age certainly play a role in the relationships between knee moment parameters and disease severity, but, as confirmed in this study, the causes are more complex than simply variations in walking speed or in age (Landry et al., 2007). Consequently, the role of other factors, including motor control, muscle strength and soft-tissue properties (Lewek et al., 2004; Hubley-Kozey et al., 2006; Rudolph et al., 2007; Adouni and Shirazi-Adi, 2014; Stanahan et al., 2015) as well as pain (Boyer, 2018), will need to be clarified in future studies. Further works should also assess the relevance of the severity index in pre-OA both for early disease detection and gait modification (Reeves and Bowling, 2011; Ulrich et al., 2020).

This study has some limitations, including the use of a single cross-sectional dataset, as discussed above. Multiple operators contributed to the gait data collection, which could have led to increased inter-individual variability and limited the detection of differences and correlations with disease severity. Nevertheless, obtaining conclusive results based on data collected by multiple operators remained a strength in view of future large-scale applications where gait recording will likely be performed by different operators. Another point worth mentioning is the multinomial logistic regression used to determine the severity index. While it is a common method, which successfully combined the moment parameters, one cannot exclude that there could be other ways to combine the parameters. This is particularly supported by the fact that some parameters were correlated to each other. It is important to note that the possible existence of alternative combinations does not affect the main findings but requires caution to not over interpret the combination obtained in this study as unique or being the best. Depending on the results of the validity studies to follow, in the future, it might be necessary comparing different combination methods. Additionally, in line with literature, this study focused on discrete knee moment parameters. Nevertheless, analyzing the knee moment curves could also reveal interesting, for example, using one-dimensional statistical parametric mapping (Friston et al., 1994; Pataky, 2012). Finally, since the severity groups differed in age and walking speed, it is possible that a fraction of the severity index reflects the variations in moment parameters with respect to age or walking speed.

5 Conclusion

This study confirmed that diverse knee moment parameters differ with disease severity. In particular, differences among severity groups were found to be consistent across studies for four parameters, including three that were frequently disregarded in prior works ($KAM_{central}$, KAM_{second}, KFM_{second}). Future studies are therefore recommended to not limit the analysis to KAM_{first} and KFM_{first}. Another important finding of this study was the possibility to combine the parameters into a severity index, which opens promising perspectives based on a single figure assessing the knee moments in their entirety. While the proposed index was shown to be reliable and correlated with disease severity, further research will be necessary to assess its validity.

Data availability statement

The data analyzed in this study is subject to the following licenses/restrictions: The data are not publicly available due to regulatory provisions. Requests to access these datasets should be directed to baptiste.ulrich@chuv.ch.

Ethics statement

The studies involving human participants were reviewed and approved by the Commission cantonale d'éthique de la recherche sur l'être humain CER-VD. The patients/participants provided their written informed consent to participate in this study.

Author contributions

Study conception and design were done by BU, TA, BJ, and JF. Data were collected and assembled by BU, JE-H, and JA.

Analysis and interpretation of the data were performed by BU, PO, TA, and JF. The article was drafted by BU, TA, and JF, and critically revised for important intellectual content by all authors. Funding was obtained by TA, BJ, and JF. The study was supervised by TA, BJ, and JF, who should be considered as last authors. All authors contributed to the article and approved the submitted version.

Funding

This study was partially funded by the Swiss National Science Foundation (SNSF grant #32003B-166433), the Lausanne Orthopedic Research Foundation and the Profectus Foundation.

Acknowledgments

The present study is part of the PhD thesis of BU (Ulrich 2021).

Conflict of interest

The authors declare that the research was conducted in the absence of any commercial or financial relationships that could be construed as a potential conflict of interest.

Publisher's note

Supplementary material

The Supplementary Material for this article can be found online at: https://www.frontiersin.org/articles/10.3389/fbioe.2023.1176471/full#supplementary-material

References

Adouni, M., and Shirazi-Adl, A. (2014). Evaluation of knee joint muscle forces and tissue stresses-strains during gait in severe OA versus normal subjects. *J. Orthop. Res.* 32 (1), 69–78. doi:10.1002/jor.22472

Ahlbäck, S. (1968). Osteoarthrosis of the knee. A radiographic investigation. *Acta. Radiol. diagn.* 227, 277:7-72–72.

Andriacchi, T. P., Alexander, E. J., Toney, M. K., Dyrby, C., and Sum, J. A. (1998). A point cluster method for *in vivo* motion analysis: Applied to a study of knee kinematics. *J. Biomech. Eng.* 120 (6), 743–749. doi:10.1115/1.2834888

Andriacchi, T. P., Griffin, T. M., Loeser, R. F., Jr, Chu, C. R., Roos, E. M., Hawker, G. A., et al. (2020). Bridging disciplines as a pathway to finding new solutions for osteoarthritis a collaborative program presented at the 2019 orthopaedic research society and the osteoarthritis research society international. *Osteoarthr. Cartil. Open* 2 (1), e100026. doi:10.1016/j.ocarto.2020.100026

Andriacchi, T. P., Mündermann, A., Smith, R. L., Alexander, E. J., Dyrby, C. O., and Koo, S. (2004). A framework for the *in vivo* pathomechanics of osteoarthritis at the knee. *Ann. Biomed. Eng.* 32 (3), 447–457. doi:10.1023/b:abme.0000017541.82498.37

Astephen, J. L., Deluzio, K. J., Caldwell, G. E., and Dunbar, M. J. (2008). Biomechanical changes at the hip, knee, and ankle joints during gait are associated with knee osteoarthritis severity. *J. Orthop. Res.* 26 (3), 332–341. doi:10.1002/jor.20496

Astephen Wilson, J. L., Stanish, W. D., and Hubley-Kozey, C. L. (2017). Asymptomatic and symptomatic individuals with the same radiographic evidence of knee osteoarthritis walk with different knee moments and muscle activity. *J. Orthop. Res.* 35 (8), 1661–1670. doi:10.1002/jor.23465

Baert, I. A., Jonkers, I., Staes, F., Luyten, F. P., Truijen, S., and Verschueren, S. M. (2013). Gait characteristics and lower limb muscle strength in women with early and established knee osteoarthritis. *Clin. Biomech.* 28 (1), 40–47. doi:10.1016/j.clinbiomech.2012.10.007

Benedetti, M. G., Catani, F., Leardini, A., Pignotti, E., and Giannini, S. (1998). Data management in gait analysis for clinical applications. *Clin. Biomech.* 13 (3), 204–215. doi:10.1016/S0268-0033(97)00041-7

Benedetti, M. G., Merlo, A., and Leardini, A. (2013). Inter-laboratory consistency of gait analysis measurements. *Gait Posture* 38 (4), 934–939. doi:10.1016/j.gaitpost.2013.04.022

Boyer, K. A. (2018). Biomechanical response to osteoarthritis pain treatment may impair long-term efficacy. *Exerc. Sport Sci. Rev.* 46 (2), 121–128. doi:10.1249/JES.0000000000000141

Chehab, E. F., Andriacchi, T. P., and Favre, J. (2017). Speed, age, sex, and body mass index provide a rigorous basis for comparing the kinematic and kinetic profiles of the lower extremity during walking. *J. Biomech.* 58, 11–20. doi:10.1016/j.jbiomech.2017.04.014

Chehab, E. F., Favre, J., Erhart-Hledik, J. C., and Andriacchi, T. P. (2014). Baseline knee adduction and flexion moments during walking are both associated with 5 year cartilage changes in patients with medial knee osteoarthritis. *Osteoarthr. Cartil.* 22 (11), 1833–1839. doi:10.1016/j.joca.2014.08.009

Cheung, R. T., Ho, K. K. W., Au, I. P. H., An, W. W., Zhang, J. H., Chan, Z. Y. S., et al. (2018). Immediate and short-term effects of gait retraining on the knee joint moments and symptoms in patients with early tibiofemoral joint osteoarthritis: A randomized controlled trial. *Osteoarthr. Cartil.* 6 (11), 1479–1486. doi:10.1016/j.joca.2018.07.011

Costello, K. W., Wilson, J. L. A., Stanish, W. D., Urquhart, N., and Hubley-Kozey, C. L. (2020). Differences in baseline joint moments and muscle activation patterns associated with knee osteoarthritis progression when defined using a clinical versus a structural outcome. *J. Appl. Biomech.* 36 (1), 39–51. doi:10.1123/jab.2019-0127

Edd, S. N., Bennour, S., Ulrich, B., Jolles, B. M., and Favre, J. (2020). Modifying stride length in isolation and in combination with foot progression angle and step width can improve knee kinetics related to osteoarthritis; A preliminary study in healthy subjects. *J. Biomech. Eng.* 142 (7), e074505. doi:10.1115/1.4046713

Efron, B., and Tibshirani, R. J. (1994). *An introduction to the bootstrap*. Florida: CRC Press.

Erhart-Hledik, J. C., Favre, J., and Andriacchi, T. P. (2015). New insight in the relationship between regional patterns of knee cartilage thickness, osteoarthritis disease severity, and gait mechanics. *J. Biomech.* 48 (14), 3868–3875. doi:10.1016/j.jbiomech.2015.09.033

Favre, J., Aissaoui, R., Jolles, B. M., de Guise, J. A., and Aminian, K. (2009). Functional calibration procedure for 3D knee joint angle description using inertial sensors. *J. Biomech.* 42 (14), 2330–2335. doi:10.1016/j.jbiomech.2009.06.025

Favre, J., and Jolles, B. M. (2016). Gait analysis of patients with knee osteoarthritis highlights a pathological mechanical pathway and provides a basis for therapeutic interventions. *EFORT Open Rev.* 1 (10), 368–374. doi:10.1302/2058-5241.1.000051

Felson, D. T. (2009). Developments in the clinical understanding of osteoarthritis. *Arthritis Res. Ther.* 11 (1), 203–211. doi:10.1186/ar2531

Friston, K. J., Holmes, A. P., Worsley, K. J., Poline, J.-P., Frith, C. D., and Frackowiak, R. S. J. (1994). Statistical parametric maps in functional imaging: A general linear approach. *Hum. Brain Mapp.* 2 (4), 189–210. doi:10.1002/hbm.460020402

Huang, S. C., Wei, I. P., Chien, H. L., Wang, T. M., Liu, Y. H., Chen, H. L., et al. (2008). Effects of severity of degeneration on gait patterns in patients with medial knee osteoarthritis. *Med. Eng. Phys.* 30 (8), 997–1003. doi:10.1016/j.medengphy.2008.02.006

Hubley-Kozey, C. L., Deluzio, K. F., Landry, S. C., McNutt, J. S., and Stanish, W. D. (2006). Neuromuscular alterations during walking in persons with moderate knee osteoarthritis. *J. Electromyogr. Kinesiol.* 16 (4), 365–378. doi:10.1016/j.jelekin.2005.07.014

Hunter, D. J., Arden, N., Conaghan, P. G., Eckstein, F., Gold, G., Grainger, A., et al. (2011). Definition of osteoarthritis on MRI: Results of a delphi exercise. *Osteoarthr. Cartil.* 19 (8), 963–969. doi:10.1016/j.joca.2011.04.017

Kean, C. O., Hinman, R. S., Bowles, K. A., Cicuttini, F., Davies-Tuck, M., and Bennell, K. L. (2012). Comparison of peak knee adduction moment and knee adduction moment

impulse in distinguishing between severities of knee osteoarthritis. *Clin. Biomech.* 27 (5), 520–523. doi:10.1016/j.clinbiomech.2011.12.007

Kellgren, J. H., and Lawrence, J. (1957). Radiological assessment of osteo-arthrosis. *Ann. Rheum. Dis.* 16 (4), 494–502. doi:10.1136/ard.16.4.494

Koo, T. K., and Li, M. Y. (2016). A guideline of selecting and reporting intraclass correlation coefficients for reliability research. *J. Chiropr. Med.* 15 (2), 155–163. doi:10.1016/j.jcm.2016.02.012

Landry, S. C., McKean, K. A., Hubley-Kozey, C. L., Stanish, W. D., and Deluzio, K. J. (2007). Knee biomechanics of moderate OA patients measured during gait at a self-selected and fast walking speed. *J. Biomech.* 40 (8), 1754–1761. doi:10.1016/j.jbiomech.2006.08.010

Lelas, J. L., Merriman, G. J., Riley, R. P., and Kerrigan, D. C. (2003). Predicting peak kinematic and kinetic parameters from gait speed. *Gait Posture* 17 (2), 106–112. doi:10.1016/S0966-6362(02)00060-7

Lewek, M. D., Rudolph, K. S., and Snyder-Mackler, L. (2004). Quadriceps femoris muscle weakness and activation failure in patients with symptomatic knee osteoarthritis. *J. Orthop. Res.* 22 (1), 110–115. doi:10.1016/S0736-0266(03)00154-2

Manal, K., Gardinier, E., Buchanan, T. S., and Snyder-Mackler, L. (2015). A more informed evaluation of medial compartment loading: The combined use of the knee adduction and flexor moments. *Osteoarthr. Cartil.* 23 (7), 1107–1111. doi:10.1016/j.joca.2015.02.779

McCullagh, P., and Nelder, J. A. (2019). Generalized linear models. *Routledge*. doi:10.1201/9780203753736

Messier, S. P., Gutekunst, D. J., Davis, C., and DeVita, P. (2005). Weight loss reduces knee-joint loads in overweight and obese older adults with knee osteoarthritis. *Arthritis Rheum.* 52 (7), 2026–2032. doi:10.1002/art.21139

Mills, K., Hunt, M. A., and Ferber, R. (2013). Biomechanical deviations during level walking associated with knee osteoarthritis: A systematic review and meta-analysis. *Arthritis Care Res.* 65 (10), 1643–1665. doi:10.1002/acr.22015

Pataky, T. C. (2012). One-dimensional statistical parametric mapping in Python. *Comput. Methods Biomech. Biomed. Engin.* 15 (3), 295–301. doi:10.1080/10255842.2010.527837

Reeves, N. D., and Bowling, F. L. (2011). Conservative biomechanical strategies for knee osteoarthritis. *Nat. Rev. Rheumatol.* 7, 113–122. doi:10.1038/nrrheum.2010.212

Richards, R., Van de Noort, J. C., Van der Esch, M., Booik, M. J., and Harlaar, J. (2018). Gait retraining using real-time feedback in patients with medial knee osteoarthritis: Feasibility and effects of a six-week gait training program. *Knee* 25 (5), 814–824. doi:10.1016/j.knee.2018.05.014

Ringdahl, E. N., and Pandit, S. (2011). Treatment of knee osteoarthritis. *Am. Fam. Physician* 83 (11), 1287–1292.

Rudolph, K. S., Schmitt, L. C., and Lewek, M. D. (2007). Age-related changes in strength, joint laxity, and walking patterns: Are they related to knee osteoarthritis? *Phys. Ther.* 87 (11), 1422–1432. doi:10.2522/ptj.20060137

Safiri, S., Kolahi, A.-A., Smith, E., Hill, C., Bettampadi, D., Mansournia, M. A., et al. (2020). Global, regional and national burden of osteoarthritis 1990-2017: A systematic analysis of the global burden of disease study 2017. *Ann. Rheum. Dis.* 79 (6), 819–828. doi:10.1136/annrheumdis-2019-216515

Schrijvers, J. C., Rutherford, D., Richards, R., Van den Noort, J. C., Van der Esch, M., and Harlaar, J. (2021). Inter-laboratory comparison of knee biomechanics and muscle activation patterns during gait in patients with knee osteoarthritis. *Knee* 29, 500–509. doi:10.1016/j.knee.2021.03.001

Stanahan, C. J., Hodges, P. W., Wrigley, T. V., Bennell, K. L., and Farrell, M. J. (2015). Organisation of the motor cortex differs between people with and without knee osteoarthritis. *Arthritis Res. Ther.* 17 (1), 1–11. doi:10.1186/s13075-015-0676-4

Thorp, L. E., Sumner, D. R., Block, J. A., Moisio, K. C., Shott, S., and Wimmer, M. A. (2006). Knee joint loading differs in individuals with mild compared with moderate medial knee osteoarthritis. *Arthritis Rheum.* 54 (12), 3842–3849. doi:10.1002/art.22247

Uhlrich, S. D., Silder, A., Beaupre, G. S., Shull, P. B., and Delp, S. L. (2018). Subject-specific toe-in or toe-out gait modifications reduce the larger knee adduction moment peak more than a non-personalized approach. *J. Biomech.* 66, 103–110. doi:10.1016/j.jbiomech.2017.11.003

Ulrich, B., Cosendey, K., Jolles, B. M., and Favre, J. (2020). Decreasing the ambulatory knee adduction moment without increasing the knee flexion moment individually through modifications in footprint parameters: A feasibility study for a dual kinetic change in healthy subjects. *J. Biomech.* 111, e110004. doi:10.1016/j.jbiomech.2020.110004

Ulrich, B. (2021). *Gait modifications for medial knee osteoarthritis*. [Lausanne, Switzerland]: University of Lausanne. [Doctoral thesis].

Wallace, I. J., Worthington, S., Felson, D. T., Jurmain, R. D., Wren, K. T., Maijanen, H., et al. (2017). Knee osteoarthritis has doubled in prevalence since the mid-20th century. *Proc. Natl. Acad. Sci. U. S. A.* 114 (35), 9332–9336. doi:10.1073/pnas.1703856114

Walter, J. P., D'Lima, D. D., Colwell, C. W., Jr, and Fregly, B. J. (2010). Decreased knee adduction moment does not guarantee decreased medial contact force during gait. *J. Orthop. Res.* 28 (10), 1348–1354. doi:10.1002/jor.21142

Weidow, J., Tranberg, R., Saari, T., and Kärrholm, J. (2006). Hip and knee joint rotations differ between patients with medial and lateral knee osteoarthritis: Gait analysis of 30 patients and 15 controls. *J. Orthop. Res.* 24 (9), 1890–1899. doi:10.1002/jor.20194

Weir, J. P. (2005). Quantifying test-retest reliability using the intraclass correlation coefficient and the SEM. *J. Strength Cond. Res.* 19 (1), 231–240. doi:10.1519/15184.1

Zabala, M. E., Favre, J., Scanlan, S. F., Donahue, J., and Andriacchi, T. P. (2013). Three-dimensional knee moments of ACL reconstructed and control subjects during gait, stair ascent, and stair descent. *J. Biomech.* 46 (3), 515–520. doi:10.1016/j.jbiomech.2012.10.010

frontiers | Frontiers in Bioengineering and Biotechnology

TYPE Brief Research Report
PUBLISHED 16 June 2023
DOI 10.3389/fbioe.2023.1190712

OPEN ACCESS

EDITED BY
Juan Ramírez,
National University of Colombia,
Medellin, Colombia

REVIEWED BY
Vasilios (Bill) Baltzopoulos, Liverpool John Moores University, United Kingdom
Willians Fernando Vieira,
Massachusetts General Hospital and Harvard Medical School, United States
Abdelwahed Barkaoui,
International University of Rabat, Morocco

*CORRESPONDENCE
S. van Drongelen,
stefan.vandrongelen@kgu.de

†PRESENT ADDRESS
J. Holder, University of Salzburg, Department of Sport and Exercise Science, Salzburg, Austria

RECEIVED 21 March 2023
ACCEPTED 06 June 2023
PUBLISHED 16 June 2023

CITATION
van Drongelen S, Holder J and Stief F (2023), Lower limb joint loading in patients with unilateral hip osteoarthritis during bipedal stance and the effect of total hip replacement.
Front. Bioeng. Biotechnol. 11:1190712.
doi: 10.3389/fbioe.2023.1190712

Lower limb joint loading in patients with unilateral hip osteoarthritis during bipedal stance and the effect of total hip replacement

S. van Drongelen[1,2]*, J. Holder[1†] and F. Stief[1,2]

[1]Department of Orthopedics (Friedrichsheim), University Hospital Frankfurt, Goethe University Frankfurt, Frankfurt, Germany, [2]Dr. Rolf M. Schwiete Research Unit for Osteoarthritis, Department of Orthopedics (Friedrichsheim), University Hospital Frankfurt, Goethe University Frankfurt, Frankfurt, Germany

Osteoarthritis of the hip is a common condition that affects older adults. Total hip replacement is the end-stage treatment to relief pain and improve joint function. Little is known about the mechanical load distribution during the activity of bipedal stance, which is an important daily activity for older adults who need to rest more frequently. This study investigated the distribution of the hip and knee joint moments during bipedal stance in patients with unilateral hip osteoarthritis and how the distribution changed 1 year after total hip replacement. Kinematic and kinetic data from bipedal stance were recorded. External hip and knee adduction moments were calculated and load distribution over both limbs was calculated using the symmetry angle. Preoperatively, the non-affected limb carried 10% more body weight than the affected limb when standing on two legs. Moreover, the mean external hip and knee adduction moments of the non-affected limb were increased compared to the affected limb. At follow-up no significant differences were observed between the patients' limbs. Preoperative and postoperative changes in hip adduction moment were mainly explained by the combination of the vertical ground reaction force and the hip adduction angle. Stance width also explained changes in the hip and knee adduction moments of the affected leg. Furthermore, as with walking, bipedal standing also showed an asymmetric mechanical load distribution in patients with unilateral hip osteoarthritis. Overall, the findings suggest the need for preventive therapy concepts that focus not only on walking but also on optimizing stance towards a balanced load distribution of both legs.

KEYWORDS

posture, ground reaction forces, external hip adduction moment, external knee adduction moment, symmetry angle

1 Introduction

Osteoarthritis (OA) is a leading cause of disability and imposes societal costs in older adults (Hunter and Bierma-Zeinstra, 2019). It is even more prevalent than in previous decades due to an ageing and increasingly obese population. Primary total hip replacement (THR) is the standard treatment for end-stage hip OA, providing pain relief and improved joint function. The demand and volume of this procedure is predicted to increase in the

coming years due to higher demand for improved mobility and quality of life in the aging population (Maradit Kremers et al., 2015).

In patients with unilateral hip OA, a pain-induced protective walking pattern results in uneven loading of the lower extremities. Pathological moments in the hip and knee joint during walking have been noted (Hurwitz et al., 1997; Shakoor et al., 2011; Schmidt et al., 2017). Despite good clinical-functional outcomes (Neuprez et al., 2020), some studies found that gait kinematics (i.e., reduced hip extension) and kinetics (i.e., lower knee adduction moments) did not normalize after THR (Foucher et al., 2007; Stief et al., 2018). The development of OA in the hip joint has been shown to be related to increased joint loading during walking (Hurwitz et al., 2001). In this context, the external hip adduction moment (HAM) has been identified as one of the most important determinants of hip contact force and joint loading (Lenaerts et al., 2009; Wesseling et al., 2015). Peak external knee adduction moments (KAM) are associated with the rate of progression and severity of knee OA (Sharma et al., 1998; Miyazaki et al., 2002). Patients with hip OA have also been shown to have altered lower limb joint mechanics during sit-to-stand tasks (Eitzen et al., 2014; Abujaber et al., 2015) and stair climbing (Queen et al., 2015), suggesting that these activities may contribute to the development of OA in adjacent joints (Jungmann et al., 2015; Joseph et al., 2016).

Although standing is an important activity of daily living (Morlock et al., 2001), there is limited information on lower extremity mechanical load distribution in patients with unilateral hip OA. It appears that patients with unilateral hip OA shift more weight to the non-affected leg during standing (Talis et al., 2008; Miura et al., 2018). However, in these studies, leg loading is expressed only as asymmetry between the legs or as uneven distribution of vertical ground reaction force between the legs. There is no information on the hip or knee joint moments of the affected and non-affected leg, nor is there detailed information on what factors influence asymmetrical leg loading. When walking on flat surfaces, patients with unilateral hip OA use compensatory strategies (i.e., greater foot progression angle and increased lateral trunk displacement toward the affected side) that directly affect HAM and KAM (Schmidt et al., 2017). It is therefore reasonable to assume that some of these compensatory strategies also occur during bipedal standing. If this is the case, the symmetry of lower limb joint moments may also be affected. Characteristic gait changes to unload the affected limb include increased lateral trunk displacement (LTD) toward the affected side (Reininga et al., 2012), altered foot progression angle (FPA) at the affected limb (Müller et al., 2012) and increased stride width (Stief et al., 2021). Information on these compensatory strategies for bipedal standing is missing, although their effects on lower limb joint moments may have implications for rehabilitation of patients with hip OA. Rehabilitation focusing on motor control to move and stand more symmetrically could be applied to patients with hip OA and after THR to modify motor strategies (Boonstra et al., 2011). This is in line with Hunter and Bierma-Zeinstra (2019), who stated that management of OA should shift from reactive to proactive and preventive measures.

The aim of the present study was to investigate load distribution before THR and the improvement in load distribution after THR during bipedal standing in patients with unilateral hip OA and finally to examine whether kinematic and kinetic variables in general and compensatory strategies in particular correlate with significant changes in joint loading. It was expected that before THR, the non-affected limb would experience greater lower limb joint moments than the affected limb in patients with unilateral hip OA. Furthermore, it was hypothesized that joint loading asymmetries in patients with unilateral hip OA would differ from those in a healthy control (HC) group and would be due in part to changes in kinematic and kinetic variables.

2 Methods

In the present study, data from patients who had participated in previous prospective studies in our clinic were analyzed (Schmidt et al., 2017; Stief et al., 2018; van Drongelen et al., 2019; van Drongelen et al., 2020). In these studies, gait analysis and radiography were performed preoperatively and 1 year after THR. The complete protocol for these studies has been described previously (Stief et al., 2018; van Drongelen et al., 2019). In addition, data from HCs with a similar age distribution that were available in our database were used for comparison.

2.1 Participants

Symptomatic patients with radiologically confirmed unilateral hip OA (Kellgren-Lawrence > 2) between the age of 30 and 80 years, who were scheduled for and received THR were considered for inclusion. Exclusion criteria were: OA of lower limb joints other than the affected hip, chronic or neuromuscular diseases, history of orthopedic surgery of the lower extremities, and use of assistance devices during walking. Only data from patients who had three valid trials of two-leg-standing measured during gait analysis in the week before and 1 year after surgery were included. Patients with a body mass index (BMI) > 35 kgm^{-2} were excluded from the analyses. Finally, data from 43 patients were included in the study (Table 1).

Seventeen participants with a similar age distribution were included as a HC collective for comparison (Table 1). Control participants were included if they had no history of orthopedic surgeries or chronic and neuromuscular disease. All patients and HCs provided written informed consent prior to participation in the original studies. The protocol was approved by the Medical Ethics Committee of the Department of Medicine, Goethe University Frankfurt (reference number 122/14 and 497/15).

2.2 Bipedal standing

An 8-camera Vicon System operating at 200 Hz (8MX T10 cameras, VICON Motion Systems, Oxford, United Kingdom) collected kinematic data, synchronously with the two force plates (Advanced Mechanical Technology, Inc., Watertown, MA, United States). Reflective markers (14 mm) were placed on anatomical landmarks according to the standardized Plug-in-Gait marker set (Kadaba et al., 1990): pelvis (anterior and posterior superior iliac spines), upper leg (lateral thigh and lateral femoral condyle), lower leg (lateral shank and lateral malleolus), foot (heel and toe), shoulder (acromion) and thorax (sternum and spine). To improve the reliability and accuracy of the gait data in the frontal plane, additional markers were placed on the medial malleolus, medial femoral condyle and greater trochanter (Stief

TABLE 1 Anthropometric data, kinetic data and kinematic data of patients with unilateral hip osteoarthritis and healthy controls.

	Healthy controls	Hip OA patients preoperatively		Hip OA patients postoperatively	
Anthropometrics					
Number of participants	17	43		43	
Males/Females	8/9	24/19		24/19	
Age (years)	56.0 (52.5–67.0)	63.0 (53.0–69.0)†		64.0 (54.0–70.0)	
Body mass (kg)	68.8 ± 13.2	80.8 ± 11.7*†		81.9 ± 12.0*	
Body height (m)	1.70 ± 0.10	1.72 ± 0.08		1.72 ± 0.08	
BMI (kgm^{-2})	23.7 ± 2.8	27.3 ± 3.6*†		27.7 ± 3.7*	
Kinetics		Affected	Non-affected	Affected	Non-affected
vGRF (Nkg^{-1})	4.95 ± 0.37	4.70 ± 0.52#	5.20 ± 0.52	4.91 ± 0.42	4.98 ± 0.44
HAM ($Nmkg^{-1}$)	0.11 ± 0.08	0.10 ± 0.10#	0.16 ± 0.13	0.15 ± 0.11	0.14 ± 0.10
KAM ($Nmkg^{-1}$)	0.01 ± 0.05	−0.01 ± 0.05#	0.02 ± 0.09	0.03 ± 0.06	0.02 ± 0.07
Kinematics		Affected	Non-affected	Affected	Non-affected
Lateral trunk displacement (°)	−0.4 ± 2.1	−0.4 ± 2.3		−0.1 ± 2.0	
Pelvic obliquity (°)	0.03 ± 1.0	−0.2 ± 2.3†		0.6 ± 1.9	
Hip abduction/adduction (°)	1.2 ± 2.0	2.0 ± 3.7	2.3 ± 4.4†	2.3 ± 3.0	1.2 ± 4.0
Knee flexion/extension (°)	2.0 (−1.8–4.3)	4.5 (0.9–8.0)†	0.6 (−2.4–5.8)†	1.6 (−1.2–3.9)	−0.3 (−3.2–3.1)
Ankle plantar/dorsiflexion (°)	5.9 (4.4–8.3)	5.1 (1.9–8.1)	5.3 (3.3–6.9)	5.1 (1.9–7.0)	5.1 (2.2–7.5)
Foot progression angle (°)	−8.4 (−11.3–−7.0)	−10.0 (−14.3–−7.9)†	−9.4 (−14.7–−5.4)	−8.8 (−11.5–−6.0)	−8.4 (−11.1–−6.1)

Values are mean values ± standard deviation, or median and interquartile range in parenthesis. The comparison between patients and healthy controls was tested with a chi-squared test (sex), Mann-Whitney test (age) and independent-sample *t*-tests (weight, height and body mass index (BMI)). Kinetic and kinematic differences between limbs were tested with dependent *t*-tests or Wilcoxon signed rank tests.

* Significant difference between patients and healthy controls.

Significant difference between affected and non-affected limb.

† Significant difference between pre and postoperative values.

Negative values indicate ipsilateral thorax displacement, ipsilateral pelvic drop, hip abduction, knee extension, plantarflexion and external foot progression angle.

Abbreviations: OA, osteoarthritis; vGRF, vertical Ground Reaction Force; HAM, external hip adduction moment; KAM, external knee adduction moment.

et al., 2013). The hip joint center was determined using a geometrical prediction method by Harrington (Harrington et al., 2007).

For the measurement, all participants were instructed to stand comfortably (barefoot) on their two legs for 10 s, with each foot resting on one of two force plates and arms at their sides. To achieve a natural balanced posture, no further instructions were given except when the thigh and pelvic markers were not visible, participants were asked to abduct their arms slightly.

Kinematic and kinetic data were exported to MATLAB for further analysis (version R2022a, The Mathworks Inc., Natick, MA, United States). The following kinematic outcome variables, based on the characteristic gait strategies (Schmidt et al., 2017), were extracted (Baker et al., 2018): mean LTD, mean pelvic obliquity, mean hip adduction, mean knee flexion/extension angle, mean ankle plantar/dorsiflexion angle and mean FPA. Here, negative LTDs refer to lateral displacements of the trunk with respect to the corresponding limb. Pelvic obliquity was negative when the pelvis dropped with respect to the corresponding limb. Adduction of the hip in the frontal plane was defined as a positive angle. Positive values for the knee indicated flexed knees, while negative values for the ankle indicated a plantar flexed ankle joint. FPA was defined as the angle of the long axis of the foot segment relative to the global coordinate system. Negative FPAs here indicate externally rotated feet. External joint moments were calculated from the force plate data and the mathematically derived joint centers by inverse dynamics analysis (Davis et al., 1991). Mean vertical ground reaction forces (vGRFs) of each limb and mean joint moments in the frontal plane for the hip and the knee joint (HAMs, KAMs) were normalized by body mass. Stance width was calculated as the distance between the ankle joint centers.

2.3 Symmetry angle

To quantify inter-limb symmetry with respect to vGRFs, HAMs, and KAMs, the symmetry angle (SA) was calculated using the following equation from Zifchock et al. (2008).

$$SA = \left| \frac{(45° - \arctan(X_L / X_R))}{90°} \right| \times 100\%$$

Where XL and XR represent left/affected and right/non-affected limb values, respectively. SA values of 0% indicate perfect symmetry. SA values of 100% indicate two values that are opposite but equal in

magnitude. The direction of asymmetry (indicated by a positive or negative value) was ignored and absolute values were used (Zifchock et al., 2008).

2.4 Statistical analyses

Statistical analyses were performed using SPSS Statistics (IBM SPSS Statistics for Windows, version 29, IBM Corp., Armonk, NY, United States). Shapiro-Wilk tests and visual inspection of Q-Q plots were used to check for normal distribution. Normally distributed parameters were compared with respect to differences between limbs (dependent *t*-test), groups (independent *t*-tests), and over time (dependent *t*-test). When data were not normally distributed, parameters were compared using Wilcoxon signed rank tests (differences between limbs and over time) and Mann-Whitney U-Tests (differences between groups). A chi-squared test was used to compare the sex distribution between groups.

The left and right sides of the HCs were randomized to a single-leg HC group for comparison with patients. Because significant HAM and KAM changes were expected in patients with unilateral hip OA, regression analysis was performed to determine predictor variables that best explained these changes. Pearson correlation coefficients were calculated to determine significant correlations between kinematic and kinetic predictor variables and HAMs and KAMs, respectively (Bortz, 1999). A stepwise multiple regression analysis was then performed if two or more parameters significantly correlated with the frontal external hip and knee joint moments. Secondary, a forward multiple regression analysis was performed using only the known compensatory strategy parameters (LTD, FPA and stance width). The level of significance was $\alpha = 0.05$.

3 Results

Participant demographics are listed in Table 1. Patients were measured preoperatively and at a mean follow-up of 12.6 ± 2.5 months after surgery. The patients had significantly higher body mass and BMI compared to HCs, at preoperatory measure (80.8 vs. 68.8 kg, $p < 0.001$; 27.3 vs. 23.7 kgm^{-2}; $p < 0.001$, respectively) and during follow-up (81.9 vs. 68.8 kg, $p < 0.001$; 27.7 vs. 23.7 kgm^{-2}; $p < 0.001$, respectively). No differences were observed in age (preoperatory 63.0 vs. 56.0 years/postoperatory 64.0 vs. 56.0 years, $p > 0.237$), height (1.72 vs. 1.70 m, $p > 0.379$) or sex distribution (24 males and 19 females vs. 8 males and 9 females, $p = 0.540$) between the patients and HCs (Table 1). HCs stood with a stance width of 18.3 ± 4.3 cm, whereas patients stood with a stance width of 20.5 ± 4.3 cm before surgery and 20.1 ± 4.3 cm after surgery. The differences between HCs and patients were not significant ($p > 0.074$). Age ($p < 0.001$), body mass ($p = 0.002$) and BMI ($p = 0.003$) were significantly higher when postoperative anthropometrics were compared with preoperative values.

3.1 Kinetics and symmetry

Preoperatively, the non-affected limb carried more body weight than the affected limb in patients with unilateral hip OA ($p = 0.003$), as expressed by the vGRF (Table 1). In addition, greater HAMs ($p = 0.007$) and KAMs ($p = 0.018$) were found for the non-affected limb than for the affected limb. Postoperatively, no differences were found between the affected and non-affected sides (Table 1). Furthermore, no differences were found between HCs and patients pre- or postoperatively.

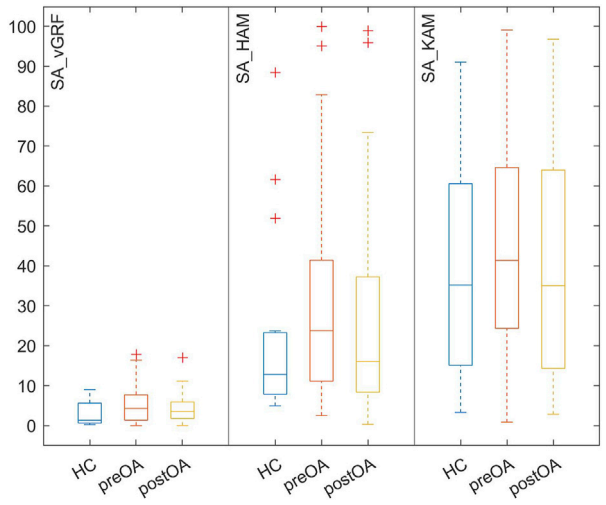

FIGURE 1
Box-and-whisker-plots of the absolute angles of symmetry (SA) of the vertical ground reaction force (vGRF) and external frontal hip (HAM) and knee (KAM) joint moments in healthy controls (HCs) and patients with hip osteoarthritis both preoperatively (preOA) and postoperatively (postOA).

During bipedal standing, no significantly increased symmetry angles (vGRF, HAM and KAM) were observed in the patients with unilateral hip OA compared with the HCs (Figure 1). Preoperatively, the symmetry angles were all higher for the patients and postoperatively the values all became smaller, but the differences between the patients and HCs never reached significance.

3.2 Kinematics

When considering the kinematics of patients with hip OA while standing on two legs (Table 1), it was found that the affected limb showed no difference from the non-affected limb both preoperatively and postoperatively. No differences were observed between HCs and patients, either preoperatively or postoperatively. Small significant changes were seen in the preoperative to postoperative comparison. The affected foot was less externally rotated, and the knees were less flexed or even extended after THR. In addition, the pelvis was no longer dropped to the affected side; postoperatively the pelvis dropped to the non-affected side with a corresponding change in hip adduction angle on the non-affected side.

3.3 Correlations and regression

All significant correlations to joint loading parameters (HAM and KAM) are shown in Table 2. Preoperatively, hip adduction angle

TABLE 2 Results from the correlation analyses.

Dependent variable preoperative	Covariate	*r*	*p*-value
HAM affected leg	hip adduction	0.586	<0.001
	vGRF	0.456	0.002
	stance width	−0.443	0.003
HAM non-affected leg	hip adduction	0.635	<0.001
	vGRF	0.506	<0.001
KAM affected leg	stance width	−0.576	<0.001
KAM non-affected leg	vGRF	0.539	<0.001
Dependent variable postoperative	**Covariate**	***r***	***p*-value**
HAM affected leg	hip adduction	0.588	<0.001
	vGRF	0.369	0.015
	stance width	−0.545	<0.001
	ankle flexion	0.353	0.020
HAM non-affected leg	hip adduction	0.642	<0.001
	stance width	−0.435	0.004
KAM affected leg	knee flexion	−0.353	0.020
	stance width	−0.409	0.006
KAM non-affected leg	knee flexion	−0.366	0.016

Abbreviations: HAM, external hip adduction moment; KAM, external knee adduction moment; vGRF, vertical Ground Reaction Force.

and vGRF were significantly correlated with HAM in both the affected and non-affected limb. A significant correlation with stance width was also found for the affected limb. A significant correlation was found between KAM and stance width in the affected limb, and between KAM and vGRF in the non-affected limb.

Postoperatively, the same significant correlations with HAM were found for the affected limb (hip adduction angle, vGRF and stance width). There was also a significant correlation with the ankle plantarflexion angle. For the non-affected limb, significant correlations with HAM were found for hip adduction angle and stance width. KAM significantly correlated with knee flexion for both the affected and the non-affected limb. A significant correlation with stance width was also found for the affected leg.

Preoperative regression analysis revealed that changes in hip adduction angle and vGRFs explained 42% of HAM changes (R^2 = 0.418; F = 14.360; $p < 0.001$) for the affected limb. Stance width did not significantly improve the outcome using this model (ΔR^2 = 0.037, ΔF = 2.673, p = 0.110). In the non-affected limb changes in hip adduction angle and vGRFs explained 61% of HAM changes (R^2 = 0.612; F = 31.569; $p < 0.001$).

Postoperatively, the regression analysis yielded a model in which hip adduction angle and vGRF explained 42% of HAM alterations (R^2 = 0.417; F = 14.310; $p < 0.001$). Adding stance width (likely due to relatively high correlation to hip adduction) and ankle flexion to the model did not result in a significant increase in the percentage of variance in HAM predicted by the model. For the non-affected limb, hip adduction angle explained 41% of the changes in HAM (R^2 = 0.413; F = 28.808; $p < 0.001$), and adding stance width did not significantly increase the outcome using this model (ΔR^2 = 0.014, ΔF = 1.004, p = 0.322). For the affected leg only 16% of the changes in KAM were explained by the changes in stance width (R^2 = 0.167; F = 8.245; p = 0.006), the inclusion of the knee flexion angle did not significantly increase the percentage of variance in KAM predicted by the model (ΔR^2 = 0.062, ΔF = 3.198, p = 0081).

Multiple regression analysis with only known parameters of the compensatory strategies showed that only stance width explained part of the variation of the external joint moments in the frontal plane (see Table 2). The other parameters (LTD and FPA) did not significantly improve the outcome using any of the models.

4 Discussion

Altered joint moments in individuals with unilateral hip OA may contribute to the development of OA in adjacent joints (Jungmann et al., 2015). To identify possible abnormal joint moments in the knee and hip joint during standing, this study quantified weight distribution and lower limb joint moments in individuals with unilateral hip OA during bipedal standing before (preoperatively) and 1 year after THR (postoperatively). The results of the current study suggest that weight distribution favoring the affected limb and few kinematic adjustments in the affected limb enable patients with unilateral hip OA to stand comfortably while

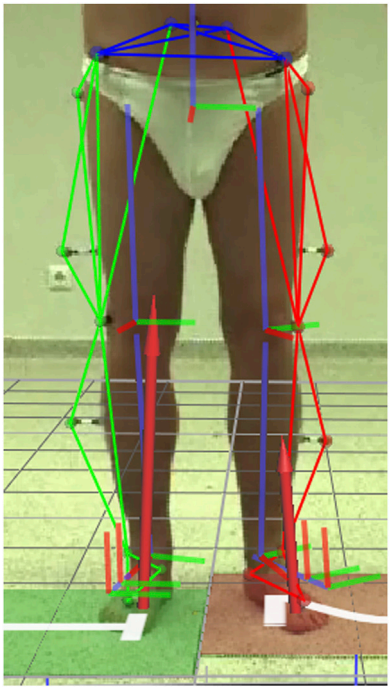

FIGURE 2
Patient with unilateral hip osteoarthritis (preoperatively) in a standing position with a frequently observed extended external foot rotation on the affected (left) side. Kinematic segments and ground reaction force are superimposed on the image.

standing on two legs before THR. At a mean follow-up of 12.6 months, asymmetries in joint loading were no longer present.

4.1 Kinetics and symmetry

To avoid pain caused by the affected hip, individuals with unilateral hip OA appear to adopt an altered bipedal standing position (Figure 2), resulting in a redistribution of lower limb joint moments. As previously noted, the non-affected limb carried more body weight than the affected limb in patients with unilateral hip OA (Talis et al., 2008; Miura et al., 2018). The non-affected limb experienced 38% greater HAMs than the affected limb, indicating a pathological loading of the hip joint. KAM tended to be a valgus moment in the affected limb, which denoted that the vertical GRF vector was slightly lateral from the estimated knee joint center rather than slightly medial, which has been shown to be physiological during walking (Cerny, 1984). During walking, patients with unilateral hip OA exhibited pathological peak external KAM and HAM in the non-affected limb (Hurwitz et al., 1997; Shakoor et al., 2011; Schmidt et al., 2017; Stief et al., 2018). Therefore, it has been suggested that the non-affected limb is at higher risk for developing OA in these joints (Hurwitz et al., 2001). Comparable results have been obtained during sit-to-stand tasks (Eitzen et al., 2014; Abujaber et al., 2015) and stair climbing (Queen et al., 2015).

Miura et al. (2018) showed that the load distribution of the operated leg was restored as early as 1 month after surgery. In the present study it was found that the load distribution and corresponding joint moments had no asymmetries between limbs at a follow-up of 12.6 months on average. Postoperative joint moments were significantly different from preoperative values [i.e., HAM appeared to be 33% higher in the affected leg after surgery (0.15 vs. 0.10 $Nmkg^{-1}$)]. No differences were observed compared with HCs. Studies also found increased HAM during walking compared to HCs (Stief et al., 2018), although in general, peak HAM values were usually lower but not significantly reduced after THR compared to HCs (Ewen et al., 2012). The increase in HAM may be due to the absence of pain and the resultant increase in vGRF after THR. However, whether other factors such as an altered moment arm due to repositioning of the hip joint center during THR surgery play a role requires further investigation.

4.2 Kinematics and correlations

In this study, it was hypothesized that patients with unilateral hip OA adopt a standing position that is significantly different from HCs to reduce the moments in the affected hip joint. However, HAMs in the affected limb were not reduced compared to normal, which partly explains the lack of significant kinematic changes compared with HCs. For example, during walking, patients with unilateral hip OA significantly bend their trunk toward the affected side (Bennett et al., 2007; Reininga et al., 2012). Consequently, HAM in the affected limb was significantly reduced during gait (Hurwitz et al., 1997; Foucher et al., 2007; Shakoor et al., 2011; Foucher and Wimmer, 2012). When standing on two legs, patients with hip OA showed minimal LTD to the affected side, which was not significantly different from HCs. Bending of the trunk towards the affected limb during bipedal standing may be detrimental in terms of postural stability or even non-feasible while at the same time the non-affected limb carries proportionally more body weight. Preoperatively, the foot of the affected limb was significantly more externally rotated during bipedal stance (Figure 2; Table 1) while the knee was more flexed (Table 1) when compared with the postoperative standing position, but not when compared with HCs. Although these kinematic changes during standing did not relate to changes in HAM, they appear to be adopted by patients with unilateral hip OA to unload the affected limb in terms of body weight distribution. Increased FPAs and knee flexion changes are typical of patients with unilateral hip OA during walking (Bennett et al., 2007; Müller et al., 2012; Schmitt et al., 2015). Previous studies on HCs have shown that large changes in LTD (Mündermann et al., 2008) and FPA (Andrews et al., 1996) are required to significantly reduce KAMs during walking. Hip adduction and plantar/dorsiflexion angle of the ankle are known control variables of sway in the medio-lateral and anterior-posterior directions, respectively (Weaver et al., 2017). Therefore, it makes sense that these variables are predictors of the hip joint moments during stance. In the present study, no kinematic differences were found between the affected and non-affected limb. The relatively small kinematic changes observed in the affected limb may be the reason why kinematics did not explain the KAM alterations preoperatively. It appears that vGRF, hip adduction and knee flexion angle explain most of the variance in HAM and KAM. However, stance width also showed correlations to HAM and KAM and since increased stance

width influences hip adduction angle, stance width indirectly contributes to explain the variance. When only compensation parameters were considered, stance width was the only parameter that mattered: stance width explained 18.9%–29.7% of the variance of HAM and 16.7%–33.2% of the variance of KAM (Table 2). From walking it is known that increasing stride width reduces knee and hip joint moments in the frontal plane (Stief et al., 2021), so increasing stance width could be a simple adaptation with a reducing effect on knee and hip joint moments in the frontal plane during standing.

4.3 Limitations

This study should be considered in the context of its limitations. Only variables that have been shown to correlate with external KAM and HAM during walking were examined. However, it is likely that patients with unilateral hip OA modify additional kinematic and kinetic parameters to stand comfortably on two legs. In addition, factors such as pain, leg length discrepancy, and pelvic or spinopelvic malalignment have been suggested to contribute toasymmetric loading (Miura et al., 2018) and were not investigated in the current study.

KAM was found to be very small because the GRF was centered on the center of rotation of the knee joint, in contrast to gait where the GRF is directed medially from the center of rotation of the knee joint (Cerny, 1984). Therefore, KAM and consequently the SA for KAM may not be the best parameters for assessing knee loading during bipedal standing. Although knee and hip joint moments in the frontal plane during dynamic activities have been widely used as an indicator of knee joint loading and to characterize intrinsic compressive loading, this parameter itself may not be sufficient to predict the mechanical properties of the cartilage, especially during standing. Therefore, future studies are needed to analyze possible relationships between knee and hip joint loading parameters and compressive properties of joint cartilage, i.e., a combination of musculoskeletal and finite element models (Harlaar et al., 2022).

5 Conclusion

In summary, our elderly patients with unilateral hip OA adopted a standing position preoperatively in which foot progression (more externally rotated) and knee flexion (more flexed) were adapted in the affected limb compared to the postoperative standing position. However, these kinematic adaptations did not explain the lower HAM and KAM in the affected limb compared with the non-affected limb. The non-affected limb experienced 38% greater HAMs than the affected limb, indicating pathological loading of the hip joint during normal standing. Postoperatively, limb load distribution and corresponding joint loads normalized, comparable to findings during walking. The altered preoperative joint moments were mainly caused by a disproportionate weight distribution, expressed by the vGRF, in favor of the affected limb. Of the compensation strategy parameters, stance width showed moderate to high correlations with HAM and KAM and also explained up to 33% of the variance. Therefore, in patients with hip OA, interdisciplinary preventive therapy concepts in which stance width could play a role should be considered to improve the loading situation.

Data availability statement

The raw data supporting the conclusion of this article will be made available by the authors, without undue reservation.

Ethics statement

The studies involving human participants were reviewed and approved by Medical Ethics Committee of the Faculty of Medicine of the Goethe University Frankfurt. The patients/participants provided their written informed consent to participate in this study. Written informed consent was obtained from the individual(s) for the publication of any potentially identifiable images or data included in this article.

Author contributions

SD and FS were involved in the design of the study. SD carried out the data analysis. SD, JH, and FS were involved in the interpretation and discussion of the results. SD took the lead in writing the manuscript. All authors contributed to the article and approved the submitted version.

Funding

This work was supported by the German Research Foundation (DFG) (Project number: 492686079). Sponsor had no involvement in this article.

Acknowledgments

The authors would like to thank Hanna Kaldowski and André Schmidt for their help with the data collection and data preparation.

Conflict of interest

The authors declare that the research was conducted in the absence of any commercial or financial relationships that could be construed as a potential conflict of interest.

Publisher's note

References

Abujaber, S. B., Marmon, A. R., Pozzi, F., Rubano, J. J., and Zeni, J. A., Jr. (2015). Sit-to-stand biomechanics before and after total hip arthroplasty. *J. Arthroplasty* 30, 2027–2033. doi:10.1016/j.arth.2015.05.024

Andrews, M., Noyes, F. R., Hewett, T. E., and Andriacchi, T. P. (1996). Lower limb alignment and foot angle are related to stance phase knee adduction in normal subjects: A critical analysis of the reliability of gait analysis data. *J. Orthop. Res.* 14, 289–295. doi:10.1002/jor.1100140218

Baker, R., Leboeuf, F., Reay, J., and Sangeux, M. (2018). "The conventional gait model - success and limitations," in *Handbook of human motion*. Editors B. Müller and S. I. Wolf (Cham: Springer International Publishing), 1–19.

Bennett, D., Ogonda, L., Elliott, D., Humphreys, L., Lawlor, M., and Beverland, D. (2007). Comparison of immediate postoperative walking ability in patients receiving minimally invasive and standard-incision hip arthroplasty: A prospective blinded study. *J. Arthroplasty* 22, 490–495. doi:10.1016/j.arth.2006.02.173

Boonstra, M. C., Schreurs, B. W., and Verdonschot, N. (2011). The sit-to-stand movement: Differences in performance between patients after primary total hip arthroplasty and revision total hip arthroplasty with acetabular bone impaction grafting. *Phys. Ther.* 91, 547–554. doi:10.2522/ptj.20090376

Bortz, J. (1999). *Statistik für Sozialwissenschaftler*. Berlin: Springer.

Cerny, K. (1984). Pathomechanics of stance. *Phys. Ther.* 64, 1851–1859. doi:10.1093/ptj/64.12.1851

Davis, R. B., Õunpuu, S., Tyburski, D., and Gage, J. R. (1991). A gait analysis data collection and reduction technique. *Hum. Mov. Sci.* 10, 575–587. doi:10.1016/0167-9457(91)90046-z

Eitzen, I., Fernandes, L., Nordsletten, L., Snyder-Mackler, L., and Risberg, M. A. (2014). Weight-bearing asymmetries during sit-to-stand in patients with mild-to-moderate hip osteoarthritis. *Gait Posture* 39, 683–688. doi:10.1016/j.gaitpost.2013.09.010

Ewen, A. M., Stewart, S., St Clair Gibson, A., Kashyap, S. N., and Caplan, N. (2012). Post-operative gait analysis in total hip replacement patients-a review of current literature and meta-analysis. *Gait Posture* 36, 1–6. doi:10.1016/j.gaitpost.2011.12.024

Foucher, K. C., Hurwitz, D. E., and Wimmer, M. A. (2007). Preoperative gait adaptations persist one year after surgery in clinically well-functioning total hip replacement patients. *J. Biomech.* 40, 3432–3437. doi:10.1016/j.jbiomech.2007.05.020

Foucher, K. C., and Wimmer, M. A. (2012). Contralateral hip and knee gait biomechanics are unchanged by total hip replacement for unilateral hip osteoarthritis. *Gait Posture* 35, 61–65. doi:10.1016/j.gaitpost.2011.08.006

Harlaar, J., Macri, E. M., and Wesseling, M. (2022). Osteoarthritis year in review 2021: Mechanics. *Osteoarthr. Cartil.* 30, 663–670. doi:10.1016/j.joca.2021.12.012

Harrington, M. E., Zavatsky, A. B., Lawson, S. E., Yuan, Z., and Theologis, T. N. (2007). Prediction of the hip joint centre in adults, children, and patients with cerebral palsy based on magnetic resonance imaging. *J. Biomech.* 40, 595–602. doi:10.1016/j.jbiomech.2006.02.003

Hunter, D. J., and Bierma-Zeinstra, S. (2019). Osteoarthritis. *Lancet* 393, 1745–1759. doi:10.1016/s0140-6736(19)30417-9

Hurwitz, D. E., Hulet, C. H., Andriacchi, T. P., Rosenberg, A. G., and Galante, J. O. (1997). Gait compensations in patients with osteoarthritis of the hip and their relationship to pain and passive hip motion. *J. Orthop. Res.* 15, 629–635. doi:10.1002/jor.1100150421

Hurwitz, D. E., Sumner, D. R., and Block, J. A. (2001). Bone density, dynamic joint loading and joint degeneration. *Cells Tissues Organs* 169, 201–209. doi:10.1159/000047883

Joseph, G. B., Hilton, J. F., Jungmann, P. M., Lynch, J. A., Lane, N. E., Liu, F., et al. (2016). Do persons with asymmetric hip pain or radiographic hip OA have worse pain and structure outcomes in the knee opposite the more affected hip? Data from the Osteoarthritis Initiative. *Osteoarthr. Cartil.* 24, 427–435. doi:10.1016/j.joca.2015.10.001

Jungmann, P. M., Nevitt, M. C., Baum, T., Liebl, H., Nardo, L., Liu, F., et al. (2015). Relationship of unilateral total hip arthroplasty (THA) to contralateral and ipsilateral knee joint degeneration - a longitudinal 3T MRI study from the Osteoarthritis Initiative (OAI). *Osteoarthr. Cartil.* 23, 1144–1153. doi:10.1016/j.joca.2015.03.022

Kadaba, M. P., Ramakrishnan, H. K., and Wootten, M. E. (1990). Measurement of lower extremity kinematics during level walking. *J. Orthop. Res.* 8, 383–392. doi:10.1002/jor.1100080310

Lenaerts, G., Mulier, M., Spaepen, A., Van der Perre, G., and Jonkers, I. (2009). Aberrant pelvis and hip kinematics impair hip loading before and after total hip replacement. *Gait Posture* 30, 296–302. doi:10.1016/j.gaitpost.2009.05.016

Maradit Kremers, H., Larson, D. R., Crowson, C. S., Kremers, W. K., Washington, R. E., Steiner, C. A., et al. (2015). Prevalence of total hip and knee replacement in the United States. *J. Bone Jt. Surg. Am.* 97, 1386–1397. doi:10.2106/jbjs.n.01141

Miura, N., Tagomori, K., Ikutomo, H., Nakagawa, N., and Masuhara, K. (2018). Leg loading during quiet standing and sit-to-stand movement for one year after total hip arthroplasty. *Physiother. Theory Pract.* 34, 529–533. doi:10.1080/09593985.2017.1422203

Miyazaki, T., Wada, M., Kawahara, H., Sato, M., Baba, H., and Shimada, S. (2002). Dynamic load at baseline can predict radiographic disease progression in medial compartment knee osteoarthritis. *Ann. Rheum. Dis.* 61, 617–622. doi:10.1136/ard.61.7.617

Morlock, M., Schneider, E., Bluhm, A., Vollmer, M., Bergmann, G., Müller, V., et al. (2001). Duration and frequency of every day activities in total hip patients. *J. Biomech.* 34, 873–881. doi:10.1016/s0021-9290(01)00035-5

Müller, M., Schwachmeyer, V., Tohtz, S., Taylor, W. R., Duda, G. N., Perka, C., et al. (2012). The direct lateral approach: Impact on gait patterns, foot progression angle and pain in comparison with a minimally invasive anterolateral approach. *Arch. Orthop. Trauma. Surg.* 132, 725–731. doi:10.1007/s00402-012-1467-x

Mündermann, A., Asay, J. L., Mündermann, L., and Andriacchi, T. P. (2008). Implications of increased medio-lateral trunk sway for ambulatory mechanics. *J. Biomech.* 41, 165–170. doi:10.1016/j.jbiomech.2007.07.001

Neuprez, A., Neuprez, A. H., Kaux, J. F., Kurth, W., Daniel, C., Thirion, T., et al. (2020). Total joint replacement improves pain, functional quality of life, and health utilities in patients with late-stage knee and hip osteoarthritis for up to 5 years. *Clin. Rheumatol.* 39, 861–871. doi:10.1007/s10067-019-04811-y

Queen, R. M., Attarian, D. E., Bolognesi, M. P., and Butler, R. J. (2015). Bilateral symmetry in lower extremity mechanics during stair ascent and descent following a total hip arthroplasty: A one-year longitudinal study. *Clin. Biomech.* 30, 53–58. doi:10.1016/j.clinbiomech.2014.11.004

Reininga, I. H., Stevens, M., Wagenmakers, R., Bulstra, S. K., Groothoff, J. W., and Zijlstra, W. (2012). Subjects with hip osteoarthritis show distinctive patterns of trunk movements during gait-a body-fixed-sensor based analysis. *J. Neuroeng Rehabil.* 9, 3. doi:10.1186/1743-0003-9-3

Schmidt, A., Meurer, A., Lenarz, K., Vogt, L., Froemel, D., Lutz, F., et al. (2017). Unilateral hip osteoarthritis: The effect of compensation strategies and anatomic measurements on frontal plane joint loading. *J. Orthop. Res.* 35, 1764–1773. doi:10.1002/jor.23444

Schmitt, D., Vap, A., and Queen, R. M. (2015). Effect of end-stage hip, knee, and ankle osteoarthritis on walking mechanics. *Gait Posture* 42, 373–379. doi:10.1016/j.gaitpost.2015.07.005

Shakoor, N., Dua, A., Thorp, L. E., Mikolaitis, R. A., Wimmer, M. A., Foucher, K. C., et al. (2011). Asymmetric loading and bone mineral density at the asymptomatic knees of patients with unilateral hip osteoarthritis. *Arthritis Rheum.* 63, 3853–3858. doi:10.1002/art.30626

Sharma, L., Hurwitz, D. E., Thonar, E. J., Sum, J. A., Lenz, M. E., Dunlop, D. D., et al. (1998). Knee adduction moment, serum hyaluronan level, and disease severity in medial tibiofemoral osteoarthritis. *Arthritis Rheum.* 41, 1233–1240. doi:10.1002/1529-0131(199807)41:7<1233::aid-art14>3.0.co;2-l

Stief, F., Böhm, H., Michel, K., Schwirtz, A., and Döderlein, L. (2013). Reliability and accuracy in three-dimensional gait analysis: A comparison of two lower body protocols. *J. Appl. Biomech.* 29, 105–111. doi:10.1123/jab.29.1.105

Stief, F., Holder, J., Feja, Z., Lotfolahpour, A., Meurer, A., and Wilke, J. (2021). Impact of subject-specific step width modification on the knee and hip adduction moments during gait. *Gait Posture* 89, 161–168. doi:10.1016/j.gaitpost.2021.07.008

Stief, F., Schmidt, A., van Drongelen, S., Lenarz, K., Froemel, D., Tarhan, T., et al. (2018). Abnormal loading of the hip and knee joints in unilateral hip osteoarthritis persists two years after total hip replacement. *J. Orthop. Res.* 36, 2167–2177. doi:10.1002/jor.23886

Talis, V. L., Grishin, A. A., Solopova, I. A., Oskanyan, T. L., Belenky, V. E., and Ivanenko, Y. P. (2008). Asymmetric leg loading during sit-to-stand, walking and quiet standing in patients after unilateral total hip replacement surgery. *Clin. Biomech.* 23, 424–433. doi:10.1016/j.clinbiomech.2007.11.010

van Drongelen, S., Kaldowski, H., Fey, B., Tarhan, T., Assi, A., Stief, F., et al. (2020). Determination of leg alignment in hip osteoarthritis patients with the EOS® system and the effect on external joint moments during gait. *Appl. Sci.* 10, 7777. doi:10.3390/app10217777

van Drongelen, S., Kaldowski, H., Tarhan, T., Assi, A., Meurer, A., and Stief, F. (2019). Are changes in radiological leg alignment and femoral parameters after total hip replacement responsible for joint loading during gait? *BMC Musculoskelet. Disord.* 20, 526. doi:10.1186/s12891-019-2832-5

Weaver, T. B., Glinka, M. N., and Laing, A. C. (2017). Stooping, crouching, and standing - characterizing balance control strategies across postures. *J. Biomech.* 53, 90–96. doi:10.1016/j.jbiomech.2017.01.003

Wesseling, M., de Groote, F., Meyer, C., Corten, K., Simon, J. P., Desloovere, K., et al. (2015). Gait alterations to effectively reduce hip contact forces. *J. Orthop. Res.* 33, 1094–1102. doi:10.1002/jor.22852

Zifchock, R. A., Davis, I., Higginson, J., McCaw, S., and Royer, T. (2008). Side-to-side differences in overuse running injury susceptibility: A retrospective study. *Hum. Mov. Sci.* 27, 888–902. doi:10.1016/j.humov.2008.03.007

frontiers | Frontiers in Bioengineering and Biotechnology

TYPE Original Research
PUBLISHED 20 June 2023
DOI 10.3389/fbioe.2023.1191868

OPEN ACCESS

EDITED BY
Simone Tassani,
Pompeu Fabra University, Spain

REVIEWED BY
Mario Ceresa,
Pompeu Fabra University, Spain
Hongfei Yang,
National University of Singapore, Singapore

*CORRESPONDENCE
Yanghui Xing,
yhxing@stu.edu.cn

RECEIVED 22 March 2023
ACCEPTED 12 June 2023
PUBLISHED 20 June 2023

CITATION
Ma X, Zeng B and Xing Y (2023), Combining 3D skeleton data and deep convolutional neural network for balance assessment during walking.
Front. Bioeng. Biotechnol. 11:1191868.
doi: 10.3389/fbioe.2023.1191868

Combining 3D skeleton data and deep convolutional neural network for balance assessment during walking

Xiangyuan Ma, Buhui Zeng and Yanghui Xing*

Department of Biomedical Engineering, Shantou University, Shantou, China

Introduction: Balance impairment is an important indicator to a variety of diseases. Early detection of balance impairment enables doctors to provide timely treatments to patients, thus reduce their fall risk and prevent related disease progression. Currently, balance abilities are usually assessed by balance scales, which depend heavily on the subjective judgement of assessors.

Methods: To address this issue, we specifically designed a method combining 3D skeleton data and deep convolutional neural network (DCNN) for automated balance abilities assessment during walking. A 3D skeleton dataset with three standardized balance ability levels were collected and used to establish the proposed method. To obtain better performance, different skeleton-node selections and different DCNN hyperparameters setting were compared. Leave-one-subject-out-cross-validation was used in training and validation of the networks.

Results and Discussion: Results showed that the proposed deep learning method was able to achieve 93.33% accuracy, 94.44% precision and 94.46% F1 score, which outperformed four other commonly used machine learning methods and CNN-based methods. We also found that data from body trunk and lower limbs are the most important while data from upper limbs may reduce model accuracy. To further validate the performance of the proposed method, we migrated and applied a state-of-the-art posture classification method to the walking balance ability assessment task. Results showed that the proposed DCNN model improved the accuracy of walking balance ability assessment. Layer-wise Relevance Propagation (LRP) was used to interpret the output of the proposed DCNN model. Our results suggest that DCNN classifier is a fast and accurate method for balance assessment during walking.

KEYWORDS

Kinect, skeleton data, deep convolutional neural network, balance assessment, machine learning

1 Introduction

Balance ability refers to the human body perceiving the body's center of gravity and controlling the body's center of gravity within the support plane through body movements (Shumway-Cook et al., 1988). It is crucial for people to maintain their daily activities of living (ADL). Balance impairment may be caused by a number of factors, including advanced age, arthritis, cerebral palsy and Parkinson's disease, of which advanced age is the most common one. With the growth of age, various functions related to balance abilities decline rapidly,

including muscle strength, eyesight, and reaction time, etc. It has been found that as many as 75% of people aged 70 and above have balance disorders (Howe et al., 2011). Balance assessment plays an important role in accurately diagnosing potential disorders, identifying fall risks, and developing treatment plans. Currently, balance assessment is usually done by physical therapists based on commonly used standardized measures, such as Berg balance scale, Tinetti balance scale and timed "up & go" test (TUG).

Walking balance assessment is an important part in a variety of balance standardized measures. For example, in Berg balance scale, subjects are required to walk from one position to another, and the physical therapist will give them scores based on their walking stability, gait and posture. In Tinetti balance scale, foot and trunk positions as well as walking path and time of subjects are considered. Similarly, the TUG test mainly use walking speed as an index to judge person's balance abilities and fall risks.

Balance ability scores in balance standardized measures are assessed based on judgments from the physical therapists, which is subjective. To address this issue, one way is to analyze the balance abilities with equipment-based and digitalized assessment methods in order to eliminate subjective opinions from physical therapists. In equipment-based and digitalized assessment methods, the motion of human body can be described with 3D skeleton data. Thus, it is possible to use 3D skeleton data to assess balance abilities during walking.

3D skeleton data can be acquired in several ways, such as Microsoft Kinect, Orbbec Astra, and Intel RealSense. Microsoft Kinect is the most popular method. Kinect can recognize and track a total of 32 human joints, covering all parts of the human body. Currently, there are a number of relevant studies on the accuracy of Kinect. Eltoukhy (Eltoukhy et al., 2017) simultaneously used Kinect and Vicon system to record the results of Star Excursion Balance Test (SEBT), and found that the kinematic error of lower limbs was less than 5° except for the front plane angle of the posterior and lateral knee joints, which were 5–7°. According to Schmitz (Schmitz et al., 2014), the accuracy and precision of joint angle measurement in 3D skeleton model obtained from Kinect are equivalent to that of the mark-based system. Khoshelham (Khoshelham, 2012) believes that the point cloud data of Kinect sensor is able to provide acceptable accuracy by comparing it with the point cloud data of high-end laser scanner. Kinect has the characteristics of low cost, portability and convenient data access, and is able to provide acceptable accuracy.

At present, there are plenty of studies on gait recognition, pathological gait classification and motion analysis using Kinect 3D skeleton data (Ahmed et al., 2014; Li et al., 2018; Bari and Gavrilova, 2019; Jun et al., 2020; Xing and Zhu, 2021), all of which have acceptable accuracy. However, further process is needed in order to assess balance abilities during walking. Balance abilities assessment during walking not only need to observe the gait, but also need to consider walking speed and other parameters. The existing methods so far are mainly designed for gait recognition and motion analysis. In this study, we aim to develop a digitalized assessment method for assessing balance abilities during walking based on 3D skeleton data collected by Kinect.

Deep convolutional neural network (DCNN) is a popular machine learning technology, and has excellent performance in the fields of image recognition (Szegedy et al., 2015; Senior et al., 2020; Li et al., 2021). Also, DCNN classifier is widely used in data and image analysis applications (Yao et al., 2019; Yu et al., 2019; Szczęsna et al., 2020; Yu et al., 2022a; Yu et al., 2022b). DCNN can achieve automatic feature extraction based on original sensor data (Alharthi et al., 2019). One of the limitations of DCNN is its opacity (Bach et al., 2015). This opacity seriously hinders the acceptance and application of DCNN model in medical diagnosis (Wolf et al., 2006). To solve this problem, Layer-wise Relevance Propagation (LRP) was proposed (Montavon et al., 2017), which uses the back propagation method to attribute part of the model prediction to the original input signal. It is possible to identify the important area of classification hoisting in the input signal, which may be used to interpret the prediction of the model. Currently, LRP has been successfully applied in image classification (Lapuschkin et al., 2017), text classification (Arras et al., 2017) and gait analysis (Horst et al., 2019).

In this study, we proposed a deep learning-based method for balance assessment during walking based on 3D skeleton data collected by Kinect. The main contributions and innovation of this study are listed as follows.

(1) Existing Kinect-based methods are only designed for gait recognition and motion analysis. We newly collected a Kinect 3D skeleton dataset with three standardized balance ability levels and specifically designed a deep learning based method for balance ability assessment during walking.
(2) To obtain better performance, we performed thorough parametric study including hyperparameters setting of DCNN and skeleton node selection. We also used LRP to interpret the output of the DCNN model.
(3) To validate the performance of the proposed method, we conducted a comparison with other commonly used machine learning methods. In addition, we migrated and applied a state of art posture classification method to the walking balance ability assessment task. The proposed method was also compared with the migrated state of art method. The results showed the superiority of the proposed method.

2 Materials and methods

2.1 Experimental subjects and balance impairment simulation

We recruited ten healthy adults aged from 21–24 as our experimental subjects, who have normal balance abilities. For balance impaired subjects, we asked the ten adults wearing age simulation suits, which are widely used for healthy people to experience functional challenges of the elderly. After wearing the suits, the young adults will have reduced motor and cognitive performance, as well as self-perception ability (Saiva et al., 2020; Vieweg and Schaefer, 2020). Additionally, the suit users will also experience a variety of other functional disabilities including reduced muscle strength, vision loss, decreased flexibility of the joints (Lauenroth et al., 2017; Bowden et al., 2020; Watkins et al., 2021), which can lead to the decline in balance as in older people. The simulation suit is shown in Figure 1. Briefly, we use wrist and ankle weights to simulate loss of muscle strength in the extremities, and use knee and elbow adjustments to limit joint flexibility. We also can adjust two ropes in front of the chest to simulate hunchback status, and tie the rope around thighs to limit step width. Additionally, special glasses were used for poor vision simulation.

FIGURE 1
Age simulation suit. **(A)**: Subject with age simulation suit; **(B)**: sticks used to restrict knee and elbow joints; **(C)**: Sandbags located on the limbs; **(D)**: Special glasses to simulate vision loss.

There are two setups of the suit to simulate two different types of balance disabilities that may happen during the aging process. Thus, for one healthy subject, we can acquire totally three standardized balance levels. Under the guidance of rehabilitation doctors, our simulation guidelines are as follows:

- Level-0: No restrictions are added, subjects walk normally.
- Level-1: Subjects are given extra weight on their wrists and ankles, and have limited knee and elbow flexibility.
- Level-2: On the basis of level-1, the conditions of hunchback and limited vision are added.

2.2 Data collection

Following simulation guidelines, every subject walked 10 times for each of the balance levels. Thus, the size of the dataset is 300 (10 subjects × 10 times × 3 balance levels). 3D skeleton data were obtained using a Kinect sensor and the corresponding software development kit named Kinect SDK. The skeleton data includes 3D coordinates of total 32 joints, and the joint hierarchy is distributed in a direction from the center of the body to the extremities. Joints includes pelvis, shoulder, elbow, wrist, hand, hang tip, thumb, hip, knee, ankle, foot, head, nose, eye, and ear, as shown in Figure 2A. Based on our preliminary studies, some of these joints including hand, hang tip, nose, eye and ear have minor impact on balance abilities, and were removed in this research. The final skeleton structure for data collection is shown in Figure 2B.

The data acquisition process by Kinect is shown in Figure 3. We set up a 4-meter long sidewalk, and the two ends of the sidewalk are the starting point and the end point respectively. The Kinect device is located 1 meter away from the end point. Subjects are required to walk from the starting point to the end point at their normal speed.

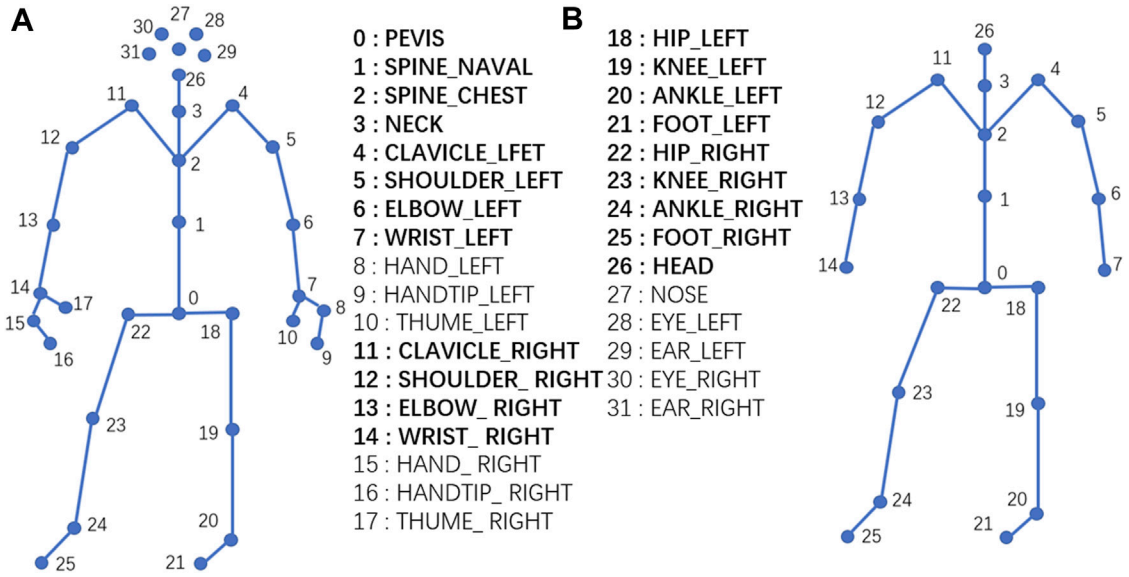

FIGURE 2
Joint diagram of human skeleton. **(A)**: The original skeleton structure from Kinect with 32 joints; **(B)**: Simplified skeleton structure for this study with 21 joints in bold font.

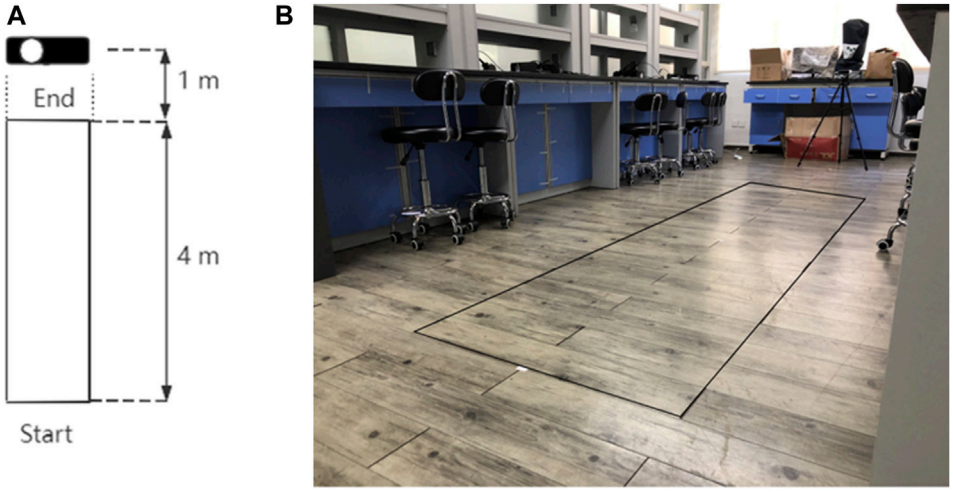

FIGURE 3
Data acquisition process with Kinect. **(A)**: Abstract figure of scene; **(B)**: Real scenarios of data acquisition process.

2.3 Deep convolutional neural network (DCNN)

Deep convolutional neural networks are frequently used for classification and recognition tasks and show great performance; therefore, some researchers also use DCNN to process 3D skeleton data (Caetano et al., 2019; Li et al., 2020). RNN, LSTM and GRU have been proposed successively for processing sequence data [text (Cho et al., 2014), audio (Yue-Hei Ng et al., 2015), video (Ballas et al., 2015)]. Because 3D skeleton data is time series sequence data, these three models can be used to process 3D skeleton data (Graves et al., 2013; Lee et al., 2019). In addition, as the human skeleton connected by the junction nodes is similar to the graph in the computer data type, there are some studies on 3D skeleton data analysis based on graph convolution network (Cheng et al., 2020; Shi et al., 2020). In summary, neural network models commonly used for skeleton data processing include DCNN, RNN and GCN. In this paper, we use convolutional networks to construct a model for processing the hierarchical assessment of dynamic balancing capability based on 3D skeleton data.

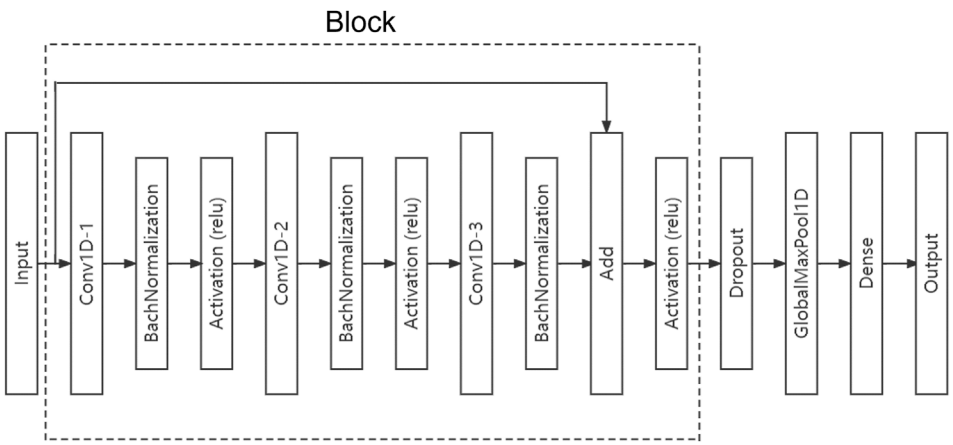

FIGURE 4
Proposed DCNN structure. DCNN mainly consists of a single or multiple residual blocks, each of which includes three convolutional layers, batch normalization layers, and Relu activation layers. We can add multiple residual blocks between input layer and dropout layer if needed.

The core building module of deep convolutional network model is the convolution layer, which mainly extracts features by applying convolution operation. Assuming that X is the input of the convolution layer, W is the weight matrix, and B is bias, the output Y of the convolution layer can be expressed as:

$$Y = Conv(W, X) + b$$

An activation function φ is usually added after the convolution operation:

$$Y = \varphi(Y)$$

The structure of the DCNN constructed in this paper is shown in Figure 4. The model consists of several residual blocks, a dropout layer, a global pooling layer and a full connection layer. Residual block is mainly composed of three convolution layers and a connection layer. Convolution layer 1 processes the input data, convolution layer 2 processes the output of convolution layer 1, convolution layer 3 processes the output of convolution layer 2, and then the connection layer merges the input of convolution layer 1 and the output of convolution layer 3. Batch Normalization and activation using Relu are required following each convolutional layer in a convolution block. In a residual block, the size of convolution kernel of convolution layer 1 is set as 5, the size of convolution kernel of convolution layer 2 is set as 3, and the size of convolution kernel of convolution layer 3 is set as 1.

2.4 Layer-wise relevance propagation (LRP)

Linear models make transparent decisions. However, complex nonlinear models are usually regarded as black box classifiers, and almost all deep artificial neural networks are composed of nonlinear models. Layer-wise Relevance propagation (LRP) is a technique for generalized interpretation of nonlinear models. We used LRP to interpret the output of the proposed DCNN model in this paper.

The LRP (Montavon et al., 2017) uses the topology of the network model itself to attribute the correlation score to the important components of the input data, so as to explain the decisions made by the model based on a given data point. Based on the conservation principle, LRP technology (Bach et al., 2015) gradually maps the prediction to a lower layer through back propagation until the input variable is reached. Neuron j receives a quantity of relevance R_j^{l+1} from upper layer neurons, and redistributes that quantity to neuron i, in proportion to $R_{i\leftarrow j}^{(l,l+1)}$ (the contribution of neuron i to the activation of neuron j in the forward pass).

$$R_{i\leftarrow j}^{(l,l+1)} = \frac{z_{ij}}{z_j} \cdot R_j^{l+1}$$

Where z_{ij} represents the measurement of the contribution from neuron i to neuron j, and z_j represents the sum of all neurons from l layer to neuron j.

2.5 Model training

2.5.1 Pre-processing of input samples

The time length of each video sample recorded in the dataset was inconsistent because different subjects may have different walking speeds. Thus, in the temporal aspect, the total number of frames of different samples was different. The total number of frames of different samples collected in this study varied from 22 frames to 38 frames.

To normalize the DCNN input size, we selected fixed 20 frames for every sample in the dataset from back to front. Occasionally, subjects did not walk immediately after receiving the command, selected from back to front could avoid the collection of few non-walking frames. Besides, since the sample data may be offset, we reoriented the input data of each sample based on the position of the pelvis joint in the first frame of each sample. Specifically, for each

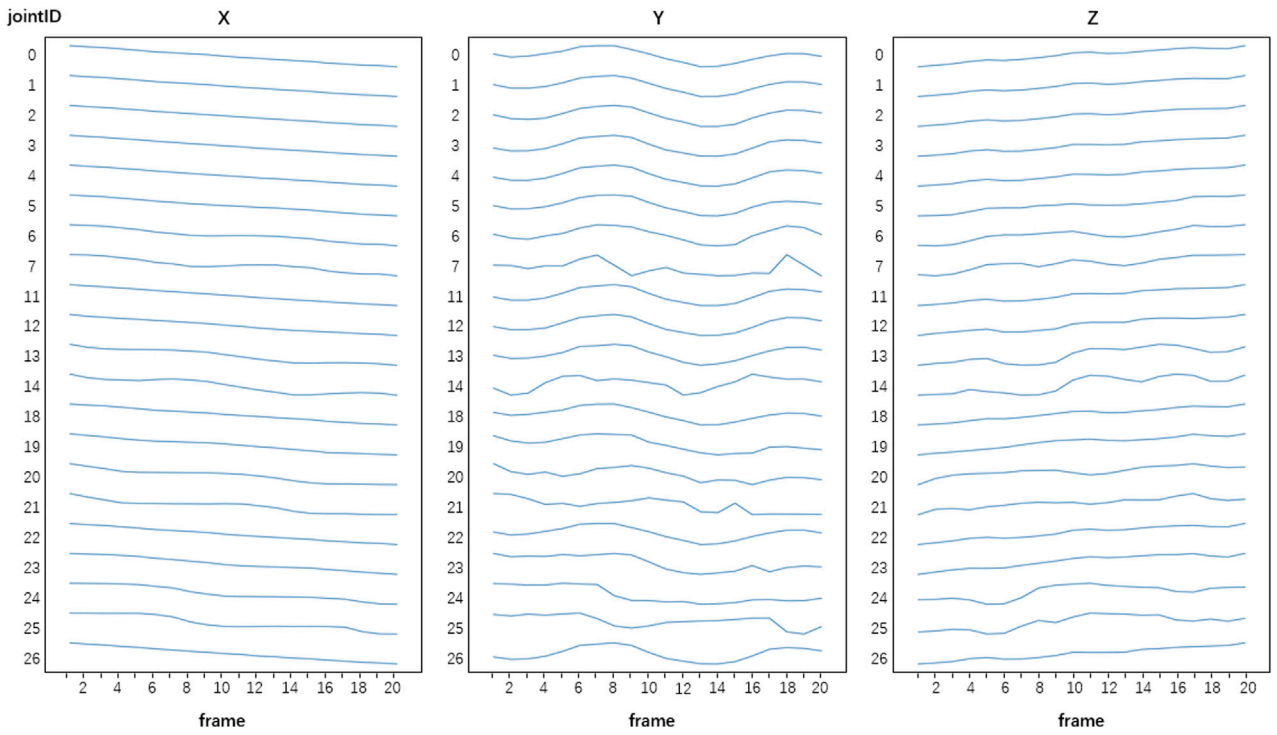

FIGURE 5
An example of a pre-processed sample. Each sample has data of 21 joints, 20 frames and three-dimensional (X, Y, Z) time-varying spatial coordinates of the joints after pre-processing.

data point in each sample, its position coordinates need to subtract the pelvis joint in the original coordinates.

2.5.2 Training-validation-test split

In this study, we obtained a dataset of 300 samples. After data pre-processing, the total number of frames of each sample was 20 frames, each frame had data of 21 human joints, and each joint had data of three-dimensional (X, Y, Z) time-varying spatial coordinates. Thus the size of an input sample was 1,260 (20 frames × 21 joints × 3 dimensions). Figure 5 show an example of a pre-processed input sample.

Since it was a relatively small dataset, we adopted leave-one-subject-out-cross-validation strategy to train and evaluate the performance of the DCNN. In each fold, one subject data was used as validation dataset, another one subject data was used as test dataset and the remaining eight subject data was used as training dataset. Finally, the size of training dataset was 240 (8 subjects × 10 times × 3 balance levels), the size of validation dataset was 30 (1 subjects × 10 times × 3 balance levels), and the size of test dataset was 30 (1 subjects × 10 times × 3 balance levels) in each fold.

2.5.3 DCNN hyperparameters setup

After parametric study, for the residual block, we set the size of kernel of residual block in the first convolutional layer to 5, the size of kernel in the second convolutional layer to 3, the size of kernel in the third convolutional layer to 1. The padding method was same, and the activation function was Relu function in every convolutional layer. The channel size of filter in convolution layer is an important parameter, we chose 64 after comparing with other size. For epoch selection, we applied the early stop method. The early stop method is a widely used method to stop training when the performance of the model on the validation dataset begins to decline, so as to avoid the problem of overfitting caused by continued training. In addition, cross-entropy was chose as the loss function and Adam optimizer with a learning rate of 0.0001 was used to train DCNN classifier.

2.5.5 Performance evaluation measures

Accuracy, Precision and F1-Score were used to measure the model, and the results from 10 test folds were then pooled together to form a complete set to calculate the average values of the measures. Accuracy, Precision and F1-score are counted by the true positive (TP), false positives (FP), true negatives (TN), and false negatives (FN). In multi-classification tasks, Precision and F1 indices need to be calculated for each category, and then arithmetic average is performed.

$$Accutacy = \frac{TP + TN}{TP + FP + TN + FN}$$

$$Precision = \frac{TP}{TP + FP}$$

$$F_1 = 2 \cdot \frac{Precision \cdot Recall}{Precision + Recall}$$

Since artificial neural networks are often seen as black boxes, methods such as SmoothGrad (Smilkov et al., 2017), Deconvnet (Springenberg et al., 2015), GuidedBackprop (Alber et al., 2018), and LRP (Montavon et al., 2017) have been proposed to remedy this

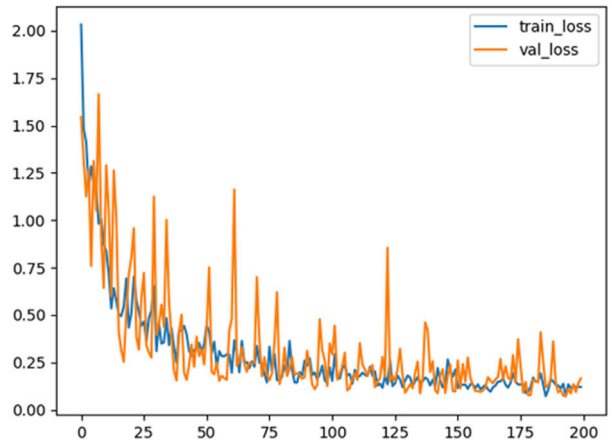

FIGURE 6
Loss function variation curve of training set and validation set. The blue line represents the loss function curve of the training dataset and the orange line represents the loss function curve of the validation dataset.

deficiency. INNvesigate is a library that implements the PattNet, PatternAttribution (Kindermans et al., 2017), and LRP methods, allowing the user to invoke them through the interface. We called LRP method based on iNNvesigate for 3D skeleton data analysis.

3 Results and discussion

3.1 Performance of proposed DCNN for balance assessment during walking

We use the proposed DCNN method to classify three different levels of balance ability during walking. With leave-one-subject-out cross-validation, the method achieved 93.33% accuracy, 94.44% precision and 94.46% F1 score. The results showed that Kinect can collect 3D skeleton data to assess the balance ability of walking subjects, and the accuracy of DCNN classification can reach an accepted level.

The loss function of balance ability classification based on the DCNN model is shown in Figure 6, where the blue line represents the loss function curve of the training dataset and the orange line represents the loss function curve of the validation dataset. We found that when Adam optimizer with learning rate of 0.0001 was used for training, the loss function value of DCNN classifier decreased as the number of iterations increased, and stabilized after 150 epochs, with a fluctuation of 0.25. The result suggests that DCNN classifier is convergent.

3.2 Parametric study of DCNN hyperparameters selection

3.2.1 Kernel size

Kernel size is an import parameter in convolution layer. The larger the convolution kernel is, the larger the receptive field is. However, a large convolution kernel will lead to a huge increase in the amount of computation and may reduce the computational performance. We compared the performance of DCNN with different kernel size and the results were showed in Table 1. After comparing the performance of DCNN with different kernel size in the residual block, we set the size of kernel in the first convolutional layer to 5, the size of kernel in the second convolutional layer to 3, the size of kernel in the third convolutional layer to 1.

3.2.2 Channel size

Channel can usually be understood as the width of model, and increasing the width allows each layer to learn richer features. However, increasing the number of channels may also affect the performance of the model. Table 2 shows the impact of different channel size on model performance. We can see that the loss function of validation dataset shows a downward trend, and the accuracy of validation dataset shows an upward trend.

3.2.3 The number of residual blocks

The number of residual blocks is also an important parameter for DCNN. Usually, the more residual blocks, the deeper the DCNN model will be, and the more accurate classification model can be fitted. However, as the depth of the model increases, it will be easy to learn the noise of input data, resulting in the phenomenon of overfitting. Table 3 shows the impact of different number of residual blocks on model performance. We can see that, as the number of residual blocks increases, the training loss value decreases, but the validation loss decreases first and then increases. When the number of residual blocks is 3, the validation loss of DCNN model reaches the minimum value, which is 0.1539, and the loss accuracy is 0.9741.

3.2.4 Optimizer

In order to obtain better performance, we use different optimizers for optimization analysis. Stochastic Gradient Descent (SGD) algorithm randomly selects a group of samples from each iteration and updates them according to the Gradient after training. Root Mean Square Propagation (RMSProp) is an exponential movement-weighted average of the binary norm of each component of the historical gradient. Adam Optimizer takes advantage of the advantages of AdaGrad and RMSProp optimizer and is considered to be quite robust to the selection of hyperparameters. Table 4 shows the performance of DCNN with different optimization methods. From Table 4, we can see that although the average epoch of Adam optimizer is larger than the others, its validation loss is smaller than the others, and fitting effect is better.

3.3 Parametric study of skeleton node selection

In order to improve the performance of the proposed DCNN classifier, we also tried to optimize skeleton node selection and subsequently to control the data input to the model. We have previously excluded some nodes (fingers, ears, and nose) in the process of data collection, but not all the remaining nodes have positive effects on the assessment of balance ability during walking.

TABLE 1 The validation loss and the validation accuracy with different kernel size.

Kernel size 1	Kernel size 2	Kernel size 3	Validation loss	Validation accuracy
1	1	1	0.2424	0.9426
1	1	3	0.2460	0.9444
1	1	5	0.2128	0.9519
1	1	7	0.2316	0.9444
1	3	1	0.2098	0.9556
1	3	3	0.2060	0.9630
1	3	5	0.1982	0.9593
1	3	7	0.2093	0.9556
1	5	1	0.1840	0.9630
1	5	3	0.1720	0.9704
1	5	5	0.2038	0.9519
1	5	7	0.1995	0.9481
1	7	1	0.2243	0.9444
1	7	3	0.1823	0.9630
1	7	5	0.1696	0.9667
1	7	7	0.1493	0.9626
3	1	1	0.2045	0.9630
3	1	3	0.2050	0.9556
3	1	5	0.1436	0.9778
3	1	7	0.2299	0.9704
3	3	1	0.1974	0.9556
3	3	3	0.1649	0.9704
3	3	5	0.2303	0.9481
3	3	7	0.1893	0.9667
3	5	1	0.1811	0.9556
3	5	3	0.1701	0.9667
3	5	5	0.1556	0.9704
3	5	7	0.2170	0.9556
3	7	1	0.1917	0.9667
3	7	3	0.1465	0.9715
3	7	5	0.2123	0.9593
3	7	7	0.1636	0.9667
5	1	1	0.1677	0.9704
5	1	3	0.2052	0.9630
5	1	5	0.1848	0.9630
5	1	7	0.1757	0.9593
5	3	1	0.1420	0.9778
5	3	3	0.2075	0.9667

(Continued on following page)

TABLE 1 (*Continued*) The validation loss and the validation accuracy with different kernel size.

Kernel size 1	Kernel size 2	Kernel size 3	Validation loss	Validation accuracy
5	3	5	0.1930	0.9667
5	3	7	0.1795	0.9667
5	5	1	0.1983	0.9667
5	5	3	0.2169	0.9630
5	5	5	0.2137	0.9630
5	5	7	0.2030	0.9593
5	7	1	0.1930	0.9667
5	7	3	0.2082	0.9444
5	7	5	0.1874	0.9630
5	7	7	0.1538	0.9635
7	1	1	0.1956	0.9667
7	1	3	0.1654	0.9630
7	1	5	0.1986	0.9593
7	1	7	0.1823	0.9704
7	3	1	0.2001	0.9593
7	3	3	0.1816	0.9741
7	3	5	0.1599	0.9704
7	3	7	0.1658	0.9630
7	5	1	0.1669	0.9667
7	5	3	0.1489	0.9704
7	5	5	0.1485	0.9630
7	5	7	0.1649	0.9715
7	7	1	0.2015	0.9630
7	7	3	0.1393	0.9615
7	7	5	0.1988	0.9667
7	7	7	0.1816	0.9593

TABLE 2 The validation loss and the validation accuracy with channel size.

Channel size	Validation loss	Validation accuracy
4	0.2455	0.9555
8	0.2196	0.9518
16	0.2215	0.9518
32	0.1489	0.9704
64	0.1411	0.9852

The body's joints are connected with each other, and some joints are dependent on the existence of other joints. For example, if we exclude elbow from input data, we should also exclude wrist data. Following this principle, we observed the performance change of DCNN classifier by selectively inputting data of specific nodes, the results were shown in Table 5.

We take the inputs of all joints as the control group (A0), and the classification accuracy was 89.83%. We found that the accuracy of the classifier increased when we excluded the hand-related data. Specifically, when the wrist and elbow (H2) were excluded, the accuracy of the classifier increased to 91%. When wrists, elbows, shoulders and clavicles were excluded (H4), the accuracy of the classifier increased to 93.67%. However, the accuracy of the classifier decreased after excluding leg-related joints. When foots, ankle, knees and hips were excluded (L4), the classifier's accuracy fell to 84.33%. Furthermore, when using only the pelvis, spine naval, spine chest (G1) data, the classifier has only 76% accuracy. When using only leg-related data, including feet, wart-form, knees and hips (G2), the classifier achieved 67.33% accuracy. The results suggest that the performance of DCNN classifier depends on data of the input joint groups.

TABLE 3 Performance of DCNN with different number of residual blocks.

The number of residual blocks	Train loss	Validation loss	Validation accuracy
1	0.1386	0.1663	0.8333
2	0.1237	0.1569	0.9556
3	0.1235	0.1539	0.9741
4	0.1001	0.1856	0.9667

TABLE 4 Performance of DCNN with different optimization methods.

Optimizer	Epoch	Validation loss	Validation accuracy
SGD	79	0.3040	0.9184
RMsProp	80	0.2982	0.9259
Adam	95	0.1539	0.9741

The results showed that data from leg and trunk are the most important in the assessment of balance during walking. These results are expected because balance is related to body's center of gravity, and leg and trunk play an important role in its position change. On the other side, human hands and upper limbs are usually moving freely during walking, thus when we exclude these data, the accuracy of the classification improved.

3.4 DCNN model interpretation with LRP

We further used LRP technique to explain DCNN decisions in the balance assessment process as shown in Figure 7, which is the representation of data contribution matrix for H4 condition which has the best accuracy performance. The darker the color, the greater the value of the matrix.

In walking (X) direction, the matrix values gradually increased with time, which implies that the importance of data roughly increased with time. In reality, when a subject is walking, his/her position in X direction is gradually increase in X direction. The relationship of position and time is dependent on step size, walking speed and some other parameters that are widely used in popular balance assessment scales. The subjects with low balance ability have smaller walking speed, step frequency and step length, thus the distance difference between subjects with different balance levels gets bigger and bigger as time frames go on.

In left-right (Y) direction, the color of the entire Y block is much lighter than the color of X and Z blocks, suggesting left-right direction is the least important one for the classification task of balance levels. We believe that this is because the movement of the body in left-right (Y) direction during walking is relatively small, leading to a failure to recognize the left-right (Y) direction difference between different balance levels.

In the up-and-down direction (Z), lower limb data (left and right) have relative darker color, suggesting ankles and legs are the important parts for the classification task of balance levels. We believed that this is because the subjects with different balance abilities have different heights of foot lifting. In some assessment scales, lifting height of foot is also an important parameter to judge the level of human balance ability. The ankle joints and foot joints

TABLE 5 Performance of different joint groups.

Group	Description	Selected joints	Accuracy	Improvement
A0	All joints	0, 1, 2, 3, 4, 5, 6, 7, 11, 12, 13, 14, 18, 19, 20, 21, 22, 23, 24, 25, 26	89.83	
T1	Joints except for head	0, 1, 2, 3, 4, 5, 6, 7, 11, 12, 13, 14, 18, 19, 20, 21, 22, 23, 24, 25	86.34	−3.49
T2	Joints expect for head, neck	0, 1, 2, 4, 5, 6, 7, 11, 12, 13, 14, 18, 19, 20, 21, 22, 23, 24, 25	86.67	−3.16
H1	Joints except for wrists	0, 1, 2, 3, 4, 5, 6, 11, 12, 13, 18, 19, 20, 21, 22, 23, 24, 25, 26	88.67	−1.16
H2	Joints except for wrists, elbows	0, 1, 2, 3, 4, 5, 11, 12, 18, 19, 20, 21, 22, 23, 24, 25, 26	91.33	1.50
H3	Joints except for wrists, elbows, shoulders	0, 1, 2, 3, 4, 11, 18, 19, 20, 21, 22, 23, 24, 25, 26	91.00	1.17
H4	Joints except for wrists, elbows, shoulders, clavicles	0, 1, 2, 3, 18, 19, 20, 21, 22, 23, 24, 25, 26	93.67	3.84
L1	Joints expert for feet	0, 1, 2, 3, 4, 5, 6, 7, 11, 12, 13, 14, 18, 19, 20, 22, 23, 24, 26	89.00	−0.83
L2	Joints expert for feet, ankles	0, 1, 2, 3, 4, 5, 6, 7, 11, 12, 13, 14, 18, 19, 22, 23, 26	88.67	−1.16
L3	Joints expert for feet, ankles, knees	0, 1, 2, 3, 4, 5, 6, 7, 11, 12, 13, 14, 18, 22, 26	87.33	−2.50
L4	Joints expert for feet, ankles, knees, hips	0, 1, 2, 3, 4, 5, 6, 7, 11, 12, 13, 14, 26	84.33	−5.50
G1	Joints only include pelvis, spine naval, spine chest	0, 1, 2	76.00	−13.83
G2	Joints only include feet, ankles, knees, hips	18, 19, 20, 21, 22, 23, 24, 25	67.33	−22.50

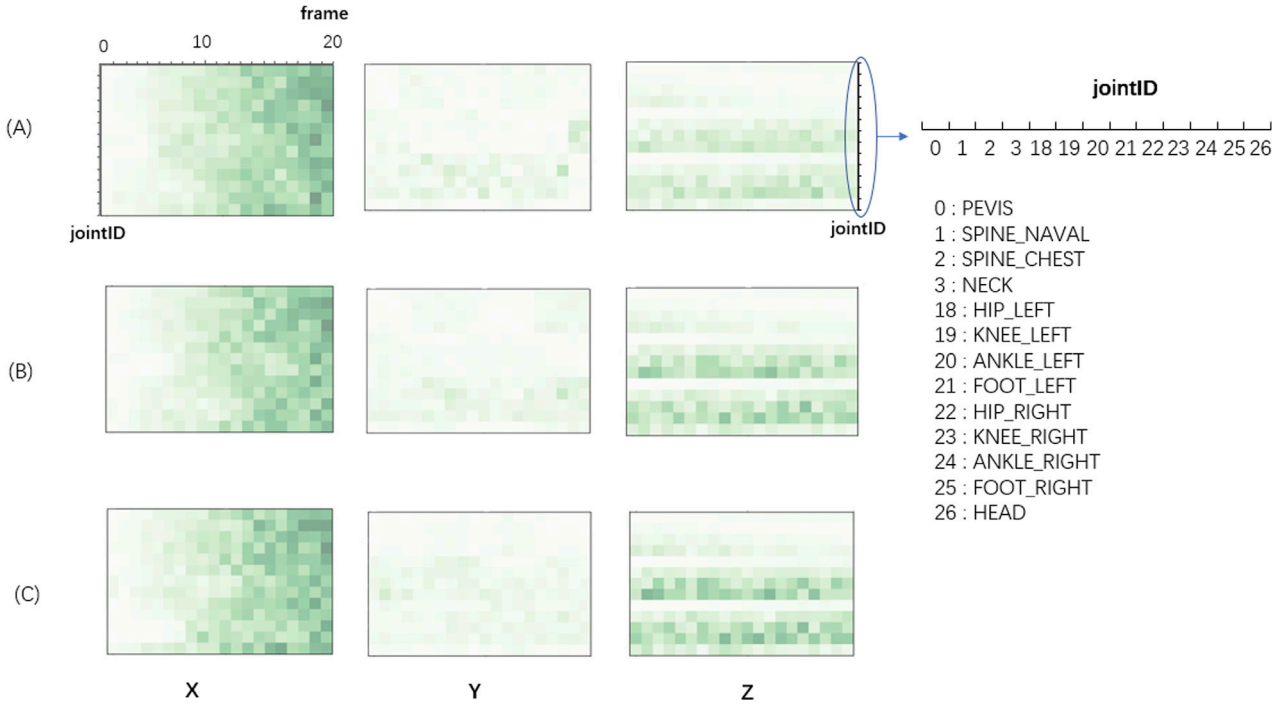

FIGURE 7
Color diagram of the contribution matrix of the sample input in the three levels of the subject. **(A)** Balance Level-0; **(B)** Balance Level-1; **(C)** Balance Level-2. The y-axis represents 13 joints in H4 skeleton node group and the x-axis represents 20 frames (time). The X refers to the front and back direction of the human body, the Y refers to the left and right direction, and the Z refers to the up-and-down direction.

vary fast in the vertical direction during the lifting of foot. Additionally, the color of normal balance group (Level-0) was lighter than the other two, suggesting normal balance group is relatively stable and has less position changes than balance impaired groups (Level-1 and Level-2).

3.5 Comparison of the proposed DCNN with traditional machine learning methods

To validate the effectiveness of the proposed DCNN method, we compared the results of DCNN with those of traditional machine learning methods, such as Naive Bayes, Random Forest and support vector machines (SVM). We used an exhaustive grid search method to compute optimal values for hyperparameters of Naive Bayes, Decision Tree, and SVM to obtain the highest recognition accuracy for all three methods. Naive Bayes is used to fit the distribution of data samples, and gaussian naive Bayes is used here. For the three hyperparameters of random forest classifier, the number of weak classifiers, evaluation criteria and maximum depth, the grid search method is used to search for optimal values. The number of weak classifiers is {50, 100, 150, 200}, the evaluation criteria is {"entropy," "gini"}, and the maximum depth is set to a range of 5–50. Random forest classifiers perform best when the number of weak classifiers is 50, the evaluation criterion is "entropy", and the maximum depth is 24. SVM classifier has three important hyperparameter kernel types, kernel coefficients and penalty parameters. The kernel type is {"RBF," "Linear," "Poly"}, the kernel coefficient is {0.0001, 0.001, 0.01, 0.1, 1.0, 10.0}, and the penalty parameter is {1, 5, 10, 100, 1,000}. When the kernel type is Linear, the kernel coefficient is 1.0, and the penalty parameter is 1, the SVM classifier can achieve the best performance. In addition, we use two LSTM layers and one full connection layer to construct the LSTM network, where the number of neurons in LSTM layer is 32, and the number of neurons in full connection layer is 32.

Table 6 shows the comparison results of DCNN and different traditional machine learning methods. Among them, Naïve Bayes performed the worst, with accuracy of 73.33%, precision of 81.71% and F1 score of 73.37%. The accuracy of SVM is 86.66%, the precision is 87.96%, and the F1 score is 86.92%. The accuracy of Random Forest is 86.66%, the precision is 87.96%, and the F1 score is 86.81%. LSTM has 83.33% accuracy, 86.71% precision and 82.83% F1 score. Compared with these methods, the performance of DCNN classifier proposed by us is better. The improvement indicated the potential of the proposed DCNN in balance ability assessment.

Because DCNN can effectively extract low and high dimensional features, it has demonstrated better performance than traditional machine learning classifiers in many areas (Khagi et al., 2019; Mete and Ensari, 2019). DCNN and LSTM are often used to process image data and sequence data respectively. In this paper, we compared the two deep learning models in our experiments, and we found that the proposed DCNN model with residual structure has better performance than LSTM. The result is consistent with other previous literatures (Bai et al., 2018), in which word-level language are studied. With the help of residual architecture, one-dimensional convolutional networks can also make effective use of historical

TABLE 6 Performance of DCNN and different traditional machine learning methods.

Classifier	Accuracy	Precision	F1-score
DCNN	93.33	94.44	93.46
SVM	86.67	87.96	86.92
Random Forest	86.67	90.47	86.81
LSTM	83.33	86.71	82.83
Naive Bayes	73.33	81.71	73.37

TABLE 7 Performance of DCNN and different CNN-based methods.

Classifier	Accuracy	Precision	F1-score
DCNN	93.33	94.44	93.46
AlexNet	90.00	90.74	89.95
VGGNet	86.67	90.48	86.11
ResNet-18	83.33	88.89	82.22

information. Therefore, in some cases, one-dimensional residual convolution networks can match or exceed the performance of LSTM.

3.6 Comparison of the proposed DCNN with commonly used CNN-based methods

To further validate the effectiveness of the proposed DCNN method, we also compared the results of DCNN with those of several commonly used CNN-based methods. These commonly used CNN-based methods including the AlexNet, the VGGNet and the ResNet-18. The hyperparameters of these three CNN-based networks were optimized to achieve better prediction accuracy.

Table 7 shows the comparison results of DCNN and different CNN-based methods. Among them, ResNet-18 performed the worst, with accuracy of 83.33%, precision of 88.89% and F1 score of 82.22%. The accuracy of AlexNet is 90.00%, the precision is 90.74%, and the F1 score is 89.95%. The accuracy of VGGNet is 86.67%, the precision is 90.48%, and the F1 score is 86.11%. Compared with these methods, the performance of DCNN classifier proposed by us is better. The architecture of the proposed DCNN is more suitable for the classification of walking balance ability task.

3.7 Comparing with posture description method

There are many studies that use Kinect for posture and motion recognition, but few studies that use Kinect to assess balance ability during walking. Although the goals of the two tasks are different, they are achieved using classification methods, so it can be considered to migrate the postures classification model to the walking balance ability classification.

To further validate the performance of the proposed method, we migrated and applied a state of art posture classification method proposed by Klishkovakaia et al. (Klishkovskaia et al., 2020). Briefly, the authors developed a low-cost and high-precision posture classification method based on posture description composed of vector lengths and angles. Movement can be described as a collection of postures. We can analyze differences in walking balance ability by establishing balance ability posture collections.

TABLE 8 Performance of DCNN and posture description method.

Method	Accuracy	Precision	F1-score
Posture description method	86.67	87.68	86.43
DCNN	93.33	94.44	93.46

The performances of the reproduced method and the proposed DCNN method are shown in Table 8. We can see that the proposed model is better in the walking balance classification task. In the classification of postures task, the difference between postures is more obvious, such as walking and standing. However, in the classification of walking balance ability task, the postures are all walking postures. Therefore, the classification of walking balance ability may need more powerful feature extraction capability, which is the strong point of DCNN method.

4 Conclusion

In this study, we used the Kinect 3D skeleton data and DCNN to assess balance abilities of human body during walking. Thorough parametric study including hyperparameters setting of DCNN and skeleton node selection was performed in order to obtain better performance. The proposed DCNN was compared with traditional machine learning methods, and the results showed that DCNN has the best performance. Our results suggest that 3D skeleton data and DCNN can be used for balance assessment with decent accuracy. The proposed method should be useful in early screening balance impaired people. It can partially replace commonly used balance measures and reduce the influence of subjective factors. In future work, we plan to further validate the proposed deep convolutional neural network model on 3D skeleton datasets from real patients. In addition, we plan to further subdivide the levels of walking balance ability to assess the patient's situation more accurately. Moreover, we plan to use multiple Kinects in combination to increase data accuracy.

Data availability statement

The original contributions presented in the study are included in the article/Supplementary material, further inquiries can be directed to the corresponding author.

Ethics statement

Ethical review and approval was not required for the study on human participants in accordance with the local legislation and institutional requirements. The patients/participants provided their written informed consent to participate in this study.

Author contributions

XM and BZ did experiments and wrote the parts of the original version of manuscript; YX designed the experiments and wrote the final version of manuscript. All authors contributed to the article and approved the submitted version.

Funding

This research was funded by Shantou University (STU Scientific Research Foundation for Talents: NF21014 to Yanghui Xing and NTF21004 to Xiangyuan Ma).

Conflict of interest

The authors declare that the research was conducted in the absence of any commercial or financial relationships that could be construed as a potential conflict of interest.

Publisher's note

References

Ahmed, M., Al-Jawad, N., and Sabir, A. T. (2014). "Gait recognition based on kinect sensor," in Process SPIE 9139, real-time image and video processing, SPIE, 15 May 2014, 63–72. doi:10.1117/12.2052588

Alber, M., Lapuschkin, S., Seegerer, P., Hägele, M., Schütt, K. T., Montavon, G., et al. (2018). iNNvestigate neural networks. arXiv preprint. Available at: https://arxiv.org/abs/1808.04260 (Accessed August 13, 2018).

Alharthi, A. S., Yunas, S. U., and Ozanyan, K. B. (2019). Deep learning for monitoring of human gait: A review. *IEEE Sensors J.* 19 (21), 9575–9591. doi:10.1109/jsen.2019.2928777

Arras, L., Horn, F., Montavon, G., Müller, K. R., and Samek, W. (2017). What is relevant in a text document? An interpretable machine learning approach. *PloS one* 12 (8), e0181142. doi:10.1371/journal.pone.0181142

Bach, S., Binder, A., Montavon, G., Klauschen, F., Müller, K. R., and Samek, W. (2015). On pixel-wise explanations for non-linear classifier decisions by layer-wise relevance propagation. *PloS one* 10 (7), e0130140. doi:10.1371/journal.pone.0130140

Bai, S., Kolter, J. Z., and Koltun, V. (2018). An empirical evaluation of generic convolutional and recurrent networks for sequence modeling. arXiv preprint. Available at: https://arxiv.org/abs/1803.01271 (Accessed April 19, 2018).

Ballas, N., Yao, L., Pal, C., and Courville, A. (2015). *Delving deeper into convolutional networks for learning video representations*. Canada: LCLR. arXiv preprint arXiv:1511.06432.

Bari, A. H., and Gavrilova, M. L. (2019). Artificial neural network based gait recognition using kinect sensor. *IEEE Access* 7, 162708–162722. doi:10.1109/access.2019.2952065

Bowden, A., Wilson, V., Traynor, V., and Chang, H. C. (2020). Exploring the use of ageing simulation to enable nurses to gain insight into what it is like to be an older person. *J. Clin. Nurs.* 29 (23-24), 4561–4572. doi:10.1111/jocn.15484

Caetano, C., Brémond, F., and Schwartz, W. R. (2019). "Skeleton image representation for 3d action recognition based on tree structure and reference joints," in 2019 32nd SIBGRAPI conference on graphics, patterns and images (SIBGRAPI), USA, Oct. 28 2019 (IEEE), 16–23.

Cheng, K., Zhang, Y., He, X., Chen, W., Cheng, J., and Lu, H. (2020). "Skeleton-based action recognition with shift graph convolutional network," in Proceedings of the IEEE/CVF conference on computer vision and pattern recognition, USA, 16-17 June 2019 (IEEE), 183–192.

Cho, K., Van Merriënboer, B., Bahdanau, D., and Bengio, Y. (2014). "On the properties of neural machine translation: Encoder-decoder approaches," in *Proceedings of SSST-8, eighth workshop on syntax, semantics and structure in statistical translation* (Canada: Association for Computational Linguistics), 103–111.

Eltoukhy, M., Kuenze, C., Oh, J., Wooten, S., and Signorile, J. (2017). Kinect-based assessment of lower limb kinematics and dynamic postural control during the star excursion balance test. *Gait posture* 58, 421–427. doi:10.1016/j.gaitpost.2017.09.010

Graves, A., Jaitly, N., and Mohamed, A. R. (2013). Hybrid speech recognition with deep bidirectional LSTM. *IEEE workshop on automatic speech recognition and understanding* (pp. 273–278). Germany, IEEE.

Horst, F., Lapuschkin, S., Samek, W., Müller, K. R., and Schöllhorn, W. I. (2019). Explaining the unique nature of individual gait patterns with deep learning. *Sci. Rep.* 9 (1), 2391–2413. doi:10.1038/s41598-019-38748-8

Howe, T. E., Rochester, L., Neil, F., Skelton, D. A., and Ballinger, C. (2011). Exercise for improving balance in older people. *Cochrane database Syst. Rev.* (11), CD004963. doi:10.1002/14651858.CD004963.pub3

Jun, K., Lee, Y., Lee, S., Lee, D. W., and Kim, M. S. (2020). Pathological gait classification using kinect v2 and gated recurrent neural networks. *IEEE Access* 8, 139881–139891. doi:10.1109/access.2020.3013029

Khagi, B., Kwon, G. R., and Lama, R. (2019). Comparative analysis of Alzheimer's disease classification by CDR level using CNN, feature selection, and machine-learning techniques. *Int. J. Imaging Syst. Technol.* 29 (3), 297–310. doi:10.1002/ima.22316

Khoshelham, K. (2012). Accuracy analysis of kinect depth data. *Int. Archives Photogrammetry, Remote Sens. Spatial Inf. Sci.* 38, 133–138. doi:10.5194/isprsarchives-5-w12-133-2011

Kindermans, P. J., Schütt, K. T., Alber, M., Müller, K. R., Erhan, D., Kim, B., et al. (2017). Learning how to explain neural networks: Patternnet and pattern attribution. arXiv preprint. Available at: https://arxiv.org/abs/1705.05598 (Accessed October 24, 2017).

Klishkovskaia, T., Aksenov, A., Sinitca, A., Zamansky, A., Markelov, O. A., and Kaplun, D. (2020). Development of classification algorithms for the detection of postures using non-marker-based motion capture systems. *Appl. Sci.* 10 (11), 4028. doi:10.3390/app10114028

Lapuschkin, S., Binder, A., Muller, K. R., and Samek, W. (2017). "Understanding and comparing deep neural networks for age and gender classification," in Proceedings of the IEEE international conference on computer vision workshops, USA, 20-23 June 1995 (IEEE), 1629–1638.

Lauenroth, A., Schulze, S., Ioannidis, A., Simm, A., and Schwesig, R. (2017). Effect of an age simulation suit on younger adults' gait performance compared to older adults' normal gait. *Res. gerontological Nurs.* 10 (5), 227–233. doi:10.3928/19404921-20170831-04

Lee, D. W., Jun, K., Lee, S., Ko, J. K., and Kim, M. S. (2019). Abnormal gait recognition using 3D joint information of multiple Kinects system and RNN-LSTM. 41st Annual International Conference of the IEEE Engineering in Medicine and Biology Society (EMBC) 23-27 July 2019, USA, (pp. 542–545). IEEE.

Li, R., Liu, Z., and Tan, J. (2018). Human motion segmentation using collaborative representations of 3D skeletal sequences. *IET Comput. Vis.* 12 (4), 434–442. doi:10.1049/iet-cvi.2016.0385

Li, Y., Xia, R., and Liu, X. (2020). Learning shape and motion representations for view invariant skeleton-based action recognition. *Pattern Recognit.* 103, 107293. doi:10.1016/j.patcog.2020.107293

Li, Q., Peng, H., Li, J., Xia, C., Yang, R., Sun, L., et al. (2021). A survey on text classification: from shallow to deep learning. arXiv preprint. Available at: https://arxiv.org/abs/2008.00364 (Accessed December 22, 2021).

Mete, B. R., and Ensari, T. (2019). "Flower classification with deep CNN and machine learning algorithms," in *2019 3rd international symposium on multidisciplinary Studies and innovative technologies (ISMSIT)* (USA: IEEE), 1–5.

Montavon, G., Lapuschkin, S., Binder, A., Samek, W., and Müller, K. R. (2017). Explaining nonlinear classification decisions with deep Taylor decomposition. *Pattern Recognit.* 65, 211–222. doi:10.1016/j.patcog.2016.11.008

Saiva, A., Abdool, P. S., Naismith, L. M., and Nirula, L. (2020). An immersive simulation to build empathy for geriatric patients with co-occurring physical and mental illness. *Acad. Psychiatry* 44, 745–750. doi:10.1007/s40596-020-01233-w

Schmitz, A., Ye, M., Shapiro, R., Yang, R., and Noehren, B. (2014). Accuracy and repeatability of joint angles measured using a single camera markerless motion capture system. *J. biomechanics* 47 (2), 587–591. doi:10.1016/j.jbiomech.2013.11.031

Senior, A. W., Evans, R., Jumper, J., Kirkpatrick, J., Sifre, L., Green, T., et al. (2020). Improved protein structure prediction using potentials from deep learning. *Nature* 577 (7792), 706–710. doi:10.1038/s41586-019-1923-7

Shi, L., Zhang, Y., Cheng, J., and Lu, H. (2020). Skeleton-based action recognition with multi-stream adaptive graph convolutional networks. *IEEE Trans. Image Process.* 29, 9532–9545. doi:10.1109/tip.2020.3028207

Shumway-Cook, A., Anson, D., and Haller, S. (1988). Postural sway biofeedback: Its effect on reestablishing stance stability in hemiplegic patients. *Archives Phys. Med. Rehabilitation* 69 (6), 395–400.

Smilkov, D., Thorat, N., Kim, B., Viégas, F., and Wattenberg, M. (2017). SmoothGrad: Removing noise by adding noise. arXiv preprint. Available at: https://arxiv.org/abs/1706.03825 (Accessed June 12, 2017).

Springenberg, J. T., Dosovitskiy, A., Brox, T., and Riedmiller, M. (2015). Striving for simplicity: The all convolutional net. arXiv preprint. Available at: https://arxiv.org/abs/1412.6806 (Accessed April 13, 2015).

Szczęsna, A., Błaszczyszyn, M., and Kawala-Sterniuk, A. (2020). Convolutional neural network in upper limb functional motion analysis after stroke. *PeerJ* 8, e10124. doi:10.7717/peerj.10124

Szegedy, C., Liu, W., Jia, Y., Sermanet, P., Reed, S., Anguelov, D., et al. (2015). "Going deeper with convolutions," in Proceedings of the IEEE conference on computer vision and pattern recognition, USA, June 21 1994 (IEEE), 1–9.

Vieweg, J., and Schaefer, S. (2020). How an age simulation suit affects motor and cognitive performance and self-perception in younger adults. *Exp. Aging Res.* 46 (4), 273–290. doi:10.1080/0361073x.2020.1766299

Watkins, C. A., Higham, E., Gilfoyle, M., Townley, C., and Hunter, S. (2021). Age suit simulation replicates in healthy young adults the functional challenges to balance experienced by older adults: An observational study. *BMJ Simul. Technol. Enhanc. Learn.* 7 (6), 581–585. doi:10.1136/bmjstel-2021-000867

Wolf, S., Loose, T., Schablowski, M., Döderlein, L., Rupp, R., Gerner, H. J., et al. (2006). Automated feature assessment in instrumented gait analysis. *Gait Posture* 23 (3), 331–338. doi:10.1016/j.gaitpost.2005.04.004

Xing, Y., and Zhu, J. (2021). Deep learning-based action recognition with 3D skeleton: A survey. *Caai Trans. Intell. Technol.* 6, 80–92. doi:10.1049/cit2.12014

Yao, G., Lei, T., and Zhong, J. (2019). A review of convolutional-neural-network-based action recognition. *Pattern Recognit. Lett.* 118, 14–22. doi:10.1016/j.patrec.2018.05.018

Yu, Y., Rashidi, M., Samali, B., Mohammadi, M., Nguyen, T. N., and Zhou, X. (2022b). Crack detection of concrete structures using deep convolutional neural networks optimized by enhanced chicken swarm algorithm. *Struct. Health Monit.* 21 (5), 2244–2263. doi:10.1177/14759217211053546

Yu, Y., Samali, B., Rashidi, M., Mohammadi, M., Nguyen, T. N., and Zhang, G. (2022a). Vision-based concrete crack detection using a hybrid framework considering noise effect. *J. Build. Eng.* 61, 105246. doi:10.1016/j.jobe.2022.105246

Yu, Y., Wang, C., Gu, X., and Li, J. (2019). A novel deep learning-based method for damage identification of smart building structures. *Struct. Health Monit.* 18 (1), 143–163. doi:10.1177/1475921718804132

Yue-Hei Ng, J., Hausknecht, M., Vijayanarasimhan, S., Vinyals, O., Monga, R., and Toderici, G. (2015). "Beyond short snippets: Deep networks for video classification," in Proceedings of the IEEE conference on computer vision and pattern recognition, USA, 17-19 June 1997 (IEEE), 4694–4702.

frontiers | Frontiers in Bioengineering and Biotechnology

TYPE Systematic Review
PUBLISHED 19 July 2023
DOI 10.3389/fbioe.2023.1192524

OPEN ACCESS

EDITED BY
Claudio Belvedere,
Rizzoli Orthopedic Institute (IRCCS), Italy

REVIEWED BY
Redha Taiar,
Université de Reims Champagne-Ardenne, France
Elbe De Villiers,
Stellenbosch University, South Africa

*CORRESPONDENCE
Qichang Mei,
meiqichang@nbu.edu.cn,
qmei907@aucklanduni.ac.nz

RECEIVED 04 April 2023
ACCEPTED 12 July 2023
PUBLISHED 19 July 2023

CITATION
Jiang H, Mei Q, Wang Y, He J, Shao E, Fernandez J and Gu Y (2023), Understanding foot conditions, morphologies and functions in children: a current review.
Front. Bioeng. Biotechnol. 11:1192524.
doi: 10.3389/fbioe.2023.1192524

Understanding foot conditions, morphologies and functions in children: a current review

Hanhui Jiang[1], Qichang Mei[1,2,3]*, Yuan Wang[1], Junhao He[1], Enze Shao[1], Justin Fernandez[3,4] and Yaodong Gu[1,2,3]

[1]Faculty of Sports Science, Ningbo University, Ningbo, China, [2]Research Academy of Grand Health, Ningbo University, Ningbo, China, [3]Auckland Bioengineering Institute, The University of Auckland, Auckland, New Zealand, [4]Department of Engineering Science, The University of Auckland, Auckland, New Zealand

This study provided a comprehensive updated review of the biological aspects of children foot morphology across different ages, sex, and weight, aiming to reveal the patterns of normal and pathological changes in children feet during growth and development. This review article comprised 25 papers in total that satisfied the screening standards. The aim was to investigate how weight changes, age and sex affect foot type, and gain a deeper understanding of the prevalent foot deformities that occur during children growth. Three different foot morphological conditions were discussed, specifically including the effect of sex and age differences, the effect of weight changes, and abnormal foot morphologies commonly documented during growth. This review found that sex, age, and weight changes would affect foot size, bony structure, foot posture, and plantar pressures during child growth. As a result of this biological nature, the children's feet generally exhibit neutral and internally rotated foot postures, which frequently lead to abnormal foot morphologies (e.g., flat foot, pronated foot, etc.). In the future, attention shall be paid to the causal factors leading to specific foot morphologies during the growth and development of children. However, sufficient evidence could not be provided due to a relatively short period of investigation and non-uniformed research methodology in the current literature. A more comprehensive and in-depth exploration is recommended to provide scientific evidence for the discovery of children foot development and personalized growth pattern.

KEYWORDS

children, foot morphology, foot posture, obesity, flatfoot, pes cavus

Introduction

The human foot, consisting of a total of 26 bones, is one of the most significant parts of the human body (Mauch et al., 2009) and crucial for locomotion. Foot bones and relevant muscles, ligaments, and tendons played significant roles in preserving the general form and ensured functions under static or dynamic conditions (Mauch et al., 2009). In general, the foot is the first to grow during early childhood (Bosch et al., 2009). According to the growth of the foot stopped first, followed by the long bones (the femur and tibia), and lastly the body (Mauch et al., 2009). Reported that the biological performance of the foot in healthy children varied with age (Manousaki et al., 2019). It was discovered that foot width decreased with growing foot length as a normalization of the foot width to length, and adjusting for proportional variations during foot development (Bruner et al., 2009).

As children grow, the foot morphology varied between sex as well. As reported in several studies (Cheng et al., 1997; El et al., 2006; Bruner et al., 2009; Muller et al., 2012; Waseda et al., 2014; Manousaki et al., 2019), the foot length (FL) of boys increased until at least the period of 15 years old, but girls showed scare increases beyond the period of 13 years old. The navicular height (NH) of the boy's foot exhibited a gradual increase starting at the at 12, followed by a rapid rise at 13, and eventually reached a plateau at 15. In contrast, females' NH rose gradually at 10, then quickly at 11, and finally hit a plateau at 16[9].

Weight fluctuations could affect foot morphology, in addition to other variables, such as age, sex, and height. In many developed nations, child obesity is currently at "epidemic" levels (Racette et al., 2003). For public health services across the world, obesity has become an increasing burden and worry for public health services across the world, which is a condition becoming more common, showing long-term medical and social effects (Wang and Lobstein, 2006). Overweight and obesity, according to the World Health Organization, are abnormal or excessive fat deposits that affect general health. Overweight is defined as a body mass index (BMI) for the age that is one standard deviation over the median of the WHO growth reference criteria for school-age children and adolescents (5–19 years). Obesity (de Onis et al., 2010) was defined as a BMI for the age that was more than two standard deviations over the WHO growth reference criterion median. Being overweight put more strain on the musculoskeletal system as kids get older, which could affect their mobility, level of physical activity, and ability to carry out age-appropriate daily tasks. Obesity could cause musculoskeletal discomfort in various body regions (Krul et al., 2009). In addition to musculoskeletal pain and discomfort, being overweight or obese also led to orthopedic issues in the foot and ankle, knee, hip, and spine (Frey and Zamora, 2007; Stovitz et al., 2008). Additionally, this change significantly raised the chance of fractures, growth issues, and developmental problems (Must and Strauss, 1999; Taylor et al., 2006). Being overweight resulted in improper plantar pressure distribution, foot anatomical changes, and foot balance issues (Fink et al., 2019; Park and Park, 2019). Reduced flexibility from the changed foot anatomy stopped children from running or walking activities (Must and Strauss, 1999; Taylor et al., 2006; Fink et al., 2019; Park and Park, 2019). Additionally, being overweight could affect the plantar arch by affecting the bone and ligament support and causing the medial longitudinal arch to collapse (Buldt et al., 2018). Flatfoot was one of the most often reported problems, according to various studies, that such change in the arch may result in related foot conditions (Sachithanandam and Joseph, 1995; Chen et al., 2013; Telfer and Bigham, 2019). However, the two were not discovered to be associated, indicating that there was no connection between obesity and flat feet, in a later set of investigations on weight change and flat feet (Song-Hua et al., 2017).

Flatfoot in quite common in children, and the prevalence was determined by several variables, and the predisposing factors are not only obesity (Abolarin et al., 2011). The prevalence of flat feet may decrease as individuals age (Rao and Joseph, 1992). People who had pes planus (flatfoot) typically exhibited midfoot pronation or hindfoot valgus. Pes planus is a condition in which the medial longitudinal arch (MLA) collapses with the midfoot touching the ground entirely or almost completely (LeGuern et al., 1997; Pfeiffer et al., 2006). The opposite of flatfoot is a pes cavus (high-arched foot), which would not drop with weight bearing. It is typically a deformity because of muscular imbalance, which may be skeletal or soft tissue, or both combined. The deformity is primarily located in the hindfoot, forefoot (midfoot and forefoot), or a combination of both, with varying degrees of severity. According to Zimon et al. (2011) the Charcot-Marie-Tooth (CMT) disease was responsible for half of the pes cavus (Brewerton et al., 1963). Research investigating the timing and progression of foot and ankle changes in children with CMT, as a genetic condition affecting the peripheral nervous system and worsens over time, revealed that approximately 1 in 2,500 individuals was affected by this condition. The weakening of the distal lower extremity, causing foot drop, sensory loss, lacking tendon reflection, muscular spasms, and inverted foot deformity was the typical symptom of CMT (Skre, 1974; Burns et al., 2009). These symptoms resulted in several functional deficits, such as foot discomfort, ankle instability, tripping, falling, poor balance, and foot pain, which would affect gait performance (Redmond et al., 2008a; Ferrarin et al., 2012; Dars et al., 2018). One major symptom was the arch deformity (LeGuern et al., 1997; Zambito et al., 2008), but not always presenting in children. Clinical study, involving 32 children diagnosed with CMT and ranging in age from 7 months to 15 years, reported that 72% exhibited bilateral high arches, while 13% had flat feet (Ghanem et al., 1996; Wines et al., 2005). The result reflected that arch disorders could affect foot morphology.

However, whether increased weight in children could increase the risk of flatfoot disease and the causation of specific foot morphology is unknown. The answer to this question has been controversial, and this study is aimed to discuss the effects of age, weight, and sex differences on foot morphology and focuses on the patterns of abnormal foot changes. The existing studies are still unable to provide sufficient evidence due to factors such as short study periods and non-uniformed research methodology. Therefore, the goal of this review study is to investigate the influence of sex, change in age and weight, and the causal factors leading to abnormal foot morphology. Knowledge could provide a scientific basis for children's growth and development and the discovery of individualized growth patterns for clinical diagnosis.

Materials and methods

The study focused on foot morphology changes in children, to discuss the normal and abnormal foot morphologies, thus summarizing the effect of sex, age, and weight differences on foot morphology, especially changes of flatfoot and high-arch foot in the midfoot. The range of this study was set at 0–18 years old according to the growth cycle of the children foot morphology (Bosch et al., 2009; Bruner et al., 2009; Mauch et al., 2009; Waseda et al., 2014; Manousaki et al., 2019), and foot changes caused by genetic or other diseases were excluded in the study. The review did not include data on human rights violations as contained in the Declaration of Helsinki, so ethics committee approval was not required.

TABLE 1 Inclusion and exclusion criteria.

	Inclusion	Exclusion
Research direction	(1) Studies in the English language; (2) Studies should focus on foot morphological changes; Prospective or retrospective studies at least involve changes in foot biomechanics or biological characteristics. In the study of abnormal foot form, the change characteristics relating injury risk to at least one biological characteristic, or plantar pressure; (3) Studies should focus on the tracking of changes in time	(1) The foot has undergone surgery; (2) Studies (apparently) published duplicate results from the same subject sample, the same results in previous publications obtained from the same group; biological features reported in the first study were excluded; (3) non-original articles (e.g., comments or conference articles); non-English articles; review; (4) no biological features of the foot
Subjects and age	children and adolescents; 0–18 years old; sample size> 1	Congenital foot disease; Other diseases lead to foot changes; Over 18 years old

Search strategy

Researchers used databases, including PubMed, Web of Science, and Google Scholar, to conduct a comprehensive literature search strategy. Since our study focused on changes in foot morphology during child development, each search string had to contain the following key words, 'Children's feet' and 'Morphology'. Therefore, the following key phrases were retrieved using Boolean search syntax, [(Children's foot) OR (Children's feet)] AND [(morphology) OR (shape) OR (foot posture)] AND (age) AND (sex), with 134 documents found; [(Children foot) OR (Children feet)] AND [(morphology) OR (shape) OR (foot posture)] AND (foot (Children foot) OR (Children feet) AND [(morphology) OR (shape) OR (foot posture)] AND [(obesity) OR (overweight)], 112 searches [(Children foot) OR (Children feet)] AND [(morphology) OR (shape) OR (foot posture)] AND [(flat foot) OR (Pes cavus) OR (CMT) OR (Foot Valgus)]. Thus, a total of 207 articles were found. The search was not limited to the publication year. Studies released before January 2023 were included. A total of 453 uncensored duplicates were considered for topics, abstracts, and keywords. All copies were removed using reference software (Endnote) and manually checked by the Investigators (HJ, QM, and YG) before the literature screening.

Inclusion and exclusion criteria

The screening conditions followed the framework construction method of (Linares-Espinos et al., 2018) and the Preferred Reporting Items for Systematic Evaluation and Meta-Analysis (PRISMA) guidelines (Moher et al., 2009).

Inclusion: (1) the language of study is English; 2) young children, children, and adolescents; 0–1 years of age; sample size >1; 3) studies focus on changes in foot morphology; prospective or retrospective studies involved at least changes in foot biomechanics or biological features; abnormal foot type studies should be about the characteristics of morphological changes and injury risk, biological features, plantar pressure; 4) studies should focus on tracer changes over time.

Exclusions: 1) congenital foot disease; other diseases causing foot changes; 18 years of age or beyond; 2) foot has undergone surgery; 3) studies that (apparently) published duplicate results from the same subject sample as in previous publications obtained from the same group; biological feature values reported in the first study were excluded; 4) non-original articles (e.g., comments or conference articles); non-English articles; review; and 5) did not address foot biological features.

Research risks

Although defining the age range of children between 0 and 18 years, there were still individual differences in studies and even external factors such as race, region, and environment that may affect foot changes. Table 1.

Result

Search results

The preliminary search data was 453 articles, and after deleting duplicates, the search yielded 238 articles. Among them, there were 64 articles about sex and age changes in children's feet. There were 52 articles on changes in the foot due to obesity and overweight. There were 122 articles on changes in specific foot types in children. After removing 100 articles from the keyword filtering in titles and abstracts; 32 studies with congenital foot disorders were excluded; 20 studies with other diseases causing foot changes were excluded; 9 studies with feet undergoing surgical treatment were excluded; 24 studies without foot biology were excluded; and 7 studies without foot morphology were excluded. Therefore, based on the screening eligibility criteria, a total of 32 studies were included for full-text screening. However, 3 studies did not meet the number of participants, 3 conference papers or reviews were excluded, and 1 study was retracted. Finally, 25 papers were found that satisfied the requirements for inclusion. Figure 1 illustrates the systematic search and selection process of the studies in detail.

Flat foot

The flattened MLA, showing that the foot type had smaller arch angle as well as greater CSI and SI factor volume, was the primary attribute of the flat foot. The typical z-value for the foot length was around −0.1 [51].

The findings from Table 2 showed that variations in skeletal architecture, foot posture, and plantar pressure distribution were influenced by differences in sex and age. These variations continued until maturity. Studies on infant foot posture have shown that boys often had flatter feet and lower arches than girls. With increasing

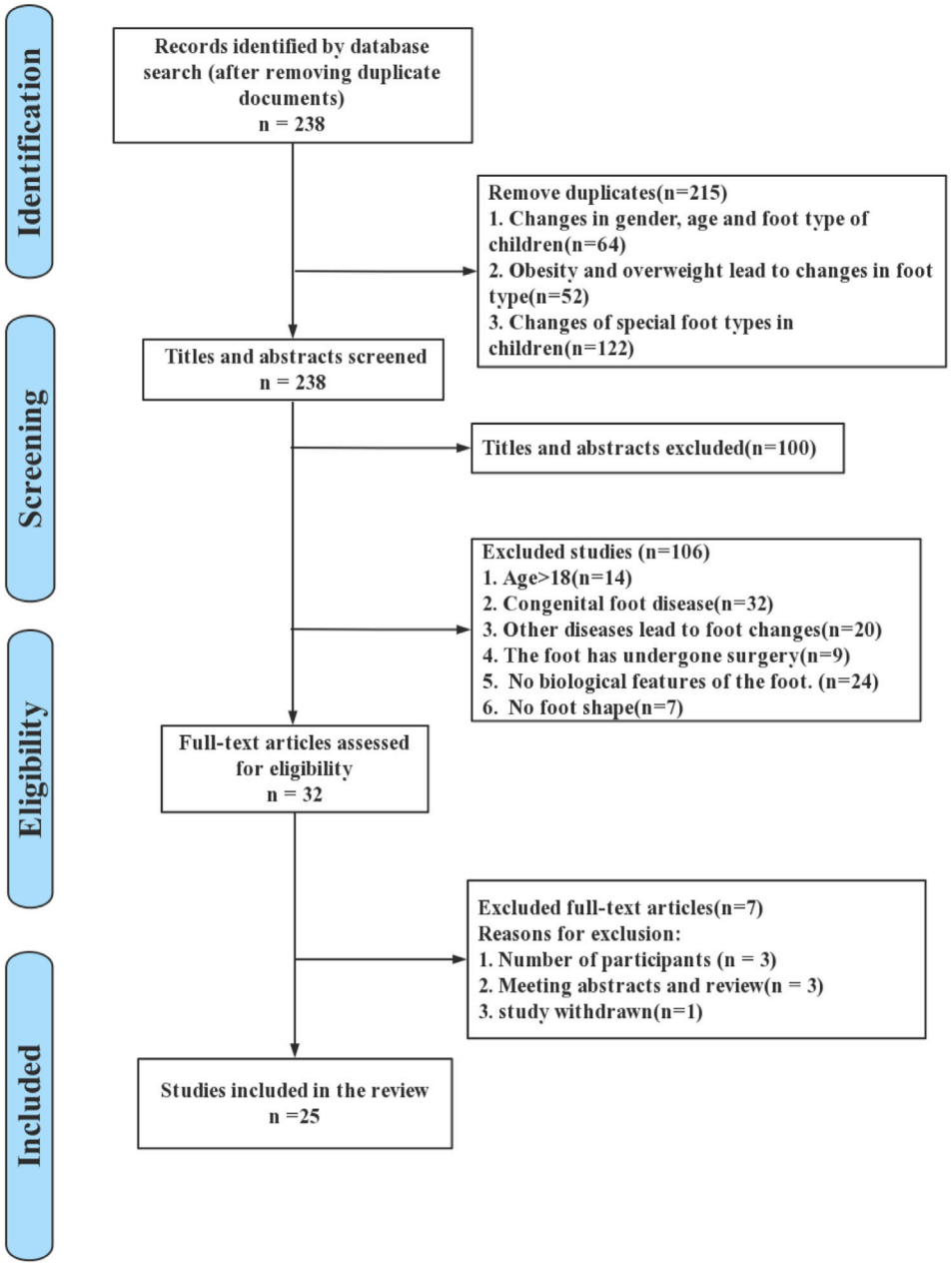

FIGURE 1
Illustration of literature search and selection process for the current study.

age, 46.7% of children aged 8–10 years had neutral feet and 53.3% had medially rotated feet (Al Kaissi et al., 2016). 56.9% of children aged 11 to 13 had neutral feet, 39.7% had medially rotated feet, and 3.4% had posteriorly rotated feet (Al Kaissi et al., 2016).

2. Ball width is the x-y distance between points B1 and B2 projected; The distance between the instep and heel, measured horizontally, is known as the instep distance. Ball girth: the area around the forefoot that corresponds to the B1, B2, and BC points. (B2: fifth metatarsal; B1: first metatarsal; BC points: projected on the z-axis. This is shown in Figure 2.)

From the results in Table 3, (Mauch et al., 2008), concluded that flatfoot occurred at a higher rate in overweight children than in other normal weight and ultralight weight. Although a considerable number of studies have concluded that weight gain during growth can indirectly or directly cause flat feet, (e.g., plantar pressure due to weight gain and flattening of the MLA), the foot prosthesis could maintain the longitudinal arch through compensatory mechanisms (Aboelnasr et al., 2019). As the central nervous system matures in children, individuals would have better motor performance and balance. This would result in better control of lower limb posture (Swallen et al., 2005). Notably, the ossification of foot structures that accompanied skeletal development would allow the arch to remain stable under weight-bearing in children (athirgamanathan et al., 2019). External tibial rotation from the in-toe position at birth to the

TABLE 2 Influence of Age and Sex on Foot type Changes

References	Participants	Sex	Age	Method	Sex result	Age result
Ana et al. (2017)	2569	1291 girls and 1278 boys	9-15	Researchers compiled data on children's age distribution and mean bilateral FPI-6 scores.	Males typically scored higher than girls did, and the left foot's FPI-6 score was substantially greater than the right foot's ($p < 0.05$).	The typical FPI-6 score for children and adolescents between the ages of 9 and 15 is 3.0-3.4, with neutral to slightly pronated foot morphology.
Al Kaissi et al. (2016)	150	71 girls and 79 boys	8-13	Determined BMI, weight, FPI and height in the bipedal, static, and relaxed position.	As compared to boys, a somewhat higher percentage of girls had pronated feet.	Children aged 8 to 10 had neutral feet in 46.7 percent of cases and pronated feet in 53.3 percent. 11.9% neutral, 39.7% pronation, and 3.4% pronation were seen in children aged 11 to 13.
Delgado-Abellan et al. (2014)	1031	534 girls and 497 boys	6-12	Measuring the barefoot condition. The boy or girl stood with both feet stilly with equally distributed weight on both feet during measurement.	The aged with the largest sex difference was 8 - 9 years old and 9 - 10 years old. Boys' feet were wider than girls' feet, and the most significant differences between boys and girls of the same age were in ball width, ball circumference, and instep height.	Through all ages evaluated the disparities in foot length increased linearly with height.
Stavlas et al. (2005)	5866	2931 girls and 2935 boys	6-17	The Harris and Beath foot printing mat was used to obtain dynamic (walking) bilateral footprints in every child	At the age of 7, 9, 11, 14 and 15, boys have a significantly higher proportion of low arch than girls of the same age	No systematic description
(Xu et al., 2018)	2543	1303 girls and 1240 boys	7-12	Record foot size through video capture system	At 7-8 and 8–9 years old for girls and 8–9 and 10–11 years old for boys, most measurements dramatically rose. The arch height, instep length and heel width of male and female had the largest increasing trend at the age of 7-12 years ($P < 0.05$). Most of the sex differences occurred at ages 8, 9, and 11.	In girls 7-8 and 8–9 years old and boys 8–9 and 10–11 years old, the majority of measurements dramatically rose. For both sexes, ages 7 to 12 years, the largest increases were seen in arch height, instep length, and heel width.
Carvalho et al. (2017)	1394	921 girls and 473 boys	10-14	determined weight, height, BMI, and FPI in the bipedal, static, and relaxed position.	With the right foot, boys scored higher than girls.	There were age differences between 11- and 13-year-old for the left foot. The 11-year-old group showed a greater tendency to pronate their feet.
Vrdoljak (2017)	2745	1370 girls and 1375 boys	2-7	Six age categories were used to separate the population of kids. The length of the foot was measured using a measuring tape, while shape was determined clinically.	In all age and sex groups, boys' and girls' left and right feet were identical in length and form.	The second and third years were when the foot grow the fastest. The foot grow by around 1 cm a year from the third to the sixth year.

Remarks: Indicators and scoring standards for the FPI-6 test: (1) Foot posture indexes (FPI-6) Palpation of the talar head; (2) symmetry of the supra- and infra-lateral malleolar curvature; (3) position of the calcaneus in the frontal plane; (4) prominence near the talonavicular joint; (5) congruence of the medial longitudinal arch, and forefoot abduction or adduction on the rearfoot are other examination criteria. The total FPI-6 score ranged from -12 to 12, with each FPI-6 item being graded on a scale of -2 to 2. Based on their FPI-6 scores, the individuals were divided into three groups: 1) 0 to 5 is considered normal; 2) >6 is considered pronated; 3) < -1 is considered supinated (Redmond et al., 2008b).

out-toe position during growth would result in a concomitant decrease in the morphology of the hindfoot exostosis (Atik and Ozyurek, 2014).

From the above analysis, it was clear that flatfoot may not be significantly correlated with changes in body mass index (Hawke et al., 2016; Aboelnasr et al., 2019). In other words, weight gain may not lead to flatfoot. (Hawke et al., 2016). found that children with greater internal rotation of the foot exhibited greater lower limb and overall body flexibility in a study of a sample of healthy asymptomatic children aged 7–15 years. Also, the findings of this study corroborated the discovery of a connection between flat feet and joint flexibility (Pfeiffer et al., 2006).

High-arch foot

Foot arch deformities were rarely seen in the early childhood population (under 3 years of age). However, as children grow, the navicular bone, the final foot bone to ossify in children between the ages of two and five, was characterized by its fallibility and formative nature. As a result, it became a crucial consideration when evaluating the foot posture of four-year-old kids. Foot navicular ossification occurred later in boys than in girls, while the prevalence of pes cavus increased highly in boys between the period of 4 and 13 years, but the prevalence of pes cavus was frequent in the girl population (Alexander and Johnson, 1989;

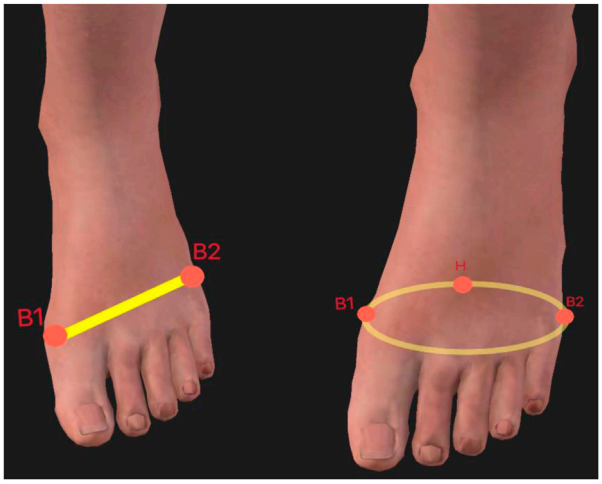

FIGURE 2
Illustration of Ball width (left) and Ball girth (right).

Aminian and Sangeorzan, 2008; Wozniacka et al., 2013; Chang et al., 2014).

Pes cavus was a common foot disorder in children while this disorder had an overall inversion of the foot, projection of the lateral edges of the foot, and inversion of the heel during standing (Wicart, 2012). This was generally caused by the deformity of pes cavus, which was cavus foot, a simple morphological feature but a normal variant often found in healthy individuals and growing children (Alexander and Johnson, 1989; Schwend and Drennan, 2003; Chang et al., 2014). While the other condition was direct cavus foot, which was the result of foot deformity and often only affected the sagittal plane (forefoot, hindfoot, or both) occurred only in the sagittal plane (forefoot, hindfoot, or both). Direct cavus foot may be associated with multiple causes, and several studies have shown that the condition was due to structural problems in the brain, spinal cord, peripheral nerves, or foot, while neurological disorders were seen primarily in the posterior cavus foot (Schwend and Drennan, 2003; Wicart, 2012). CMT was the most common neurologically caused disorder in this condition (Burns et al., 2009). The risk of deterioration in childhood can generally be averted with the right conservative care (orthotic realignment of the foot) (Wicart, 2012).

Discussion

Influence of sex and age differences

Changes in foot morphology in children were gradual over time, particularly the growth of foot length and width. The critical age for foot development was 6 years, and (Waseda et al., 2014). found that children's foot length increased rapidly from the age of 6 years. Changes in foot morphology characteristics were minimal during the age interval of 10–11 years and stabilized at 12 years (Cheng et al., 1997; El et al., 2006; Catan et al., 2020). Cheng et al. (Cheng et al., 1997) found that children's foot length and width increased by an average of 8–10 mm per year between the ages of 6–12 years. (Muller et al., 2012). reported that the length and width of the foot grew with age, it was demonstrated that the growth rate of foot length practically hit a plateau at 13 years for girls and 14 years for boys at that point (Evans et al., 2012; Waseda et al., 2014).

In terms of sex differences, the change in the foot was comparable, however, there could be variations between 8 and 10 years old (Delgado-Abellan et al., 2014). According to (Cheng et al., 1997), until the age of 3 years, variations in foot length and width in males were comparable to those in girls. Boys' feet development increased after the age of 3 years. At the age of 9, boys and girls showed considerable disparities, according to research by Bosch, Gerss, and Rosenbaum (Bosch et al., 2010). Nevertheless, no information regarding foot length was provided in this investigation. (Stavlas et al., 2005). found that the average annual foot length growth rate was 4.3% for boys and 3.9% for girls. The study also revealed that the fastest growth rates were observed at ages 8-9 and 10-11 for boys, and ages 7-8 and 8-9 for girls. Thus, peak growth rates occur earlier in girls than in boys. The age of 7–12 years was the stage of rapid growth in foot arch height among Chinese boys and girls. Studies showed that the navicular height of boys' feet would increase from 6 to 13 years of age (Szczepanowska-Wolowiec et al., 2021). The navicular or talar navicular joint line was often used to determine the height of medial longitudinal arch. Between the ages of 8 and 13, the arch height of girls rose. The arch height ratio in boys was practically flat until age 11 but considerably rose from age 11 to 13. The formula for the arch height ratio is AHR (%) = navicular height*100/ foot length. Girls' arch height ratios were largely flat until age 10 but considerably rose between age 10 and 12.

Foot morphology changed with growth and development. (Ana et al., 2017). performed the Foot Posture Index (FPI) test for both feet among 2,569 children aged 9–15 years during 2016–2018. The FPI was a clinical diagnostic tool designed to quantify the grade of foot position (posture), such as neutral, internally rotated, or posteriorly rotated. The index was developed using a simple six-factor method to assess foot morphology, to obtain simple and quantitative postures (Al Kaissi et al., 2016). It was reported that girls had a higher percentage of rotated feet than boys, and boys presented higher FPI-6 scores than girls, suggesting that boys had flatter feet and that children and adolescents aged 9–15 years had neutral or mildly internally rotated foot morphology. (Heidi and Priv, 2015). conducted a study on foot morphology in infants who just started walking independently. The study showed that boys' feet were flatter and had a lower arch than girls' feet, indicating that males were more likely than girls to have higher FPI-6 scores from an early age.

In other words, the effect of sex differences on foot morphology may be present since birth, and such a condition may exist during growth. The effect of age differences on the foot was also presented from the time of birth, and because of the age difference, the foot width and length grew at different rates, which was a dynamic process. (Al Kaissi et al., 2016). observed differences between children and adult populations, with children generally presenting a neutral foot and internally rotated foot stance, and (Wilkerson and Mason, 2000) found that adults generally presented a neutral foot stance. The study discovered that with increased muscle mass, myelination of motor neurons, and subsequently enhanced muscular strength from puberty forward, the medial longitudinal arch (MLA) had stronger support. This function would contribute to the development of a neutral foot.

In studies of normal foot type, characteristics of foot morphology could be evaluated by footprint, foot index, FPI,

TABLE 3 Influence of Obesity and Overweight on Foot Types

References	Participants	Age	Category	Method	Result
Agnieszka and Edyta, (2015)	207	4-6	OW	Measurements included body weight, height, body mass index, and Clarke's and gamma angles. Correlations between sex, nutritional health, and variations in foot arch height were also examined.	The proportion of overweight and obese boys and girls increased between the ages of 4 and 6, and those with extra body weight tended to have collapsed medial longitudinal arches of the foot.
Stewart et al. (2018)	3713	3-18	OB	Analysis of pediatric foot dimensions of children's feet (foot length [FL] and foot width [FW])	When compared to their obese counterparts, FL and FW were substantially shorter in male and female patients of normal weight.
Mauch et al. (2008)	2887	2-14	N, UW, OW	Twelve relevant 3D foot measures were taken while the feet were in an upright bipedal position using a 3D foot scanner. The age, sex, height, and weight of the children were also recorded.	Among underweight children, there was a larger percentage of thin feet (65-7%) compared to flat (4-50%), robust (89-100%), and short (21–70%) feet. The disparities were considerably more obvious in the overweight kids. Age-related increases in robustness (69-337%) and flat feet (53-128%) were seen.
da Rocha et al. (2014)	40	6-10	N, OW	Whether individuals were standing on one foot or two feet, the researchers measured the foot sensitivity and plantar pressure and compared the results between the feet and legs of obese and non-obese persons.	Children who are overweight have fewer sensitive feet and more plantar pressure. In addition, sensitivity in various foot areas was comparable in obese and non-obese children.
Gijon-Nogueron et al. (2017)	1798	6-12	OW, OB	Each had their height and weight assessed, and the body mass index (BMI) was computed. The foot posture is described using the foot posture index (FPI).	Body mass does not appear to have a significant impact on static foot posture in children between the ages of 6 and 12.
Jimenez-Ormeno et al. (2013)	1032	6-12	N, OW, OB	The body mass index was determined using measurements of height and weight. Obese, overweight, and normal-weight children were identified. An instatic, three-dimensional foot digitizer was used to measure the foot morphology.	Overweight and obese kids develop bigger feet than their normal-weight peers.
Escalona-Marfil et al. (2022)	575	5-10	N, OW, OB, UW	Foot posture and form evaluation (FPI) and body composition measurement	The findings of this study show that children with normal weight, children who are overweight or obese, as well as children who are underweight, have different foot measurements (FPI, AHI, and MFW).

Remarks: 1. OW=overweight; OB=obeity; N=normal; UW=under weight

manual measurement, and camera acquisition. A large sample of data and studies reported (Alexander and Johnson, 1989; Aminian and Sangeorzan, 2008; Heidi and Priv, 2015; Hawke et al., 2016; Escalona-Marfil et al., 2022) that incorrect gait and walking postures and related external factors were the causes of foot disorders in children.

Influence of body weight variations

Apart from the above factors of age and sex, variations in body weight and height could also lead to changes in the biological structure of the foot (Waseda et al., 2014; Bailly et al., 2022). Being overweight has implications for foot structure, including alterations of anatomical structure, abnormalities in plantar pressure distribution, and balance (Bruner et al., 2009; Waseda et al., 2014; Manousaki et al., 2019; Bailly et al., 2022). BMI is a popular tool for assessing overweight and obesity as a straightforward measure of the connection between weight and height. The overweight individuals have higher ratios of arch collapse due to thicker layers of adipose tissue (Swallen et al., 2005). Medial section of the plantar foot in a group of 8-year-old children had denser adipose tissue, and the height of longitudinal arch was lower in these observations (Wilkerson and Mason, 2000). (Agnieszka and Edyta, 2015) found that being overweight had a negative effect on the longitudinal arch in preschool children. In preschoolers, no correlation between BMI and the height of the transverse arch was found, but in preschoolers of normal weight, the height of longitudinal arch was significantly increased. In contrast, a trend towards the decreasing longitudinal arch height in overweight and obese boys and girls was found. (da Rocha et al., 2014). concluded that foot sensitivity was lower in obese children than non-obese children. Obese children showed similar sensitivity in all foot regions, while non-obese children were able to differentiate the intensities of touch on different regions. Studies showed that higher sensitivity to touch was associated with higher receptor density, which decreased with age. Therefore, the lower sensitivity in obese children may be due to lower receptor density per surface area unit (Kozłowska, 1988), but this is only theory at this time, and no particular experimental verification of this assumption has been carried out. Future studies may consider examining the receptor density of foot surface area in obese, overweight, normal, and ultralight children as per age group and BMI groups. (Lee et al., 2013).

Overweight boys during childhood may have bigger feet, indicating that obesity may be a major factor affecting foot growth (as determined by the size recorded in the available data set). The structural characteristics of the foot in obese children were

wider and thicker, which may increase the peak plantar pressure and vertical peak pressure during gait. Lower footprint angle (FA), higher Chippaux-Smirak index (CSI), higher plantar pressure (Lobstein and Frelut, 2003), higher arch index (AI), and greater footprint area (Stovitz et al., 2008) were found in obese children feet. Children with high body weight may show less degree of variations in the foot morphology or the changes might be gradual or subtle. Thus, (Jimenez-Ormeno et al., 2013), suggested that being overweight may be an important factor affecting foot development in prepubescent students at school. (Mauch et al., 2008). found that low percentage of flatfoot was observed in underweight children. However, the likelihood of flat feet rises with age, although this is highly documented in overweight children.

Obesity would lead to the compensation of foot arch, and either indirectly or directly contribute to the development of flat feet (Sachithanandam and Joseph, 1995; Chen et al., 2013; Song-Hua et al., 2017; Buldt et al., 2018; Telfer and Bigham, 2019). However, a recent study of 728 children between 3 and 15 years old found a relationship between weight and foot morphology (Evans and Karimi, 2015). While Evans (Evans and Karimi, 2015) refuted that heavier children had flatter feet, and further emphasized no association between increased body weight and flatfeet among children. Whilst this statement contradicted with several studies (Sachithanandam and Joseph, 1995; Lobstein and Frelut, 2003; Chen et al., 2013; Telfer and Bigham, 2019), which may be a convergent prediction of the foot morphology in overweight and obese children. Currently, weight reduction was not employed as a treatment in the traditional treatment of flat feet due to obesity. Therefore, it was suggested that further follow-up studies should be conducted focusing on this issue. Yet, alterations in foot morphology brought on by excess weight may cause discomfort or pain and may increase reluctance to exercise, which might result in body weight growth. Considering the development of healthy children, increased attention is still required, especially for physical activity and diet control.

Abnormal foot type

Pes planus (flat foot)

The influence of weight, sex, and age was discussed for the development of flat feet. (Evans et al., 2012). found that between the age of 5–10 years, girls had higher arches than boys. (Ana et al., 2017). investigated 2,569 Japanese kids between the age of 9–15 using the FPI-6, discovering that kids exhibited neutral or moderate internal rotation in standing posture, with a mean score of 3–3.4. Based on a sample of 140 children aged 7–10 years, (Aboelnasr et al., 2019), used FPI-6 screening to identify a sample of 31 kids with flat feet. Basic anthropometric measurements were compared between subjects designated with flat feet, reporting that waist size was associated with foot morphology (although not significantly), but conversely, a "fatter" waist was less associated with flat feet. In other words, weight gain and flat feet were unrelated. In a study by (Hawke et al., 2016), basic data on 30 healthy, asymptomatic kids aged 7 to 15 were gathered, including height and weight (BMI), Beighton score, Foot Posture Index-6 (FPI), and lower extremity evaluation. A correlation between flat feet and joint flexibility was discovered, and internal foot rotation was associated with lower limb and overall body flexibility in healthy and asymptomatic children, but not related with the ankle flexibility (Aboelnasr et al., 2019), which was consistent with a previous statement (Hawke et al., 2016). This finding supported that neutral and internally rotated foot postures predominated over other foot postures, as reported by Evans (Evans et al., 2012) that being overweight would not cause flat feet.

The current review discussed flatfoot based on asymptomatic participants, focusing on the effect of growth and development on the biological shape of the children foot and the potential cause of flatfoot.

Pes cavus (high arch)

Cavus foot was used to describe the foot type that had high arch as a typical characteristic. High arch may be caused by a high pitch angle in the hindfoot, hyperflexion of the plantar aspect in the forefoot, or hyperflexion of the midfoot. In complex cases, the cavus foot may be driven by a narrow pitch-heel angle and a possible torsional component in the midfoot. The components of the venous cavity showed increased pronation and pitch of the hindfoot, plantar flexion of the midfoot, and pronation and inversion of the forefoot. The shape of the foot cavity is associated with changes in foot mechanics.

(Alexander and Johnson, 1989) stated that arch deformities were rarely observed in young children (under 3 years) but may occur as children grow. The etiology could be attributed to problems in the brain, spinal cord, peripheral nerves, or foot structure. When motor imbalances occurred before skeletal maturation, the healthy bone morphology may result in substantial changes. When cavernous cavities were acquired after skeletal maturation, there may be little or no change in foot morphology. Two-thirds of adults with symptomatic cavus foot have an underlying neurological condition. CMT disease was the most prevalent. The findings of (Wozniacka et al., 2013) indicated that a high prevalence of high arched feet. Those with symptomatic cavus feet were two-thirds more likely to have a neurological disorder. The most common disease among children and teenagers between the ages of 4 and 13 was the CMT disease. On the right foot, 66.5% of children had high arches, compared to 61.4% on the left, and girls were more likely to have high arches than boys. (Chang et al., 2014). studied static foot morphology, including foot navicular height and arch volume during sitting and standing in 27 children aged 2–6 years. The study found that the arch volume index (AVI) was significantly correlated with pressure changes in the midfoot (Stovitz et al., 2008), which implied that AVI measured in the static position could be correlated with dynamic changes in mid-foot lower-foot loading. However, there was no correlation between AVI and mean pressure and force throughout the stance phase (Evans et al., 2012). As the arch height decreasing, the pressure and force on the medial metatarsal and midfoot plantar increased (Villarroya et al., 2009). Compared with NH, the correlation between arch volume and foot pressure distribution is higher, so the cause of high arch formation may come from changes in foot structure (Putti et al., 2010). Foot structure may alter over time because of weight fluctuations, foot growth, and development, which could eventually cause musculoskeletal disease to manifest.

The studies included in the current review were based on asymptomatic participants, comparing to the different foot types and those asymptomatic individuals who seem healthy but have higher risks of musculoskeletal diseases.

Conclusion

This review study mainly investigated three issues, including (1) how age and sex variations affect changes in foot morphology, (2) the effect of weight changes on foot morphology, and (3) common abnormal foot morphology during the growth and development of children. Key finding of this review was that sex, age, and weight change would affect foot size, bony structure, foot posture, and plantar pressures during childhood. As per this biological nature, children feet generally exhibit neutral and internally rotated foot postures, which frequently contribute to abnormal foot morphologies (e.g., flat feet and high-arched feet).

This review comprehensively synthesized several published evidence in previous studies, while future studies may consider focusing on the contribution of other factors to specific foot shapes during child development (in addition to the studies presented here) and further expand the information of the research and application of foot morphologies and conditions in children, thus providing comprehensive knowledge for healthy children development.

Data availability statement

The original contributions presented in the study are included in the article/Supplementary material, further inquiries can be directed to the corresponding author.

Author contributions

Conceptualization: HJ, QM, and YG; methodology: HJ, QM, YW, JH, and ES; writing—original draft preparation: HJ, QM, YW, and ES; writing—review and editing: JF and YG; supervision: QM and YG; project administration: QM and YG; funding acquisition: QM and YG. All authors contributed to the article and approved the submitted version.

Funding

This study was supported by the National Natural Science Foundation of China (No. 12202216), Ningbo Natural Science Foundation, Ningbo University Teaching and Research project (JYXM2023051), SRIP project of Ningbo University (No. 2023SRIP0501, No. 2023SRIP0510 and No. 2023SRIP0502) and K. C. Wong Magna Fund in Ningbo University.

Conflict of interest

The authors declare that the research was conducted in the absence of any commercial or financial relationships that could be construed as a potential conflict of interest.

Publisher's note

All claims expressed in this article are solely those of the authors and do not necessarily represent those of their affiliated organizations, or those of the publisher, the editors and the reviewers. Any product that may be evaluated in this article, or claim that may be made by its manufacturer, is not guaranteed or endorsed by the publisher.

References

Aboelnasr, E. A., El-Talawy, H. A., Abdelazim, F. H., and Hegazy, F. A. (2019). Sensitivity and specificity of normalized truncated navicular height in assessment of static foot posture in children aged 6-12 years. *Hong Kong Physiother. J.* 39, 15–23. doi:10.1142/S1013702519500021

Abolarin, T., Aiyegbusi, A., Tella, A., and Akinbo, S. (2011). Predictive factors for flatfoot: The role of age and footwear in children in urban and rural communities in South West Nigeria. *Foot (Edinb)* 21, 188–192. doi:10.1016/j.foot.2011.07.002

Agnieszka, J. S., and Edyta, M. (2015). Effect of excessive body weight on foot arch changes in preschoolers. *J. Am. Podiatric Med. Assoc.* 105, 313–319. doi:10.7547/14-101.1

Al Kaissi, A., Kenis, V., Chehida, F., Hofstaetter, J., Grill, F., and Ganger, R. (2016). Lower limbs deformities in patients with McCune-Albright syndrome: Tomography and treatment. *Afr. J. Paediatr. Surg. AJPS* 13, 125–130. doi:10.4103/0189-6725.187808

Alexander, I. J., and Johnson, K. A. (1989). Assessment and management of pes cavus inn Charcot-Marie-Tooth disease. *Clin. Orthop.* 246, 273–281. doi:10.1097/00003086-198909000-00038

Aminian, A., and Sangeorzan, B. J. (2008). The anatomy of cavus foot deformity. *Foot Ankle Clin.* 13, 191–198. doi:10.1016/j.fcl.2008.01.004

Ana, M., Morente-Bernal, M. F., Román-Bravo, P. D., Saucedo-Badía, J. F., Alonso-Ríos, J. A., and Montiel-Luque, A. (2017). Influence of age, sex, and anthropometric determinants on the foot posture index in a pediatric population. *J. Am. Podiatric Med. Association.March* 107 (2), 124–129. doi:10.7547/14-097

athirgamanathan, B., Silva, P., and Fernandez, J. (2019). Implication of obesity on motion, posture and internal stress of the foot: An experimental and finite element analysis. *Comput. Methods Biomech. Biomed. Engin* 22, 47–54. doi:10.1080/10255842.2018.1527320

Atik, A., and Ozyurek, S. (2014). Flexible flatfootness. *North. Clin. Istanbul* 1, 57–63. doi:10.14744/nci.2014.29292

Bailly, R., Lempereur, M., Thepaut, M., Pons, C., Houx, L., and Brochard, S. (2022). Relationship between 3D lower limb bone morphology and 3D gait variables in children with uni and bilateral Cerebral Palsy. *Gait Posture* 92, 51–59. doi:10.1016/j.gaitpost.2021.11.011

Bosch, K., Gerss, J., and Rosenbaum, D. (2010). Development of healthy children's feet-Nine-year results of a longitudinal investigation of plantar loading patterns. *Gait Posture* 32, 564–571. doi:10.1016/j.gaitpost.2010.08.003

Bosch, K., Nagel, A., Weigend, L., and Rosenbaum, D. (2009). From "first" to "last" steps in life - pressure patterns of three generations. *Clin. Biomech.* 24, 676–681. doi:10.1016/j.clinbiomech.2009.06.001

Brewerton, D. A., Sandifer, P. H., and Sweetnam, D. R. (1963). IDIOPATHIC" pes cavus: AN investigation into its aetiology. *Br. Med. J.* 2, 659–661. doi:10.1136/bmj.2.5358.659

Bruner, E., Mantini, S., Guerrini, V., Ciccarelli, A., Giombini, A., Borrione, P., et al. (2009). Preliminary shape analysis of the outline of the baropodometric foot: Patterns of covariation, allometry, sex and age differences, and loading variations. *J. Sports Med. Phys. Fit.* 49, 246–254.

Buldt, A. K., Allan, J. J., Landorf, K. B., and Menz, H. B. (2018). The relationship between foot posture and plantar pressure during walking in adults: A systematic review. *Gait Posture* 62, 56–67. doi:10.1016/j.gaitpost.2018.02.026

Burns, J., Ryan, M. M., and Ouvrier, R. A. (2009). Evolution of foot and ankle manifestations in children with CMT1A. *Muscle & Nerve* 39, 158–166. doi:10.1002/mus.21140

Carvalho, B. K. G., Penha, P. J., Penha, N. L. J., Andrade, R. M., Ribeiro, A. P., and João, S. M. A. (2017). The influence of gender and body mass index on the FPI-6 evaluated foot posture of 10- to 14-year-old school children in são paulo, Brazil: A cross-sectional study. *J. foot ankle Res.* 10, 1. doi:10.1186/s13047-016-0183-0

Catan, L., Amaricai, E., Onofrei, R. R., Popoiu, C. M., Iacob, E. R., Stanciulescu, C. M., et al. (2020). The impact of overweight and obesity on plantar pressure in children and adolescents: A systematic review. *Int. J. Environ. Res. public health* 17, 6600. doi:10.3390/ijerph17186600

Chang, H. W., Chieh, H. F., Lin, C. J., Su, F. C., and Tsai, M. J. (2014). The relationships between foot arch volumes and dynamic plantar pressure during midstance of walking in preschool children. *PloS one* 9, e94535. doi:10.1371/journal.pone.0094535

Chen, K. C., Tung, L. C., Yeh, C. J., Yang, J. F., Kuo, J. F., and Wang, C. H. (2013). Change in flatfoot of preschool-aged children: A 1-year follow-up study. *Eur. J. Pediatr.* 172, 255–260. doi:10.1007/s00431-012-1884-4

Cheng, J. C. Y., Leung, S. S., Leung, A. K., Guo, X., Sher, A., and Mak, A. F. (1997). Change of foot size with weightbearing - a study of 2829 children 3 to 18 years of age. *Clin. Orthop. Relat. Res.* 342, 123–131. doi:10.1097/00003086-199709000-00019

da Rocha, E. S., Klein Bratz, D. T., Gubert, L. C., de David, A., and Carpes, F. P. (2014). Obese children experience higher plantar pressure and lower foot sensitivity than non-obese. *Clin. Biomech.* 29, 822–827. doi:10.1016/j.clinbiomech.2014.05.006

Dars, S., Uden, H., Banwell, H. A., and Kumar, S. (2018). The effectiveness of non-surgical intervention (foot orthoses) for paediatric flexible pes planus: A systematic review: Update. *PloS one* 13, e0193060. doi:10.1371/journal.pone.0193060

de Onis, M., Blossner, M., and Borghi, E. (2010). Global prevalence and trends of overweight and obesity among preschool children. *Am. J. Clin. Nutr.* 92, 1257–1264. doi:10.3945/ajcn.2010.29786

Delgado-Abellan, L., Aguado, X., Jimenez-Ormeno, E., Mecerreyes, L., and Alegre, L. M. (2014). Foot morphology in Spanish school children according to sex and age. *Ergonomics* 57, 787–797. doi:10.1080/00140139.2014.895055

El, O., Akcali, O., Kosay, C., Kaner, B., Arslan, Y., Sagol, E., et al. (2006). Flexible flatfoot and related factors in primary school children: A report of a screening study. *Rheumatol. Int.* 26, 1050–1053. doi:10.1007/s00296-006-0128-1

Escalona-Marfil, C., Prats-Puig, A., Ortas-Deunosajut, X., Font-Lladó, R., Ruiz-Tarrazo, X., and Evans, A. M. (2022). Children's foot parameters and basic anthropometry - do arch height and midfoot width change? *Eur. J. Pediatr.* 182, 777–784. doi:10.1007/s00431-022-04715-1

Evans, A. M., and Karimi, L. (2015). The relationship between paediatric foot posture and body mass index: Do heavier children really have flatter feet? *J. foot ankle Res.* 8, 46. doi:10.1186/s13047-015-0101-x

Evans, A. M., Rome, K., and Peet, L. (2012). The foot posture index, ankle lunge test, Beighton scale and the lower limb assessment score in healthy children: A reliability study. *J. foot ankle Res.* 5, 1. doi:10.1186/1757-1146-5-1

Ferrarin, M., Bovi, G., Rabuffetti, M., Mazzoleni, P., Montesano, A., Pagliano, E., et al. (2012). Gait pattern classification in children with Charcot-Marie-Tooth disease type 1A. *Gait Posture* 35, 131–137. doi:10.1016/j.gaitpost.2011.08.023

Fink, P. W., Shultz, S. P., D'Hondt, E., Lenoir, M., and Hills, A. P. (2019). Multifractal analysis differentiates postural sway in obese and nonobese children. *Mot. Control* 23, 262–271. doi:10.1123/mc.2016-0085

Frey, C., and Zamora, J. (2007). The effects of obesity on orthopaedic foot and ankle pathology. *Foot Ankle Int.* 28, 996–999. doi:10.3113/fai.2007.0996

Ghanem, I., Zeller, R., and Seringe, R. (1996). Foot deformities in children with hereditary motor and sensory neuropathy. *Revue De Chir. Orthop. Reparatrice De L Appareil Moteur* 82, 152–160.

Gijon-Nogueron, G., Montes-Alguacil, J., Martinez-Nova, A., Alfageme-Garcia, P., Cervera-Marin, J. A., and Morales-Asencio, J. M. (2017). Overweight, obesity and foot posture in children: A cross-sectional study. *J. Paediatr. Child Health* 53, 33–37. doi:10.1111/jpc.13314

Hawke, F., Rome, K., and Evans, A. M. (2016). The relationship between foot posture, body mass, age and ankle, lower-limb and whole-body flexibility in healthy children aged 7 to 15 years. *J. foot ankle Res.* 9, 14. doi:10.1186/s13047-016-0144-7

Heidi, U., and Priv, D. D. (2015). Gender-specific differences of the foot during the first year of walking.*FOOT ANKLE Int.* 12, 582–587. doi:10.1177/107110070402500812

Jimenez-Ormeno, E., Aguado, X., Delgado-Abellan, L., Mecerreyes, L., and Alegre, L. M. (2013). Foot morphology in normal-weight, overweight, and obese schoolchildren. *Eur. J. Pediatr.* 172, 645–652. doi:10.1007/s00431-013-1944-4

Kozłowska, A. (1988). Studying tactile sensitivity - population approach. *Anthropol. Rev.* 61, 3–30. doi:10.18778/1898-6773.61.01

Krul, M., van der Wouden, J. C., Schellevis, F. G., van Suijlekom-Smit, L. W. A., and Koes, B. W. (2009). Musculoskeletal problems in overweight and obese children. *Ann. Fam. Med.* 7, 352–356. doi:10.1370/afm.1005

Lee, K. M., Chung, C. Y., Sung, K. H., Kim, T. W., Lee, S. Y., and Park, M. S. (2013). Femoral anteversion and tibial torsion only explain 25% of variance in regression analysis of foot progression angle in children with diplegic cerebral palsy. *J. neuroengineering rehabilitation* 10, 56. doi:10.1186/1743-0003-10-56

LeGuern, E., Gouider, R., Mabin, D., Tardieu Bs, S., Birouk, N., Parent, P., et al. (1997). Patients homozygous for the 17p11.2 duplication in Charcot-Marie-Tooth type 1A disease. *Ann. Neurology* 41, 104–108. doi:10.1002/ana.410410117

Linares-Espinos, E., Hernández, V., Domínguez-Escrig, J., Fernández-Pello, S., Hevia, V., Mayor, J., et al. (2018). Methodology of a systematic review. *Actas Urol. Esp. Engl. Ed.* 42, 499–506. doi:10.1016/j.acuro.2018.01.010

Lobstein, T., and Frelut, M. L. (2003). Prevalence of overweight among children in Europe. *Obes. Rev.* 4, 195–200. doi:10.1046/j.1467-789x.2003.00116.x

Manousaki, E., Esbjornsson, A. C., Mattsson, L., and Andriesse, H. (2019). Correlations between the Gait Profile Score and standard clinical outcome measures in children with idiopathic clubfoot. *Gait Posture* 71, 50–55. doi:10.1016/j.gaitpost.2019.04.009

Mauch, M., Grau, S., Krauss, I., Maiwald, C., and Horstmann, T. (2009). A new approach to children's footwear based on foot type classification. *Ergonomics* 52, 999–1008. doi:10.1080/00140130902803549

Mauch, M., Grau, S., Krauss, I., Maiwald, C., and Horstmann, T. (2008). Foot morphology of normal, underweight and overweight children. *Int. J. Obes.* 32, 1068–1075. doi:10.1038/ijo.2008.52

Moher, D., Liberati, A., Tetzlaff, J., and Altman, D. G.PRISMA Group (2009). Preferred reporting items for systematic reviews and meta-analyses: The PRISMA statement. *PLoS Med.* 6, e1000097. doi:10.1371/journal.pmed.1000097

Muller, S., Carlsohn, A., Muller, J., Baur, H., and Mayer, F. (2012). Static and dynamic foot characteristics in children aged 1-13 years: A cross-sectional study. *Gait Posture* 35, 389–394. doi:10.1016/j.gaitpost.2011.10.357

Must, A., and Strauss, R. S. (1999). Risks and consequences of childhood and adolescent obesity. *Int. J. Obes.* 23, S2–S11. doi:10.1038/sj/ijo/0800852

Park, S. Y., and Park, D. J. (2019). Comparison of foot structure, function, plantar pressure and balance ability according to the body mass index of young adults. *Osong Public Health Res. Perspect.* 10, 102–107. doi:10.24171/j.phrp.2019.10.2.09

Pfeiffer, M., Kotz, R., Ledl, T., Hauser, G., and Sluga, M. (2006). Prevalence of flat foot in preschool-aged children. *Pediatrics* 118, 634–639. doi:10.1542/peds.2005-2126

Putti, A. B., Arnold, G. P., and Abboud, R. J. (2010). Foot pressure differences in men and women. *Foot Ankle Surg.* 16, 21–24. doi:10.1016/j.fas.2009.03.005

Racette, S. B., Deusinger, S. S., and Deusinger, R. H. (2003). Obesity: Overview of prevalence, etiology, and treatment. *Phys. Ther.* 83, 276–288. doi:10.1093/ptj/83.3.276

Rao, U. B., and Joseph, B. (1992). The influence of footwear on the prevalence of flat foot. A survey of 2300 children. *J. bone Jt. Surg. Br. volume* 74, 525–527. doi:10.1302/0301-620x.74b4.1624509

Redmond, A. C., Burns, J., and Ouvrier, R. A. (2008a). Factors that influence health-related quality of life in Australian adults with Charcot-Marie-Tooth disease. *Neuromuscul. Disord.* 18, 619–625. doi:10.1016/j.nmd.2008.05.015

Redmond, A. C., Crane, Y. Z., and Menz, H. B. (2008b). Normative values for the foot posture index. *J. foot ankle Res.* 1, 6. doi:10.1186/1757-1146-1-6

Sachithanandam, V., and Joseph, B. (1995). The influence of footwear on the prevalence of flat foot. A survey of 1846 skeletally mature persons. *J. Bone Jt. Surgery-British* 77B, 254–257. doi:10.1302/0301-620x.77b2.7706341

Schwend, R. M., and Drennan, J. C. (2003). Cavus foot deformity in children. *J. Am. Acad. Orthop. Surg.* 11, 201–211. doi:10.5435/00124635-200305000-00007

Skre, H. (1974). Genetic and clinical aspects of Charcot-Marie-Tooth's disease. *Clin. Genet.* 6, 98–118. doi:10.1111/j.1399-0004.1974.tb00638.x

Song-Hua, Y., Lu, W., and Kuan, Z. (2017). Effects of different movement modes on plantar pressure distribution patterns in obese and non-obese Chinese children. *Gait Posture* 57, 28–34. doi:10.1016/j.gaitpost.2017.05.001

Stavlas, P., Grivas, T. B., Michas, C., Vasiliadis, E., and Polyzois, V. (2005). The evolution of foot morphology in children between 6 and 17 years of age: A cross-sectional study based on footprints in a mediterranean population. *J. foot ankle Surg. official Publ. Am. Coll. Foot Ankle Surg.* 44, 424–428. doi:10.1053/j.jfas.2005.07.023

Stewart, C., Morrison, M., and Ryan, M. (2018). Associations between obesity and pediatric foot dimensions. *J. Am. Podiatric Med. Assoc.* 108, 383–389. doi:10.7547/16-172

Stovitz, S. D., Pardee, P. E., Vazquez, G., Duval, S., and Schwimmer, J. B. (2008). Musculoskeletal pain in obese children and adolescents. *Acta Paediatr.* 97, 489–493. doi:10.1111/j.1651-2227.2008.00724.x

Swallen, K. C., Reither, E. N., Haas, S. A., and Meier, A. M. (2005). Overweight, obesity, and health-related quality of life among adolescents: The national longitudinal study of adolescent health. *Pediatrics* 115, 340–347. doi:10.1542/peds.2004-0678

Szczepanowska-Wolowiec, B., Sztandera, P., Kotela, I., and Zak, M. (2021). Vulnerability of the foot's morphological structure to deformities caused by foot loading paradigm in school-aged children: A cross-sectional study. *Sci. Rep.* 11, 2749. doi:10.1038/s41598-021-82475-y

Taylor, E. D., Theim, K. R., Mirch, M. C., Ghorbani, S., Tanofsky-Kraff, M., Adler-Wailes, D. C., et al. (2006). Orthopedic complications of overweight in children and adolescents. *Pediatrics* 117, 2167–2174. doi:10.1542/peds.2005-1832

Telfer, S., and Bigham, J. J. (2019). The influence of population characteristics and measurement system on barefoot plantar pressures: A systematic review and meta-regression analysis. *Gait Posture* 67, 269–276. doi:10.1016/j.gaitpost.2018.10.030

Villarroya, M. A., Esquivel, J. M., Tomás, C., Moreno, L. A., Buenafé, A., and Bueno, G. (2009). Assessment of the medial longitudinal arch in children and adolescents with obesity: Footprints and radiographic study. *Eur. J. Pediatr.* 168, 559–567. doi:10.1007/s00431-008-0789-8

Vrdoljak, O. (2017). Anthropometric measurements of foot length and shape in children 2 to 7 years of age. *Period. Biol.* 119, 125–129. doi:10.18054/pb.v119i2.4508

Wang, Y., and Lobstein, T. (2006). Worldwide trends in childhood overweight and obesity. *Int. J. Pediatr. Obes.* 1, 11–25. doi:10.1080/17477160600586747

Waseda, A., Suda, Y., Inokuchi, S., Nishiwaki, Y., and Toyama, Y. (2014). Standard growth of the foot arch in childhood and adolescence--derived from the measurement results of 10,155 children. *Foot Ankle Surg.* 20, 208–214. doi:10.1016/j.fas.2014.04.007

Wicart, P. (2012). Cavus foot, from neonates to adolescents. *Orthop. traumatology, Surg. Res. OTSR* 98, 813–828. doi:10.1016/j.otsr.2012.09.003

Wilkerson, R. D., and Mason, M. A. (2000). Differences in men's and women's mean ankle ligamentous laxity. *Iowa Orthop. J.* 20, 46–48.

Wines, A. P., Chen, D., Lynch, B., and Stephens, M. M. (2005). Foot deformities in children with hereditary motor and sensory neuropathy. *J. Pediatr. Orthop.* 25, 241–244. doi:10.1097/01.bpo.0000151057.39485.4b

Wozniacka, R., Bac, A., Matusik, S., Szczygiel, E., and Ciszek, E. (2013). Body weight and the medial longitudinal foot arch: High-arched foot, a hidden problem? *Eur. J. Pediatr.* 172, 683–691. doi:10.1007/s00431-013-1943-5

Xu, M., Hong, Y., Li, J. X., and Wang, L. (2018). Foot morphology in Chinese school children varies by sex and age. *Med. Sci. Monit.* 24, 4536–4546. doi:10.12659/MSM.906030

Zambito, A., Dall'oca, C., Polo, A., Bianchini, D., and Aldegheri, R. (2008). Spina bifida occulta. Foot deformities, enuresis and vertebral cleft: Clinical picture and neurophysiological assessment. *Eur. J. Phys. rehabilitation Med.* 44, 437–440.

Zimon, M., Baets, J., Fabrizi, G. M., Jaakkola, E., Kabzinska, D., Pilch, J., et al. (2011). Dominant GDAP1 mutations cause predominantly mild CMT phenotypes. *Neurology* 77, 540–548. doi:10.1212/WNL.0b013e318228fc70

frontiers | Frontiers in Bioengineering and Biotechnology

TYPE Original Research
PUBLISHED 20 July 2023
DOI 10.3389/fbioe.2023.1198120

OPEN ACCESS

EDITED BY
Juan Ramírez,
National University of Colombia,
Medellin, Colombia

REVIEWED BY
Lorenzo Rum,
University of Sassari, Italy
Mihaela Baritz,
Transilvania University of Brașov,
Romania
Chiara Palmisano,
University Hospital Würzburg, Germany

*CORRESPONDENCE
P. De Blasiis,
paolo.deblasiis@unicampania.it

†These authors have contributed equally to this work

RECEIVED 31 March 2023
ACCEPTED 03 July 2023
PUBLISHED 20 July 2023

CITATION
De Blasiis P, Caravaggi P, Fullin A, Leardini A, Lucariello A, Perna A, Guerra G and De Luca A (2023), Postural stability and plantar pressure parameters in healthy subjects: variability, correlation analysis and differences under open and closed eye conditions.
Front. Bioeng. Biotechnol. 11:1198120.
doi: 10.3389/fbioe.2023.1198120

Postural stability and plantar pressure parameters in healthy subjects: variability, correlation analysis and differences under open and closed eye conditions

P. De Blasiis[1*†], P. Caravaggi[2†], A. Fullin[1,3†], A. Leardini[2], A. Lucariello[4], A. Perna[5], G. Guerra[5] and A. De Luca[1]

[1]Department of Mental and Physical Health and Preventive Medicine, Section of Human Anatomy, University of Campania "Luigi Vanvitelli", Naples, Italy, [2]Movement Analysis Laboratory, IRCCS Istituto Ortopedico Rizzoli, Bologna, Italy, [3]Department of Advanced Biomedical Sciences, University of Naples "Federico II", Naples, Italy, [4]Department of Sport Sciences and Wellness, University of Naples "Parthenope", Naples, Italy, [5]Department of Medicine and Health Sciences "Vincenzo Tiberio", University of Molise, Campobasso, Italy

Introduction: The "postural control system" acts through biomechanical strategies and functional neuromuscular adaptations to maintain body balance under static and dynamic conditions. Postural stability and body weight distribution can be affected by external sensory inputs, such as different visual stimuli. Little information is available about the influence of visual receptors on stabilometric and plantar pressure parameters. The aim of this study was to analyze variability, correlations, and changes in these parameters under open- (OE) and closed-eye (CE) conditions.

Methods: A total of 31 stabilometric and plantar pressure parameters were acquired in 20 young and healthy adults during baropodometric examination performed in bipedal standing under both visual conditions. Variability of parameters was evaluated via the coefficient of variation, correlation analysis via Pearson's R2, and statistical differences via the Wilcoxon test.

Results: High intra-subject repeatability was found for all plantar pressure parameters and CoP-speed (CV < 40%) under OE and CE conditions, while CoP-sway area (CoPsa) and length surface function (LSF) showed larger variability (CV > 50%). Mean and peak pressures at midfoot and total foot loads showed the least number of significant correlations with other parameters under both visual conditions, whereas the arch-index and rearfoot loads showed the largest number of significant correlations. The limb side significantly affected most plantar pressure parameters. A trend of larger LSF and lower CoPsa and mean and peak pressures at the right forefoot was found under the CE condition.

Discussion: The present study provides a deeper insight into the associations between postural stability and foot load. Interesting postural adaptations, particularly with respect to different visual stimuli, the effect of the dominant side, and the specific role of the midfoot in balance control were highlighted.

KEYWORDS

posture, postural control, foot, baropodometry, stabilometry, pressure plate, visual control

1 Introduction

Postural stability represents the ability of the "postural control system" (PCS) (Takakusaki, 2017) in maintaining the vertical projection of the body center of mass (COM) within the feet contact area (Patti et al., 2018). This function of the central nervous system relies on biomechanical strategies and neuromuscular adaptation to stabilize the position of the body segments against the force of gravity (Ivanenko and Gurfinkel, 2018) and to maintain balance (Moffa et al., 2020) during different motor tasks. Bipedal standing is characterized by postural parameters in the sagittal plane (De Blasiis et al., 2021a) resulting from the synergic actions of anti-gravity muscles on the human skeleton to ensure minimal COM oscillations and low energy expenditure (Gagey et al., 1998).

Body oscillations can be quantitatively assessed by baropodometry using stabilometric tests (Rosário, 2014; Baumfeld et al., 2017). Several

TABLE 1 Description and legend of plantar pressure and stabilometric parameters. Forefoot (Ff); midfoot (Mf); rearfoot (Rf); mean pressure (Pmean); maximum pressure (Pmax); center-of-pressure speed (CoP-speed); center-of-pressure sway area (CoPsa); length surface function (LSF); arch index (AI); and foot contact area (FCA).

Legend	Plantar pressure and stabilometric parameters		Description
1	Load Tf [%]	Left	Percentage of body weight distribution
2	Load Tf [%]	Right	
3	Load Rf [%]	Left	Percentage of body weight distribution at the rearfoot
4	Load Rf [%]	Right	
5	Load Mf [%]	Left	Percentage of body weight distribution at the midfoot
6	Load Mf [%]	Right	
7	Load Ff [%]	Left	Percentage of body weight distribution at the forefoot
8	Load Ff [%]	Right	
9	Pmean Tf [KPa]	Left	Mean pressure at the total foot
10	Pmean Tf [KPa]	Right	
11	Pmean Rf [KPa]	Left	Mean pressure at the rearfoot
12	Pmean Rf [KPa]	Right	
13	Pmean Mf [KPa]	Left	Mean pressure at the midfoot
14	Pmean Mf [KPa]	Right	
15	Pmean Ff [KPa]	Left	Mean pressure at the forefoot
16	Pmean Ff [KPa]	Right	
17	Pmax Tf [KPa]	Left	Peak pressure at the total foot
18	Pmax Tf [KPa]	Right	
19	Pmax Rf [KPa]	Left	Peak pressure at the rearfoot
20	Pmax Rf [KPa]	Right	
21	Pmax Mf [KPa]	Left	Peak pressure at the midfoot
22	Pmax Mf [KPa]	Right	
23	Pmax Ff [KPa]	Left	Peak pressure at the forefoot
24	Pmax Ff [KPa]	Right	
25	FCA [mm^2]	Left	Foot contact area
26	FCA [mm^2]	Right	
27	AI [%]	Left	Ratio between the midfoot contact area and foot contact area (without toes)
28	AI [%]	Right	
29	CoPsa [mm^2]		Area of an ellipse containing the trajectory of the center of pressure
30	CoP-speed [mm/s]		Average velocity of the center of pressure
31	LSF [mm^{-1}]		Ratio between the distance covered by the center of pressure (CoP-length) and CoP sway area (CoPsa)

plantar-pressure-based measures have been proposed to evaluate postural stability: center of pressure (CoP), CoP-sway area (CoPsa), CoP-speed, and length surface function (LSF) (Fullin et al., 2022) (Table 1). In addition, the morphology of the foot contact area and body weight distribution across different plantar regions can be analyzed under static and dynamic conditions (Rosário, 2014; Fullin et al., 2022) using plantar pressure parameters (percentages of body weight distribution, mean and peak pressures, and arch index).

All baropodometric parameters are affected by the continuous postural adaptations performed by the PCS, which integrates sensory inputs (somatosensory, visual, and vestibular) and elaborates motor outputs stabilizing the whole-body posture (Gagey et al., 1998). In particular, the contribution of the visual receptor to postural control has been investigated for its impact across different scientific fields (Stoffregen et al., 2000; Bellizzi et al., 2011; Nishiike et al., 2013). Maintaining balance control in vision-loss conditions is supported mainly by the vestibular and proprioceptive receptors, through postural adjustments that may be assessed quantitatively and instrumentally.

Quantifying the physiological variation of stabilometric and plantar pressure parameters in a normal population is critical to define the reference values to assess pathological conditions and identify the most reliable parameters to be used in the clinical setting and research. The intra-subject and intra-day variability in stabilometric and plantar pressure parameters have been reported in healthy subjects under open- (OE) (Fullin et al., 2022) and closed-eye (CE) conditions (Samson and Crowe, 1996; Gagey and Weber, 2010; Hébert-Losier and Murray, 2020). The inter-subject variability in a young healthy population in OE during the same day (Fullin et al., 2022), two sessions 1 week apart (Alves and Porfirio Borel, 2018), and intra-session and inter-session over 2 weeks (Baldini et al., 2013) has also been assessed. Several studies defined the standard reference values of the aforementioned parameters under OE conditions (Ohlendorf et al., 2019; Fullin et al., 2022) and under static OE and CE conditions (Prieto et al., 1996; Tanaka et al., 2000; Hue et al., 2006; Vieira Tde et al., 2009; Bellizzi et al., 2011; Baldini et al., 2013; Santana Castro et al., 2021; Nishiike et al., 2013; Rodríguez-Rubio et al., 2020; De Blasiis et al., 2021b; Quialheiro et al., 2021; Scoppa and Gallamini, 2021), reporting greater CoPsa, CoP-speed, and CoP-length in CE.

While several stabilometric parameters are affected by visual stimuli, little information is available on which baropodometric parameters characterize the different visual conditions. The aim of this study was to evaluate the effect of visual stimuli on postural stability and plantar pressure parameters in a young and healthy population and to analyze variability, correlations, and changes in these parameters under OE and CE conditions.

2 Materials and methods

A total of 20 healthy subjects (7 M, 13 F; age = 20.2 ± 0.9 years; right-limb dominance = 20/20; height = 1.69 ± 0.09 m; weight = 61.94 ± 8.58 kg; BMI = 21.6 ± 1.7 kg/m^2) were recruited at the Motion Analysis Laboratory of the Anatomy Department at the University of Campania L.Vanvitelli, Naples, Italy. Ethical review and approval were waived for this study due to the nature of this pilot study, which required the recruitment of a small population of healthy participants tested for standard plantar pressure parameters during bipedal standing posture. The following inclusion criteria were used: absence of pain, no surgery in the last 6 months, no muscle-skeletal injury in the last 3 months, no dental surgery or use of dental implants, no prostheses or use of corrective orthoses, no neurological or visual disease, no skeletal dysmorphism, and no cognitive impairment. Participants were evaluated in an anatomical upright bipedal posture with the arms relaxed along the body close to the thighs and the head in the neutral position using a 200 × 50 cm 10,000 sensors/m^2 pressure plate (P-Walk FM12050 BTS-Bioengineering, Milan, Italy), sampling at 50 Hz (Figures 1A, B), following the international standardization criteria for baropodometric tests (Scoppa and Gallamini, 2017). The exceptions were for the visual target, placed 2.8 m away from the subject, and for the distance between the feet, self-selected by each participant with the indication to place the feet close but not together and to find a comfortable posture (Tarantola et al., 1997; Chiari et al., 2002). Four stabilometric exams of 30 s were performed on each participant under OE and CE conditions (Figure 1A, B). Each participant was allowed to sit down and rest before each trial, maintaining the same feet position in all the trials (Chiari et al., 2002). To ensure a correct postural examination, the tests were performed in silence and in a room with a level floor and white walls. The pressure plate was weight-calibrated before each measurement following the procedure recommended by the manufacturer. The following clinically relevant stabilometric and plantar pressure parameters were measured: center-of-pressure sway area (CoPsa; mm^2); length surface function (LSF; mm^{-1}); center-of-pressure speed (CoP-speed; mm/sec); total foot (Tf), rearfoot (Rf), midfoot (Mf), and forefoot (Ff) loads (%); mean and peak pressures (Pmean and Pmax; KPa) at Rf, Mf, and Ff; the foot contact area (FCA; mm^2); and arch index (AI; %) (Figure 1C–F; Table 1) (Fullin et al., 2022). All plantar pressure parameters were calculated for both left (l) and right (r) sides. Mean pressure parameters at Rf, Mf, and Ff were calculated as the ratio between weight and area calculated for each region. Load parameters were normalized to body weight (%BW). For each parameter, intra-subject (inter-trial) variability was assessed via the coefficient of variation (CV) across four trials for each subject. Possible correlations between pairs of stabilometric and plantar pressure parameters were assessed under OE and CE conditions via Pearson's correlation analysis (R^2). The effects of the side and the visual conditions were tested via the non-parametric Wilcoxon paired test. A Bonferroni correction was applied to the significance level (adjusted α = 0.005) to account for the multiple correlation analyses and for the multiple paired comparisons between OE and CE conditions. Statistical analysis was performed using MATLAB (MathWorks) and R (R Core Team. R, 2018).

3 Results

3.1 Variability in stabilometric and plantar pressure parameters under OE and CE conditions

Figure 2 depicts the boxplots (median 25%–75%) for each parameter of the CV distribution across subjects. The CVs were sorted in ascending order along the *x*-axis by the median value. High repeatability (median CV < 20%) was observed for all plantar

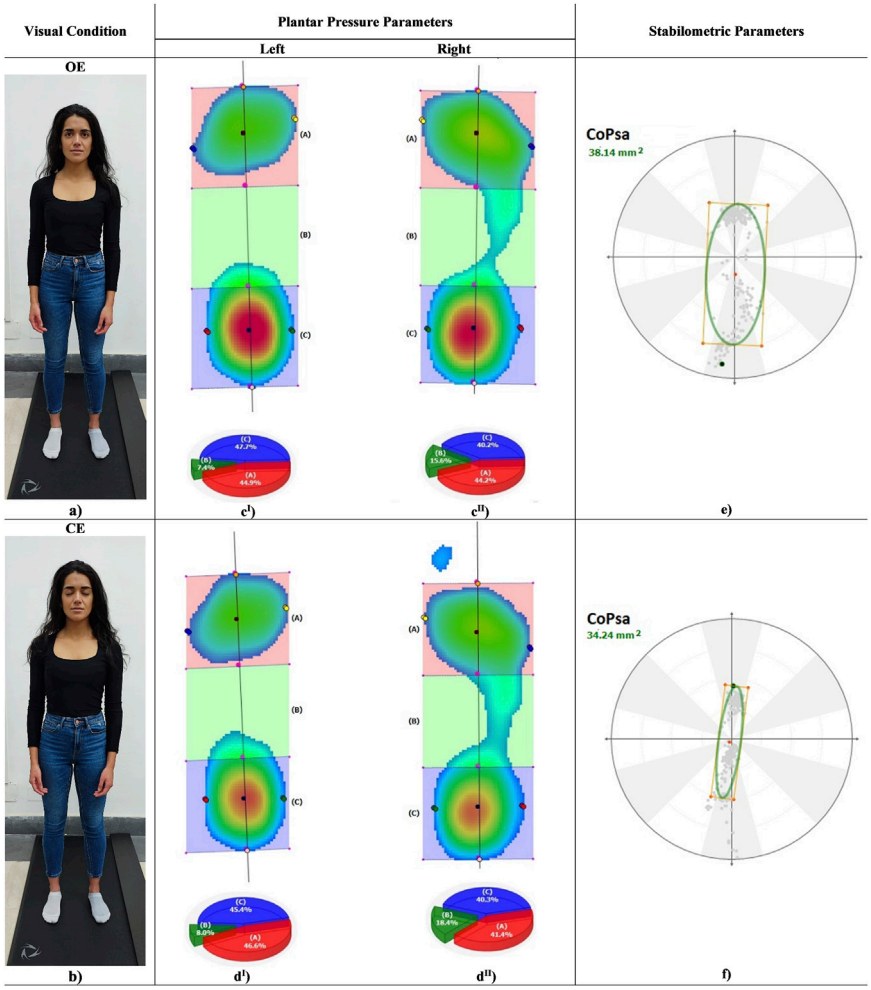

FIGURE 1
Left, a subject in anatomical standing posture in OE **(a)** and CE **(b)** conditions. Centre, color maps of plantar pressure distribution at rearfoot, midfoot and forefoot during standing in OE **(c^I, c^{II})** and CE **(d^I, d^{II})**. Right, center of pressure sway area (CoPsa) in OE **(e)** and CE **(f)**.

pressure parameters and CoP-speed under both visual conditions, except for right AI in OE (median CV = ~40%). CoPsa and LSF showed the largest variability (median CV > 50%).

3.2 Correlation analysis across stabilometric and plantar pressure parameters under OE and CE conditions

Figure 3 illustrates the outcome of the multiple correlation analysis between pairs of stabilometric and plantar pressure parameters under OE and CE conditions. The R^2 of the correlation between each pair of parameters are graphically reported in a 31 x 31 matrix, using round markers whose size represents the magnitude of a statistically significant correlation between a parameter on the *x*-axis and a parameter on the *y*-axis. Positive correlations are represented by green round markers and negative correlations by black round markers. The *X*-axis parameters were sorted in ascending order by the number of statistically significant correlations (corrected $\alpha < 0.005$) with other parameters. CoP-speed and Pmean Mf (r) were identified as the most independent parameters in OE, showing no correlation with other parameters. In CE, the most independent parameters were Pmean Mf (r), Pmax Mf (r), and LSF; unlike what was observed in OE, CoP-speed was positively correlated with Pmax Rf (l, r), Pmean Rf (l), Load Rf (l), Pmax Tf (l), and CoPsa. A few correlations (≤ 6) were found in OE and CE for Load Tf (l,r), Pmean Mf (l) and Ff (l, r), Pmax Mf (l) and Ff (l, r), and CoPsa. All other parameters showed a larger number of correlations (>6) under both visual conditions.

3.3 Inter-side (left vs. right) comparison of plantar pressure parameters

The distribution of stabilometric and plantar pressure parameters under each visual condition is reported as median and 25% and 75% percentiles in Table 2. Significant differences were found between the left and right sides for all parameters ($p < 0.005$), except for Load Ff, Pmean Tf, Pmean Mf, and Pmax Mf under both visual conditions and for Pmax Rf in OE (Table 2). In particular, significant parameters were larger in the right side under both visual conditions, except for Rf.

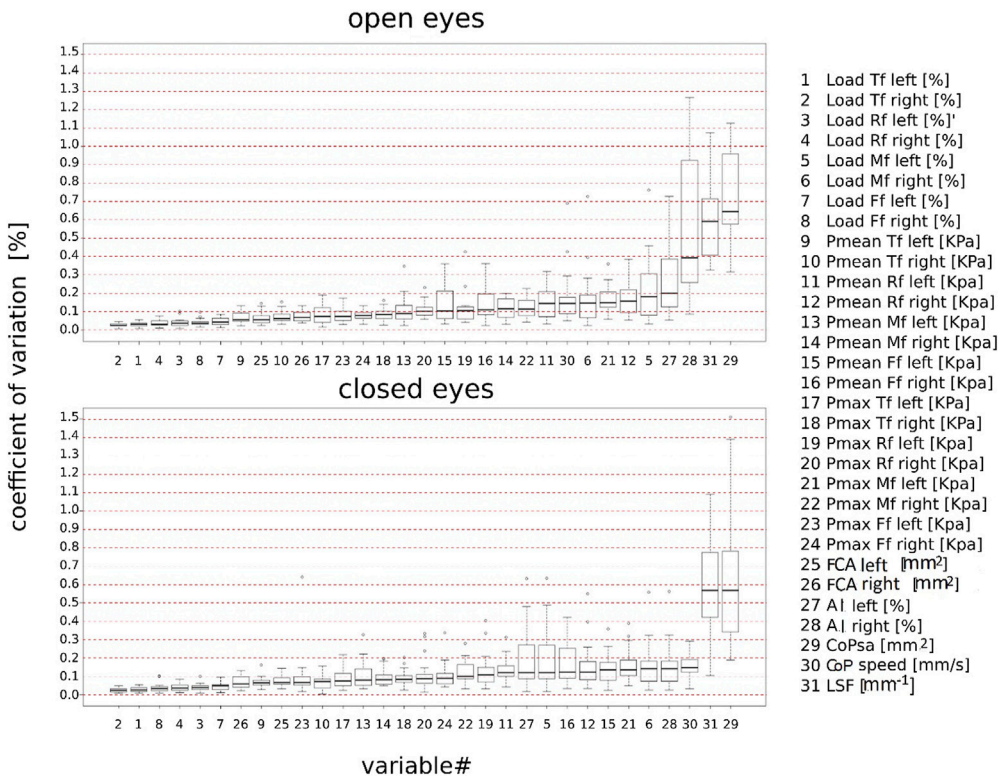

FIGURE 2
Boxplot of the intra-subject coefficient of variation (%) of stabilometric and plantar pressure parameters sorted in ascending order according to the median values under open- and closed-eye conditions. Total foot (Tf); forefoot (Ff); midfoot (Mf); rearfoot (Rf); mean pressure (Pmean); maximum pressure (Pmax); center-of-pressure speed (CoP-speed); length surface function (LSF); center-of-pressure sway area (CoPsa); arch index (AI); and foot contact area (FCA).

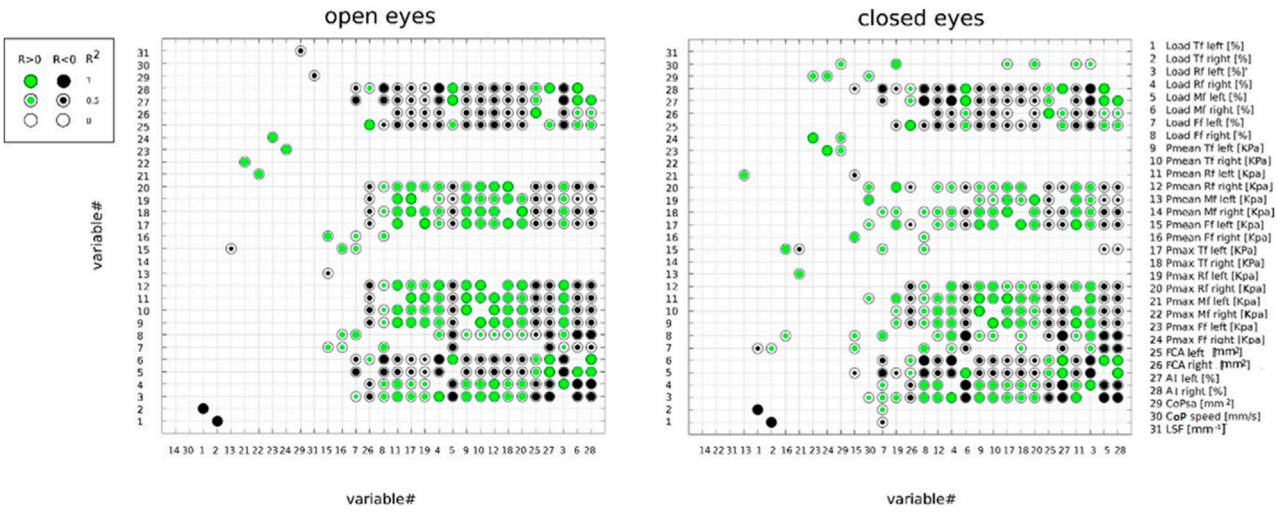

FIGURE 3
Correlation between pairs of stabilometric and plantar pressure parameters, assessed under open- and closed-eye conditions by Pearson's correlation analysis (R^2). Positive and negative correlations are represented by green and black round markers, respectively. The parameters were ordered from left to right on the *X*-axis in ascending order according to the number of statistically significant correlations with other parameters. The α level of significance was corrected to 0.005 accounting for the multiple correlations. Total foot (Tf); forefoot (Ff); midfoot (Mf); rearfoot (Rf); mean pressure (Pmean); maximum pressure (Pmax); center-of-pressure speed (CoP-speed); length surface function (LSF); center-of-pressure sway area (CoPsa); arch index (AI); and foot contact area.

TABLE 2 Inter-subject median and percentiles (25% and 75%) of plantar pressure and stabilometric parameters; significant differences (*p*-value = = 0.005) between left and right (Wilcoxon paired test) and between open and closed eyes (Wilcoxon signed test). Forefoot (Ff); midfoot (Mf); rearfoot (Rf); mean pressure (Pmean); maximum pressure (Pmax); center-of-pressure speed (CoP-speed); center-of-pressure sway area (CoPsa); length surface function (LSF); arch index (AI); and foot contact area (FCA).

Plantar pressure and stabilometric parameters	Side	Open eyes (OE)		Closed eyes (CE)		*p*-value inter-visual condition (OE vs. CE)
		Median (25%; 75%)	*p*-value inter-sides (right vs. left)	Median (25%; 75%)	*p*-value intra-group (right vs. left)	
Load Tf [%]	Left	46.46 (45.65; 48.70)	< **0.001**	47.53 (46.15; 49)	< **0.001**	0.224
	Right	53.54 (51.30; 54.35)		52.48 (51.00; 53.85)		0.224
Load Rf [%]	Left	41.19 (36.53; 44.95)	**0.001**	41.84 (35.83; 45.03)	**0.001**	0.469
	Right	36.95 (33.88; 42.00)		37.44 (34.43; 41.80)		0.420
Load Mf [%]	Left	14.05 (8.58; 25.13)	**0.001**	14.91 (9.05; 26.48)	< **0.001**	0.419
	Right	20.79 (12.98; 24.95)		21.42 (13.45; 24.70)		0.370
Load Ff [%]	Left	43.91 (41.03; 45.05)	0.133	43.16 (40.35; 44.53)	0.13	0.329
	Right	43.05 (40.85; 43.85)		41.99 (39.20; 44.25)		0.312
Pmean Tf [KPa]	Left	24.04 (22.96; 27.89)	0.393	23.45 (22.27; 26.49)	0.108	0192
	Right	24.39 (22.79; 27.32)		23.54 (21.94; 25.70)		0.101
Pmean Rf [KPa]	Left	27.35 (23.83; 35.58)	< **0.001**	27 (23.44; 32.43)	**0.004**	0.261
	Right	23.19 (18.70; 31)		22.02 (18.02; 33.17)		0.395
Pmean Mf [KPa]	Left	16.38 (15; 18.75)	0.026	15.88 (15; 18.25)	0.154	0.312
	Right	18.25 (17.00; 20)		17.75 (15.75; 18.50)		0.068
Pmean Ff [KPa]	Left	59.07 (53.15; 67.85)	< **0.001**	57.66 (47.31; 62.64)	**0.003**	0.212
	Right	69.92 (60.34; 83.98)		59.22 (55.71; 69.20)		0.040
Pmax Tf [KPa]	Left	62.78 (57.32; 71.52)	**0.001**	60.57 (58.09; 68.64)	< **0.001**	0.335
	Right	58.90 (53.27; 65.87)		57.08 (52.11; 64.55)		0.234
Pmax Rf [KPa]	Left	67.25 (59.50; 80.50)	0.025	64.5 (56.63; 68.13)	**0.002**	0.192
	Right	63.25 (55.75; 71)		58.47 (53.06; 6.06)		0.115
Pmax Mf [KPa]	Left	30.87(27.25; 36.63)	0.053	31.38 (27.50; 37.25)	0.332	0.469
	Right	35.75 (31.75; 37.94)		34 (29.5; 35.7)		0.084

(Continued on following page)

TABLE 2 (*Continued*) Inter-subject median and percentiles (25% and 75%) of plantar pressure and stabilometric parameters; significant differences (*p*-value = = 0.005) between left and right (Wilcoxon paired test) and between open and closed eyes (Wilcoxon signed test). Forefoot (Ff); midfoot (Mf); rearfoot (Rf); mean pressure (Pmean); maximum pressure (Pmax); center-of-pressure speed (CoP-speed); center-of-pressure sway area (CoPsa); length surface function (LSF); arch index (AI); and foot contact area (FCA).

Plantar pressure and stabilometric parameters	Side	Open eyes (OE)		Closed eyes (CE)		*p*-value inter-visual condition (OE vs. CE)
		Median (25%; 75%)	*p*-value inter-sides (right vs. left)	Median (25%; 75%)	*p*-value intra-group (right vs. left)	
Pmax Ff [KPa]	Left	44.50 (41.75; 49.25)	< **0.001**	42.50 (41.22; 45.75)	**0.001**	0.352
	Right	49.63 (48.25; 55)		47.47 (45.25; 49.13)		0.011
FCA [mm^2]	Left	118 (97.31; 134.44)	< **0.001**	120.25 (100.88; 139.31)	< **0.001**	0.303
	Right	132.5(112.19; 160.38)		136 (116.88; 164.94)		0.201
AI [%]	Left	14.05 (8.57; 25.27)	**0.002**	14.92 (9.05; 26.48)	< **0.001**	0.419
	Right	20.63 (12.98; 24.95)		21.43 (13.44; 24.71)		0.370
CoPsa [mm^2]		28.80 (23.50; 41.69)		24.98 (13.17; 29.22)		0.055
CoP-speed [mm/s]		3.44 (3.13; 3.970)		3.24 (3.00; 3.93)		0.192
LSF [mm^{-1}]		4.69 (3.80; 7.10)		7.85 (5.28; 9.68)		0.040

Bold values are highlight statistical significance ($p < 0.005$).

3.4 Intra-side comparison of stabilometric and plantar pressure parameters under OE and CE conditions

Table 2 reports the inter-subject median and percentile (25% and 75%) distributions of all parameters under both visual conditions. No significant differences were observed in stabilometric and plantar pressure parameters between OE and CE ($p \leq 0.005$). However, a trend for larger LSF and lower CoPsa, Pmean, and Pmax Ff (r) was found in CE.

4 Discussion

Postural sway and plantar pressure parameters in the upright standing position can be modulated in response to different visual inputs (Stoffregen et al., 2000; Bellizzi et al., 2011; Nishiike et al., 2013). Understanding the effects of open- and closed-eye conditions on these parameters and on their variability is important for their interpretation in clinical and research investigations.

The first aim of the present study was to analyze the intra-subject variability in stabilometric and plantar pressure parameters in healthy subjects during the bipedal standing test under OE and CE conditions. The coefficient of variation was lower than 20% in CE and OE across all parameters, except for the right arch index in CE (≤40%) and CoPsa and LSF (≥50%) under both visual conditions. These findings are partly in agreement with a review that identified mean pressure, percentage of body weight distribution, and foot contact area as some of the most reliable measures (Hébert-Losier and Murray, 2020). The outcome of the variability analysis under the CE condition is also in agreement with what was observed previously in OE (Figure 2) (Fullin et al., 2022); thus, the variability in stabilometric and plantar pressure parameters does not seem to be affected by the different visual conditions. The only exception is the right arch index, which suggests a greater dynamic role of the dominant foot with respect to the postural adaptations occurring with closed eyes.

To the best of the authors' knowledge, this study is the first to investigate the correlations between pairs of postural stability and plantar pressure parameters under both visual conditions. In order to better highlight and visually determine the overall outcome of the correlation analysis, a novel graphical approach was established (Figure 3). This visual representation allows for a faster and more comprehensive understanding of which parameters are more independent (i.e., less correlated to other parameters) in the characterization of the phenomenon, especially when several parameters are under investigation. Markers' dimensions and colors allow us to quickly identify the magnitude and direction of each correlation. According to the outcome of the present study (Figure 3), mean and peak pressures at midfoot and total foot loads (l, r) were among the most independent parameters under both visual conditions, whereas arch index (l, r) and rearfoot loads (l, r) were among the most correlated with other parameters. In particular, CoP-speed and mean pressure at the midfoot were identified as the most independent parameters in OE. Under the CE condition, mean and peak pressures at midfoot (r > l) and LSF were the most independent parameters. Unlike what was observed in OE, CoP-speed in CE was positively correlated with the following variables: Pmax rearfoot (l, r), Pmax total foot (l), Pmean and load rearfoot (l), and CoPsa. These

positive correlations, associated with the high reliability of CoP-speed, seem to suggest a different control mechanism of body sway with closed eyes compared to open eyes, underlying a possible functional relationship of CoP-speed with the CoP sway area and rearfoot load in the non-dominant side. The length surface function also showed different correlations between the two visual conditions. As predictable, it was negatively correlated with CoPsa in OE since it represents the ratio between the distance covered by the CoP during a standing trial (CoP-length) and CoPsa, whereas it was independent in CE (i.e., showed no significant correlations with other parameters). This different behavior between open and closed eyes is the opposite of what occurs for CoP-speed and could likely be explained by the mutual relationship of CoP-speed and LSF with CoP-length.

The present study provides a deeper insight into the effects of visual stimuli on stabilometric and plantar pressure parameters, which were previously reported in OE (Fullin et al., 2022). In agreement with what was found in OE (Fullin et al., 2022), significant differences were observed between the dominant (right) and non-dominant (left) sides for several parameters (Table 2). In particular, loads were significantly lower at the rearfoot and significantly larger at the midfoot of the dominant side under both visual conditions. In terms of mean and peak pressures, a significant decrease at the rearfoot and a significant increase at the forefoot were found in the dominant side under both visual conditions. This finding was also associated with a larger foot contact area and a larger percentage of the midfoot contact area (larger AI) in the dominant side for OE and CE (Table 2). According to previous studies (Hennig and Sterzing, 2009; Machado et al., 2015), the midfoot seems to be the most sensitive region to both tactile and vibration stimuli; therefore, it could be hypothesized that the midfoot plays an important role in the balance control mechanism. The larger midfoot contact area found in the dominant side would increase the number of receptors responsible for the spatial orientation of the body center of mass in contact with the ground. This seems to be consistent with the outcome of the correlation analysis (Figure 3), which showed that mean and peak pressures at the midfoot are two of the most independent parameters and thus are good indicators for the characterization of the balance control under both visual conditions.

The visual stimulus affected several parameters (Table 2). In particular, a trend for larger LSF and lower CoPsa and mean and peak pressures at the forefoot in the right side was found in CE with respect to the OE condition (Fullin et al., 2022). Unlike what was reported in other studies (Prieto et al., 1996; Tanaka et al., 2000; Hue et al., 2006; Vieira Tde et al., 2009; Bellizzi et al., 2011; Baldini et al., 2013; Santana Castro et al., 2021; Nishiike et al., 2013; Rodríguez-Rubio et al., 2020; De Blasiis et al., 2021b; Quialheiro et al., 2021; Scoppa and Gallamini, 2021), CoPsa and CoP-speed were not larger in the CE condition. This finding could be probably explained by the effect of the longer visual target distance with respect to the clinical stabilometry standardization (Tarantola et al., 1997; Tanaka et al., 2000; Chiari et al., 2002). Indeed, this variable has been shown to be positively correlated with CoPsa and CoP-speed (Stoffregen et al., 2000).

The limitations to the study were the relatively small sample size, due to the rather strict inclusion criteria, particularly for visual and dental impairments; it should also be noted that while most parameters showed normal distribution, the normality assumption was not guaranteed for all parameters, and this violation may have slightly affected the outcome of the correlation analysis. Moreover, the self-selected feet position may be considered a methodological bias, but the indication to place the feet close but not together in order to obtain a comfortable upright bipedal standing posture may be a good standardization method according to the neurophysiological principle of the natural postural control strategy instead of imposing an unnatural posture. In addition, the position of the visual target (2.8 m away from the subject) may have affected the stabilometric and plantar pressure measurements under the OE condition; in particular, an increase in CoPsa with the increasing target distance has been reported (Stoffregen et al., 2000). The effect of the visual target distance should be investigated in future studies.

The present study aided in establishing the most reliable and independent stabilometric and plantar pressure parameters for the evaluation of bipedal standing posture under open- and closed-eye conditions in a healthy young population. As expected, significant differences were observed between the left and right sides and between correlations under two visual conditions. While more data from a larger population should be sought, the study has highlighted the importance of the dominant side and the specific role of the midfoot in the balance control.

Data availability statement

The raw data supporting the conclusion of this article will be made available by the authors, without undue reservation.

Ethics statement

Ethical review and approval was not required for the study on human participants in accordance with the local legislation and institutional requirements. The patients/participants provided their written informed consent to participate in this study. Written informed consent was obtained from the individual(s) for the publication of any potentially identifiable images or data included in this article.

Author contributions

PD, AF, and PC conceived and designed the study. PD and AF recruited the healthy subjects and performed stabilometric examinations. PD, AF, and PC contributed to analysis and interpretation of the data and drafted the first article. ALe, ALu, AP, GG, and ADL critically revised the content. All authors contributed to the article and approved the submitted version.

Acknowledgments

The authors thank “Ortopedia Formisano S.R.L.” for supplying the pressure plate and for providing valuable technical support.

Conflict of interest

The authors declare that the research was conducted in the absence of any commercial or financial relationships that could be construed as a potential conflict of interest.

Publisher's note

References

Alves, R., and Porfirio Borel, W. (2018). Test-retest reliability of baropodometry in young asyntomatic individuals during semi static and dynamic analysis. *Fisioter. Mov.* 31, e003114. doi:10.1590/1980-5918.031.AO14

Baldini, A., Nota, A., Assi, V., Ballanti, F., and Cozza, P. (2013). Intersession reliability of a posturo-stabilometric test, using a force platform. *J. Electromyogr. Kinesiol.* 23, 1474–1479. doi:10.1016/j.jelekin.2013.08.003

Baumfeld, D., Baumfeld, T., da Rocha, R. L., Macedo, B., Raduan, F., Zambelli, R., et al. (2017). Reliability of baropodometry on the evaluation of plantar load distribution: A transversal study. *Biomed. Res. Int.* 2017, 1–4. doi:10.1155/2017/5925137

Bellizzi, M., Rizzo, G., Bellizzi, G., Ranieri, M., Fanelli, M., Megna, G., et al. (2011). Electronic baropodometry in patients affected by ocular torticollis. *Strabismus* 19 (1), 21–25. doi:10.3109/09273972.2010.545469

Chiari, L., Rocchi, L., and Cappello, A. (2002). Stabilometric parameters are affected by anthropometry and foot placement. *Clin. Biomech. (Bristol, Avon)* 17 (9-10), 666–677. PMID: 12446163. doi:10.1016/s0268-0033(02)00107-9

De Blasiis, P., Fullin, A., Sansone, M., Del Viscovo, L., Napolitano, F., Terracciano, C., et al. (2021a). Quantitative evaluation of upright posture by x-ray and 3D stereophotogrammetry with a new marker set protocol in late onset pompe disease. *J. Neuromuscul. Dis.* 8 (6), 979–988. doi:10.3233/JND-210663

De Blasiis, P., Fullin, A., Caravaggi, P., Lus, G., Melone, M. A., Sampaolo, S., et al. (2021b). Long-term effects of asymmetrical posture in boxing assessed by baropodometry. *J. Sports Med. Phys. Fit.* 62, 350–355. doi:10.23736/S0022-4707.21.12040-7

Fullin, A., Caravaggi, P., Picerno, P., Mosca, M., Caravelli, S., De Luca, A., et al. (2022). Variability of postural stability and plantar pressure parameters in healthy subjects evaluated by a novel pressure plate. *Int. J. Environ. Res. Public Health* 19 (5), 2913. doi:10.3390/ijerph19052913

Gagey, P. M., Martinerie, J., Pezard, L., and Benaim, C. (1998). Static balance is controlled by a non-linear dynamic system. *Ann. d'oto-laryngologie de Chir. cervico faciale,* 115 (3), 161–168.

Gagey, P. M., and Weber, B. (2010). Study of intra-subject random variations of stabilometric parameters. *Med. Biol. Eng. Comput.* 48, 833–835. doi:10.1007/s11517-010-0656-4

Hébert-Losier, K., and Murray, L. (2020). Reliability of centre of pressure, plantar pressure, and plantar-flexion isometric strength measures: A systematic review. *Gait Posture* 75, 46–62. doi:10.1016/j.gaitpost.2019.09.027

Hennig, E. M., and Sterzing, T. (2009). Sensitivity mapping of the human foot: Thresholds at 30 skin locations. *Foot Ankle Int.* 30 (10), 986–991. doi:10.3113/fai.2009.0986

Hue, O., Simoneau, M., Marcotte, J., Berrigan, F., Doré, J., Marceau, P., et al. (2006). Body weight is a strong predictor of postural stability. *Gait Posture* 26 (1), 32–38. doi:10.1016/j.gaitpost.2006.07.005

Ivanenko, Y., and Gurfinkel, V. S. (2018). Human postural control. *Front. Neurosci.* 12, 171. doi:10.3389/fnins.2018.00171

Santana Castro, K. J., Cruz Salomão, R., Feitosa, N. Q., Jr., Dutra Henriques, L., Rozin Kleiner, A. F., Belgamo, A., et al. (2021). Changes in plantar load distribution in legally blind subjects. *PLOS ONE* 16(4):e0249467. doi:10.1371/journal.pone.0249467

Machado, Á. S., Bombach, G. D., Duysens, J., and Carpes, F. P. (2015). Differences in foot sensitivity and plantar pressure between young adults and elderly. *Arch. Gerontol. Geriatr.* 63, 67–71. doi:10.1016/j.archger.2015.11.005

Moffa, S., Perna, A., Candela, G., Cattolico, A., Sellitto, C., De Blasiis, P., et al. (2020). Effects of hoverboard on balance in young soccer athletes. *J. Funct. Morphol. Kinesiol.* 5, 60. doi:10.3390/jfmk5030060

Nishiike, S., Okazaki, S., Watanabe, H., Akizuki, H., Imai, T., Uno, A., et al. (2013). The effect of visual-vestibulosomatosensory conflict induced by virtual reality on postural stability in humans. *J. Med. Investig.* 60 (3-4), 236–239. doi:10.2152/jmi.60.236

Ohlendorf, D., Doerry, C., Fisch, V., Schamberger, S., Erbe, C., Wanke, E. M., et al. (2019). Standard reference values of the postural control in healthy young female adults in Germany: An observational study. *BMJ Open* 9, e026833. doi:10.1136/bmjopen-2018-026833

Patti, A., Bianco, A., S¸ahin, Nes¸e., Sekulic, D., Paoli, A., Iovane, A., et al. (2018). Postural control and balance in a cohort of healthy people living in Europe. *Medicine* 97, 52, e13835. doi:10.1097/MD.0000000000013835

Prieto, T. E., Myklebust, J. B., Hoffmann, R. G., Lovett, E. G., and Myklebust, B. M. (1996). Measures of postural steadiness: Differences between healthy young and elderly adults. *IEEE Trans. Biomed. Eng. Sep.* 43 (9), 956–966. doi:10.1109/10.532130

Quialheiro, A., Maestri, T., Zimermann, T. A., Ziemann, R. M. D. S., Silvestre, M. V., Maio, J. M. B., et al. (2021). Stabilometric analysis as a cognitive function predictor in adults over the age of 50: A cross-sectional study conducted in a memory clinic. *J. Bodyw. Mov. Ther.* 27, 640–646. doi:10.1016/j.jbmt.2021.04.007

R Core Team. R (2018). *A language and environment for statistical computing*. Vienna, Austria: R Foundation for Statistical Computing. Available online: https://www.R-project.org (accessed on December 12, 2022).

Rodríguez-Rubio, P. R., Bagur-Calafat, C., López-de-Celis, C., Bueno-Gracía, E., Cabanas-Valdés, R., Herrera-Pedroviejo, E., et al. (2020). Validity and reliability of the satel 40 Hz stabilometric force platform for measuring quiet stance and dynamic standing balance in healthy subjects. *Int. J. Environ. Res. Public Health* 17 (21), 7733. doi:10.3390/ijerph17217733

Rosário, J. L. (2014). A review of the utilization of baropodometry in postural assessment. *J. Bodyw. Mov. Ther.* 18 (2), 215–219. doi:10.1016/j.jbmt.2013.05.016

Samson, M., and Crowe, A. (1996). Intra-subject inconsistencies in quantitative assessments of body sway. *Gait Posture* 4, 252–257. doi:10.1016/0966-6362(95)01050-5

Scoppa, F., and Gallamini, M. (2017). Clinical stabilometry standardization: Feet position in the static stabilometric assessment of postural stability. *Acta Med. Mediterr.* 33, 707. doi:10.19193/0393-6384_2017_4_105

Scoppa, F., and Gallamini, M. (2021). Clinical stabilometry standardization: Feet position in the static stabilometric assessment of postural stability. *Acta Med. Mediterr.* 33, 707. doi:10.19193/0393-6384_2017_4_105

Stoffregen, T. A., Pagulayan, R. J., Bardy, B. G., and Hettinger, L. J. (2000). Modulating postural control to facilitate visual performance. *Hum. Mov. Sci.* 19, 203–220. doi:10.1016/S0167-9457(00)00009-9

Takakusaki, K. (2017). Functional neuroanatomy for posture and gait control. *J. Mov. Disord.* 10, 1–17. doi:10.14802/jmd.16062

Tanaka, H., Nakashizuka, M., Uetake, T., and Itoh, T. (2000). The effects of visual input on postural control mechanisms: An analysis of center-of-pressure trajectories using the auto-regressive model. *J. Hum. Ergol.* 1–2. doi:10.11183/jhe1972.29.15

Tarantola, J., Nardone, A., Tacchini, E., and Schieppati, M. (1997). Human stance stability improves with the repetition of the task: Effect of foot position and visual condition. *Neurosci. Lett.* 228 (2), 75–78. doi:10.1016/s0304-3940(97)00370-4

Vieira Tde, M., de Oliveira, L. F., and Nadal, J. (2009). An overview of age-related changes in postural control during quiet standing tasks using classical and modern stabilometric descriptors. *J. Electromyogr. Kinesiol. Dec* 19 (6), e513–e519. doi:10.1016/j.jelekin.2008.10.007

frontiers | Frontiers in Bioengineering and Biotechnology

TYPE Original Research
PUBLISHED 12 December 2023
DOI 10.3389/fbioe.2023.1282024

OPEN ACCESS

EDITED BY
Claudio Belvedere,
Rizzoli Orthopedic Institute (IRCCS), Italy

REVIEWED BY
Xiaolong Zeng,
Guangzhou University of Chinese Medicine, China
Jonathan Rylander,
Baylor University, United States

*CORRESPONDENCE
Marco Recenti,
marcor@ru.is

†These authors have contributed equally to this work and share first authorship

RECEIVED 23 August 2023
ACCEPTED 22 November 2023
PUBLISHED 12 December 2023

CITATION
Ricciardi C, Ponsiglione AM, Recenti M, Amato F, Gislason MK, Chang M and Gargiulo P (2023), Development of soft tissue asymmetry indicators to characterize aging and functional mobility.
Front. Bioeng. Biotechnol. 11:1282024.
doi: 10.3389/fbioe.2023.1282024

Development of soft tissue asymmetry indicators to characterize aging and functional mobility

Carlo Ricciardi[1,2†], Alfonso Maria Ponsiglione[1,2†], Marco Recenti[2*], Francesco Amato[1], Magnus Kjartan Gislason[2], Milan Chang[3] and Paolo Gargiulo[2,4]

[1]Department of Electrical Engineering and Information Technology, University of Naples "Federico II", Naples, Italy, [2]Institute of Biomedical and Neural Engineering, Reykjavik University, Reykjavik, Iceland, [3]The Icelandic Gerontological Research Institute, Landspitali University Hospital, Reykjavik, Iceland, [4]Department of Science, Landspitali University Hospital, Reykjavik, Iceland

Introduction: The aging population poses significant challenges to healthcare systems globally, necessitating a comprehensive understanding of age-related changes affecting physical function. Age-related functional decline highlights the urgency of understanding how tissue composition changes impact mobility, independence, and quality of life in older adults. Previous research has emphasized the influence of muscle quality, but the role of tissue composition asymmetry across various tissue types remains understudied. This work develops asymmetry indicators based on muscle, connective and fat tissue extracted from cross-sectional CT scans, and shows their interplay with BMI and lower extremity function among community-dwelling older adults.

Methods: We used data from 3157 older adults from 71 to 98 years of age (mean: 80.06). Tissue composition asymmetry was defined by the differences between the right and left sides using CT scans and the non-Linear Trimodal Regression Analysis (NTRA) parameters. Functional mobility was measured through a 6-meter gait (Normal-GAIT and Fast-GAIT) and the Timed Up and Go (TUG) performance test. Statistical analysis included paired t-tests, polynomial fitting curves, and regression analysis to uncover relationships between tissue asymmetry, age, and functional mobility.

Results: Findings revealed an increase in tissue composition asymmetry with age. Notably, muscle and connective tissue width asymmetry showed significant variation across age groups. BMI classifications and gait tasks also influenced tissue asymmetry. The Fast-GAIT task demonstrated a substantial separation in tissue asymmetry between normal and slow groups, whereas the Normal-GAIT and the TUG task did not exhibit such distinction. Muscle quality, as reflected by asymmetry indicators, appears crucial in understanding age-related changes in muscle function, while fat and connective tissue play roles in body composition and mobility.

Discussion: Our study emphasizes the importance of tissue asymmetry indicators in understanding how muscle function changes with age in older individuals, demonstrating their role as risk factor and their potential employment in clinical assessment. We also identified the influence of fat and connective tissue on body

composition and functional mobility. Incorporating the NTRA technology into clinical evaluations could enable personalized interventions for older adults, promoting healthier aging and maintaining physical function.

KEYWORDS

aging, asymmetry, CT scan, body mass index, gait speed, soft tissue, muscle, sarcopenia

Introduction

The rapidly growing older population has become a significant healthcare concern in most developed societies (Kalseth and Halvorsen, 2020). With advances in healthcare and technology, people are living longer and healthier lives, but there is an urgent need to develop strategies to address the unique challenges of aging, including health disparities, social isolation, and financial insecurity (WHO, 2020). One of the most prominent manifestations of aging is functional decline, resulting in decreased muscle strength, an increased risk for falls, gait and balance problems, and chronic pain which highly affects the independency of older adults (Chatterjee et al., 2021).

Mobility, which is defined as the ability to move without assistance (Ostir et al., 2015; Treacy et al., 2022) is crucial for older adults to manage independent daily life (Visser et al., 2005; Schaap et al., 2013). Lower extremity function (LEF) is a critical measure of mobility and is frequently used as a clinical screening tool (Guralnik et al., 2000; Chang et al., 2013). The age-related decline in muscle mass and strength (Visser et al., 2005; Schaap et al., 2013) impacts the ability to walk quickly and efficiently in older adults, which ultimately leading to a slower gait speed over time (Goodpaster et al., 2006; Schaap et al., 2013; Reinders et al., 2015).

Sarcopenia, which refers to the simultaneous decline in skeletal muscle size and quality, has consistently been associated with various pathophysiological mechanisms that ultimately result in reduced lean tissue mass and the gradual fat infiltration of non-contractile tissue into lean muscle. This condition increases the risk of disability and mortality (Young et al., 1985; Kalyani et al., 2014). In older adults, there is often an asymmetrical distribution of muscle volume accompanied by a decrease in muscle mass and strength (Stagi et al., 2021). The asymmetry in muscle volume, particularly in the lower extremities, has been identified as a contributing factor to slower walking speed among older adults (Laroche et al., 2012; Lee et al., 2019; Mertz et al., 2019). Previous research has shown that older adults with asymmetrical muscle and fat mass exhibit poor physical performance in areas such as gait speed, balance, strength, and flexibility (Laroche et al., 2012; Miller et al., 2015; Lee et al., 2019; Mertz et al., 2019). These studies assessed muscle and fat mass asymmetry using techniques such as dual-energy X-ray absorptiometry (DEXA) (Lee et al., 2019; Mertz et al., 2019), computed tomography (CT) (Miller et al., 2015), and muscle strength measurements (Laroche et al., 2012). While existing studies have primarily focused on assessing muscle asymmetry using techniques such as dual-energy X-ray absorptiometry (DEXA), computed tomography (CT), and muscle strength measurements, there is a gap in the literature regarding asymmetry in other soft tissues of the legs, such as fat or connective tissue.

In recent years, our research group has focused on studying sarcopenia and has developed an approach based on analyzing features extracted from the radiodensitometric distribution of x-ray CT scans of mid-thigh cross-sectional images. This approach is known as the non-linear trimodal regression analysis (NTRA) (Edmunds et al., 2016; Edmunds et al., 2018). The NTRA features, consisting of 11 patient-specific parameters that characterize the quantity and quality of muscle, fat, and connective tissues using Hounsfield Unit (HU) radiodensitometric values, have shown predictive potential in classifying comorbidities such as diabetes and hypertension using Machine Learning (ML) in the older population (Recenti et al., 2020a). Additionally, ML algorithms have been employed in conjunction with the NTRA features to classify cardiac pathophysiologies, Body Mass Index (BMI), and isometric leg strength, achieving classification metrics with accuracy rates exceeding 95% (Ricciardi et al., 2020a; Recenti et al., 2020b; Recenti et al., 2021a). These features have also mediated the relationship between physical activity and lower extremity function (LEF) in aging individuals (Edmunds et al., 2021). Furthermore, previous studies observed that muscle features exhibit more significant variations compared to fat and connective tissues with regard to age and physical activity levels (Recenti et al., 2021b).

Despite the growing recognition of the importance of muscle quality and mobility (Simonsick et al., 2008; Reinders et al., 2015; Gonzalez et al., 2020; Borghi et al., 2022; Khaleghi et al., 2023), there still exists a lack of studies examining asymmetry and its implications regarding mobility in older adults. In contrast to previous studies focusing solely on NTRA features for one leg, a new approach assessing asymmetries in NTRA features may provide insight into how asymmetry in these three tissue types in the thigh relates to age and lower extremity function (LEF) among older adults. Furthermore, it may offer potential implications for the clinical assessment of age-related or changes in muscle quality and mobility among older adults (Harris et al., 2007). The aim of the current study is to investigate the differences between right and left legs using the NTRA features, establishing a set of asymmetry indicators, and assessing their relationships with age, BMI, gait speed and time up and go (TUGO). Data was from the large cohort of the AGES-Reykjavik study based on community-dwelling older adults in Iceland (Harris et al., 2007).

Materials and methods

Ages-Reykjavik dataset

The AGES-Reykjavik dataset includes, for the present study, a total of 3157 healthy elderly subjects from 71 to 98 years of age

TABLE 1 AGES Dataset: Sex differences and mean age in respect to BMI classes.

	BMI			
	<18.5	18.5–25	25–30	>30
Subject, N	53	1092	1341	667
Age, yrs, Mean (SD)	76.81 (5.98)	75.44 (5.97)	74.73 (5.96)	73.77 (5.96)
Male, N	21	466	561	269
Female, N	32	626	780	398

(mean: 80.06). All the participants were measured in a series of multimetric assessments including CT-scans, BMI and LEF performance tests (Harris et al., 2007). Informed signed consent was given by all participants. The ethical approval was certified by the Icelandic National Bioethics Committee (RU Code of Ethics, Paragraph 3—Article 2—Higher Education Institution Act 63/2006). A limited number of subjects was not able to complete one or more gait performance test due to different reasons so the total number of subjects considered for each of the next measurements can be lower than 3157 because of the presence of missing values in the dataset.

Anthropometric data

Heigh and weight of each subject were objectively measured (Chang et al., 2013; Recenti et al., 2021a) and BMI was determined by dividing the weight in kilograms by the square of the height in meters.

For the asymmetry analysis four BMI classes have been defined as follows (Table 1) (WHO, 2021):

- Class 1: BMI <18.5: below-normal (N = 53)
- Class 2: 18.5 < BMI <25: normal (N = 1092)
- Class 3: 25 < BMI <30: above-normal (N = 1341)
- Class 4: BMI >30: overweight (N = 667)

LEF performance tests

To assess the LEF, two tests were conducted: the 6-meter walk test and the Timed Up and Go Test (TUG) (Chang et al., 2013). The 6-meter gait walk test included two measurements, normal-GAIT and fast-GAIT, in meters per second (m/s). The test is reliable when performed standardly and well tolerated by elderly individuals (Cesari et al., 2005). Two gait speed data were consequently extracted: Normal Gait Speed and Fast Gait Speed. The normal gait has been proved to be strongly linked to disability, risk of fall and mortality (Guralnik et al., 2000; Studenski et al., 2011; Nakakubo et al., 2018) while the fast gait speed represents the maximum walking speed of older individual which is used as a predictor of frailty, falls, and mobility limitation (White et al., 2013).

The normal-GAIT Task, two classes have been defined using a threshold based on the distribution of the speed (equal to 1 m/s) (defined as *v_norm*) to carry out the task and adapted from the literature (Day and Lord, 2018) and reported as follows:

- Class 1: *v_norm* < 1 m/s: slow (N = 1966)
- Class 2: *v_norm* > 1 m/s: normal (N = 1084)

Similarly, for the fast-GAIT Task two classes have been defined using a threshold based on the distribution of the speed 1.3 m/s (defined as *v_fast*) to carry out the task and adapted from the literature (Day and Lord, 2018) and reported as follows:

- Class 1: *v_fast* < 1.3 m/s: slow (N = 1957)
- Class 2: *v_fast* > 1.3 m/s: normal (N = 800)

The TUG measured the time in seconds, it took for participants to stand up from a seated position (height of the chair: 45.5 cm), walk a distance of 3 m, turn around, walk back to the chair, and sit down again (Podsiadlo and Richardson, 1991). TUG is a valuable screening tool for detecting balance issues in older adults and is also used as a predictor of decline in daily activities (Newton, 1997). During the test, participants were allowed to wear their own footwear, and if needed, a cane or walker could be used. The time recorded for the first complete trial was used for the analysis (Chang et al., 2013).

The TUG has been defined in four classes using thresholds based on the distribution of the time to carry out the task and adapted from the literature (Podsiadlo and Richardson, 1991) and reported as follows:

- Class 1: TUG <10 s: fast (N = 660)
- Class 2: 10 s < TUG <13 s: average (N = 1333)
- Class 3: 13 s < TUG <29 s: slow (N = 1044)
- Class 4: TUG >29 s: very slow (N = 16)

Table 2 shows the dataset population age and sex characteristics with a focus on the LEF tests and their classes.

CT acquisition

All individuals included in the AGES-Reykjavík database underwent scanning using a 4-row CT detector system with a voltage setting of 120-kV (Sensation; Siemens Medical Systems, Erlangen, Germany). The scanned area spanned from the iliac crest to the knee. Prior to transaxial imaging, accurate positions were established by measuring the maximum length of the femur on an anterior-posterior localizer image, followed by locating the midpoint of the femoral long axis. Subsequent to CT image acquisition, a single 10 mm section was extracted from the middle of the thigh for each participant, positioned equidistantly between the acetabulum of the hip joint and the knee joint (Harris et al., 2007). The pixel elements within each slice were then subjected to processing using the NTRA method, enabling the derivation of personalized radiodensitometric value distributions ranging from −200 to 200 HU.

Non-linear trimodal regression analysis (NTRA) and asymmetry indicators

As mentioned previously, this study utilized the NTRA method to computationally characterize each distribution of HU. The NTRA

TABLE 2 AGES Dataset: Sex differences and mean age in respect to LEF tests.

	Normal-GAIT		Fast-GAIT		TUG			
	<1 m/s	>1 m/s	<1.3 m/s	>1.3 m/s	<10 s	10–13 s	13–29 s	>29 s
Subject, N	1966	1084	1957	800	660	1333	1044	16
Age, yrs Mean (SD)	79.97 (4.90)	80.04 (4.98)	80.05 (4.86)	79.92 (4.94)	79.91 (4.95)	80.05 (4.85)	80.14 (4.90)	80.06 (5.68)
Male, N	821	456	812	352	298	553	423	8
Female, N	1145	628	1145	448	362	780	621	8

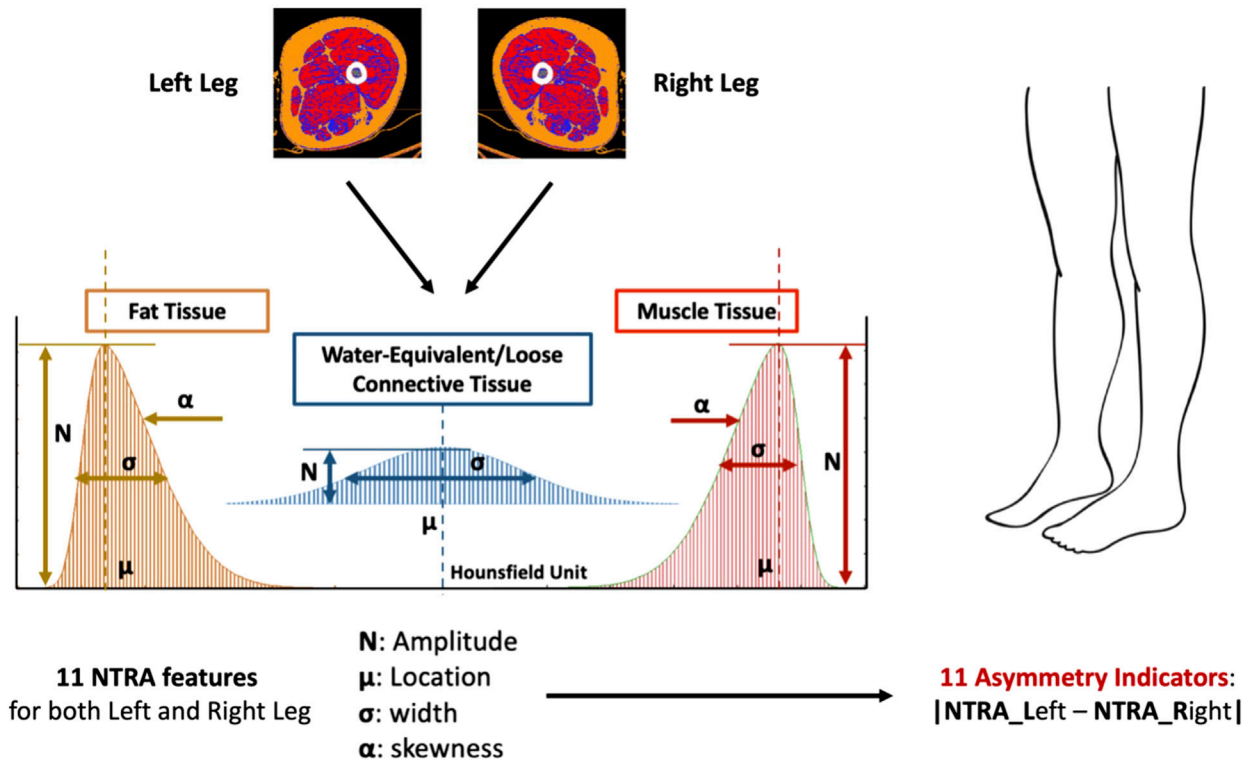

FIGURE 1
The 11 NTRA features are extracted from CT scan of both legs for a total of 22 NTRA features per subject. The Asymmetry Indicators are then computed as the absolute value of the NTRA difference between Left and Right legs. Each subject will have a total of 11 Asymmetry Indicators.

method, originally described in the study by Edmunds et al., 2016, treats each HU distribution as a quasi-probability density function that is defined by three Gaussian distributions. This definition arises from the hypothesis that HU distributions of cross-sectional soft tissues exhibit three distinct peaks or modes, corresponding to three separate tissue types with their own specific ranges of linear attenuation coefficients in the HU domain. These tissue types and their corresponding HU ranges are as follows: adipose or fat tissue [-200 to −10 HU], loose connective tissue [-9 to 40 HU], and lean muscle [41 to 200 HU]. The general form of this quasi-probability density function, representing the trimodal nature, can be expressed as Eq. 1, where N denotes the amplitude, μ represents the location, and σ indicates the width of the distribution. The parameter α captures the asymmetry (skewness) of the fat and muscle distributions, with a value of zero (non-skewed) assigned to the central connective tissue distribution.

$$\sum_{i=1}^{3}\varphi\left(x,N_i,\mu_i,\sigma_i,\alpha_i\right)=\sum_{1}^{3}\frac{N_i}{\sigma_i\sqrt{2\pi}}e^{-\frac{(x-\mu_i)^2}{2\sigma_i^2}}erfc\left(\frac{\alpha_i\left(x-\mu_i\right)}{\sigma_i\sqrt{2}}\right) \quad (1)$$

By employing a generalized reduced gradient algorithm and minimizing the standard error at each radio-absorption bin, theoretical HU distribution curves were generated, enabling the extraction of a total of 11 subject-specific NTRA parameters, 4 (N, μ, σ, α) from fat and muscle and 3 (N, μ, σ) from connective tissue (Figure 1).

The Asymmetry Indicators are computed as the absolute value of the NTRA difference between the values extracted from the left and the right legs (Eq. 2). Consequently, a total of 11 NTRA Asymmetry values is evaluated for each subject (Figures 1, 2).

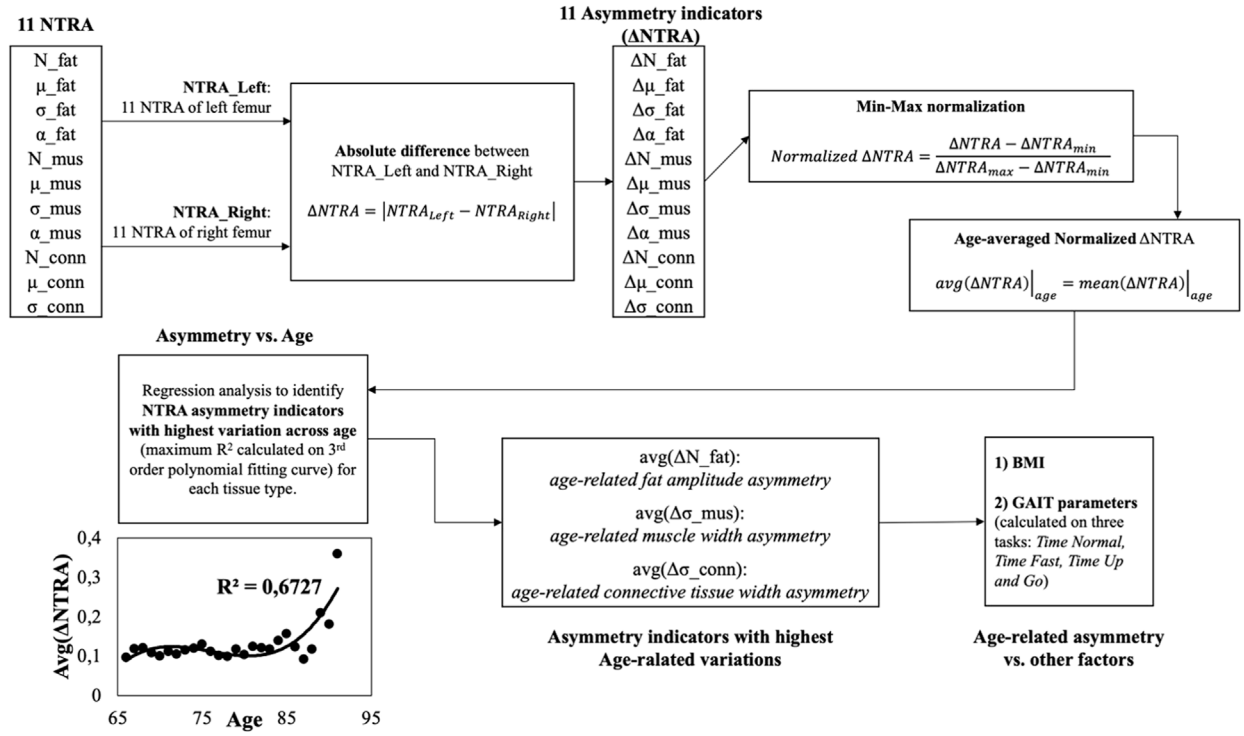

FIGURE 2
Workflow of the present study. Starting from the values of the 11 NTRA parameters for each leg (right $NTRA_{Right_i}$ and left $NTRA_{Left_i}$) (see block n.1 of Figure 2), the asymmetry indicators were calculated according to the following formula (see block n.2 of Figure 2)..

$$\Delta\text{NTRA} = |\,\text{NTRA}_{\text{Left}} - \text{NTRA}_{\text{Right}}| \quad (2)$$

Statistical analysis

The first analysis to find an overall asymmetry was performed by running a paired *t*-test to compare right and left NTRA parameters of each patient. The uncertainty level was set at 0.05. This test is used to investigate the presence of a difference between the right and the left NTRA parameter of each patient.

Then, the analytical workflow shown in Figure 2 has been adopted and described in the following.

$$\begin{gathered} Asymmetry\ indicator\ based\ on\ NTRA\ parameter \\ = \Delta NTRA_i = \left|NTRA_{Left_i} - NTRA_{Right_i}\right| \\ with\ i = 1, 2, \ldots .11\ indicating\ the\ i-th\ among \\ the\ 11\ NTRA\ indices\ \left(e.g., NTRA_{Left_1} = N_{fat}\ of\ the\ left\ leg\right) \end{gathered}$$

The results are 11 left-right leg asymmetry indicators, $\Delta NTRA_i$, (see block n. 3 of Figure 2).

These resulted indicators have been normalized using the min-max method according to the following formula (see block n. 4 of Figure 2):

$$\begin{aligned} normalized\ \Delta NTRA_i &= n\Delta NTRA_i \\ &= \frac{\Delta NTRA_i - \min\left(\Delta NTRA_i\right)}{\max\left(\Delta NTRA_i\right) - \min\left(\Delta NTRA_i\right)} \end{aligned}$$

Then the arithmetic mean of the normalized $\Delta NTRA_i$ for each age category has been calculated (see block n. 5 of Figure 2):

$$age-averaged\ asymmetry\ indicator = avg\left(\Delta NTRA_i\right)\big|_{age=y} = \frac{1}{Ny}\sum_{k=1}^{Ny} n\Delta NTRA_i|_k$$

$$\begin{gathered} with\ y = 65, 66 \ldots, 95 = patient\ age\ (in\ years), \\ Ny = number\ of\ patients\ with\ age = y, \\ n\Delta NTRA_i|_k\ is\ the\ value\ of\ the\ i-th \\ n\Delta NTRA\ beloging\ to\ the\ k\text{–}th\ patient\ with\ age = y. \end{gathered}$$

Afterwards, the age-averaged asymmetry indicators have been plotted against the age groups and a regression curve (by means of 3-rd order polynomial fitting curves) was adopted to model the asymmetry trends vs. age and to study the relationships between subjects' age and the degree of asymmetry (see block n. 6 of Figure 2). Based on the coefficient of determination (R^2) of the fitting curves, the asymmetry indicator with highest determination coefficient was chosen for each tissue type (fat, muscle and connective tissue) and have been moved for further analysis (see block n. 7 of Figure 2).

Finally, the degree of asymmetry was analyzed by grouping the data according to other physiological parameters, i.e., BMI, normal gait speed, fast gait speed, TUG (see block n. 8 of Figure 2). All the analyses were conducted using IBM SPSS v.27.

TABLE 3 Statistical analysis through a paired *t*-test to show the overall differences between right and left NTRA parameters per each tissue.

NTRA		Tissue types from the mid-thigh cross-sectional CT								
		Fat			Muscle			Connective tissue		
Parameter	Side	M	SD	*p*	M	SD	*p*	M	SD	*p*
N	L	135.16	69.92	0.004	184.84	42.06	0.008	90.05	25.10	0.009
	R	137.48	71.81		186.41	41.36		91.10	25.03	
μ	L	11.95	7.76	0.004	23.14	6.18	<0.001	44.61	10.15	0.024
	R	11.59	7.20		22.65	5.95		45.01	9.66	
σ	L	−106.22	7.47	0.079	61.71	3.37	0.055	−46.4	26.80	0.010
	R	−106.42	7.01		61.6	3.23		−45.3	26.06	
α	L	0.018	0.14	0.807	3.09	0.67	<0.001			
	R	0.019	0.17		3.15	0.63				

CT: computed tomography, N: amplitude, μ: location, σ: width, α: skewness, L: left, R: right M: mean; SD: standard deviation; *p*: *p*-value.

TABLE 4 Determination coefficients of the third order polynomial fitting curves used (ΔNTRA) to fit the 11 age-averaged normalized values of the asymmetry indicators.

NTRA parameter	Tissue types		
	Fat	Muscle	Connective tissue
	R^2	R^2	R^2
avg (ΔN)	**0.50**	0.31	0.36
avg (Δμ)	0.23	0.34	0.21
avg (Δσ)	0.21	**0.76**	**0.75**
avg (Δα)	0.18	0.16	

N: amplitude, μ: location, σ: width, α: skewness, R^2: coefficient of determination.

Results

NTRA paired t-tests

Table 3 shows the results of the statistical analysis conducted on AGES dataset to compare the values of the right and the left NTRA parameter of each patient. A paired *t*-test was conducted to show the overall differences.

Table 3 shows that amplitude and location of each tissue were statistically significantly different ($p < 0.005$ for each parameter). Connective tissue had also a statistically significant difference in width ($p = 0.01$) and muscle had a statistically significant difference in skewness ($p < 0.001$) and a trend in width ($p = 0.055$). These results already provide with an idea of overall presence of asymmetry in the analyzed patients.

Asymmetry vs. age

By averaging the normalized asymmetry indicators (ΔNTRA) across the age groups and by fitting the age-related trends using a third order polynomial fitting curves, it was possible to determine the NTRA asymmetry indicators with the highest variation explained by the fitting model (i.e., highest determination coefficients, R^2) across age for each tissue type (fat, muscle, and connective tissue). The corresponding R^2 values are reported in Table 4 and the age-related trends for the three identified ΔNTRA with highest age-related variations are displayed in Figure 3.

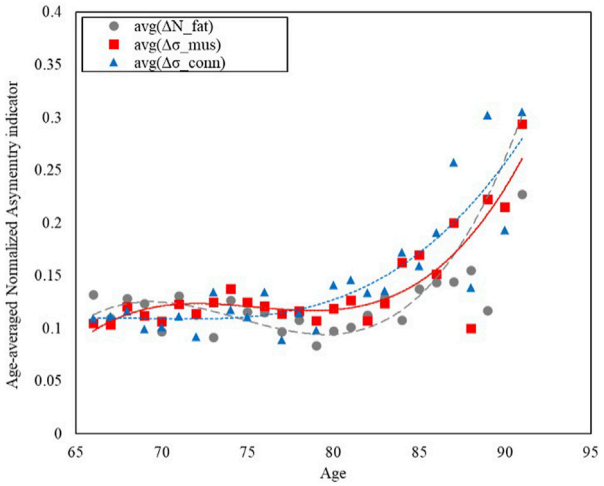

FIGURE 3
Trends of the age-averaged normalized values of the NTRA asymmetry indicators exhibiting most significant variation across population age for: Fat (avg(ΔN_{fat}), grey circles), Muscle (avg($\Delta\sigma_{mus}$), red squares), and Connective Tissue (avg($\Delta\sigma_{conn}$), blue triangles). Third order polynomial fitting curves are also reported for each data series: Fat (avg(ΔN_{fat}), grey dashed line), Muscle (avg($\Delta\sigma_{mus}$), red line), and Connective Tissue (avg($\Delta\sigma_{conn}$), blue dotted line).

Figure 3 shows how the asymmetry increases with age, with a growing trend that has been modelled with third order polynomial fitting curves for the three NTRA parameters exhibiting most significant variation across the population age for each tissue category, namely, N_{fat}, σ_{mus}, and σ_{conn}.

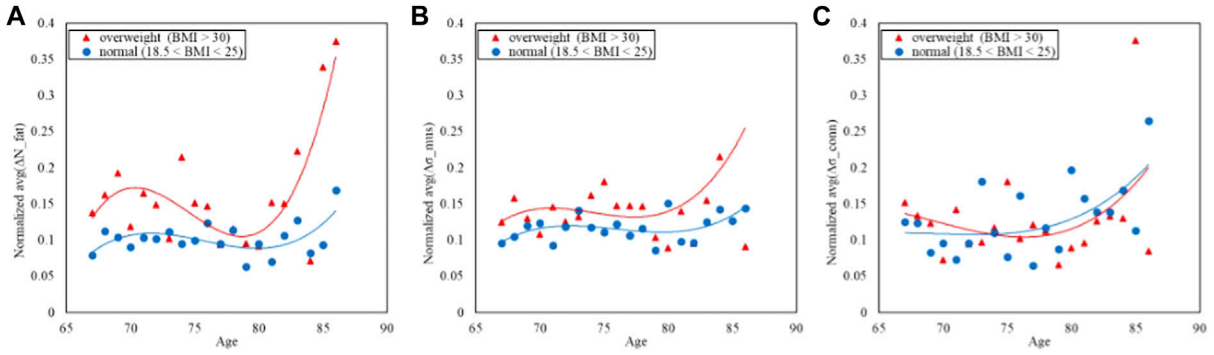

FIGURE 4
Trends of the age-averaged normalized values of ΔN_{fat} **(A)**, $\Delta\sigma_{mus}$ **(B)**, and $\Delta\sigma_{conn}$ **(C)** based on BMI groups, namely, overweight (red triangles) and normal (blue circles). Third order polynomial fitting curves are also reported for both overweight (red line) and normal (blue line) groups.

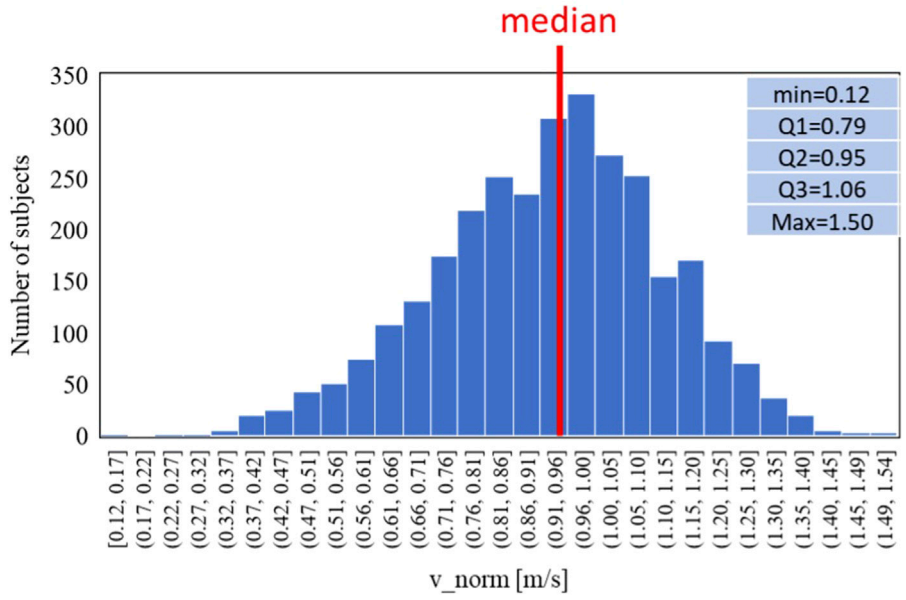

FIGURE 5
Data distribution of the normal-GAIT task reference parameter (*v_norm*).

Asymmetry vs. BMI

The values of the above selected NTRA asymmetry features have been investigated across the BMI groups as reported in Figure 4, following the four classes defined previously.

Figure 4 displays the comparison of the trends in the NTRA asymmetry indicators. The separability between normal and overweight BMI classes is far more evident in both the fat and muscle NTRA asymmetry parameters, where the average asymmetry is higher in the overweight group than the normal one. In the case of the connective tissue, the plot does not show appreciable separation among the two groups.

Asymmetry vs. Gait

The study of potential confounding factors and covariates has been also carried out grouping the population according to the three LEF formerly defined (Gait Normal Task, Gait Fast Task and Gait TUG).

Figures 5, 6 refer to the normal-GAIT Task and report respectively the distribution of the speed to carry out the task (equal to 1 m/s) and the relative trends split according to the classes defined previously.

Similarly Figures 7, 8 report respectively the distribution of the speed in fast-GAIT (median 1.3 m/s) and the trends by a fast-GAIT Task.

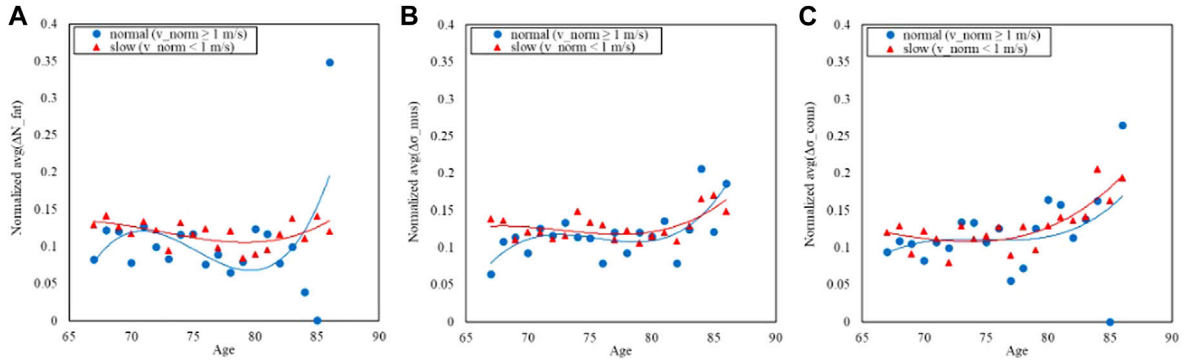

FIGURE 6
Trends of the age-averaged normalized values of ΔN_{fat} **(A)**, $\Delta\sigma_{mus}$ **(B)**, and $\Delta\sigma_{conn}$ **(C)** based on GAIT Normal Task groups, namely, slow (red triangles) and normal (blue circles). Third order polynomial fitting curves are also reported for both slow (red line) and normal (blue line) groups.

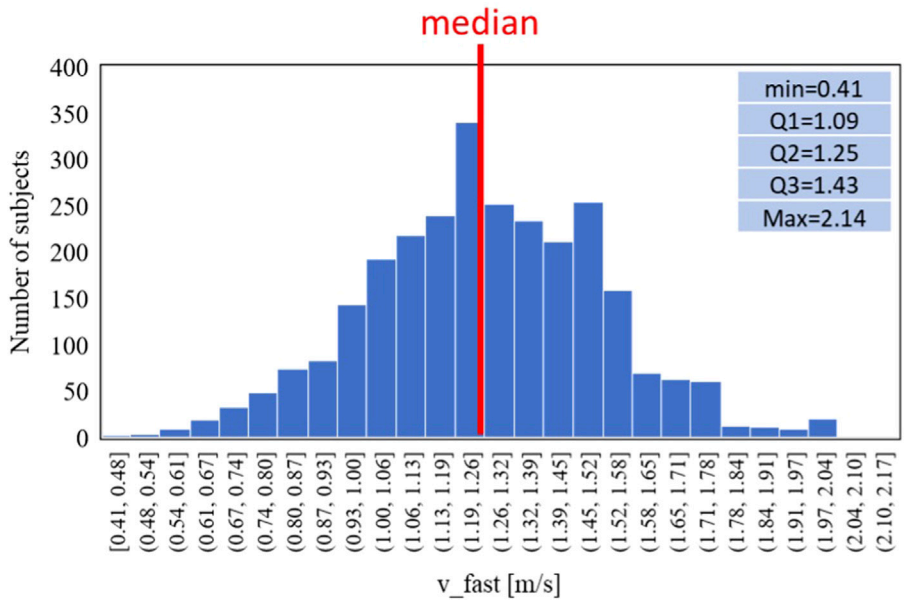

FIGURE 7
Data distribution of the fast-GAIT task reference parameter (*v_fast*).

Finally, the same analysis is shown for the TUG: Figure 9 shows the distribution of the time while Figure 10 shows the trends split according to the TUG classes.

Figures 6, 8, 10 show how the Fast Task (Figure 8) can separate the normal and slow groups, thus confirming to be a confounding factor that could influence the asymmetry trend with age. On the contrary, Normal Task (Figure 6) and TUG (Figure 10) are not able to enhance the difference between the groups of subjects, thereby not showing a markable different trends of the asymmetry with age.

Discussion

Summary

This study aimed to explore whether there existed a connection between soft tissue composition asymmetry (heterogeneity), as defined by radiodensity analysis of thigh CT scans, and the functional mobility of the older Icelandic population. Our findings revealed that the asymmetry in tissue composition grows more pronounced with advancing age. Indeed, we observed that CT

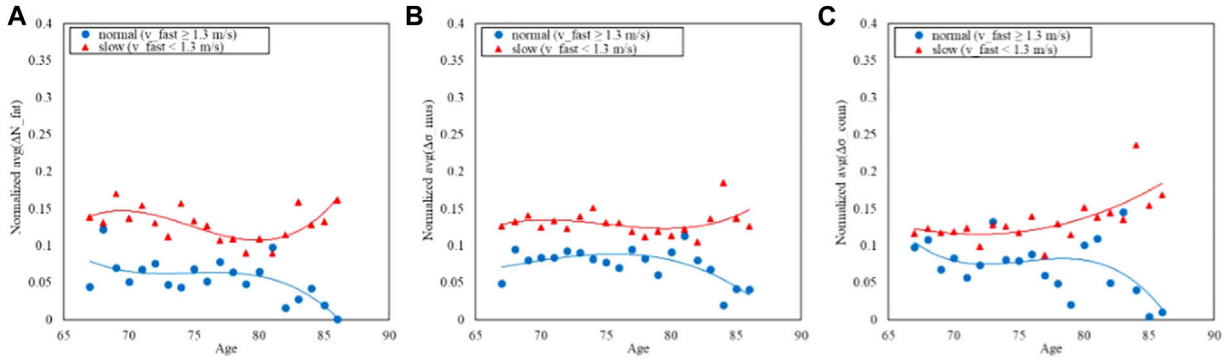

FIGURE 8
Trends of the age-averaged normalized values of ΔN_{fat} **(A)**, $\Delta\sigma_{mus}$ **(B)**, and $\Delta\sigma_{conn}$ **(C)** based on GAIT Fast Task groups, namely, slow (red triangles) and normal (blue circles). Third order polynomial fitting curves are also reported for both slow (red line) and normal (blue line) groups.

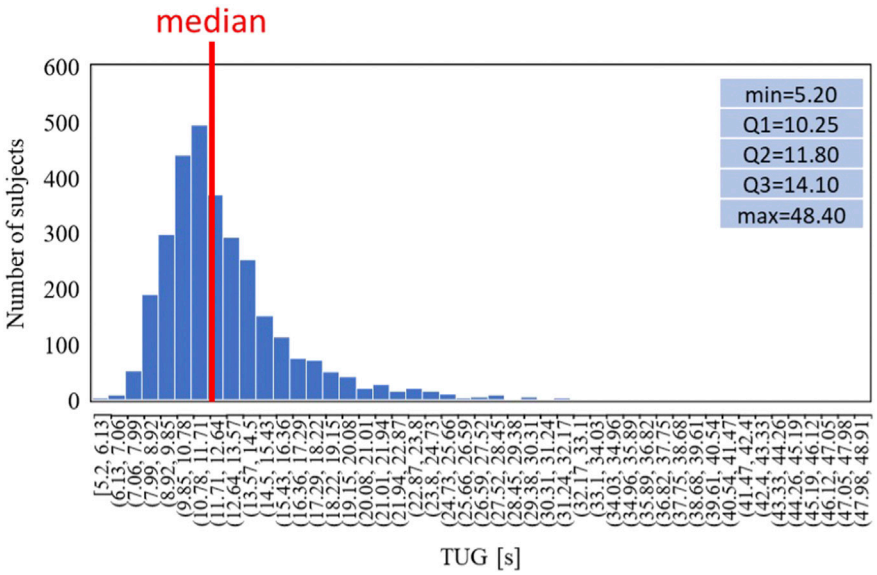

FIGURE 9
Data distribution of the TUG task.

densitometric distribution can provide indicators of asymmetry in tissue composition (heterogeneity). The main results showed that tissue asymmetry increases with age with a nonlinear trend that could be modeled with third order polynomial curve to quantitatively describe up to 76% of the variation in the asymmetry across age. Moreover, our observations suggested that relationships between age and asymmetry could be also influenced by further possible confounding factors, such as BMI and mobility functions. The results also confirmed that the tissue composition asymmetry is a valuable indicator for evaluating age-related changes in muscle condition and provided insights for both musculoskeletal conditions and mobility function in older individuals. Particularly, three types of tissue composition including muscle, fat, and connective tissue provided comprehensive understanding of the intrinsic relationships between muscle quality, aging, and physical function. Recognizing the critical role of maintaining mobility function, especially among those at high risk of functional decline (Simonsick et al., 2008), our study underscores the importance of asymmetry information. Aligning with previous research (Wilkinson et al., 2018), our findings highlight that differences in muscle mass between the right and left thighs can result in imbalances affecting strength and function, particularly in movements like walking or climbing stairs. Variations in fat distribution impact body weight distribution, potentially influencing gait, and balance (Gonzalez et al., 2020; Khaleghi et al., 2023), while the connective tissue between muscle and fat in the thigh serves as a predictor of incident of mobility disability (Schaap et al., 2013; Reinders et al., 2015; Borghi et al., 2022). Despite the growing recognition of the importance of this asymmetry information, there is a notable absence of studies examining its

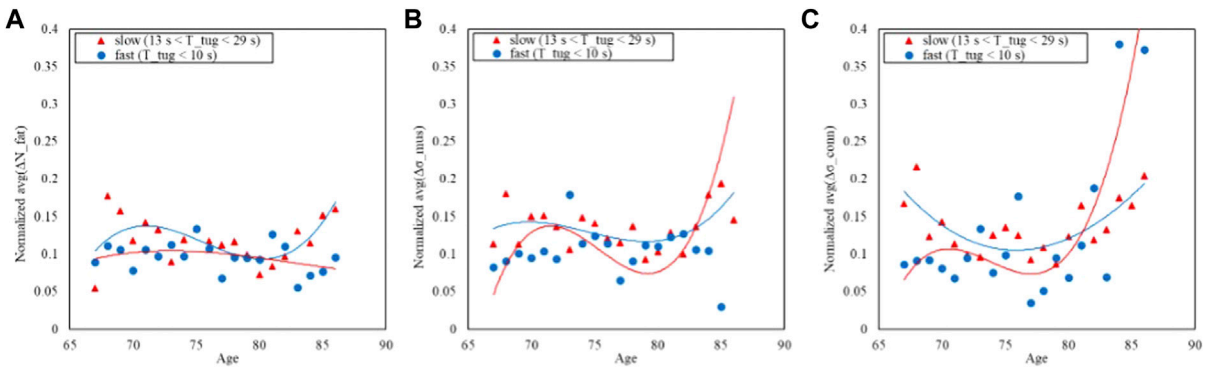

FIGURE 10
Trends of the age-averaged normalized values of ΔN_{fat} **(A)**, $\Delta\sigma_{mus}$ **(B)**, and $\Delta\sigma_{conn}$ **(C)** based on GAIT TUG groups, namely, slow (red triangles) and fast (blue circles). Third order polynomial fitting curves are also reported for both slow (red line) and normal (blue line) groups.

implications in designing effective interventions to improve and sustain mobility function in older adults. Therefore, asymmetries in different tissue types can be a potential determinants of mobility limitation among older adults as well. In this context, the information regarding asymmetry in different tissue types in the thigh area can guide the targeted interventions and rehabilitation strategies to enhance the mobility.

Asymmetry and physical function

Quantitative loss of muscle over age is a well-known condition in older adults (Curtis et al., 2015). Decline of muscle mass and function, defined as "sarcopenia," is closely linked to impaired physical function and an increased risk of mortality in the aging population (Cawthon, 2015; Clark, 2019). Regarding the muscle aging in older adults, it is vital to recognize that the decline of muscle function is not only due to the loss of muscle mass but also other factors that affect the muscle quality including muscle composition and fatty infiltration (Goodpaster et al., 2006; Reinders et al., 2015). The asymmetry condition in the muscle strength among older adults was also reported in few studies (Skelton et al., 2002; Perry et al., 2007), and one recent study reported that asymmetry in lower extremity strength was associated with functional mobility among older community-living older adults (Lee et al., 2019).

Muscle quality and physical function

The aging process in muscle is widely associated with myofibrosis, a condition marked by an elevated presence of fibrous connective tissue along with a diminished ability for muscle regeneration which may cause a gradual replacement of muscle tissue with fibrous connective tissue (Wang and Zhou, 2022). This process is still relatively unknown but elevated levels of myofibrosis appear closely linked with increased perimuscular subcutaneous adipose tissue, leading to a subsequent rise in chronic low-grade inflammation (Zoico et al., 2013). The accumulation of fat and connective tissues in skeletal muscle contribute to significant muscle impairment in older individuals (Correa-de-Araujo and Hadley, 2014) which could potentially contribute to age-related variations in physical performance (Correa-de-Araujo and Hadley, 2014; Correa-de-Araujo et al., 2017). The current research offers a more holistic understanding of age-related transformations within the musculoskeletal system by encompassing not only muscle and fat tissue but also considering muscle quality in relation to connective tissue among older adults.

Asymmetry indicators and age-related trends

Only a limited number of studies have explored the muscle quality of older adults which included connective tissue using thigh CT scans among older adults (Recenti et al., 2020a; Ricciardi et al., 2020a; Recenti et al., 2021b). Previous study reported that these three tissue types had high correlation with lower extremity functions and BMI (Edmunds et al., 2018; Recenti et al., 2021a). The current study further explored the potential association between asymmetry in the three tissue types, age, and physical function. The results revealed that the asymmetry in muscle and connective tissue width play as major contributors to the variation across different age groups. These results emphasize the potential role of these tissue components in age-related changes and their impact on physical function which is in line with previous research (Zoico et al., 2013; Lee et al., 2019).

Our findings add a new perspective to understanding how different tissue components collectively contribute to functional mobility and overall physical wellbeing by looking at asymmetrical condition in the three types of soft tissues analyzed with NTRA on the mid-tight CT scan. The significant differences observed in all the tissues asymmetry indicators highlight the distinct characteristics of each tissue type. Connective tissue asymmetry's difference in width reflects its potential involvement in age-related changes underlying the not negligible impact of the connective tissue itself in the sarcopenia studies. Differences in skewness and width in muscle tissue asymmetry suggest alterations in muscle quality, which might be linked to muscle function, mobility, and overall physical performance. The asymmetry in fat tissue amplitude variations across age indicate

that adipose tissue plays a pivotal role in age-related changes which reflect changes in body composition, metabolism, and the potential influence of adipose tissue on muscle function with aging (Ribisl et al., 2007). The asymmetry indicators were also able to differentiate levels of BMI among the older Icelandic population of the AGES dataset. The correlation between asymmetry indicators and BMI highlights the potential influence of body composition on tissue distribution and physical function. This could be especially relevant for understanding the impact of obesity on musculoskeletal health and mobility in older adults. This might reflect alterations in body composition, metabolism, and the potential influence of adipose tissue on muscle function (Correa-de-Araujo et al., 2020). Similarly, asymmetry in muscle tissue across age suggests their contribution to changes in musculoskeletal structure and function over time as both weak muscle strength and high BMI is higher associated with poorer physical performance (Hardy et al., 2013). Our findings revealed that the asymmetry indicators in all three tissue types were able to separate normal and slow groups in Fast-GAIT task. The separation of normal and slow groups suggests that asymmetry has the potential to serve as a marker of gait performance and mobility status. They could be utilized to identify individuals who might be at a higher risk of age-related decline in physical function or those who may require tailored interventions to maintain or improve their mobility and overall health. Although TUG tests are well recognized as a predictor of fall or frailty among older individuals (Savva et al., 2013; Barry et al., 2014) the lack of differentiation in asymmetry for the TUG task emphasizes that not all functional tasks may be equally influenced by tissue asymmetry, reflecting the multifaceted nature of physical function. However, incorporating assessments of tissue asymmetry, including muscle, fat, and connective tissue, into clinical evaluations could provide a more nuanced evaluation of muscle health and potential mobility issues in older adults. This approach may allow healthcare professionals to better tailor treatment plans and interventions to address specific tissue-related challenges.

The identification of a relationship between tissue asymmetry and functional mobility suggests new directions for further research. Investigating the underlying mechanisms linking these tissue asymmetries to mobility and exploring the potential influence of different factors including lifestyle, genetics, and exercise could lead to a deeper understanding of musculoskeletal aging processes.

Limitations and strengths

The strength of the study is the comprehensive analysis on the tissue composition, including muscle, fat, and connective tissue, which provides a holistic understanding of age-related changes. Further, the incorporation of functional mobility tasks including Normal-GAIT, Fast-GAIT, and TUG enhances the relevance of the findings to the real-world physical performance test with muscle quality. The study findings offer potential insights for developing clinical assessment tools that could aid in identifying individuals at risk of functional decline.

The study includes some limitations. First, the cross-sectional nature of the study restricted the ability to establish causal relationships between tissue composition asymmetry and age-related changes or functional performance. Future research could consider incorporating longitudinal designs, which would provide a more comprehensive understanding of the dynamic interplay between tissue asymmetry, aging, and various functional outcomes including comorbidities that typically affect the elderly population. A potential future development could be the employment of machine learning classification algorithms to longitudinally predict comorbidities like cardiac pathophysiology, diabetes, and hypertension utilizing the asymmetry indicators as input including an in-depth feature importance analysis. Second, the study's sample size might limit the generalizability of findings to broader populations. The current study is a cross-sectional study based secondary analysis and the available data is only for those who completed the physical performance test at the measurement site. Therefore, it is possible that those with available data may have been healthier than those who were excluded or not completed the measurement. Despite the thousands of subjects included in this research, larger and more diverse samples, with a wider range of demographic characteristics and health statuses may further enhance our findings. Thirdly, the study's asymmetry measurements might not have captured the full complexity of tissue composition and its impact on functional mobility. Utilizing multi-dimensional assessments that encompass factors like muscle strength, flexibility, and coordination could offer a more holistic view for the relationship between tissue asymmetry and functional outcomes in older adults. The study considers limited factors like BMI and gait speed. Future analyses with additional data such as genetics, comorbidities, and lifestyle factors with advanced statistical methods and machine learning predictive approaches might contribute to new insights on the observed outcomes. A further limitation of this study is the use CT scan to analyze old people: CT is typically reserved for specific diagnostic purposes when the benefits outweigh the risks. A recent study demonstrated a significant association between CT scans and blood tumors in young subjects (Bosch de Basea Gomez et al., 2023). This underscores the need for caution in the use of CT scans, prompting a recommendation for further research and clinical exploration to limit their unnecessary application.

Additionally, with a particular reference to the investigated muscle asymmetry indicator ($\Delta\sigma_{mus}$), it is worth noting that this reflects the heterogeneity in the muscle tissue, and it may have important implications in the clinical assessment of age-related or pathologic changes in muscle quality (Harris-Love et al., 2019). Therefore, future work will aim at investigating physiological phenomena involved in the tissue asymmetry changes and analyzing other confounding factors through advanced data analysis approaches with aim of defining novel robust quantitative metrics to monitor healthy aging.

Conclusion

In conclusion, the investigation on asymmetry across various tissue types of muscle, fat, and connective tissue provides a further understanding of the multifaceted factors influencing musculoskeletal health. The significant contributions of the NTRA features in particular muscle and connective tissue width asymmetry indicators to variations across age groups presented their potential roles. These findings suggest that tissue asymmetry could

have significant diagnostic and prognostic value as markers for age-related declines and mobility restrictions which provide possibilities for early interventions and personalized treatments. Furthermore, the study's limitations emphasize the need for future research, including longitudinal studies and more extensive participant samples, to fully elucidate the underlying mechanisms and potential applications of tissue composition asymmetry in aging and physical function. The long-term goal of our research is to define robust quantitative metrics to effectively monitor healthy aging and gain a deeper understanding of the impact of tissue composition on physical function in older adults.

Data availability statement

The datasets presented in this article are not readily available because the AGES I-II dataset cannot be made publicly available, since the informed consent signed by the participants prohibits data sharing on an individual level, as outlined by the study approval by the Icelandic National Bioethics Committee (RU Code of Ethics, Paragraph 3—Article 2—Higher Education Institution Act 63/2006). Requests to access the datasets should be directed to Hjartavernd—The Icelandic Heart Association: afgreidsla@hjarta.is.

Ethics statement

The studies involving humans were approved by the Icelandic National Bioethics Committee (RU Code of Ethics, Paragraph 3—Article 2—Higher Education Institution Act 63/2006). The studies were conducted in accordance with the local legislation and institutional requirements. The participants provided their written informed consent to participate in this study.

Author contributions

CR: Conceptualization, Investigation, Methodology, Visualization, Writing–original draft, Validation. AP: Conceptualization, Investigation, Methodology, Visualization, Writing–original draft, Validation. MR: Conceptualization, Investigation, Visualization, Writing–original draft, Writing–review and editing, Data curation. FA: Supervision, Writing–review and editing. MG: Conceptualization, Data curation, Formal Analysis, Writing–review and editing. MC: Methodology, Supervision, Visualization, Writing–original draft, Writing–review and editing. PG: Conceptualization, Funding acquisition, Project administration, Resources, Supervision, Writing–review and editing.

Funding

The author(s) declare that no financial support was received for the research, authorship, and/or publication of this article.

Acknowledgments

The authors wish to thank the University Hospital Landspitali and Reykjavik University for the infrastructural support and Hjartavernd—The Icelandic Heart Association for the collaboration and access to the data.

Conflict of interest

The authors declare that the research was conducted in the absence of any commercial or financial relationships that could be construed as a potential conflict of interest.

The author(s) declared that they were an editorial board member of Frontiers, at the time of submission. This had no impact on the peer review process and the final decision.

Publisher's note

References

Barry, E., Galvin, R., Keogh, C., Horgan, F., and Fahey, T. (2014). Is the Timed up and Go test a useful predictor of risk of falls in community dwelling older adults: a systematic review and meta-analysis. *BMC Geriatr.* 14, 14. doi:10.1186/1471-2318-14-14

Borghi, S., Bonato, M., La Torre, A., Banfi, G., and Vitale, J. A. (2022). Interrelationship among thigh intermuscular adipose tissue, cross-sectional area, muscle strength, and functional mobility in older subjects. *Med. Baltim.* 101 (26), e29744. doi:10.1097/MD.0000000000029744

Bosch de Basea Gomez, M., Thierry-Chef, I., Harbron, R., Hauptmann, M., Byrnes, G., Bernier, M. O., et al. (2023). Risk of hematological malignancies from CT radiation exposure in children, adolescents and young adults. *Nat. Med.* 2023, 1–9. doi:10.1038/s41591-023-02620-0

Cawthon, P. M. (2015). Assessment of lean mass and physical performance in sarcopenia. *J. Clin. Densitom.* 18 (4), 467–471. doi:10.1016/j.jocd.2015.05.063

Cesari, M., Kritchevsky, S. B., Penninx, B. W., Nicklas, B. J., Simonsick, E. M., Newman, A. B., et al. (2005). Prognostic value of usual gait speed in well-functioning older people—results from the Health, Aging and Body Composition Study. *J. Am. Geriatr. Soc.* 53, 1675–1680. doi:10.1111/j.1532-5415.2005.53501.x

Chang, M., Saczynski, J. S., Snaedal, J., Bjornsson, S., Einarsson, B., Garcia, M., et al. (2013). Midlife physical activity preserves lower extremity function in older adults: age gene/environment susceptibility-Reykjavik study. *J. Am. Geriatr. Soc.* 61, 237–242. doi:10.1111/jgs.12077

Chatterjee, P., Pedrini, S., Stoops, E., Goozee, K., Villemagne, V. L., Asih, P. R., et al. (2021). Plasma glial fibrillary acidic protein is elevated in cognitively normal older adults at risk of Alzheimer's disease. *Transl. Psychiatry* 11, 27–10. doi:10.1038/s41398-020-01137-1

Clark, B. C. (2019). Neuromuscular changes with aging and sarcopenia. *J. frailty aging* 8, 7–9. doi:10.14283/jfa.2018.35

Correa-de-Araujo, R., Addison, O., Miljkovic, I., Goodpaster, B. H., Bergman, B. C., Clark, R. V., et al. (2020). Myosteatosis in the context of skeletal muscle function deficit: an interdisciplinary workshop at the National Institute on Aging. *Front. physiology* 11, 963. doi:10.3389/fphys.2020.00963

Correa-de-Araujo, R., and Hadley, E. (2014). Skeletal muscle function deficit: a new terminology to embrace the evolving concepts of sarcopenia and age-related muscle dysfunction. *Journals Gerontology Ser. A Biomed. Sci. Med. Sci.* 69 (5), 591–594. doi:10.1093/gerona/glt208

Correa-de-Araujo, R., Harris-Love, M. O., Miljkovic, I., Fragala, M. S., Anthony, B. W., and Manini, T. M. (2017). The need for standardized assessment of muscle quality in skeletal muscle function deficit and other aging-related muscle dysfunctions: a symposium report. *Front. physiology* 8, 87. doi:10.3389/fphys.2017.00087

Curtis, E., Litwic, A., Cooper, C., and Dennison, E. (2015). Determinants of muscle and bone aging. *J. Cell. physiology* 230 (11), 2618–2625. doi:10.1002/jcp.25001

Day, B. L., and Lord, S. R. (2018). *Balance, gait, and falls*. Elsevier.

Edmunds, K., Gíslason, M., Sigurðsson, S., Guðnason, V., Harris, T., Carraro, U., et al. (2018). Advanced quantitative methods in correlating sarcopenic muscle degeneration with lower extremity function biometrics and comorbidities. *PloS one* 13 (3), e0193241. doi:10.1371/journal.pone.0193241

Edmunds, K. J., Árnadóttir, Í., Gíslason, M. K., Carraro, U., and Gargiulo, P. (2016). Nonlinear trimodal regression analysis of radiodensitometric distributions to quantify sarcopenic and sequelae muscle degeneration. *Comput. Math. Methods Med.* 2016, 1–10. doi:10.1155/2016/8932950

Edmunds, K. J., Okonkwo, O. C., Sigurdsson, S., Lose, S. R., Gudnason, V., Carraro, U., et al. (2021). Soft tissue radiodensity parameters mediate the relationship between self-reported physical activity and lower extremity function in AGES-Reykjavík participants. *Sci. Rep.* 11 (1), 20173. doi:10.1038/s41598-021-99699-7

Gonzalez, M., Gates, D. H., and Rosenblatt, N. J. (2020). The impact of obesity on gait stability in older adults. *J. Biomech.* 100, 109585. doi:10.1016/j.jbiomech.2019.109585

Goodpaster, B. H., Park, S. W., Harris, T. B., Kritchevsky, S. B., Nevitt, M., Schwartz, A. V., et al. (2006). The loss of skeletal muscle strength, mass, and quality in older adults: the health, aging and body composition study. *J. Gerontol. A Biol. Sci. Med. Sci.* 61, 1059–1064. doi:10.1093/gerona/61.10.1059

Guralnik, J. M., Ferrucci, L., Pieper, C. F., Leveille, S. G., Markides, K. S., Ostir, G. V., et al. (2000). Lower extremity function and subsequent disability consistency across studies, predictive models, and value of gait speed alone compared with the short physical performance battery. *J. Gerontol. A Biol. Sci. Med. Sci.* 55, M221–M231. doi:10.1093/gerona/55.4.M221

Hardy, R., Cooper, R., Aihie Sayer, A., Ben-Shlomo, Y., Cooper, C., Deary, I. J., et al. (2013). Body mass index, muscle strength and physical performance in older adults from eight cohort studies: the HALCyon programme. *PloS one* 8 (2), e56483. doi:10.1371/journal.pone.0056483

Harris, T. B., Launer, L. J., Eiriksdottir, G., Kjartansson, O., Jonsson, P. V., Sigurdsson, G., et al. (2007). Age, gene/environment susceptibility–Reykjavik study: multidisciplinary applied phenomics. *Amer. J. Epidemiol.* 165 (9), 1076–1087. doi:10.1093/aje/kwk115

Harris-Love, M. O., Gonzales, T. I., Wei, Q., Ismail, C., Zabal, J., Woletz, P., et al. (2019). Association between muscle strength and modeling estimates of muscle tissue heterogeneity in young and old adults. *J. Ultrasound Med.* 38 (7), 1757–1768. doi:10.1002/jum.14864

Kalseth, J., and Halvorsen, T. (2020). Health and care service utilisation and cost over the life-span: a descriptive analysis of population data. *BMC Health Serv. Res.* 20, 435. doi:10.1186/s12913-020-05295-2

Kalyani, R. R., Corriere, M., and Ferrucci, L. (2014). Age-related and disease-related muscle loss: the effect of diabetes, obesity, and other diseases. *lancet Diabetes and Endocrinol.* 2 (10), 819–829. doi:10.1016/s2213-8587(14)70034-8

Khaleghi, M. M., Emamat, H., Marzban, M., Farhadi, A., Jamshidi, A., Ghasemi, N., et al. (2023). The association of body composition and fat distribution with dysmobility syndrome in community-dwelling older adults: bushehr Elderly Health (BEH) program. *BMC Musculoskelet. Disord.* 24 (1), 809. doi:10.1186/s12891-023-06934-5

Laroche, D. P., Cook, S. B., and Mackala, K. (2012). Strength asymmetry increases gait asymmetry and variability in older women. *Med. Sci. Sports Exerc* 44, 2172–2181. doi:10.1249/MSS.0b013e31825e1d31

Lee, E. J., Lee, S. A., Soh, Y., Kim, Y., Won, C. W., and Chon, J. (2019). Association between asymmetry in lower extremity lean mass and functional mobility in older adults living in the community. *Med. Baltim.* 98, e17882. doi:10.1097/MD.0000000000017882

Mertz, K. H., Reitelseder, S., Jensen, M., Lindberg, J., Hjulmand, M., Schucany, A., et al. (2019). Influence of between-limb asymmetry in muscle mass, strength, and power on functional capacity in healthy older adults. *Scand. J. Med. Sci. Sports* 29, 1901–1908. doi:10.1111/sms.13524

Miller, R. R., Eastlack, M., Hicks, G. E., Alley, D. E., Shardell, M. D., Orwig, D. L., et al. (2015). Asymmetry in CT scan measures of thigh muscle 2 Months after hip fracture: the Baltimore hip studies. *J. Gerontol. Ser. A* 70, 1276–1280. doi:10.1093/gerona/glv053

Nakakubo, S., Doi, T., Makizako, H., Tsutsumimoto, K., Hotta, R., Kurita, S., et al. (2018). Association of walk ratio during normal gait speed and fall in community-dwelling elderly people. *Gait posture* 66, 151–154. doi:10.1016/j.gaitpost.2018.08.030

Newton, R. A. (1997). Balance screening of an inner city older adult population. *Arch. Phys. Med. Rehabil.* 78, 587–591. doi:10.1016/s0003-9993(97)90423-8

Ostir, G. V., Berges, I. M., Ottenbacher, K. J., Fisher, S. R., Barr, E., Hebel, J. R., et al. (2015). Gait speed and dismobility in older adults. *Arch. Phys. Med. Rehabil.* 96, 1641–1645. doi:10.1016/j.apmr.2015.05.017

Perry, M. C., Carville, S. F., Smith, I. C. H., Rutherford, O. M., and Newham, D. J. (2007). Strength, power output and symmetry of leg muscles: effect of age and history of falling. *Eur. J. Appl. physiology* 100, 553–561. doi:10.1007/s00421-006-0247-0

Podsiadlo, D., and Richardson, S. (1991). The timed "Up and Go": a test of basic functional mobility for frail elderly persons. *J. Am. Geriatr. Soc.* 39, 142–148. doi:10.1111/j.1532-5415.1991.tb01616.x

Recenti, M., Ricciardi, C., Edmunds, K., Gislason, M. K., and Gargiulo, P. (2020b). Machine learning predictive system based upon radiodensitometric distributions from mid-thigh CT images. *Eur. J. Transl. Myology* 30 (1), 121–124. doi:10.4081/ejtm.2019.8892

Recenti, M., Ricciardi, C., Edmunds, K., Jacob, D., Gambacorta, M., and Gargiulo, P. (2021b). Testing soft tissue radiodensity parameters interplay with age and self-reported physical activity. *Eur. J. Transl. myology* 31 (3), 9929. doi:10.4081/ejtm.2021.9929

Recenti, M., Ricciardi, C., Edmunds, K. J., Gislason, M. K., Sigurdsson, S., Carraro, U., et al. (2020a). Healthy aging within an image: using muscle radiodensitometry and lifestyle factors to predict diabetes and hypertension. *IEEE J. Biomed. Health Inf.* 25 (6), 2103–2112. doi:10.1109/jbhi.2020.3044158

Recenti, M., Ricciardi, C., Monet, A., Jacob, D., Ramos, J., Gislason, M., et al. (2021a). Predicting body mass index and isometric leg strength using soft tissue distributions from computed tomography scans. *Health Technol.* 11, 239–249. doi:10.1007/s12553-020-00498-3

Reinders, I., Murphy, R. A., Koster, A., Brouwer, I. A., Visser, M., Garcia, M. E., et al. (2015). Muscle quality and muscle fat infiltration in relation to incident mobility disability and gait speed decline: the age, gene/environment susceptibility-reykjavik study. *J. Gerontol. A Biol. Sci. Med. Sci.* 70, 1030–1036. doi:10.1093/gerona/glv016

Ribisl, P. M., Lang, W., Jaramillo, S. A., Jakicic, J. M., Stewart, K. J., Bahnson, J., et al. (2007). Exercise capacity and cardiovascular/metabolic characteristics of overweight and obese individuals with type 2 diabetes: the Look AHEAD clinical trial. *Diabetes care* 30 (10), 2679–2684. doi:10.2337/dc06-2487

Ricciardi, C., Edmunds, K. J., Recenti, M., Sigurdsson, S., Gudnason, V., Carraro, U., et al. (2020a). Assessing cardiovascular risks from a mid-thigh CT image: a tree-based machine learning approach using radiodensitometric distributions. *Sci. Rep.* 10 (1), 2863. doi:10.1038/s41598-020-59873-9

Savva, G. M., Donoghue, O. A., Horgan, F., O'Regan, C., Cronin, H., and Kenny, R. A. (2013). Using timed up-and-go to identify frail members of the older population. *J. Gerontol. Ser. A* 68 (4), 441–446. doi:10.1093/gerona/gls190

Schaap, L. A., Koster, A., and Visser, M. (2013). Adiposity, muscle mass, and muscle strength in relation to functional decline in older persons. *Epidemiol. Rev.* 35, 51–65. doi:10.1093/epirev/mxs006

Simonsick, E. M., Newman, A. B., Visser, M., Goodpaster, B., Kritchevsky, S. B., Rubin, S., et al. (2008). Mobility limitation in self-described well-functioning older adults: importance of endurance walk testing. *J. Gerontol. A Biol. Sci. Med. Sci.* 63 (8), 841–847. doi:10.1093/gerona/63.8.841

Skelton, D. A., Kennedy, J., and Rutherford, O. M. (2002). Explosive power and asymmetry in leg muscle function in frequent fallers and non-fallers aged over 65. *Age ageing* 31 (2), 119–125. doi:10.1093/ageing/31.2.119

Stagi, S., Moroni, A., Micheletti Cremasco, M., and Marini, E. (2021). Body composition symmetry in long-term active middle-aged and older individuals. *Int. J. Environ. Res. Public Health* 18, 5956. doi:10.3390/ijerph18115956

Studenski, S., Perera, S., and Patel, K. (2011). Gait speed and survival in older adults. *JAMA* 305 (1), 50–58. doi:10.1001/jama.2010.1923

Treacy, D., Hassett, L., Schurr, K., Fairhall, N. J., Cameron, I. D., and Sherrington, C. (2022). Mobility training for increasing mobility and functioning in older people with frailty. *Cochrane Database Syst. Rev.* 2022, CD010494. doi:10.1002/14651858.CD010494.pub2

Visser, M., Goodpaster, B. H., Kritchevsky, S. B., Newman, A. B., Nevitt, M., Rubin, S. M., et al. (2005). Muscle mass, muscle strength, and muscle fat infiltration as predictors of incident mobility limitations in well-functioning older persons. *J. Gerontol. A Biol. Sci. Med. Sci.* 60, 324–333. doi:10.1093/gerona/60.3.324

Wang, X., and Zhou, L. (2022). The many roles of macrophages in skeletal muscle injury and repair. *Front. Cell Dev. Biol.* 10, 952249. doi:10.3389/fcell.2022.952249

White, D. K., Neogi, T., Nevitt, M. C., Peloquin, C. E., Zhu, Y., Boudreau, R. M., et al. (2013). Trajectories of gait speed predict mortality in well-functioning older adults: the Health, Aging and Body Composition study. *J. Gerontol. A Biol. Sci. Med. Sci.* 68 (4), 456–464. doi:10.1093/gerona/gls197

WHO (2020). UN decade of healthy ageing 2021-2030. Available at: https://www.who.int/initiatives/decade-of-healthy-ageing (Accessed August 8, 2023).

WHO (2021). Obesity and overweight (WHO fact sheet No. 311). Available at: https://www.who.int/news-room/fact-sheets/detail/obesity-and-overweight (Accessed August 23, 2023).

Wilkinson, D. J., Piasecki, M., and Atherton, P. J. (2018). The age-related loss of skeletal muscle mass and function: measurement and physiology of muscle fibre atrophy and muscle fibre loss in humans. *Ageing Res. Rev.* 47, 123–132. doi:10.1016/j.arr.2018.07.005

Young, A., Stokes, M., and Crowe, M. (1985). The size and strength of the quadriceps muscles of old. *Clin. Physiol. Oxf. Engl.* 5 (2), 145–154. doi:10.1111/j.1475-097x.1985.tb00590.x

Zoico, E., Corzato, F., Bambace, C., Rossi, A. P., Micciolo, R., Cinti, S., et al. (2013). Myosteatosis and myofibrosis: relationship with aging, inflammation and insulin resistance. *Archives gerontology geriatrics* 57 (3), 411–416. doi:10.1016/j.archger.2013.06.001

frontiers | Frontiers in Neurology

TYPE Original Research
PUBLISHED 03 January 2024
DOI 10.3389/fneur.2023.1303215

OPEN ACCESS

EDITED BY
Claudio Belvedere,
Rizzoli Orthopedic Institute (IRCCS), Italy

REVIEWED BY
Giorgio Cassiolas,
Rizzoli Orthopedic Institute (IRCCS), Italy
Anjali Sivaramakrishnan,
The University of Texas Health Science Center at San Antonio, United States

*CORRESPONDENCE
Kazunori Sato
ksatoh@juntendo.ac.jp

RECEIVED 27 September 2023
ACCEPTED 04 December 2023
PUBLISHED 03 January 2024

CITATION
Sato K, Yamazaki Y, Kameyama Y, Watanabe K, Kitahara E, Haruyama K, Takahashi Y, Fujino Y, Yamaguchi T, Matsuda T, Makabe H, Isayama R, Murakami Y, Tani M, Honaga K, Hatori K, Oji Y, Tomizawa Y, Hatano T, Hattori N and Fujiwara T (2024) Factor analysis for construct validity of a trunk impairment scale in Parkinson's disease: a cross-sectional study. *Front. Neurol.* 14:1303215. doi: 10.3389/fneur.2023.1303215

Factor analysis for construct validity of a trunk impairment scale in Parkinson's disease: a cross-sectional study

Kazunori Sato[1]*, Yuta Yamazaki[1], Yoshihiro Kameyama[1], Koji Watanabe[1], Eriko Kitahara[1], Koshiro Haruyama[2], Yoko Takahashi[2], Yuji Fujino[2], Tomofumi Yamaguchi[2], Tadamitsu Matsuda[2], Hitoshi Makabe[2], Reina Isayama[1], Yuhei Murakami[1], Mami Tani[1], Kaoru Honaga[1], Kozo Hatori[1], Yutaka Oji[3], Yuji Tomizawa[3], Taku Hatano[3], Nobutaka Hattori[3] and Toshiyuki Fujiwara[1,2]

[1]Department of Rehabilitation Medicine, Juntendo University Graduate School of Medicine, Tokyo, Japan, [2]Department of Physical Therapy, Faculty of Health Science, Juntendo University, Tokyo, Japan, [3]Department of Neurology, Juntendo University Hospital, Tokyo, Japan

Objectives: To investigate the construct validity of the Trunk Impairment Scale (TIS), which was developed to assess trunk impairment in patients with stroke, in patients with Parkinson's disease (PD).

Design: This retrospective, cross-sectional study enrolled consecutive PD inpatients. Correlation analysis was performed to clarify whether the TIS assessment was related to other balance functions, lower extremity muscle strength, or walking ability. Factor analysis was performed to see how the background factors of TIS differ from balance function, lower limb muscle strength, and walking ability.

Results: Examining the data of 471 patients with PD, there were relationships between TIS and the Mini-Balance Evaluation Systems Test ($r = 0.67$), Barthel Index ($r = 0.57$), general lower limb extension torque ($r = 0.51$), two-minute walk test ($r = 0.54$), Hoehn and Yahr stage ($r = -0.61$), and Movement Disorder Society Unified Parkinson's Disease Rating Scale part III total points ($r = -0.59$). Factor analysis showed that TIS items were divided into three factors (an abdominal muscles and righting reflex component; a perception and verticality component; and a rotational component), differing from other scales that included clinical assessment items.

Conclusion: The TIS can be useful for assessing the underlying trunk impairment as a basis for activities of daily living, gait function, and balance ability in patients with PD.

KEYWORDS

Parkinson's disease, trunk impairment, rehabilitation, physical therapy, factor analysis

Introduction

Parkinson's disease (PD) is a progressive neurodegenerative disease with loss of dopaminergic neurons in the substantia nigra pars compacta that causes bradykinesia, muscle rigidity, and resting tremor. Patients with PD also have axial symptoms, such as postural instability, gait disturbance, and postural abnormalities, during the advanced stages of the disease (1). Factors thought to cause axial symptoms include lower extremity muscle weakness, bradykinesia, rigidity, abnormal pattern of postural reflexes, dystonia, reduced gait automaticity, impaired proprioception, and impaired cognitive function, as well as poor trunk function (2–5). It is also known that trunk impairment is often observed (6).

Previous studies reported that trunk impairment is associated with postural instability, postural abnormality, and gait disturbance that reduce quality of life in patients with PD (3, 7–9). However, a battery of tests for trunk impairment focused on the trunk angle in one plane or the motor function and mobility of the trunk, and these studies separated each other. Moreover, they did not include an assessment of the perceptual aspect (6, 10–13). Proprioception and sensory integration are crucial for trunk function, but they were found to be impaired in patients with PD (14–16). Therefore, a comprehensive evaluation of trunk impairment for patients with PD should be a single assessment battery and include the perceptual aspect, in addition to the motor function and trunk deviation angle.

The Trunk Impairment Scale (TIS) reported by Fujiwara et al. (17) was originally developed to comprehensively assess the trunk impairment of patients with stroke based on the motor and perceptual aspects with seven items (1. perception of trunk verticality; 2, 3. trunk rotation muscle strength on the right and left sides; 4, 5. righting reflex on the right and left sides; 6. verticality; and 7. abdominal muscle strength). The TIS had good reliability and validity in patients with stroke (17). The TIS can predict functional prognosis in patients with early stroke and is an indicator of functional improvement in patients with PD (18, 19). However, the construct validity of TIS reported by Fujiwara has not been examined in patients with PD. This study aimed to assess the trunk impairment of patients with PD using the TIS reported by Fujiwara and to confirm its construct validity. Another objective was to analyze how the TIS is related to disease severity and various physical functions and to determine its clinical usefulness.

Methods

Study design

This retrospective, cross-sectional study was conducted with the approval of the Research Ethics Committee, Faculty of Medicine, Juntendo University (E22-0157-H01). Informed consent was obtained in the form of an opt-out on the website. This study is reported following the STrengthening the Reporting of OBservational studies in Epidemiology (STROBE) statement (20).

No previous study reported trunk function in PD including perceptual aspects in its assessment items without TIS reported by Fujiwara; therefore, a sample size calculation for analyzing correlations was considered based on a small effect size ($r = 0.2$), significance level of 0.01, and power of 0.95 to minimize the probability of committing type II error (21). Sample size calculations were performed with G*Power 3.1 (21). Since the medical record data from regular practice are expected to contain many deficiencies, over 431 patients' medical record data were included in the study.

Study subjects

A total of 482 consecutive patients with PD of all ages who were admitted to the hospital from January 2019 to April 2022 and underwent rehabilitation were included in the study. The patients had been clinically diagnosed with established and probable Parkinson's disease according to the Movement Disorder Society Clinical Diagnostic Criteria (1) by neurologists specialized in movement disorders.

The exclusion criteria included patients who were diagnosed with other neurodegenerative diseases (e.g., progressive supranuclear palsy or multiple system atrophy), had complications that severely impaired their physical performance (e.g., orthopedic disease, internal disease, or psychiatric disease), or patients who refused to participate in this research project. In addition, patients with significant missing records were also excluded.

Assessment items

Based on updated medical records when patients with PD visited the hospital, the data of age, sex, duration of disease, duration of levodopa medication, body mass index, Hoehn and Yahr stage, Levodopa Daily Dose (LDD), and Levodopa Equivalent Daily Dose (LEDD) were collected. Part II-Activity Daily living items of the Movement Disorder Society Unified Parkinson's Disease Rating Scale (MDS-UPDRS) and Highest ON medication state of part III-Motor items of MDS-UPDRS were collected from updated medical records by neurologists specialized in movement disorders. The physical functions of the TIS, Barthel Index, Mini-Balance Evaluation Systems Test (Mini-BESTest), two-minute walk test, general lower extremity extension torque using the Strength Ergo 240, and handgrip force were assessed by physical therapists. The assessments of physical function were performed 60 to 120 min after oral dosing with confirmed ON-medication status. Each assessment for the physical functions is described in detail below.

Trunk impairment scale

The TIS consists of seven items: (1) perception of trunk verticality; (2, 3) trunk rotation muscle strength on the right and left sides; (4, 5) righting reflex on the right and left sides; (6) verticality; and (7) abdominal muscle strength. Each item is evaluated on a scale of 0 to 3, with a maximum score of 21 points; a higher score represents better trunk function. The required duration for the completion of the TIS is approximately 5 min. The Appendix shows the details of the TIS's definition, procedures, and scoring criteria (17).

Postural instability and gait dysfunction

Postural instability and gait dysfunction (PIGD) was assessed with the PIGD sub-score of MDS-UPDRS part III (item 3.9 Arising from

chair, 3.10 Gait, 3.11 Freezing of gait, 3.12 Postural stability, 3.13 Posture) (22).

Specific balance abilities were measured with the Mini-Balance Evaluation Systems Test (Mini-BESTest), which consists of four different balance aspects (Anticipatory postural adjustments, Automatic postural responses, Sensory orientation, and Dynamic gait) with the highest score of 28 points (23); higher scores indicate better balance ability. Gait performance was assessed with a two-minute walk test (24, 25).

Strength of the upper and lower extremities and foot bradykinesia

General lower limb extension muscle strength was evaluated with the isokinetic mode of Strength Ergo 240 (SE240: Mitsubishi Electric Engineering Corporation, Tokyo, Japan) (19). The rotational speed was set at 50/min, and the backrest angle was set at 110 degrees during the measurement period. After orientation to strength measurement, the patients kicked pedals with five consecutive drives, and peak torque was calculated.

Handgrip force was measured using the CAMRY dynamometer (CAMRY EH101, Sensun Weighing Apparatus Group Ltd., Guangdong, China) in the sitting position with the humerus vertical and a 90-degree flexed elbow according to previous reports to avoid unexpected falls during the measurement (26, 27).

In addition to the assessments above, MDS-UPDRS part III item 7 toe-tapping was evaluated to clarify foot movement as a distal part of lower bradykinesia (22).

Statistical analysis

All data were tested for normality using the Shapiro–Wilk test. To investigate the construct validity of the TIS, the relationships between TIS and MDS-UPDRS items, Mini-BESTest, BI, Strength of Extremities, and Hoehn and Yahr stage were analyzed using Spearman's correlation coefficients. To analyze confounding factors within parameters other than the TIS, multiple regression analysis was performed. To analyze the relationships of background factors in each item on the TIS and other physical functions, factor analysis with Promax rotation was used. To determine the number of factors before the factor analysis, the Bayesian information criterion was applied to allow for more objective calculations even with a large sample size. Other determination methods such as the Kaiser-Guttman criterion and scree plot were not used in this study due to the risk of overestimation or uncertain features of visual judgment methods. Randomly occurring missing values were complemented using the multiple imputation method. All statistical analyses were performed with the statistical software R version 4.2.0 for Windows, and the significance level was set at $p < 0.05$.

Results

After applying the exclusion criteria, data of 471 patients were selected for this study (Figure 1). Data of 11 patients with PD were excluded due to significant missing medical records.

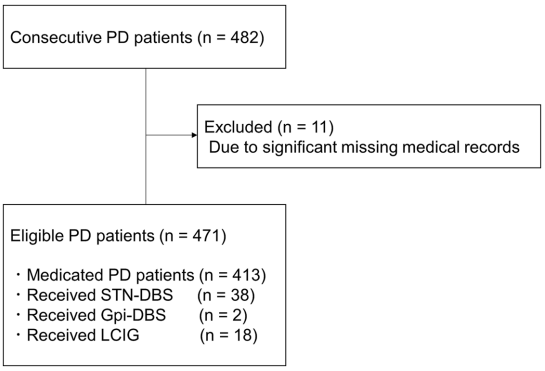

FIGURE 1
Schematic flow chart of study participants. PD, Parkinson's disease; STN-DBS, Subthalamic Nucleus Deep Brain Stimulation; Gpi-DBS, Globus Pallidus Internus Deep Brain Stimulation; LCIG, Levodopa-carbidopa intestinal gel therapy.

TABLE 1 Demographic data of the participants.

Age, years, mean (SD)	65.7 (10.6)
Sex, female/male, *n* (%)	237 (50.3)/234 (49.7)
Body height, cm, mean (SD)	159.9 (10.6)
Body weight, kg, mean (SD)	57.1 (40.8)
Body mass index, mean (SD)	22.2 (14.2)
Duration of disease, years, mean (SD)	12.1 (7.5)
Duration of medication, years, means (SD)	10.4 (8.2)
Hoehn and Yahr stage, median (IQR)	2.0 (1)
MDS-UPDRS part III, median (IQR)	22.0 (18.5)
Barthel Index, median (IQR)	80.0 (30.0)
Mini-BESTest total score, median (IQR)	19.0 (10.0)
Deep brain stimulation setting	
Pulse, microseconds, mean (SD)	54.9 (19.2)
Hz, mean (SD)	130.4 (40.1)
mA, mean (SD)	2.5 (0.9)
LDD, mg, mean (SD)	636.4 (947.8)
LEDD, mg, mean (SD)	283.5 (496.0)

Data are mean (SD), *n* (%), or median (IQR) values. SD, standard deviation; IQR, interquartile range; MDS-UPDRS, movement disorders society-unified Parkinson's disease rating scale; Mini-BESTest, Mini-Balance Evaluation Systems Test; LDD, levodopa daily dose; LEDD, levodopa equivalent daily dose.

Fifty-eight patients had previously received device-aided therapy, such as Subthalamic Nucleus Deep Brain Stimulation implantation (38 patients), Globus Pallidus Internus Deep Brain Stimulation implantation (2 patients), and Levodopa-carbidopa intestinal gel therapy (18 patients). Table 1 shows the demographic data of the eligible cases.

Spearman's correlation coefficients showed moderate positive correlations between the TIS and the Mini-BESTest ($r = 0.66$, $p < 0.001$), Barthel Index ($r = 0.57$, $p < 0.001$), general lower limb extension torque ($r = 0.51$, $p < 0.001$), and the two-minute walk test ($r = 0.54$, $p < 0.001$). There were moderate negative correlations between the TIS and Hoehn and Yahr stage ($r = -0.58$, $p < 0.001$),

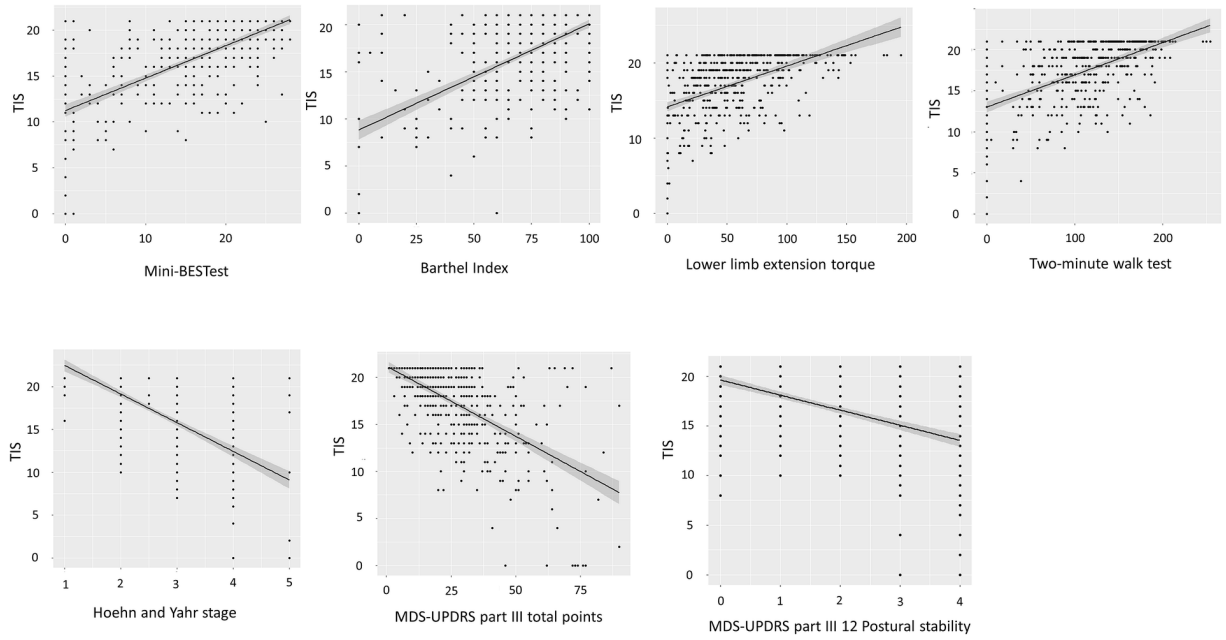

FIGURE 2
Scatter plots depicting the relationship between the TIS and associated assessment parameters. Spearman's correlation coefficients show a positive association of the TIS (range 0–21 points) and Mini-BESTest (range 0–28 points). Spearman's correlation coefficients show negative associations of the TIS (range 0–21 points) and Hoehn and Yahr stage (range 1–5) and MDS-UPDRS part III total points (range 0–132 points). TIS, Trunk Impairment Scale; Mini-BESTest, Mini-Balance Evaluation Systems Test; MDS-UPDRS, Movement Disorders Society-unified Parkinson's disease rating scale.

MDS-UPDRS part III total points ($r = -0.55$, $p < 0.001$), and part III Postural stability ($r = -0.51$, $p < 0.001$) (Figure 2). In the other functions or general state, the TIS was weakly correlated with handgrip force ($r = 0.46$, $p < 0.001$), age ($r = -0.37$, $p < 0.001$), MDS-UPDRS part III toe-tapping ($r = -0.34$, $p < 0.001$), Arising from chair ($r = -0.48$, $p < 0.001$), Gait ($r = -0.49$, $p < 0.001$), Freezing of gait ($r = -0.42$, $p < 0.001$), and Posture ($r = -0.45$, $p < 0.001$). There were negligible correlations between the TIS and MDS-UPDRS part II Turning in bed ($r = -0.29$, $p < 0.001$), body mass index ($r = 0.16$, $p = 0.007$), duration of disease ($r = -0.16$, $p < 0.001$), duration of levodopa medication ($r = -0.16$, $p < 0.001$), and LEDD ($r = 0.15$, $p = 0.0014$).

Table 2 shows the results of multiple regression analysis between the TIS and age, body height, body weight, duration of disease, years, Barthel Index, LEDD, MDS-UPDRS II Turning in bed, MDS-UPDRS III total score, Hoehn and Yahr stage, Mini-BESTest total score, general lower extremity extension torque, two-minute walk test, and handgrip force. The analysis showed that the independent variables Barthel Index ($\beta = 0.14$, $p = 0.01$), MDS-UPDRS II Turning in bed ($\beta = -0.12$, $p = 0.002$), Hoehn and Yahr stage ($\beta = -0.16$, $p = 0.003$), and Mini-BESTest total score ($\beta = 0.27$, $p = 0.00003$) contributed significantly to the dependent variable TIS.

The Bayesian information criterion analysis yielded seven factors in the MDS-UPDRS part II Turning in bed, MDS-UPDRS III Toe tapping, PIGD score (Arising from chair, Gait, Freezing of gait, Postural stability, Posture), Mini-BESTest sub-score (Anticipatory postural adjustments, Automatic postural responses, Sensory orientation, and Dynamic gait), TIS sub-score (Perception of trunk verticality, Trunk rotation muscle strength on the right and left side, Righting reflex on the left and right side, Verticality, Abdominal muscle strength), general lower extremity extension torque, two-minute walk test, and handgrip force. The factor analysis with Promax rotation indicated that the first factor included the MDS-UPDRS II Turning in bed, MDS-UPDRS III Toe tapping, and PIGD score (Arising from chair, Gait, Freezing of gait, Postural stability, Posture). The second factor consisted of the Mini-BESTest sub-score (Anticipatory postural adjustments, Automatic postural responses, Sensory orientation, and Dynamic gait), and the two-minute walk test. The third factor comprised the TIS righting reflex on the left side, TIS righting reflex on the right side, and TIS abdominal muscle strength. The fourth factor included the TIS trunk rotation muscle strength on the right side and TIS trunk rotation muscle strength on the left side. The fifth factor involved the TIS perception of trunk verticality and TIS verticality. The sixth factor covered the general lower extremity extension torque, two-minute walk test, and handgrip force. The seventh factor included the MDS-UPDRS III Postural stability and Mini-BESTest Automatic postural responses (Table 3). All 7 factors showed moderate or low correlations with each other (Table 4).

Discussion

The TIS was developed specifically to assess trunk function in patients with stroke. This is the first study to show that the TIS based on the motor function of the trunk and perceptual aspects had high construct validity. The present results showed that the TIS was correlated to disease severity, activities of daily living, limb strength, gait, and balance ability in patients with PD. Based on the results of correlation and multiple regression analysis, TIS may evaluate the

TABLE 2 Multiple regression analysis between the TIS total score and demographic and other clinical assessments.

	β	VIF	p value
Age	0.01	1.56	0.87
Body height	−0.01	1.58	0.73
Body weight	0.02	1.11	0.58
Duration of disease	0.02	1.08	0.63
Barthel index	0.14	2.75	0.01**
Levodopa equivalent daily dose	0.04	1.06	0.27
MDS-UPDRS II 9 Turning in bed	−0.12	1.36	0.002**
MDS-UPDRS III total score	−0.08	2.75	0.14
Hoehn and Yahr stage	−0.16	2.64	0.003**
Mini-BESTest total score	0.27	4.06	0.00003***
General lower extremity extension torque	0.01	3.18	0.93
Two-minute walk test	0.05	2.60	0.35
Handgrip force	0.07	2.39	0.16

$R^2 = 0.52$, $p < 0.0001$. *$p < 0.05$, **$p < 0.01$. β, standardized partial regression coefficient; VIF, variance inflation factor; R2, multiple coefficient of determination; MDS-UPDRS, movement disorders society-unified Parkinson's disease rating scale; Mini-BESTest, Mini Balance Evaluation Systems Test; TIS, Trunk Impairment Scale.

TABLE 3 Factor loading matrix for 21 variables after promax rotation for the physical performance data.

	Factor 1	Factor 2	Factor 3	Factor 4	Factor 5	Factor 6	Factor 7
MDS-UPDRS II 9 Turning in bed	**0.51**	0.049	−0.071	−0.044	−0.122	−0.109	−0.197
MDS-UPDRS III 7 Toe tapping	**0.459**	−0.111	−0.034	0.022	−0.048	0.107	0.067
MDS-UPDRS III 9 Arising from chair	**0.882**	−0.114	−0.033	−0.005	0.065	−0.007	−0.084
MDS-UPDRS III 10 Gait	**0.843**	0.046	0.04	−0.021	0.033	−0.03	0.175
MDS-UPDRS III 11 Freezing of gait	**0.848**	−0.024	−0.048	−0.002	0.082	0.052	0.016
MDS-UPDRS III 12 Postural stability	**0.323**	0.124	−0.012	0.063	0.018	−0.098	**0.684**
MDS-UPDRS III 13 Posture	**0.533**	0.04	0.117	−0.009	−0.177	0.037	0.293
Mini-BESTest Anticipatory postural adjustment	−0.204	**0.776**	−0.015	−0.026	−0.021	−0.082	−0.062
Mini-BESTest Automatic postural responses	−0.035	**0.338**	0.024	−0.029	−0.016	0.054	**−0.435**
Mini-BESTest Sensory orientation	−0.101	**0.869**	−0.026	−0.023	0.043	0	0.112
Mini-BESTest Dynamic gait	−0.189	**0.746**	0.018	−0.002	−0.011	0.035	0.028
TIS perception of trunk verticality	0.042	0.04	0.023	−0.025	**0.781**	−0.009	0.061
TIS trunk rotation muscle strength on the right side	−0.014	−0.033	−0.134	**1.165**	−0.07	−0.023	0.067
TIS trunk rotation muscle strength on the left side	0.021	−0.003	0.139	**0.582**	0.104	0.02	−0.076
TIS righting reflex on the left side	−0.018	−0.014	**0.962**	−0.031	0.019	−0.025	−0.016
TIS righting reflex on the right side	−0.005	−0.02	**1.051**	−0.114	−0.023	0.005	0.009
TIS verticality	0.063	−0.012	−0.031	−0.052	**0.987**	−0.001	−0.014
TIS abdominal muscle strength	0.026	0.118	**0.334**	0.275	0.049	0.025	−0.078
General lower extremity extension torque	0.025	0.001	−0.032	−0.011	−0.014	**0.894**	−0.076
Two-minute walk test	−0.164	**0.462**	−0.042	0.034	−0.013	**0.315**	0.038
Handgrip force	−0.018	−0.065	0.028	−0.025	0.017	**0.821**	−0.011
Sum of squared loadings	3.19	2.31	2.21	1.80	1.67	1.62	0.87
Proportion of variance	0.15	0.11	0.11	0.09	0.08	0.08	0.04
Cumulative proportion of variance	0.15	0.26	0.37	0.45	0.53	0.61	0.65

Bold values indicate loadings > 0.30. MDS-UPDRS, movement disorders society-unified Parkinson's disease rating scale; Mini-BESTest, Mini Balance Evaluation Systems Test; TIS, Trunk Impairment Scale.

TABLE 4 Factor correlations.

	Factor 1	Factor 2	Factor 3	Factor 4	Factor 5	Factor 6	Factor 7
Factor 1	1	0.444	0.646	−0.461	−0.56	−0.573	−0.55
Factor 2		1	0.585	−0.599	−0.64	−0.756	−0.641
Factor 3			1	−0.525	−0.687	−0.663	−0.546
Factor 4				1	0.52	0.694	0.601
Factor 5					1	0.602	0.493
Factor 6						1	0.702
Factor 7							1

trunk function related to balance function, disease severity, ADL function, lower limb strength, and which is different from the effects of age and BMI. The factors of the TIS were constructed with three different aspects (abdominal muscles and righting reflex component, perception and verticality component, and rotational component), and it differed from other factors that included clinical assessment items of Mini-BESTest, MDS-UPDRS part II Turning in bed, part III Postural instability and gait disturbance scores, two-minute walk test, and limb muscle strength. The TIS can be used to understand trunk impairment itself in patients with PD.

According to the previous studies, the factor analysis of TIS in patients with stroke did not divide the number of factors into multiple numbers, whereas multiple numbers were seen in patients with PD. The trunk impairment in stroke presents mainly with hypotonic hemiparesis, whereas PD presents with a variety of trunk impairments, including rigidity of trunk muscles (7), reduced righting reflexes (5), and altered vertical axis perception (5, 28). Although the results of this factor analysis might reflect the difference in the number of samples covered, there might be differences in background characteristics between stroke and PD.

After analyzing various factors such as MDS-UPDRS, Mini-BESTest, upper and lower extremity muscle strength, balance ability, and gait function, only the TIS was divided into three factors, even though these factors were correlated. Given that the Mini-BESTest is tailored explicitly to assess equilibrium in both standing and ambulatory scenarios, it was likely subjected to factor analysis as a single domain. The TIS administered in a supine or seated posture, and its broader assessment beyond mere motoric capacities of achievable or unattainable, might reflect why it was stratified into distinct domains during factor analysis. The elements that the TIS could capture separately were the [1] trunk righting reflex and abdominal muscle strength component, [2] the trunk rotation component, and [3] the verticality and vertical axis perception component, and it has been reported that, in PD, the trunk righting reflex and muscle strength (5), trunk rotation (9, 12), and vertical axis perception (5, 28) were decreased. The TIS in the present study is considered to be an assessment scale that is constructed to reflect these factors. The results of the factor analysis in the present study also suggest that the TIS may be an assessment index that can provide a more detailed evaluation of trunk dysfunction in patients with PD, which is difficult to obtain with other assessments.

In the clinical setting, trunk function is considered to be important for rolling over, but the TIS was not related to the MDS-UPDRS part II Turning in bed item in the present study. A previous study recruited only patients with PD with mild disease severity and showed that bed roll ability was related to trunk motor function, which was different from the result of the present study (6). One possible explanation is that these results might reflect the assessment method differences between the TIS, which reflects trunk dysfunction accurately by physical examination, and the MDS-UPDRS part II Turning in bed item, which allows turning movements even with compensatory movements, by questionnaire evaluation.

Previous studies have reported that trunk function in patients with PD affects ADL performance (6, 12), balance function, and gait function (7, 16). In the present study, the direct impact on trunk function on multiple regression analysis resulted in a low contribution rate, as indicated by the standard partial regression coefficients, although there were significant differences. Therefore, it is unlikely that ADL, balance function, and walking ability have a strong influence on trunk function due to these factors. From a clinical perspective, although ADL, balance function, and walking ability are correlated with trunk function, it is unlikely that they are confounding factors that influence trunk function. Rather, it is possible that trunk function influences ADLs, balance function, and walking ability.

Evaluation scales that separately quantify trunk function, balance function, and gait function in patients with PD have been scarce, making it difficult to capture the relationships among trunk function, balance function, and gait function in patients with PD, as well as trunk function itself. Since the TIS can comprehensively capture the trunk function of patients with PD from the motor and perceptual aspects, the clinical application of this assessment is considered highly meaningful.

The present study has some limitations. First, because this was a cross-sectional study, predictive factors of TIS itself or effect for the other physical functions such as balance function, and minimum clinically important difference could not be analyzed. Therefore, an additional cohort study should be planned. Second, the subjects in this study were only clinically diagnosed with PD, not pathologically confirmed. Third, this study did not contain the aspect of nonmotor symptoms and fluctuations of dopaminergic medications. A future study should include the assessment of nonmotor features and fluctuations of dopaminergic medications. In addition, it is necessary to conduct randomized, controlled studies to clarify the causal relationship to determine whether the improvement in trunk function captured by the TIS analyzed in the present study leads to an improvement in physical function in patients with PD.

Conclusion

The TIS can evaluate three different components including motor and perceptual aspects of trunk function separately from limb muscle

strength, balance function, and parkinsonism. These findings suggest that the TIS can be useful for exploring the underlying trunk impairment as a basis for activities of daily living, gait function, and balance ability in patients with PD.

Data availability statement

The raw data supporting the conclusions of this article will be made available by the authors, without undue reservation.

Ethics statement

The studies involving humans were approved by Research Ethics Committee, Faculty of Medicine, Juntendo University. The studies were conducted in accordance with the local legislation and institutional requirements. The ethics committee/institutional review board waived the requirement of written informed consent for participation from the participants or the participants' legal guardians/next of kin because informed consent was obtained in the form of an opt-out on the website.

Author contributions

KS: Conceptualization, Data curation, Formal analysis, Investigation, Methodology, Software, Validation, Writing – original draft, Writing – review & editing. YY: Data curation, Investigation, Writing – review & editing. YK: Data curation, Investigation, Writing – review & editing. KW: Data curation, Investigation, Writing – review & editing. EK: Data curation, Investigation, Writing – review & editing. KHar: Writing – review & editing. YTa: Writing – review & editing. YF: Writing – review & editing. TY: Writing – review & editing. TM: Writing – review & editing. HM: Writing – review & editing. RI: Writing – review & editing. YM: Writing – review & editing. MT: Writing – review & editing. KHo: Writing – review & editing. KHat: Writing – review & editing. YO: Writing – review & editing. YTo: Writing – review & editing. TH: Writing – review & editing. NH: Project administration, Supervision, Writing – review & editing. TF: Methodology, Project administration, Supervision, Writing – review & editing.

Funding

The author(s) declare that no financial support was received for the research, authorship, and/or publication of this article.

Acknowledgments

The authors would like to thank the medical staff of the Laboratory of Rehabilitation Medicine, Juntendo University Graduate School of Medicine for their support.

Conflict of interest

The authors declare that the research was conducted in the absence of any commercial or financial relationships that could be construed as a potential conflict of interest.

The author(s) declared that they were an editorial board member of Frontiers, at the time of submission. This had no impact on the peer review process and the final decision.

Publisher's note

Supplementary material

The Supplementary material for this article can be found online at: https://www.frontiersin.org/articles/10.3389/fneur.2023.1303215/full#supplementary-material

References

1. Postuma RB, Berg D, Stern M, Poewe W, Olanow CW, Oertel W, et al. MDS clinical diagnostic criteria for Parkinson's disease. *Mov Disord.* (2015) 30:1591–601. doi: 10.1002/mds.26424

2. Mak MK, Pang MY, Mok V. Gait difficulty, postural instability, and muscle weakness are associated with fear of falling in people with Parkinson's disease. *Parkinsons Dis.* (2012) 2012:901721. doi: 10.1155/2012/901721

3. Artigas NR, Franco C, Leao P, Rieder CR. Postural instability and falls are more frequent in Parkinson's disease patients with worse trunk mobility. *Arq Neuropsiquiatr.* (2016) 74:519–23. doi: 10.1590/0004-282X20160074

4. Fasano A, Canning CG, Hausdorff JM, Lord S, Rochester L. Falls in Parkinson's disease: a complex and evolving picture. *Mov Disord.* (2017) 32:1524–36. doi: 10.1002/mds.27195

5. Bloem BR. Postural instability in Parkinson's disease. *Clin Neurol Neurosurg.* (1992) 94:41–5. doi: 10.1016/0303-8467(92)90018-x

6. Verheyden G, Willems AM, Ooms L, Nieuwboer A. Validity of the trunk impairment scale as a measure of trunk performance in people with Parkinson's disease. *Arch Phys Med Rehabil.* (2007) 88:1304–8. doi: 10.1016/j.apmr.2007.06.772

7. Cano-de-la-Cuerda R, Vela-Desojo L, Miangolarra-Page JC, Macías-Macías Y, Muñoz-Hellín E. Axial rigidity and quality of life in patients with Parkinson's disease: a preliminary study. *Qual Life Res.* (2011) 20:817–23. doi: 10.1007/s11136-010-9818-y

8. Spildooren J, Vercruysse S, Heremans E, Galna B, Vandenbossche J, Desloovere K, et al. Head-pelvis coupling is increased during turning in patients with Parkinson's disease and freezing of gait. *Mov Disord.* (2013) 28:619–25. doi: 10.1002/mds.25285

9. Yang WC, Hsu WL, Wu RM, Lu TW, Lin KH. Motion analysis of axial rotation and gait stability during turning in people with Parkinson's disease. *Gait Posture.* (2016) 44:83–8. doi: 10.1016/j.gaitpost.2015.10.023

10. Wright WG, Gurfinkel VS, Nutt J, Horak FB, Cordo PJ. Axial hypertonicity in Parkinson's disease: direct measurements of trunk and hip torque. *Exp Neurol.* (2007) 208:38–46. doi: 10.1016/j.expneurol.2007.07.002

11. Huxham F, Baker R, Morris ME, Iansek R. Head and trunk rotation during walking turns in Parkinson's disease. *Mov Disord.* (2008) 23:1391–7. doi: 10.1002/mds.21943

12. Franco CR, Leão P, Townsend R, Rieder CR. Reliability and validity of a scale for measurement of trunk mobility in Parkinson's disease: trunk mobility scale. *Arq Neuropsiquiatr*. (2011) 69:636–41. doi: 10.1590/s0004-282x2011000500012

13. Bridgewater KJ, Sharpe MH. Trunk muscle performance in early Parkinson's disease. *Phys Ther*. (1998) 78:566–76. doi: 10.1093/ptj/78.6.566

14. Carpenter MG, Bloem BR. Postural control in Parkinson patients: a proprioceptive problem? *Exp Neurol*. (2011) 227:26–30. doi: 10.1016/j.expneurol.2010.11.007

15. Vaugoyeau M, Hakam H, Azulay JP. Proprioceptive impairment and postural orientation control in Parkinson's disease. *Hum Mov Sci*. (2011) 30:405–14. doi: 10.1016/j.humov.2010.10.006

16. Wright WG, Gurfinkel VS, King LA, Nutt JG, Cordo PJ, Horak FB. Axial kinesthesia is impaired in Parkinson's disease: effects of levodopa. *Exp Neurol*. (2010) 225:202–9. doi: 10.1016/j.expneurol.2010.06.016

17. Fujiwara T, Liu M, Tsuji T, Sonoda S, Mizuno K, Akaboshi K, et al. Development of a new measure to assess trunk impairment after stroke (trunk impairment scale): its psychometric properties. *Am J Phys Med Rehabil*. (2004) 83:681–8. doi: 10.1097/01.phm.0000137308.10562.20

18. Ishiwatari M, Honaga K, Tanuma A, Takakura T, Hatori K, Kurosu A, et al. Trunk impairment as a predictor of activities of daily living in acute stroke. *Front Neurol*. (2021) 12, 12:665592. doi: 10.3389/fneur.2021.665592

19. Sato K, Hokari Y, Kitahara E, Izawa N, Hatori K, Honaga K, et al. Short-term motor outcomes in Parkinson's disease after subthalamic nucleus deep brain stimulation combined with post-operative rehabilitation: a pre-post comparison study. *Parkinsons Dis*. (2022) 2022:8448638. doi: 10.1155/2022/8448638

20. von Elm E, Altman DG, Egger M, Pocock SJ, Gøtzsche PC, Vandenbroucke JP. Strengthening the reporting of observational studies in epidemiology (STROBE) statement: guidelines for reporting observational studies. *BMJ*. (2007) 335:806–8. doi: 10.1136/bmj.39335.541782.AD

21. Faul F, Erdfelder E, Lang AG, Buchner A. G*power 3: a flexible statistical power analysis program for the social, behavioral, and biomedical sciences. *Behav Res Methods*. (2007) 39:175–91. doi: 10.3758/bf03193146

22. Goetz CG, Tilley BC, Shaftman SR, Stebbins GT, Fahn S, Martinez-Martin P, et al. Movement Disorder Society-sponsored revision of the unified Parkinson's disease rating scale (MDS-UPDRS): scale presentation and clinimetric testing results. *Mov Disord*. (2008) 23:2129–70. doi: 10.1002/mds.22340

23. Franchignoni F, Horak F, Godi M, Nardone A, Giordano A. Using psychometric techniques to improve the balance evaluation systems test: the mini-BESTest. *J Rehabil Med*. (2010) 42:323–31. doi: 10.2340/16501977-0537

24. Bohannon RW, Bubela D, Magasi S, McCreath H, Wang YC, Reuben D, et al. Comparison of walking performance over the first 2 minutes and the full 6 minutes of the six-minute walk test. *BMC Res Notes*. (2014) 7:269. doi: 10.1186/1756-0500-7-269

25. Bohannon RW, Wang YC, Gershon RC. Two-minute walk test performance by adults 18 to 85 years: normative values, reliability, and responsiveness. *Arch Phys Med Rehabil*. (2015) 96:472–7. doi: 10.1016/j.apmr.2014.10.006

26. Vargas-Pinilla OC, Rodríguez-Grande EI. Reproducibility and agreement between three positions for handgrip assessment. *Sci Rep*. (2021) 11:12906. doi: 10.1038/s41598-021-92296-8

27. Huang L, Liu Y, Lin T, Hou L, Song Q, Ge N, et al. Reliability and validity of two hand dynamometers when used by community-dwelling adults aged over 50 years. *BMC Geriatr*. (2022) 22:580. doi: 10.1186/s12877-022-03270-6

28. Doherty KM, van de Warrenburg BP, Peralta MC, Silveira-Moriyama L, Azulay JP, Gershanik OS, et al. Postural deformities in Parkinson's disease. *Lancet Neurol*. (2011) 10:538–49. doi: 10.1016/s1474-4422(11)70067-9

frontiers | Frontiers in Bioengineering and Biotechnology

TYPE Original Research
PUBLISHED 05 January 2024
DOI 10.3389/fbioe.2023.1297068

OPEN ACCESS

EDITED BY
Simone Tassani,
Pompeu Fabra University, Spain

REVIEWED BY
Marco Recenti,
Reykjavík University, Iceland
Giorgio Davico,
Alma Mater Studiorum—University of Bologna, Italy

*CORRESPONDENCE
Qiuxia Zhang,
qxzhang@suda.edu.cn
Yuefeng Hao,
13913109339@163.com

RECEIVED 19 September 2023
ACCEPTED 11 December 2023
PUBLISHED 05 January 2024

CITATION
Kong L, Zhang Z, Bao J, Zhu X, Tan Y, Xia X, Zhang Q and Hao Y (2024), Influences of cognitive load on center of pressure trajectory of young male adults with excess weight during gait initiation. *Front. Bioeng. Biotechnol.* 11:1297068. doi: 10.3389/fbioe.2023.1297068

Influences of cognitive load on center of pressure trajectory of young male adults with excess weight during gait initiation

Lingyu Kong[1], Zhiqi Zhang[1], Jiawei Bao[2], Xinrui Zhu[3], Yong Tan[1], Xihao Xia[4], Qiuxia Zhang[1]* and Yuefeng Hao[5,6]*

[1]School of Physical Education, Soochow University, Suzhou, China, [2]School of Mathematical Sciences, Soochow University, Suzhou, China, [3]Rehabilitation Medicine Department, Xuzhou Rehabilitation Hospital, Xuzhou, China, [4]Wuxi 9th People's Hospital Affiliated to Soochow University, Wuxi, China, [5]Orthopedics and Sports Medicine Center, The Affiliated Suzhou Hospital of Nanjing Medical University, Suzhou, China, [6]Gusu School, Nanjing Medical University, Suzhou, China

Introduction: Falls and fall-related injuries in young male adults with excess weight are closely related to an increased cognitive load. Previous research mainly focuses on analyzing the postural control status of these populations performing cognitive tasks while stabilized walking progress but overlooked a specific period of walking known as gait initiation (GI). It is yet unknown the influences of cognitive load on this population's postural control status during GI.

Objective: This study aimed to determine the influences of cognitive load on the center of pressure (CoP) trajectory of young male adults with excess weight during GI.

Design: A controlled laboratory study.

Methods: Thirty-six male undergraduate students were recruited and divided into normal-weight, overweight, and obese groups based on their body mass index (BMI). Participants' CoP parameters during GI under single and dual-task conditions were collected by two force platforms. A mixed ANOVA was utilized to detect significant differences.

Results: Compared with the normal-weight group, the obese group showed significant changes in the duration and CoP parameters during sub-phases of GI, mainly reflecting prolonged duration, increased CoP path length, higher mediolateral CoP displacement amplitude, and decreased velocity of anteroposterior CoP displacement. During GI with 1-back task, significantly increased mediolateral CoP displacement amplitude occurred in the obese group. During GI with 2-back task, the obese group had increased CoP path length, higher mediolateral CoP displacement amplitude, as well as a decreased velocity of CoP displacement.

Conclusion: Based on the changes in CoP parameters during GI with cognitive tasks, young male adults with excess weight, mainly obese ones, have compromised postural stability. During GI with a difficult cognitive task, obese young male adults are more susceptible to deterioration in their lateral postural balance. These findings indicate that the increased cognitive load could exacerbate obese young male adults' postural control difficulty during GI

under dual-task conditions, putting them at a higher risk of experiencing incidents of falls. Based on these findings, we offer suggestions for therapists to intervene with these young male adults to ensure their safety of GI.

KEYWORDS

cognition, gait initiation, overweight, obesity, postural control

1 Introduction

At present, over 1.9 billion and more than 600 million individuals have excess weight and can be classified as overweight or obese, respectively (Barone et al., 2020). Aged 18–35 years is an influential period for excessive weight gain and unhealthy weight-related behaviors (Lytle et al., 2017). Excess weight can decrease the capacity of young adults to properly use proprioceptive information for postural control, making them have almost twice the fall risks as their normal-weight counterparts (Fjeldstad et al., 2008). In the population of young adults, males are more susceptible to falls and injuries for their slip-induced fall risks notably increased along the transversal direction under certain conditions (Wu et al., 2012). Based on these reasons, it is imperative to assess the motor performance of young male adults with excess weight to evaluate their safety and provide a theoretical basis for preventing them from experiencing dangerous events.

Gait initiation (GI), the transient period between standing posture and steady-state walking, involves the correct preparation and execution of a sequence of movements. Individuals not only need to shift their weight and transition the base of support voluntarily but also need to generate an appropriate propulsion force to reach the required gait speed and control the disequilibrium led by the walking progression (Hass et al., 2004; Colné et al., 2008). Analyzing biomechanical performance during GI in young male adults with excess weight, including the calculation of center of pressure (CoP) parameters (e.g., CoP displacement amplitude and velocity of CoP displacement), can provide deep insights into their postural control status, having important implications regarding their fall prevention (Cau et al., 2014; Hirjaková et al., 2018). However, currently, there is a lack of studies comparing the differences in CoP parameters between normal-weight and excess-weight ones during GI, which hinders researchers from gaining a deeper understanding of postural control status among these populations.

Maintaining a stable and sustained posture requires correct neuromuscular control, which relies on sufficient cognitive resources. Dual-task conditions are common in daily life, especially those involving the simultaneous performance of both cognitive and motor tasks (Brauer et al., 2001), in which cognitive tasks will compete with motor tasks for cognitive resources. This competition leads to uneven resource allocation between the two tasks, resulting in a decline in performance or quality in one or both tasks (Yogev-Seligmann et al., 2008). Even though walking is considered a motor activity that does not require a great degree of conscious thought, individuals may still be unstable and at risk of falling if they have difficulty reasonably dividing their attention into motor and cognitive tasks during walking under dual-task conditions (Fraser et al., 2017). Excessive body weight increase has been associated with a higher risk for impaired cognitive function (Volkow et al., 2009). Young male adults with excess weight have neurocognitive deficits, like impairments in the efficiency of central processing (Tsai et al., 2019), which might make them more dangerous while walking and dealing with cognitive tasks simultaneously. Numerous studies have explored the performance of individuals with excess weight during walking under dual-task conditions (Wu et al., 2016; Shaik et al., 2022). But, few studies evaluated the CoP parameters of young male adults during GI under dual-task conditions, making the underlying postural control mechanisms in young male adults with excess weight during GI under dual-task conditions remain unknown.

Cognitive load is a vital influence contributor to behaviors (Byrd-Bredbenner et al., 2016). Once cognitive load increases, the difficulty of maintaining postural stability will become more apparent, potentially impairing an individual's ability to actively control their balance (Small et al., 2021). In previous research, influences of cognitive overload were primarily observed in the impairment of gait control, as evidenced by alterations in the gait parameters (Xu et al., 2023). Considering that excess weight is usually accompanied by cognitive function inhibition compared with normal-weight peers (Moss et al., 2023; Wernberg et al., 2023), this means that the increased cognitive load may specifically influence the postural control of overweight or obese young male adults, putting them at a higher risk of falling. Some researchers have suggested that future research should thoroughly analyze secondary cognitive tasks with different difficulty levels to better understand the GI performance of individuals with excess weight under dual-task conditions (Qu et al., 2021). However, this aspect has not been explored yet.

In summary, the purpose of the current study was to further investigate the differences in CoP parameters among young male adults with normal weight and excess weight during GI with different difficult levels of cognitive tasks, determining the influences of cognitive load on CoP parameters of young male adults with excess weight during GI. We made three assumptions.

1) There are differences in CoP parameters during GI between normal-weight and young male adults with excess weight.
2) During GI with cognitive tasks, young male adults with normal weight and those with excess weight had different CoP parameters.
3) During GI with a higher cognitive load, obese young male adults may have different CoP parameters compared with those who are normal weight or even overweight.

2 Materials and methods

2.1 Participants

In this study, thirty-six male undergraduate students were recruited from Soochow University. The study applied the following inclusion criteria: i) individuals aged between 18 and 35 years (Lytle et al., 2017),

TABLE 1 General characteristics of participants.

Characteristics	Body weight			*F*-value	*p*-value
	Normal-weight (*n* = 12)	Overweight (*n* = 12)	Obese (*n* = 12)		
Age (years)	22.8 ± 2.7	22.9 ± 3.0	22.4 ± 2.5	0.113	0.894
Height (m)	1.72 ± 0.06	1.71 ± 0.04	1.73 ± 0.07	0.514	0.603
Weight (kg)	62.1 ± 7.7	74.5 ± 5.7	93.2 ± 8.1	56.246	**<0.001**[a]
BMI (kg/m^2)	20.9 ± 1.5	25.6 ± 1.5	31.1 ± 1.4	152.577	**<0.001**[a]
Preferred swing leg during GI					
Left	3	7	5	—	
Right	9	5	7		

[a]*p*-values < 0.017 for normal-weight group vs. overweight group vs. obese group.
The meaning of the bold values is that significant statistical differences exist.

ii) individuals with normal or corrected-to-normal vision, iii) no history of neurological disorders, and iv) no history of musculoskeletal disorders, as well as no self-reported severe physical diseases that could impede locomotion. After explaining the experimental protocol, all participants signed written informed consent before the experiment. They were evenly classified into the normal-weight group, overweight group, and obese group, according to the classification criteria for overweight and obesity in China [i.e., normal-weight: 18.5≤ body mass index (BMI) ≤23.9 kg/m^2; overweight: 24.0≤ BMI ≤27.9 kg/m^2; obesity: BMI ≥28.0 kg/m^2] (National Health and Family Planning Commission of the People's Republic of China, 2013). The researchers asked participants to walk three times consecutively from a standing position in order to determine their preferred swung leg during GI. The participants' data is presented in Table 1. This study received ethical approval from the Soochow University Human Research Institutional Review Board.

2.2 Test equipment

A screen (U55H3, Haier, China) was set at the endpoint of a 5-m linear walkway (Simonet et al., 2022). CoP parameters during GI were collected by two force platforms (9287B, KISTLER, Switzerland) sequentially embedded in the walkway along the progression direction 1 cm apart. An 8-camera motion capture system (Vicon, Oxford, United Kingdom) was used to collect spatial data from reflective markers placed on the participants' feet, following the scheme provided by the Conventional Gait Model 2.0 (Vicon 2020). The motion capture system and force platforms were synchronized with the sampling rates at 100 and 1,000 Hz, respectively.

2.3 N-back task

The N-back is a continuous performance task requiring high cognitive resources. In this study, a series of letters (from "A" to "J") were randomly presented in a sequence using a visual procedure on the screen. Participants had to monitor these letters and decide whether each letter in a sequence was consistent with the one that appeared N steps ago. The presentation of letters was controlled by E-Prime software 2.0 (Psychology Software Tools, Sharpsburg, PA, United States). Before the presentation of each letter, a cross character appeared on the screen for 500 ms. Subsequently, the letter was displayed for 500 ms, and the participants were given 1,500 ms to respond. The N-back tasks used in this study were constructed using lists of 25 plus N letters, comprising 20 percent "yes" and 80 percent "no" responses (Wrightson et al., 2016). Additionally, the list used in each experiment was different.

Cognitive tasks consist of two difficulty levels: easy (1-back task) and difficulty (2-back task), which require low and high cognitive demand and impose different levels of cognitive load during walking-related movements, respectively (Patelaki et al., 2023). For 1-back task, if the current letter presented is consistent with the previous one, that is a "target" stimulus requiring a "yes" response; once the current letter presented is inconsistent with the previous one, that is, a "not target" stimulus, the participants have to make a "no" response (Nocera et al., 2013). Similarly, for 2-back task, participants have to compare the current letter to the one presented two steps earlier and make a "yes" or "no" response (Nocera et al., 2013). The first letter of 1-back task and the first two letters of 2-back task did not require a response.

2.4 Experimental procedure

Before the formal experiment, participants were given 10 min to train in the N-back task to familiarize themselves with the procedure of N-back tasks. In the formal experiment, the participants started each trial by standing barefoot on the first force platform. They maintained an upright posture with their arms at their sides, fixed their heads in a neutral position, and looked straight ahead with their eyes. The initial positioning of the feet was self-selected and then subsequently marked to ensure consistent foot placement and stance width throughout the experimental procedure. Each participant walked from the start point to the endpoint under single and dual-task conditions.

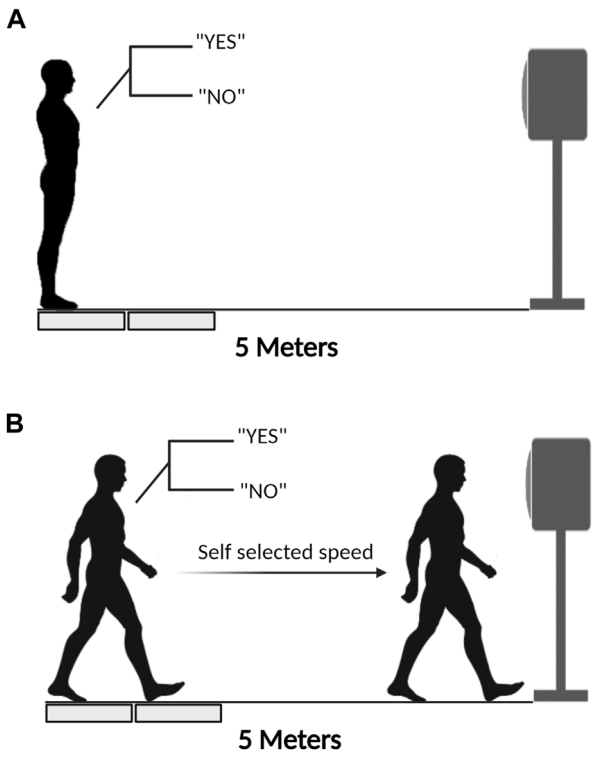

FIGURE 1
The experimental procedure during GI under dual-task conditions. **(A)**: Participants stand on the force platform and respond according to the N-back task requirements; **(B)**: Make a response according to the N-back task requirements and initiate gait simultaneously.

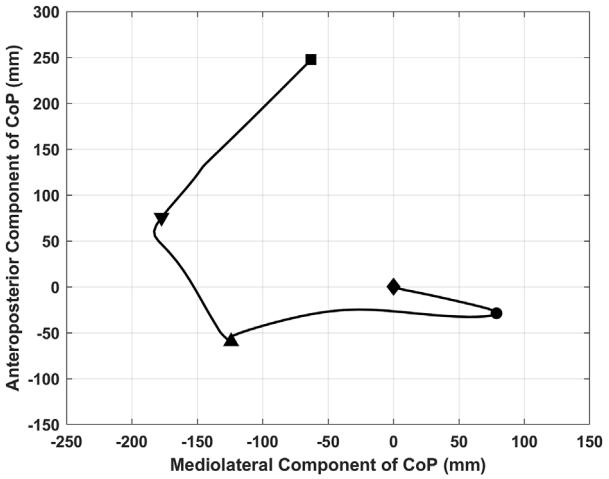

FIGURE 2
The division of GI and the meanings of landmarks. ◆: Onset of the GI period and the imbalance phase; ●: End of the imbalance phase and onset of the unloading phase; ▲: Onset of the monopedal phase and the end of the unloading phase; ▼: End of the monopedal phase and the onset of the bipedal phase; ■: End of the bipedal phase and the GI period.

2.4.1 Single-task condition

Participants stood on the force plate, as mentioned above. Once a letter with an illuminated light appeared on the screen, participants needed to initiate gait and walk along the 5-m walkway. A successful trial under the single-task condition was defined as one where the participants' preferred swung leg during GI correctly stepped on the second force platform, with the foot not exceeding the edge of the force platform, and test equipment successfully captured trial data.

2.4.2 Dual-task conditions

Participants stood on the force plate, as described above. According to the requirements of the N-back test, participants need to respond continuously as accurately and quickly as possible (Figure 1A). No feedback was given during or after each trial or block. Until the end of the list, the letter with an illuminated light would appear and cue participants to initiate gait. Participants must respond correctly, followed by the N-back test requirement, and immediately initiate gait and walk to the endpoint (Figure 1B). A 5-min gap was set between each 1- and 2-back task, allowing participants to relax. A successful trial under the dual-task condition was defined as one in which participants achieved complete accuracy in the N-back tasks (to ensure that participants really focused on performing cognitive tests) and their preferred swung leg during GI stepped on the second force platform, with their foot not exceeding the edge of the force platform, and test equipment successfully captured trial data. Those trials of participants who fail to meet the accuracy requirement of N-back tasks during GI with cognitive tasks will not be used for analysis. Finally, all participants need to conduct three successful trials under single- and dual-task conditions, respectively.

2.5 Dependent variables

The data obtained from successful trials were analyzed using MATLAB software (R2023a, MATLAB, Mathworks, Inc., Natick, MA, United States). Moment and force components were low-pass filtered at 10 Hz (Butterworth, fourth order), and then CoP parameters were calculated.

According to five landmarks, the GI was divided into four sub-phases. Specifically, those landmarks were successively representing: 1) the CoP started deviation toward the swing leg; 2) the CoP completely under the rear foot of the swing leg; 3) the heel of the swing leg left off the ground; 4) the foot of the swing leg contacted ground; and 5) the toe of the stance leg left from the ground. The four sub-phases are sequentially named as imbalance, unloading, monopedal standing, and bipedal standing phases. The imbalance phase was characterized by the CoP deviation towards the swing leg, followed by a transfer to the posterior end of the swinging leg. Deviation onset was determined as the time point when mediolateral (ML) CoP displacement exceeded three standard deviations from its baseline. The baseline was calculated as the mean value of ML CoP displacement in the 1,500 ms period before the visual cue of the last letter was presented (Uemura et al., 2012; Yousefi et al., 2020). The unloading phase represented the movement of the CoP towards the initial stance foot and stopped under the initial stance foot. The monopedal standing phase started with the forward displacement of CoP, which was at the instant of transition to the single-limb stance and ended with the heel strike of the swing leg (Davidson and Wolpert, 2005). Swing leg heel contact was determined as the

moment when the vertical ground reaction force measured by the second force platform exceeded 10 N (Qu et al., 2021). The bipedal standing phase started from the forward shift of CoP and continued until the toe-off of the stance limb (Davidson and Wolpert, 2005). Stance leg toe-off was the moment when the toe marker increased by 10 mm in the vertical direction from static upright standing. The division of GI is shown in Figure 2.

Dependent variables for the assessment included spatial-temporal variables of sub-phases: duration, CoP length path, CoP speed, anteroposterior (AP) and ML CoP displacement amplitude, and velocity of AP and ML CoP displacement. Among them, AP and ML CoP displacement amplitude were calculated using Eqs 1, 2. In these equations, x and y represent the CoP position in the AP and ML directions, respectively.

$$\text{AP CoP displacement amplitude (cm)} = |\text{y end} - \text{y onset}| \quad (1)$$

$$\text{ML CoP displacement amplitude (cm)} = |\text{x end} - \text{x onset}| \quad (2)$$

The velocity of AP and ML CoP displacement were calculated using Eqs 3, 4. The variable n represents the number of data points, and 1,000 is the sampling frequency.

$$\text{Velocity of AP CoP displacement}\left(\frac{\text{cm}}{\text{s}}\right) = \frac{\text{AP CoP displacement amplitude}^{*}1000}{(n_{end} - n_{onset})} \quad (3)$$

$$\text{Velocity of ML CoP displacement}\left(\frac{\text{cm}}{\text{s}}\right) = \frac{\text{ML CoP displacement amplitude}^{*}1000}{(n_{end} - n_{onset})} \quad (4)$$

2.6 Statistical analysis

The mean value of the three successful trials under single- and dual-task conditions, respectively, was used for statistical analysis. Data analysis was performed using SPSS version 26 for Windows (SPSS Inc., Chicago, IL, United States). Continuous variables were presented as mean ± standard deviation (SD). The data distribution for each variable was assessed using the Shapiro-Wilk test. If the data distribution was non-normal, it was transformed for subsequent analysis using the Box-Cox transformation, to become normally distributed, i.e.,

$$y^T = \begin{cases} \dfrac{y^\lambda - 1}{\lambda}, & \lambda \neq 0; \\ \ln y, & \lambda = 0, \end{cases}$$

where y is the original variable, y^T represents the corresponding transformed variable, and λ is a parameter, which is supposed to be most efficient when maximizing the log-likelihood. Those non-normal variables that need Box-Cox transformed were marked in Tables, and their corresponding optimal λ values and confidence intervals can be found in the Supplementary Material.

A mixed ANOVA with a Greenhouse-Geisser correction was utilized to detect the between-subjects effect of group (normal-weight, overweight, and obese), the within-subjects effect of task condition (baseline, 1-back, and 2-back), and the interaction effect between group and task. Statistical significance was concluded when p-values < 0.05, and Eta partial square (η^2) was used to display the effect size. Post-hoc comparisons among groups and tasks were applied Bonferroni correction, and statistical significance was concluded when p-values < 0.017. In case a significant interaction was detected, a simple effects analysis was conducted. During the simple effects analysis, when performing the *post hoc* analysis among groups, the statistical significance was set at p-values < 0.0056.

3 Results

3.1 Duration

There were significant main effects of the group on the duration of the imbalance phase (F = 4.086, p = 0.026, η^2 = 0.198) and the bipedal standing phase (F = 7.262, p = 0.002, η^2 = 0.306) (Table 2). Post hoc analysis found no significant difference in the paired comparison between any two groups regarding the duration of the imbalance phase (p > 0.017); The obese group (0.24 ± 0.05 s) showed a more prolonged duration of the bipedal standing phase than the normal-weight group (0.19 ± 0.04 s) (p = 0.002).

There were significant main effects of the task on the duration of the imbalance phase (F = 13.871, p < 0.001, η^2 = 0.296) and the bipedal standing phase (F = 7.534, p = 0.002, η^2 = 0.186) (Table 2). Post hoc analysis found that the duration of the imbalance phase with 1-back task (0.26 ± 0.07 s) and 2-back task (0.29 ± 0.07 s) was more prolonged than that with single task (0.23 ± 0.06 s) (p = 0.004; p < 0.001); The duration of the bipedal standing phase with 2-back task (0.22 ± 0.05 s) was more prolonged than that with single task (0.20 ± 0.04 s) (p = 0.009).

3.2 CoP path length and CoP speed

There were significant main effects of the group on the CoP path length during the imbalance phase (F = 5.128, p = 0.012, η^2 = 0.237), the unloading phase (F = 3.949, p = 0.029, η^2 = 0.193), and the bipedal standing phase (F = 8.337, p = 0.001, η^2 = 0.336) (Table 3). Post hoc analysis found that the obese group (8.34 ± 2.60 cm) showed more increased CoP path length during the imbalance phase than the normal-weight group (5.81 ± 2.41 cm) (p = 0.010); No significant differences were found in the paired comparison between any two groups regarding the CoP path length during the unloading phase (p > 0.017); The obese group (42.27 ± 5.16 cm) showed more increased CoP path length during the bipedal standing phase than the normal-weight group (35.62 ± 6.34 cm) (p = 0.001).

There were significant main effects of the task on the CoP path length during the imbalance phase (F = 3.157, p = 0.049, η^2 = 0.087), and the CoP speed during the bipedal standing phase (F = 7.943, p = 0.001, η^2 = 0.194) (Table 3). Post hoc analysis found that no significant differences were found in the paired comparison between any two tasks regarding the CoP path length during the imbalance phase (p > 0.017); The CoP speed during the bipedal standing phase with 2-back task (183.33 ± 39.29 cm/s) was more decreased than that with single task (208.90 ± 41.03 cm/s) (p = 0.003).

There were also significant interaction effects between task and group on the CoP length path during the unloading phase (F = 2.685, p = 0.039, η^2 = 0.140) and the CoP speed during the bipedal standing phase (F = 3.618, p = 0.010, η^2 = 0.180) (Table 3). Simple effects analysis displayed that the CoP path length during the unloading

TABLE 2 Results of the duration of sub-phases of GI (unit: s).

Variables	Task	Body weight			Main effect *p*-value		Interaction effect *p*-value
		Normal-weight (n = 12)	Overweight (n = 12)	Obese (n = 12)	Group	Task	Group × task
Imbalance phase[a]	Single	0.21 ± 0.07	0.23 ± 0.04	0.24 ± 0.06	**0.026**	**<0.001**[c,d]	0.814
	1-back	0.23 ± 0.06	0.28 ± 0.07	0.28 ± 0.07			
	2-back	0.25 ± 0.06	0.31 ± 0.07	0.31 ± 0.07			
Unloading phase[a]	Single	0.36 ± 0.21	0.32 ± 0.14	0.28 ± 0.07	0.778	0.958	0.791
	1-back	0.30 ± 0.10	0.26 ± 0.05	0.30 ± 0.05			
	2-back	0.30 ± 0.07	0.28 ± 0.06	0.29 ± 0.06			
Monopedal standing phase	Single	0.30 ± 0.09	0.31 ± 0.05	0.31 ± 0.05	0.218	0.568	0.443
	1-back	0.27 ± 0.09	0.31 ± 0.04	0.29 ± 0.08			
	2-back	0.26 ± 0.07	0.32 ± 0.08	0.31 ± 0.08			
Bipedal standing phase	Single	0.18 ± 0.04	0.20 ± 0.03	0.21 ± 0.04	**0.002**[b]	**0.002**[d]	0.132
	1-back	0.19 ± 0.05	0.21 ± 0.02	0.24 ± 0.05			
	2-back	0.19 ± 0.03	0.21 ± 0.04	0.26 ± 0.04			

[a]Box-Cox transformation was implemented to this variable.
[b]*p*-values <0.017 for normal-weight group vs. obese group.
[c]*p*-values <0.017 for single task vs. 1-back task.
[d]*p*-values <0.017 for single task vs. 2-back task.
The meaning of the bold values is that significant statistical differences exist.

phase with single and 1-back task had no significant differences among the three groups; The obese group (21.18 ± 2.69 cm) showed more increased CoP path length during the unloading phase with 2-back task than the normal-weight group (15.90 ± 3.28 cm) (p = 0.002) (Figure 3). The CoP speed during the bipedal standing phase with single, 1- and 2-back tasks had no significant differences between any two groups ($p > 0.0056$).

3.3 CoP displacement amplitude

There were significant main effects of the group on the ML CoP displacement amplitude during the imbalance phase (F = 6.258, p = 0.005, η^2 = 0.275), the unloading phase (F = 5.346, p = 0.010, η^2 = 0.245), and the bipedal standing phase (F = 17.631, $p < 0.001$, η^2 = 0.517) (Table 4). Post hoc analysis found that the obese group (6.63 ± 2.19 cm) showed higher ML CoP displacement amplitude during the imbalance phase than the normal-weight group (4.13 ± 2.12 cm) (p = 0.004); The obese group (18.73 ± 2.96 cm) showed higher ML CoP displacement amplitude during the unloading phase than the normal-weight group (14.21 ± 4.29 cm) (p = 0.008); The obese group (26.60 ± 4.77 cm) showed higher ML CoP displacement amplitude during the bipedal standing phase than the normal-weight group (17.06 ± 3.73 cm) ($p < 0.001$) and the overweight group (21.34 ± 4.16 cm) (p = 0.008).

There was significant main effects of the task on the AP CoP displacement amplitude during the bipedal standing phase (F = 4.092, p = 0.021, η^2 = 0.110) (Table 4). Post hoc analysis found that the AP CoP displacement amplitude during the bipedal standing phase with 2-back task (22.11 ± 5.38 cm) was lower than that with single task (21.48 ± 6.26 cm) (p = 0.005).

There were also significant interaction effects between task and group on the ML CoP displacement amplitude during the imbalance phase (F = 2.690, p = 0.039, η^2 = 0.140) and the unloading phase (F = 3.060, p = 0.022, η^2 = 0.156). Simple effects analysis displayed that the ML CoP displacement amplitude during the imbalance phase with single task had no statistical differences among the three groups. The obese group (6.96 ± 2.17 cm) showed higher ML CoP displacement amplitude during the imbalance phase with 1-back task than the normal-weight group (3.64 ± 2.12 cm) (p = 0.001); The obese group (7.40 ± 1.88 cm) showed higher ML CoP displacement amplitude during the imbalance phase with 2-back task than the normal-weight group (4.26 ± 1.97 cm) (p = 0.001) (Figure 4A). Additionally, the ML CoP displacement amplitude during the unloading phase with single task had no significant differences among the three groups. The obese group (18.76 ± 2.88 cm) showed higher ML CoP displacement amplitude during the unloading phase with 1-back task than the normal-weight group (13.52 ± 3.98 cm) (p = 0.003); The obese group (20.18 ± 2.69 cm) showed higher ML CoP displacement amplitude during the unloading phase with 2-back task than the normal-weight group (13.90 ± 3.38 cm) ($p < 0.001$) (Figure 4B).

3.4 Velocity of CoP displacement

There was a significant main effects of the group on the velocity of AP CoP displacement during the bipedal standing phase (F = 3.716, p = 0.035, η^2 = 0.184) (Table 5). Post hoc analysis found no significant difference in the paired comparison between any two

TABLE 3 Results of CoP path length and CoP speed (unit: cm and cm/s).

Variables	Task	Body weight			Main effect *p*-value		Interaction effect *p*-value
		Normal-weight (n = 12)	Overweight (n = 12)	Obese (n = 12)	Group	Task	Group × task
CoP path length							
Imbalance phase	Single	5.72 ± 2.68	6.96 ± 3.13	7.42 ± 3.28	**0.012**[b]	**0.049**	0.664
	1-back	5.29 ± 2.37	7.41 ± 1.91	8.43 ± 2.59			
	2-back	6.41 ± 2.23	7.75 ± 2.04	9.18 ± 1.53			
Unloading phase[a]	Single	17.24 ± 5.51	18.41 ± 4.47	18.18 ± 2.76	**0.029**	0.343	**0.039**
	1-back	15.45 ± 3.98	16.79 ± 3.84	19.63 ± 2.97			
	2-back	15.90 ± 3.28	17.24 ± 4.40	21.18 ± 2.69			
Monopedal standing phase[a]	Single	11.82 ± 3.74	12.79 ± 2.76	13.29 ± 4.57	0.972	0.670	0.397
	1-back	12.91 ± 3.46	12.28 ± 1.97	11.74 ± 3.44			
	2-back	12.06 ± 3.43	12.58 ± 3.34	12.17 ± 3.54			
Bipedal standing phase[a]	Single	34.87 ± 7.44	41.79 ± 2.84	43.95 ± 6.12	**0.001**[b]	0.204	0.055
	1-back	35.36 ± 6.62	40.08 ± 4.57	43.17 ± 4.21			
	2-back	36.64 ± 5.19	40.48 ± 4.44	39.68 ± 4.28			
CoP speed							
Imbalance phase[a]	Single	30.98 ± 18.16	31.12 ± 13.98	32.86 ± 16.32	0.354	0.427	0.611
	1-back	23.61 ± 10.52	27.33 ± 7.17	33.36 ± 16.10			
	2-back	26.11 ± 7.08	25.37 ± 7.45	31.28 ± 9.77			
Unloading phase[a]	Single	64.21 ± 41.20	65.85 ± 34.75	68.57 ± 19.73	0.099	0.731	0.756
	1-back	55.39 ± 16.83	64.58 ± 15.91	68.28 ± 16.46			
	2-back	54.64 ± 14.07	63.63 ± 17.04	77.02 ± 18.45			
Monopedal standing phase	Single	42.59 ± 17.12	43.00 ± 12.19	44.03 ± 14.84	0.387	0.881	0.211
	1-back	50.81 ± 14.30	40.43 ± 8.37	40.51 ± 12.60			
	2-back	47.01 ± 5.61	40.96 ± 15.62	40.50 ± 12.80			
Bipedal standing phase[a]	Single	194.82 ± 34.06	213.09 ± 31.05	218.79 ± 53.76	0.350	**0.001**[c]	**0.010**
	1-back	191.90 ± 45.80	195.42 ± 37.78	183.54 ± 44.05			
	2-back	195.26 ± 38.17	196.38 ± 38.09	158.37 ± 31.38			

[a]Box-Cox transformation was implemented to this variable.
[b]*p*-values <0.017 for normal-weight group vs. obese group.
[c]*p*-values <0.017 for single task vs. 2-back task.
The meaning of the bold values is that significant statistical differences exist.

groups regarding the velocity of AP CoP displacement during the bipedal standing phase ($p > 0.017$).

There was a significant main effects of the task on the velocity of AP CoP displacement during the bipedal standing phase ($F = 11.652$, $p < 0.001$, $\eta^2 = 0.261$) (Table 5). Post hoc analysis found that the velocity of AP CoP displacement during the bipedal standing phase with 1-back task (154.54 ± 34.29 cm/s) and 2-back task (146.60 ± 36.81 cm/s) were more decreased than that with single task (172.48 ± 37.06 cm/s) ($p = 0.012$; $p < 0.001$).

There was also a significant interaction effect between group and task on the velocity of AP displacement during the bipedal standing phase ($F = 3.869$, $p = 0.007$, $\eta^2 = 0.190$). Simple effects analysis displayed that the velocity of AP displacement during the bipedal standing phase with single and 1-back tasks showed no statistical differences among the three groups; The obese group (118.03 ± 22.00 cm/s) showed more decreased velocity of AP displacement during the bipedal standing phase with 2-back task than the normal-weight group (165.88 ± 35.35 cm/s) ($p = 0.001$) (Figure 5).

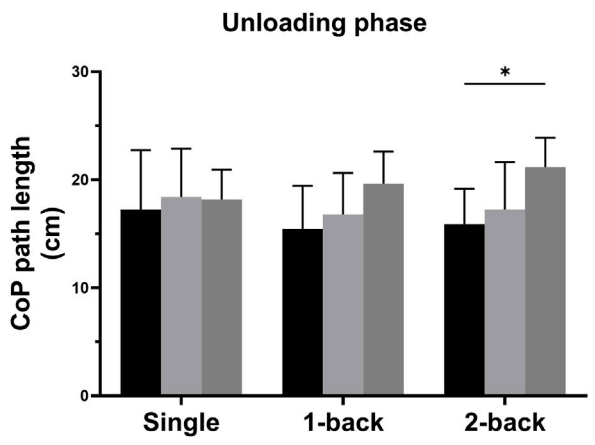

FIGURE 3
Simple analysis results in CoP path length during the unloading phase. * p-values < 0.0056.

4 Discussion

4.1 Influence of excess weight on young male adults' CoP parameters

Consistent with our assumption 1, differences in CoP parameters during GI were observed among young male adults with normal weight and excess weight in this study. Specifically, we observed that compared with normal-weight young male adults, young male adults with excess weight, mainly those who were obese, exhibited increased CoP path length and higher ML CoP displacement during the sub-phases of GI, while overweight ones did not exhibit differences with normal-weight ones. The results of increased CoP path length suggest that the adductor hip muscles of obese young male adults could have more activations during GI because adductor hip muscles are fundamental for GI in assisting the shifting of CoP from one side leg to the opposite leg for obese young male adults who have poor intrinsic coordination and greater burden in CoP transfer. Once the activation of the hip adductor muscles is reduced, it will result in a shorter CoP path length, as reported by Vrieling et al. (2008) and Cimolin et al. (2017).

However, the increased CoP path length in this study also suggests that obese young male adults could have an unbalance in muscle strength between the adductor and abductor muscles, influencing their postural control in ML direction during GI. The reason for this finding is that dynamic postural balance control needs appropriate intensity muscle contractions of all proximal muscles of the lower limbs during walking, but obese individuals have a relative weakness in the specific contractile performance and quality of hip abductor muscles (Fenato et al., 2021), like gluteus medius, compared with normal-weight ones. The partial lower extremity muscle over-contraction destabilizes the overall body frame and increases the challenge of maintaining postural control in the frontal plane for obese individuals. This finding is consistent with Horsak et al. (2019), the disequilibrium in the strength of the hip abductor and adductor muscles during GI intensifies the level of difficulty in maintaining postural control in the frontal plane for obese individuals. Besides, we also found that obese young male adults have increased displacement amplitude in ML direction during sub-phases of GI, which is consistent with the previous studies that obese individuals have more ML displacement during walking and dynamic balance tests (do Nascimento et al., 2017; McGraw et al., 2000). This finding further proves that, compared with their normal-weight counterparts, obese young males have more difficulty in terms of maintaining lateral stability.

Apart from the CoP parameters, this study showed that although the mean value of the time spent in the imbalance phase of young male adults with excess weight is slightly higher than that of the normal-weight group, there were no significant differences, suggesting regardless of whether young male adults have excess weight or not, the time spent adjusting their posture in advance for the CoP transfer from swing their leg to the stance leg maybe exist slight differences but not obvious enough. Besides, our results suggest that obese young male adults have a prolonged duration of the bipedal standing phase, which may be because more time consumption during this phase is helpful in improving their walking stability, as reported by Duffell et al. (2014). But in contrast with our results, the previous studies believed that obese individuals prolong the imbalance phase to achieve as much posture preparation as possible and take functional adaptation aimed at improving stability by prolonged monopedal standing phase (Cau et al., 2014; Cimolin et al., 2017). The reason for such difference can be attributed to the severity of obesity among the participants in the previous study being much higher than that of the young male adults recruited in our study. Considering that severely obese individuals had the lowest levels of mobility (Hergenroeder et al., 2011), we speculate that this factor amplified the differences in the duration of sub-phases between normal-weight and obese individuals, making their results different from ours. Our findings on the differences in sub-phase duration of GI likely apply more to moderately obese young male adults than severely obese ones.

4.2 Cognitive task influences on CoP parameters of young male adults with excess weight

Our results demonstrated that cognitive tasks placed additional demands on cognitive resources, resulting in differences in CoP parameters during GI among young male adults with excess weight and those with normal weight, which supports our assumption 2.

We observed that during the imbalance phase and unloading phase with cognitive tasks, obese young male adults showed distinctly increased ML CoP displacement amplitude. The reason for such results might due to although when encountering cognitive tasks during motion processing, individuals will employ an adaptive postural control strategy to regulate the CoP displacement amplitude during GI to counteract trunk sway with minimal interference from the additional cognitive task (Mille et al., 2014), but most sub-phases of GI put high demands on postural control and once obese individuals face dual-task constraints, their lateral movements and force organization strategy will be modified (Menegoni et al., 2009; Hung et al., 2013; Cimolin et al., 2017), which can lead to abnormal lateral displacement. These findings suggest that for obese young male adults, the compensatory strategy they used for lateral balance during GI with cognitive tasks might have

TABLE 4 Results of CoP displacement amplitude (unit: cm).

Variables	Task	Body weight			Main effect *p*-value		Interaction effect *p*-value
		Normal-weight (n = 12)	Overweight (n = 12)	Obese (n = 12)	Group	Task	Group × task
Imbalance phase							
AP	Single	2.86 ± 1.83	3.46 ± 1.49	3.83 ± 2.36	0.171	0.208	0.906
	1-back	3.31 ± 1.55	4.02 ± 1.12	4.00 ± 1.56			
	2-back	3.21 ± 1.52	4.27 ± 1.17	4.21 ± 1.50			
ML	Single	4.51 ± 2.34	5.65 ± 2.74	5.54 ± 2.21	**0.005**[b]	0.187	**0.039**
	1-back	3.64 ± 2.12	5.86 ± 1.55	6.96 ± 2.17			
	2-back	4.26 ± 1.97	5.88 ± 1.68	7.40 ± 1.88			
Unloading phase							
AP[a]	Single	2.72 ± 1.36	2.87 ± 1.63	1.80 ± 1.27	0.114	0.248	0.133
	1-back	2.96 ± 1.66	1.69 ± 1.03	1.29 ± 0.84			
	2-back	2.92 ± 2.40	1.72 ± 1.22	2.17 ± 1.50			
ML	Single	15.21 ± 5.45	16.49 ± 4.43	17.25 ± 2.78	**0.010**[b]	0.311	**0.022**
	1-back	13.52 ± 3.98	15.89 ± 3.73	18.76 ± 2.88			
	2-back	13.90 ± 3.38	16.48 ± 4.43	20.18 ± 2.69			
Monopedal standing phase							
AP[a]	Single	10.70 ± 3.48	11.83 ± 2.69	11.98 ± 4.12	0.968	0.681	0.300
	1-back	11.83 ± 3.24	11.21 ± 1.94	10.61 ± 3.11			
	2-back	11.16 ± 3.43	11.59 ± 3.36	10.81 ± 3.12			
ML[a]	Single	2.45 ± 1.72	2.56 ± 1.32	3.26 ± 1.43	0.186	0.346	0.729
	1-back	2.03 ± 1.58	2.66 ± 1.43	2.85 ± 1.71			
	2-back	1.99 ± 1.41	2.19 ± 1.23	3.06 ± 1.30			
Bipedal standing phase							
AP[a]	Single	30.23 ± 6.39	34.63 ± 4.44	34.23 ± 5.13	0.245	**0.021**[d]	0.059
	1-back	30.17 ± 5.95	33.19 ± 4.61	32.85 ± 2.33			
	2-back	31.20 ± 5.32	32.19 ± 4.87	29.58 ± 2.94			
ML	Single	16.34 ± 4.82	21.71 ± 4.19	26.39 ± 5.36	**<0.001**[b, c]	0.345	0.673
	1-back	17.15 ± 3.76	20.65 ± 3.44	26.46 ± 5.38			
	2-back	17.70 ± 2.41	21.67 ± 4.99	26.97 ± 3.80			

[a]Box-Cox transformation was implemented to this variable.
[b]*p*-values <0.017 for normal-weight group vs. obese group.
[c]*p*-values <0.017 for overweight group vs. obese group.
[d]*p*-values <0.017 for single task vs. 2-back task.
The meaning of the bold values is that significant statistical differences exist.

been ineffective, causing deterioration of their postural control and stability.

Moreover, we did not observe that normal-weight and overweight young male adults have significant differences in the parameters of CoP during GI with cognitive tasks. This finding is consistent with Qu et al. (2021), who used random number generation as the cognitive task for participants and did not find differences in the parameters that can reflect postural stability during GI, like margin of stability between normal-weight and overweight young adults. Although they issue that only when the cognitive task reaches a certain level of difficulty, it could amplify differences in postural control status between young male adults with excess weight and normal weight during GI, the cognitive task we employed in this study were N-back tasks which can impose

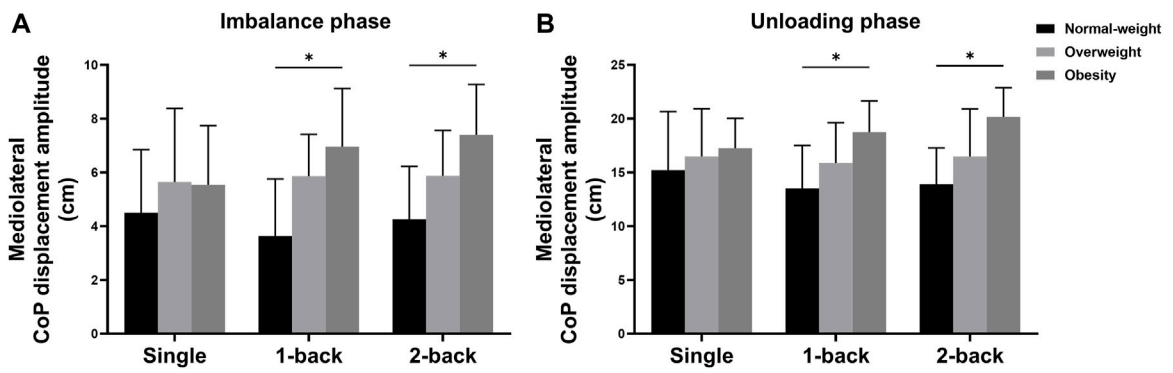

FIGURE 4
Simple analysis results in **(A)** ML CoP displacement amplitude during the imbalance phase and **(B)** ML CoP displacement amplitude during the unloading phase. * p-values < 0.0056.

greater cognitive demands than random number generation. Considering this point, we believe that the lack of differences in CoP parameters between normal weight and overweight young male adults during GI with cognitive tasks is not due to insufficient difficulty in cognitive tasks. Instead, it may be because the performance of these young male adults during GI with cognitive tasks may not have obvious differences.

4.3 Higher cognitive load influences on CoP parameters of young male adults with excess weight

Consistent with the previous studies that individuals with greater adiposity commonly have poor postural control performance, especially reflected in less effective control in the ML CoP displacement (Tsiros et al., 2019; Saraiva et al., 2023), we observed that obese young male adults showed higher ML CoP displacement and increased CoP path length during GI with difficult-level cognitive tasks, and these results reveal that a higher cognitive load could make it difficult for obese young male adults to maintain postural stability.

It is particularly prioritized for individuals to maintain the magnitude of ML CoP displacements within a reasonable range during GI under dual-task conditions (Uemura et al., 2012; Russo and Vannozzi, 2021). But obese individuals usually need more attentional resources to control their stance leg to maintain postural stability than non-obese participants when performing complex postural control tasks (Mignardot et al., 2010), particularly from the imbalance phase to the unloading phase, individuals need to gradually transfer their entire body weight to the initial stance leg for helping the swing leg step forward (Crenna et al., 2006), higher demand is placed on the ability of obese individuals to maintain balance in supporting themselves on a single-leg compared to single task condition. Difficult cognitive tasks occupied a large number of attentional resources, making obese young male adults' defects in single-leg control amplified, which could be the main reason for the differences in their displacement amplitude and CoP path length compared to normal-weight young male adults.

Moreover, in this study, we observed that the velocity of AP CoP displacement during the bipedal standing phase with the difficult cognitive task was significantly decreased in obese young male adults compared with the normal-weight ones but not with the overweight ones. This result is inconsistent with our assumption 3. Still, it shows that increased cognitive load during GI will make obese young male adults have obvious differences in CoP parameters compared to normal-weight ones. This finding suggests that the appearance of cognitive tasks has further reduced obese ones' quality of GI performance due to the velocity of CoP displacement, which is a functional performance indicator, and its value positively correlates with GI performance quality (Esfandiari et al., 2020). The decreased velocity can be attributed to individuals' cognitive function not being able to meet the requirements of GI and deal with cognitive tasks simultaneously. As reported by Shaik et al. (2022), obesity is typically associated with an increase in young adults' attentional cost of walking, resulting in a decreased gait speed of dual-task walking.

This result also suggests that when obese young male adults simultaneously dealing with difficult cognitive tasks while GI, they perform more CoP velocity adjustments in the AP direction than their normal-weight counterparts. The reason for such change is that the largest CoP displacement usually occurs during the bipedal standing phase (van Mierlo et al., 2021), and high requirements were placed for individuals to control CoP in the AP direction. But increased attentional demands are required to achieve the cognitive task goal and maintain postural control simultaneously, making excess weight individuals usually produce AP instability in postural control (Menegoni et al., 2009; Hung et al., 2013). The decreased CoP velocity is helping them compensate for a declined ability to perform multiple tasks at once successfully and safely, as reported by the previous studies (Uemura et al., 2012; Cau et al., 2014), that is, accelerating the body forward is not a priority for obese ones, and the reduced velocity in the AP direction is the continuous effort counteracting their relative instability during GI.

4.4 Practical implication

This study provided insights into the influences of cognitive load on obese young male adults during GI under dual-task

TABLE 5 Results of velocity of CoP displacement (unit: cm/s).

Variables	Task	Body weight			Main effect *p*-value		Interaction effect *p*-value
		Normal-weight (n = 12)	Overweight (n = 12)	Obese (n = 12)	Group	Task	Group × task
Imbalance phase							
AP[a]	Single	15.74 ± 11.86	15.61 ± 7.49	17.17 ± 11.61	0.899	0.573	0.993
	1-back	14.79 ± 7.39	14.99 ± 5.03	15.64 ± 7.87			
	2-back	13.55 ± 6.34	14.22 ± 5.42	14.88 ± 7.91			
ML[a]	Single	24.50 ± 14.93	25.29 ± 12.08	24.97 ± 12.51	0.172	0.135	0.146
	1-back	16.34 ± 9.20	21.60 ± 5.62	27.66 ± 13.63			
	2-back	17.74 ± 7.47	19.16 ± 5.63	25.13 ± 8.40			
Unloading phase							
AP[a]	Single	10.47 ± 8.28	9.66 ± 7.28	6.18 ± 3.55	0.167	0.481	0.357
	1-back	9.78 ± 4.59	6.58 ± 4.44	4.61 ± 3.43			
	2-back	10.23 ± 9.48	6.47 ± 5.06	8.61 ± 8.20			
ML[a]	Single	58.62 ± 41.11	60.92 ± 35.54	65.35 ± 19.96	0.051	0.761	0.675
	1-back	49.33 ± 17.64	61.14 ± 15.60	65.34 ± 16.42			
	2-back	47.96 ± 14.57	60.84 ± 16.96	73.38 ± 17.83			
Monopedal standing phase							
AP	Single	38.42 ± 15.38	39.70 ± 11.49	39.74 ± 13.58	0.360	0.866	0.145
	1-back	46.68 ± 13.65	37.05 ± 8.98	36.44 ± 11.34			
	2-back	43.37 ± 6.32	37.47 ± 14.44	36.13 ± 12.14			
ML[a]	Single	9.71 ± 7.61	8.51 ± 4.90	10.94 ± 5.12	0.468	0.465	0.896
	1-back	7.98 ± 6.04	8.56 ± 4.30	10.04 ± 6.87			
	2-back	7.95 ± 5.78	7.84 ± 5.49	10.19 ± 4.43			
Bipedal standing phase							
AP[a]	Single	169.37 ± 33.22	177.01 ± 32.92	171.06 ± 46.33	**0.035**	**<0.001**[b, c]	**0.007**
	1-back	163.37 ± 40.92	161.22 ± 29.28	139.04 ± 28.52			
	2-back	165.88 ± 35.35	155.90 ± 34.47	118.03 ± 22.00			
ML[a]	Single	91.05 ± 20.89	110.33 ± 23.74	130.75 ± 34.43	0.077	0.111	0.189
	1-back	94.74 ± 27.52	101.17 ± 25.68	113.70 ± 39.62			
	2-back	95.62 ± 22.97	105.12 ± 28.82	108.11 ± 25.96			

[a]Box-Cox transformation was implemented to this variable.
[b]*p*-values <0.017 for single task vs. 1-back task.
[c]*p*-values <0.017 for single task vs. 2-back task.
The meaning of the bold values is that significant statistical differences exist.

conditions, which could be valuable in the training and rehabilitation of these populations. Firstly, since obese young male adults are unable to correctly move their CoP and transfer body weight as healthy normal-weight do during GI, treatment personnel should modify their dietary habits to improve their metabolic profile and provide them with sufficient exercise to achieve weight loss (Lambert et al., 2017; Balasekaran et al., 2023), which is equally necessary for overweight young male adults. Although the difference between their CoP parameters and normal-weight ones is not significant enough, if their dietary structure is not adjusted, they are also likely to be obese and have similar problems during GI. Secondly, dealing with cognitive tasks can exacerbate lateral posture control disorders during GI. Treatment personnel should pay attention to correcting the unhealthy lifestyle habits of obese ones, such as using their phones while GI (Shahidian et al.,

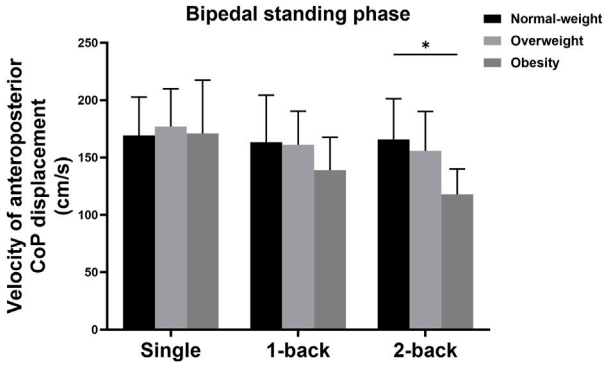

FIGURE 5
Simple analysis results in velocity of AP CoP displacement during the bipedal standing phase. * p-values < 0.0056.

2022). Finally, since obese young male adults have the most pronounced lateral posture control disorders during GI with a higher cognitive load, treatment personnel should provide additional training on the cognitive capacity of obese young male adults to enhance their capacity to make appropriate judgments in complex environments might be greatly beneficial (Shaik et al., 2022), especially effective in reducing lateral falls and preventing related injuries, like femoral neck and hip fractures (Cameron et al., 2011; Wu et al., 2016; Gonzalez et al., 2023).

4.5 Limitations

The limitations of this study should be taken into consideration. Following previous research that investigated GI performance in the obese population (Cau et al., 2014; Hirjaková et al., 2018; Qu et al., 2021), this study only grouped young male adults based on BMI and did not use the differentiation between limb and trunk circumference as inclusions for filtering young male adults with excess weight. In addition, although CoP parameters can reflect postural control problems, this study did not analyze kinematic parameters or muscle activation status. Further analysis is needed to examine the differences in these indicators among young male adults with normal weight and excess weight during GI. Moreover, based on the purpose of our study, we only recruited young male adults. Due to the movement performance of individuals with excess weight being different in individuals of different sexes (Menegoni et al., 2009), it is still necessary to conduct similar experiments in young female adults to find their characteristics of CoP parameters during GI. Finally, the number of participants in this study is relatively limited, which may have restricted the efficiency of our results, and there is a need to expand the sample size in future research to verify the findings of this study further.

5 Conclusion

The present study preliminarily explores the influence of excess weight and cognitive load on CoP parameters during GI, providing insights into postural control deficiency in young male adults with excess weight. Overall, cognitive load compromises the postural stability of obese young male adults during GI. Especially dealing with higher cognitive load during GI, obese young male adults will experience increased difficulty transferring their CoP, suffer more postural instability and have a higher risk of lateral falling than normal-weight young male adults. Further research will be necessary to determine the most effective exercise or training method for obese young male adults to achieve safe GI.

Data availability statement

The raw data supporting the conclusion of this article will be made available by the authors, without undue reservation.

Ethics statement

The studies involving humans were approved by the Soochow University Human Research Institutional Review Board. The studies were conducted in accordance with the local legislation and institutional requirements. The participants provided their written informed consent to participate in this study.

Author contributions

LK: Conceptualization, Data curation, Formal Analysis, Investigation, Methodology, Project administration, Resources, Software, Validation, Visualization, Writing–original draft, Writing–review and editing. ZZ: Conceptualization, Investigation, Methodology, Resources, Validation, Writing–original draft. JB: Formal Analysis, Methodology, Software, Validation, Visualization, Writing–review and editing. XZ: Investigation, Methodology, Validation, Writing–original draft. YT: Investigation, Resources, Validation, Writing–review and editing. XX: Investigation, Resources, Validation, Writing–review and editing. QZ: Funding acquisition, Project administration, Supervision, Validation, Writing–review and editing. YH: Project administration, Supervision, Validation, Writing–review and editing.

Funding

The author(s) declare financial support was received for the research, authorship, and/or publication of this article. This study was supported by Jiangsu University Philosophy and Social Science Research Major Project (2023SJZD143), the Program of Jiangsu Science and Technology Department (BK20211083), and the Program of Suzhou Health Commission (SZXK202111).

Acknowledgments

The authors are grateful to all the young males who participated in this study; to Feng Ye and Ke Ma at Soochow University for their help in organizing this experimental project; to Zhanyu Yu at Jiangsu Normal University and Yan Zheng at Soochow University for their help in rechecking the use of statistical methods in this manuscript.

Conflict of interest

The authors declare that the research was conducted in the absence of any commercial or financial relationships that could be construed as a potential conflict of interest.

Publisher's note

All claims expressed in this article are solely those of the authors and do not necessarily represent those of their affiliated organizations, or those of the publisher, the editors and the reviewers. Any product that may be evaluated in this article, or claim that may be made by its manufacturer, is not guaranteed or endorsed by the publisher.

Supplementary material

The Supplementary Material for this article can be found online at: https://www.frontiersin.org/articles/10.3389/fbioe.2023.1297068/full#supplementary-material

References

Balasekaran, G., Mayo, M., and Ng, Y. C. (2023). Effects of large exercise-induced weight loss on insulin sensitivity and metabolic risk factors in young males with obesity. J. Sports. Med. Phys. *Fit.* 63, 1075–1083. doi:10.23736/S0022-4707.23.14846-8

Barone, I., Giordano, C., Bonofiglio, D., Andò, S., and Catalano, S. (2020). The weight of obesity in breast cancer progression and metastasis: clinical and molecular perspectives. *Semin. Cancer. Biol.* 60, 274–284. doi:10.1016/j.semcancer.2019.09.001

Brauer, S. G., Woollacott, M., and Shumway-Cook, A. (2001). The interacting effects of cognitive demand and recovery of postural stability in balance-impaired elderly persons. *J. Gerontol. A Biol. Sci. Med. Sci.* 56, M489–M496. doi:10.1093/gerona/56.8.m489

Byrd-Bredbenner, C., Quick, V., Koenings, M., Martin-Biggers, J., and Kattelmann, K. K. (2016). Relationships of cognitive load on eating and weight-related behaviors of young adults. *Eat. Behav.* 21, 89–94. doi:10.1016/j.eatbeh.2016.01.002

Cameron, I. D., Kurrle, S., Quine, S., Sambrook, P., March, L., Chan, D., et al. (2011). Increasing adherence with the use of hip protectors for older people living in the community. *Osteoporos. Int.* 22 (2), 617–626. doi:10.1007/s00198-010-1334-y

Cau, N., Cimolin, V., Galli, M., Precilios, H., Tacchini, E., Santovito, C., et al. (2014). Center of pressure displacements during gait initiation in individuals with obesity. *J. Neuroeng. Rehabil.* 11, 82. doi:10.1186/1743-0003-11-82

Cimolin, V., Cau, N., Galli, M., Santovito, C., Grugni, G., and Capodaglio, P. (2017). Gait initiation and termination strategies in patients with Prader-Willi syndrome. *J. Neuroeng. Rehabil.* 14 (1), 44. doi:10.1186/s12984-017-0257-7

Colné, P., Frelut, M. L., Pérès, G., and Thoumie, P. (2008). Postural control in obese adolescents assessed by limits of stability and gait initiation. *Gait Posture* 28 (1), 164–169. doi:10.1016/j.gaitpost.2007.11.006

Crenna, P., Carpinella, I., Rabuffetti, M., Rizzone, M., Lopiano, L., Lanotte, M., et al. (2006). Impact of subthalamic nucleus stimulation on the initiation of gait in Parkinson's disease. *Exp. Brain Res.* 172 (4), 519–532. doi:10.1007/s00221-006-0360-7

Davidson, P. R., and Wolpert, D. M. (2005). Widespread access to predictive models in the motor system: a short review. *J. Neural. Eng.* 2 (3), S313–S319. doi:10.1088/1741-2560/2/3/S11

do Nascimento, J. A., Silva, C. C., Dos Santos, H. H., de Almeida Ferreira, J. J., and de Andrade, P. R. (2017). A preliminary study of static and dynamic balance in sedentary obese young adults: the relationship between BMI, posture and postural balance. *Clin. Obes.* 7 (6), 377–383. doi:10.1111/cob.12209

Duffell, L. D., Southgate, D. F., Gulati, V., and McGregor, A. H. (2014). Balance and gait adaptations in patients with early knee osteoarthritis. *Gait Posture* 39 (4), 1057–1061. doi:10.1016/j.gaitpost.2014.01.005

Esfandiari, E., Sanjari, M. A., Jamshidi, A. A., Kamyab, M., and Yazdi, H. R. (2020). Gait initiation and lateral wedge insole for individuals with early knee osteoarthritis. *Clin. Biomech. (Bristol, Avon)* 80, 105163. doi:10.1016/j.clinbiomech.2020.105163

Fenato, R. R., Araujo, A. C. F., and Guimarães, A. T. B. (2021). Comparison of gluteus medius strength between individuals with obesity and normal-weight individuals: a cross-sectional study. *Bmc. Musculoskelet. Disord.* 22 (1), 584. doi:10.1186/s12891-021-04470-8

Fjeldstad, C., Fjeldstad, A. S., Acree, L. S., Nickel, K. J., and Gardner, A. W. (2008). The influence of obesity on falls and quality of life. *Dyn. Med.* 7, 4. doi:10.1186/1476-5918-7-4

Fraser, S. A., Li, K. Z., Berryman, N., Desjardins-Crépeau, L., Lussier, M., Vadaga, K., et al. (2017). Does combined physical and cognitive training improve dual-task balance and gait outcomes in sedentary older adults? *Front. Hum. Neurosci.* 10, 688. doi:10.3389/fnhum.2016.00688

Gonzalez, N., Nahmias, J., Schubl, S., Swentek, L., Smith, B. R., Nguyen, N. T., et al. (2023). Obese adolescents have higher risk for severe lower extremity fractures after falling. *Pediatr. Surg. Int.* 39 (1), 235. doi:10.1007/s00383-023-05524-9

Hass, C. J., Gregor, R. J., Waddell, D. E., Oliver, A., Smith, D. W., Fleming, R. P., et al. (2004). The influence of Tai Chi training on the center of pressure trajectory during gait initiation in older adults. *Arch. Phys. Med. Rehabil.* 85 (10), 1593–1598. doi:10.1016/j.apmr.2004.01.020

Hergenroeder, A. L., Wert, D. M., Hile, E. S., Studenski, S. A., and Brach, J. S. (2011). Association of body mass index with self-report and performance-based measures of balance and mobility. *Phys. Ther.* 91 (8), 1223–1234. doi:10.2522/ptj.20100214

Hirjaková, Z., Šuttová, K., Kimijanová, J., Bzdúšková, D., and Hlavačka, F. (2018). Postural changes during quiet stance and gait initiation in slightly obese adults. *Physiol. Res.* 67 (6), 985–992. doi:10.33549/physiolres.933870

Horsak, B., Schwab, C., Baca, A., Greber-Platzer, S., Kreissl, A., Nehrer, S., et al. (2019). Effects of a lower extremity exercise program on gait biomechanics and clinical outcomes in children and adolescents with obesity: a randomized controlled trial. *Gait Posture* 70, 122–129. doi:10.1016/j.gaitpost.2019.02.032

Hung, Y. C., Gill, S. V., and Meredith, G. S. (2013). Influence of dual-task constraints on whole-body organization during walking in children who are overweight and obese. *Am. J. Phys. Med. Rehabil.* 92 (6), 461–471. doi:10.1097/PHM.0b013e31828cd59d

Lambert, E. A., Sari, C. I., Eikelis, N., Phillips, S. E., Grima, M., Straznicky, N. E., et al. (2017). Effects of moxonidine and low-calorie diet: cardiometabolic benefits from combination of both therapies. *Obes. (Silver Spring)* 25 (11), 1894–1902. doi:10.1002/oby.21962

Lytle, L. A., Laska, M. N., Linde, J. A., Moe, S. G., Nanney, M. S., Hannan, P. J., et al. (2017). Weight-gain reduction among 2-year college students: the CHOICES RCT. *Am. J. Prev. Med.* 52 (2), 183–191. doi:10.1016/j.amepre.2016.10.012

McGraw, B., McClenaghan, B. A., Williams, H. G., Dickerson, J., and Ward, D. S. (2000). Gait and postural stability in obese and nonobese prepubertal boys. *Arch. Phys. Med. Rehabil.* 81 (4), 484–489. doi:10.1053/mr.2000.3782

Menegoni, F., Galli, M., Tacchini, E., Vismara, L., Cavigioli, M., and Capodaglio, P. (2009). Gender-specific effect of obesity on balance. *Obes. (Silver Spring)* 17 (10), 1951–1956. doi:10.1038/oby.2009.82

Mignardot, J. B., Olivier, I., Promayon, E., and Nougier, V. (2010). Obesity impact on the attentional cost for controlling posture. *PLoS One* 5 (12), e14387. doi:10.1371/journal.pone.0014387

Mille, M. L., Simoneau, M., and Rogers, M. W. (2014). Postural dependence of human locomotion during gait initiation. *J. Neurophysiol.* 112 (12), 3095–3103. doi:10.1152/jn.00436.2014

Moss, S., Zhang, X., Tamplain, P., and Gu, X. (2023). Overweight/obesity and socio-demographic disparities in children's motor and cognitive function. *Front. Psychol.* 14, 1134647. doi:10.3389/fpsyg.2023.1134647

National Health and Family Planning Commission of the People's Republic of China (2013). *WS/T 428-2013 Criteria of weight for adults*. Beijing: Standards Press of China.

Nocera, J. R., Roemmich, R., Elrod, J., Altmann, L. J., and Hass, C. J. (2013). Effects of cognitive task on gait initiation in Parkinson disease: evidence of motor prioritization? *J. Rehabil. Res. Dev.* 50 (5), 699–708. doi:10.1682/jrrd.2012.06.0114

Patelaki, E., Foxe, J. J., McFerren, A. L., and Freedman, E. G. (2023). Maintaining task performance levels under cognitive load while walking requires widespread

reallocation of neural resources. *Neuroscience* 532, 113–132. doi:10.1016/j.neuroscience.2023.09.012

Qu, X., Hu, X., and Tao, D. (2021). Gait initiation differences between overweight and normal weight individuals. *Ergonomics* 64 (8), 995–1001. doi:10.1080/00140139.2021.1896788

Russo, Y., and Vannozzi, G. (2021). Anticipatory postural adjustments in forward and backward single stepping: task variability and effects of footwear. *J. Biomech.* 122, 110442. doi:10.1016/j.jbiomech.2021.110442

Saraiva, M., Vilas-Boas, J. P., Fernandes, O. J., and Castro, M. A. (2023). Effects of motor task difficulty on postural control complexity during dual tasks in young adults: a nonlinear approach. *Sensors (Basel).* 23 (2), 628. doi:10.3390/s23020628

Shahidian, H., Begg, R., and Ackland, D. C. (2022). The influence of cell phone usage on dynamic stability of the body during walking. *J. Appl. Biomech.* 38 (6), 365–372. doi:10.1123/jab.2021-0374

Shaik, A. R., Al Qahtani, M., Ahmad, F., Shaphe, M. A., Alghadir, A. H., Alduhishy, A., et al. (2022). Impacts of adiposity on the attentional cost of sensory-motor performance associated with mobility in a dual-task paradigm. *Int. J. Environ. Res. Public. Health.* 19 (20), 13118. doi:10.3390/ijerph192013118

Simonet, A., Delafontaine, A., Fourcade, P., and Yiou, E. (2022). Postural organization of gait initiation for biomechanical analysis using force platform recordings. *J. Vis. Exp.* doi:10.3791/64088

Small, G. H., Brough, L. G., and Neptune, R. R. (2021). The influence of cognitive load on balance control during steady-state walking. *J. Biomech.* 122, 110466. doi:10.1016/j.jbiomech.2021.110466

Tsai, C. L., Pan, C. Y., Chen, F. C., Huang, T. H., Tsai, M. C., and Chuang, C. Y. (2019). Differences in neurocognitive performance and metabolic and inflammatory indices in male adults with obesity as a function of regular exercise. *Exp. Physiol.* 104 (11), 1650–1660. doi:10.1113/EP087862

Tsiros, M. D., Brinsley, J., Mackintosh, S., and Thewlis, D. (2019). Relationships between adiposity and postural control in girls during balance tasks of varying difficulty. *Obes. Res. Clin. Pract.* 13 (4), 358–364. doi:10.1016/j.orcp.2019.06.003

Uemura, K., Yamada, M., Nagai, K., Shinya, M., and Ichihashi, N. (2012). Effect of dual-tasking on the center of pressure trajectory at gait initiation in elderly fallers and non-fallers. *Aging. Clin. Exp. Res.* 24 (2), 152–156. doi:10.1007/BF03325161

van Mierlo, M., Vlutters, M., van Asseldonk, E. H. F., and van der Kooij, H. (2021). Centre of pressure modulations in double support effectively counteract anteroposterior perturbations during gait. *J. Biomech.* 126, 110637. doi:10.1016/j.jbiomech.2021.110637

Volkow, N. D., Wang, G. J., Telang, F., Fowler, J. S., Goldstein, R. Z., Alia-Klein, N., et al. (2009). Inverse association between BMI and prefrontal metabolic activity in healthy adults. *Obes. (Silver Spring)* 17 (1), 60–65. doi:10.1038/oby.2008.469

Vrieling, A. H., van Keeken, H. G., Schoppen, T., Otten, E., Halbertsma, J. P., Hof, A. L., et al. (2008). Gait initiation in lower limb amputees. *Gait Posture* 27 (3), 423–430. doi:10.1016/j.gaitpost.2007.05.013

Wernberg, C. W., Grønkjær, L. L., Gade Jacobsen, B., Indira Chandran, V., Krag, A., Graversen, J. H., et al. (2023). The prevalence and risk factors for cognitive impairment in obesity and NAFLD. *Hepatol. Commun.* 7 (7), e00203. doi:10.1097/HC9.0000000000000203

Wrightson, J. G., Ross, E. Z., and Smeeton, N. J. (2016). The effect of cognitive-task type and walking speed on dual-task gait in healthy adults. *Mot. Control.* 20, 109–121. doi:10.1123/mc.2014-0060

Wu, X., Lockhart, T. E., and Yeoh, H. T. (2012). Effects of obesity on slip-induced fall risks among young male adults. *J. Biomech.* 45 (6), 1042–1047. doi:10.1016/j.jbiomech.2011.12.021

Wu, X., Nussbaum, M. A., and Madigan, M. L. (2016). Executive function and measures of fall risk among people with obesity. *Percept. Mot. Ski.* 122 (3), 825–839. doi:10.1177/0031512516646158

Xu, Y., Geng, C., Tang, T., Huang, J., and Hou, Y. (2023). How to prevent cognitive overload in the walking-arithmetic dual task among patients with Parkinson's disease. *Bmc. Neurol.* 23 (1), 205. doi:10.1186/s12883-023-03231-5

Yogev-Seligmann, G., Hausdorff, J. M., and Giladi, N. (2008). The role of executive function and attention in gait. *Mov. Disord.* 23 (3), 329–342. doi:10.1002/mds.21720

Yousefi, M., Sadeghi, H., Ilbiegi, S., Ebrahimabadi, Z., Kakavand, M., and Wikstrom, E. A. (2020). Center of pressure excursion and muscle activation during gait initiation in individuals with and without chronic ankle instability. *J. Biomech.* 108, 109904. doi:10.1016/j.jbiomech.2020.109904

frontiers | Frontiers in Bioengineering and Biotechnology

TYPE Original Research
PUBLISHED 07 March 2024
DOI 10.3389/fbioe.2024.1348977

OPEN ACCESS

EDITED BY
Simone Tassani,
Pompeu Fabra University, Spain

REVIEWED BY
Marco Recenti,
Reykjavík University, Iceland
Giorgio Davico,
Alma Mater Studiorum-University of Bologna, Italy

*CORRESPONDENCE
A. Burssens,
arne.burssens@ugent.be

RECEIVED 03 December 2023
ACCEPTED 19 February 2024
PUBLISHED 07 March 2024

CITATION
Peiffer M, Duquesne K, Delanghe M, Van Oevelen A, De Mits S, Audenaert E and Burssens A (2024), Quantifying walking speeds in relation to ankle biomechanics on a real-time interactive gait platform: a musculoskeletal modeling approach in healthy adults. *Front. Bioeng. Biotechnol.* 12:1348977. doi: 10.3389/fbioe.2024.1348977

Quantifying walking speeds in relation to ankle biomechanics on a real-time interactive gait platform: a musculoskeletal modeling approach in healthy adults

M. Peiffer[1,2,3], K. Duquesne[1,2], M. Delanghe[2], A. Van Oevelen[1,2], S. De Mits[4,5], E. Audenaert[1,2,6,7] and A. Burssens[1,2]*

[1]Department of Orthopaedics and Traumatology, Ghent University Hospital, Ghent, Belgium, [2]Department of Human Structure and Repair, Ghent University, Ghent, Belgium, [3]Foot & Ankle Research and Innovation Lab (FARIL), Department of Orthopaedic Surgery, Massachusetts General Hospital, Harvard Medical School, Boston, MA, United States, [4]Department of Rheumatology, Ghent University Hospital, Ghent, Belgium, [5]Smart Space, Ghent University Hospital, Ghent, Belgium, [6]Department of Trauma and Orthopaedics, Addenbrooke's Hospital, Cambridge University Hospitals NHS Foundation Trust, Cambridge, United Kingdom, [7]Department of Electromechanics, Op3Mech Research Group, University of Antwerp, Antwerp, Belgium

Background: Given the inherent variability in walking speeds encountered in day-to-day activities, understanding the corresponding alterations in ankle biomechanics would provide valuable clinical insights. Therefore, the objective of this study was to examine the influence of different walking speeds on biomechanical parameters, utilizing gait analysis and musculoskeletal modelling.

Methods: Twenty healthy volunteers without any lower limb medical history were included in this study. Treadmill-assisted gait-analysis with walking speeds of 0.8 m/s and 1.1 m/s was performed using the Gait Real-time Analysis Interactive Lab (GRAIL®). Collected kinematic data and ground reaction forces were processed via the AnyBody® modeling system to determine ankle kinetics and muscle forces of the lower leg. Data were statistically analyzed using statistical parametric mapping to reveal both spatiotemporal and magnitude significant differences.

Results: Significant differences were found for both magnitude and spatiotemporal curves between 0.8 m/s and 1.1 m/s for the ankle flexion ($p < 0.001$), subtalar force ($p < 0.001$), ankle joint reaction force and muscles forces of the M. gastrocnemius, M. soleus and M. peroneus longus ($\alpha = 0.05$). No significant spatiotemporal differences were found between 0.8 m/s and 1.1 m/s for the M. tibialis anterior and posterior.

Discussion: A significant impact on ankle joint kinematics and kinetics was observed when comparing walking speeds of 0.8 m/s and 1.1 m/s. The findings of this study underscore the influence of walking speed on the biomechanics of the ankle. Such insights may provide a biomechanical rationale for several therapeutic and preventative strategies for ankle conditions.

KEYWORDS

gait-analysis, ankle joint, musculoskeletal modelling, computational biomechanics, walking speed

1 Introduction

It is calculated that a human being undergoes approximately 6,000 steps a day. (Althoff et al., 2017; Paluch et al., 2022; Tison et al., 2022). Therefore, any discrepancy between the joint's load-bearing capacity and the actual load it experiences often precipitates pathological changes within the ankle joint (Peiffer et al., 2023). Given the diversity in individual gait patterns, it is plausible that certain patterns may be associated with specific pathologies, such as ankle osteoarthrosis (Jarchi et al., 2018; Horst et al., 2021).

Gait analysis enables clinicians and researchers to investigate kinematic and kinetic parameters. This crucial biomechanical information can subsequently be used to establish diagnoses, evaluate therapeutic interventions, guide rehabilitation and more (van Dijsseldonk et al., 2018; Peri et al., 2019). However, current literature lacks comprehensive discussion on the influence of walking speed on the kinematics and kinetics of the ankle joint. It is a common approach to compare the gait biomechanics of pathological individuals to those of healthy individuals during gait analysis studies. However, it is essential to consider the influence of walking speed on an individual's gait pattern, as pathological individuals often exhibit slower walking speeds compared to healthy adults. Booij et al. have previously shown that comparing total knee replacement patients with controls depends on the walking speed, and have provided a solution for speed correction using principal component analysis and full waveform analysis by use of statistical parametric mapping (Booij et al., 2021). Failing to account for this crucial factor can impede the validity and interpretability of the comparison (Fukuchi et al., 2019). Moreover, investigating pace in gait-analysis is not trivial. Several studies have previously investigated the influence of pace on ankle biomechanics, observing a higher range of motion, joint and muscle force in the ankle with increasing speed. Clinical protocols typically encompass walking distances ranging from 4 m to 10 m (Fineberg et al., 2013; van Hoeve et al., 2017; Schreiber and Moissenet, 2019; Klöpfer-Krämer et al., 2020; Alexander et al., 2021). However, the measurement of steady-state gait using these short tests presents several challenges in terms of standardization, as walking involves natural fluctuations in gait speed due to acceleration and deceleration. These factors can significantly impact the mean gait speed observed during such measurements. Treadmill-assisted gait analysis facilitates precise control and adjustment of the subject's pace, presenting a potential solution for these inherent limitations. It is imperative to acknowledge that the locomotor patterns observed on the treadmill may exhibit constraints, as ambulation on a treadmill differs from overground walking. (Liu et al., 2016; Krumpoch et al., 2021).

FIGURE 1
Shows the treadmill-assisted gait platform surrounded with screens to create a virtual reality experience to minimize the influence on the usual gait pattern.

The Gait Real-time analysis Interactive Lab (GRAIL, MotekForce Link Amsterdam BV, Netherlands) is a novel self-paced treadmill-assisted gait platform that incorporates a synchronized virtual reality environment on a semicircular screen (Figure 1). The instrument has found application in prior research endeavors; however, such applications have been circumscribed. The GRAIL remains distinctive as a platform uncommonly employed in the majority of medical centers. It takes the form of a treadmill-assisted gait platform encircled by screens, facilitating the creation of a virtual reality environment for the patient. It has been mostly used in previous studies focusing on balance training and motor control in patients with a history of stroke (de Rooij et al., 2021; Van Bladel et al., 2023), neuromuscular (Gagliardi et al., 2018; van Dijsseldonk et al., 2018) and chronic respiratory diseases (Liu et al., 2016). In case of age-related ankle problems, such as ankle arthritis, the GRAIL could stand out as an instrumental tool for in-depth exploration of the ankle's biomechanical changes. Its integration into clinical practice has the potential to revolutionize treatment approaches by facilitating precise examinations and informed decision-making, ultimately improving the overall management of this age-related condition.

Advances in computational dynamics, such as those facilitated by the AnyBody Modeling System (Anybody Technology A/S, Aalborg, Denmark) (Damsgaard, 2006) or OpenSim (Delp et al., 2007; Seth et al., 2018), offer valuable tools for investigating internal forces and moments in the ankle joint, as well as muscle forces. By integrating anatomical data with motion capture information, it utilizes inverse dynamic optimization techniques to simulate the biomechanical behavior of the musculoskeletal system (Damsgaard, 2006; Van Houcke et al., 2020; Peiffer et al., 2022).

Therefore, this study aims to explore the potential impact of walking speed on ankle kinetics and kinematics using treadmill-assisted gait analysis. We will measure these variables at different pace, with the collected data subsequently analyzed via musculoskeletal modelling and simulations, where after statistical parametric mapping will be used to identify potential time-continuous differences (Liu et al., 2016; Motek, 2023). We hypothesize that higher walking speeds will lead to alterations in

TABLE 1 Demographic characteristics of the study population.

Age (yrs), mean (range) +- SD	28,75 +- 11,35 (19–50)
Gender distribution	12 females/8 males
Height (m), mean (range) +- SD	1,73 +- 0,11 (1,56–1,93)
Weight (kg), mean (range) +- SD	66,10 +- 9,75 (50–82)
BMI (kg/m^2), mean	21,44 +- 2,13 (17,51–28,60)

the ankle kinematics, joint reaction, and muscle forces on a real-time interactive gait platform.

2 Materials and methods

2.1 Study population

A total of twenty healthy subjects volunteered to participate in this study. Demographic characteristics of our study population are listed in Table 1. Inclusion criteria consisted of an age between eighteen and 50 years old and being in a healthy and active condition without pre-existing ankle-, knee- or hip pathology or surgery during their lifetime. Exclusion criteria consisted of any medical history that could interfere with gait patterns and a musculoskeletal visual analogue pain rating scale higher than three at the moment of investigation (Karcioglu et al., 2018). The study was conducted in accordance with the Declaration of Helsinki and the Guidelines for Good Clinical Practice. The Institutional Review Board approved this study (IRB B6702021000905). Written consent was obtained from each subject prior to testing. The methodological framework of this study is presented in Figure 2.

2.2 Gait-analysis protocol

A total of 56 retro-reflective markers were stuck on the skin of the lower limbs on palpable landmarks. The marker protocol was based on a previous study by Kim et al. (Kim et al., 2018), which combined the plug-in-gait marker set and Oxford foot marker set along with three additional toe markers as seen in Figure 3 (Kadaba et al., 1989; Stebbins et al., 2006).

Motion capture was performed using the treadmill-assisted GRAIL (MotekForce Link Amsterdam BV, Netherlands). A virtual environment was projected on the 180° semicircular screen, involving a straight, endless path with industrial components on the side as depicted in Figure 1. In Figure 4, a flowchart of the gait-analysis protocol is presented. First, a static calibration record was performed, which comprised the participant standing upright with lower and upper limbs outstretched, palms facing forward, and a straight head. Subsequently, a 6-min familiarization walking trial at 1.1 m/s was performed. Collected gait-analysis consisted of 60 s at 1.1 m/s, followed by 60 s of slow walking at 0.8 m/s. Before each new pace, 1 minute of non-collected gait-analysis was performed for the participant to get used to the new pace (familiarization). Kinematic and Ground Reaction Force (GRF) data were saved and exported as. c3d files. It is demonstrated that healthy adults normally choose to walk at about 1.3 m s^{-1} (Bohannon, 1997). We selected a walking speed of 0.8 m/s, because this could also serve as a baseline reference in a patient cohort, as it demonstrated that patients with age related diseases like ankle osteoarthritis have an average walking speed of 0.8 m s^{-1} (Ingrosso et al., 2008). Additionally, we opted for 1.1 m/s as it is slightly below the mean walking speed, acknowledging that individuals tend to walk more slowly on a treadmill compared to

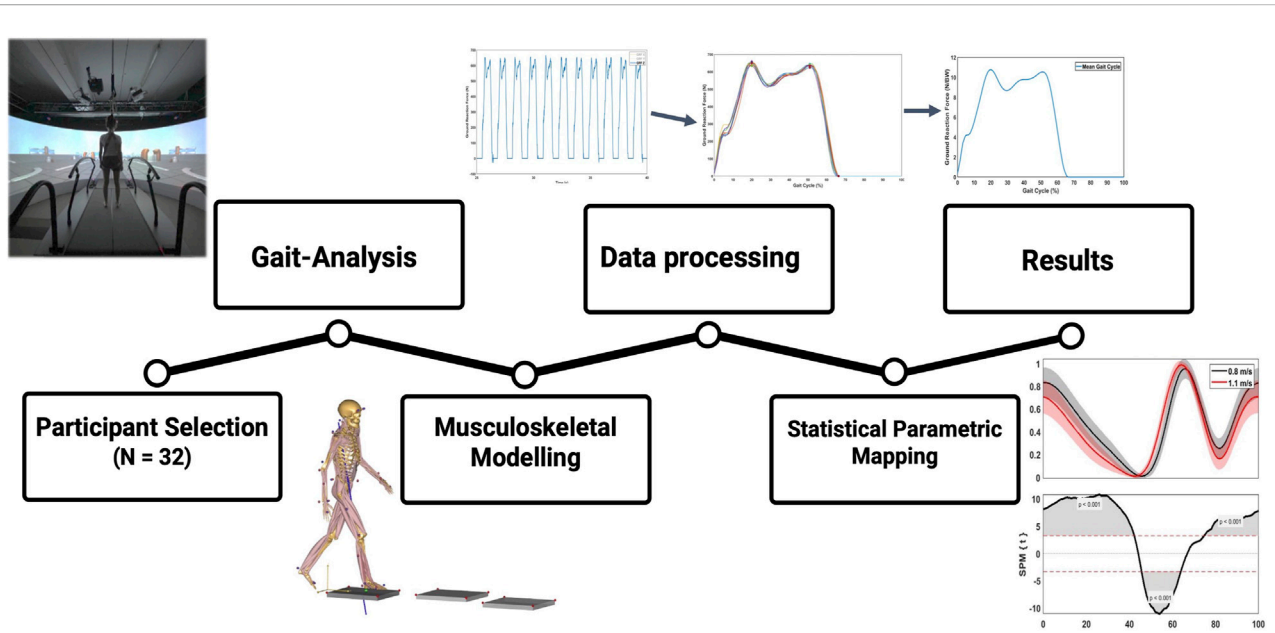

FIGURE 2
Methodology framework of this study. First, marker-based gait-analysis was performed in 20 young, healthy volunteers. Second, kinematics and GRF's were transferred to AnyBody® for musculoskeletal modelling and calculation of kinetic results. Third, raw results were processed in Matlab® to perform time normalization and statistical parametric mapping.

10.3389/fbioe.2024.1348977

FIGURE 3
Marker protocol of the lower limb.

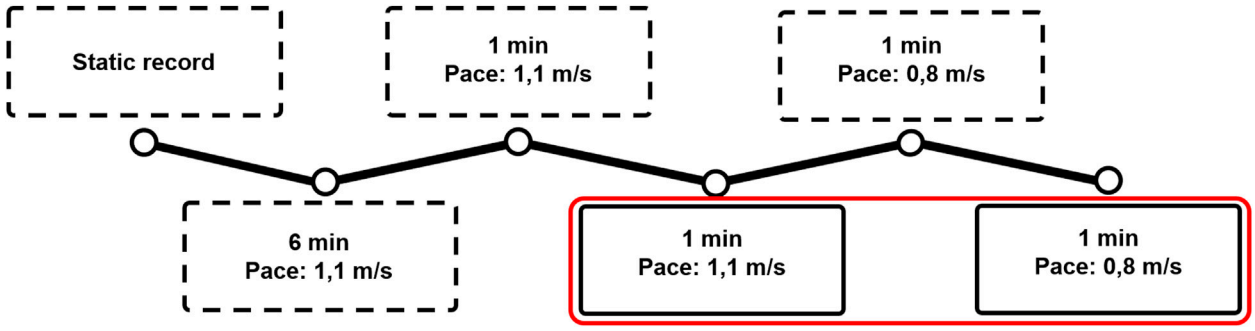

FIGURE 4
The protocol used for the gait analysis: First, a static trial and a 6-min familiarization walking trial at 1.1 m/s were performed. After that, the participant walked 1 min at each speed without analysis to get familiarized to the speed. First, 60 gait cycles at 1.1 m/s were collected, after which 60 cycles at 0.8 m/s were collected. Dotted frames represent non-collected trials, whereas the red frame represent the collected trials.

overground walking and being able to have a faster control speed to compare patients in rehabilitation (being able to increase their walking speed on the treadmill but not yet to the extent of 1.3 m/s) (Song et al., 2020). The choice of outcome measures is based on their established relevance in previous examinations of ankle biomechanics (Riley et al., 2001; Liu et al., 2006; Fukuchi et al., 2019; Alexander et al., 2021).

2.3 Musculoskeletal modelling

Kinematic and GRF data were imported into the Anybody Modelling System (AMS version 7.1.0, Anybody Technology, Aalborg, Denmark). The Twente Lower Extremity Model (TLEM 2.0) which includes a two-segment foot model (modelling the ankle and subtalar joints separately), was scaled to each participant's size using the length-mass-fat law proposed by Rasmussen and others (Rasmussen et al., 2005). The ankle and subtalar joint were modeled as a revolute joint with one rotational degree of freedom to allow flexion/extension and inversion/eversion motion, respectively. Joint kinematics were optimized by minimizing the differences between the experimental markers (captured by the cameras mounted on the GRAIL system) and the corresponding virtual markers on the models. Kinetics were calculated by using an inverse dynamics-based algorithm, implemented in the AnyBody Modelling System. Joint reaction forces (JRF) and joint moments were calculated at the rotation center of the respective joint. Muscle forces were scaled by use of the length-mass-fat scaling law and predicted to balance the

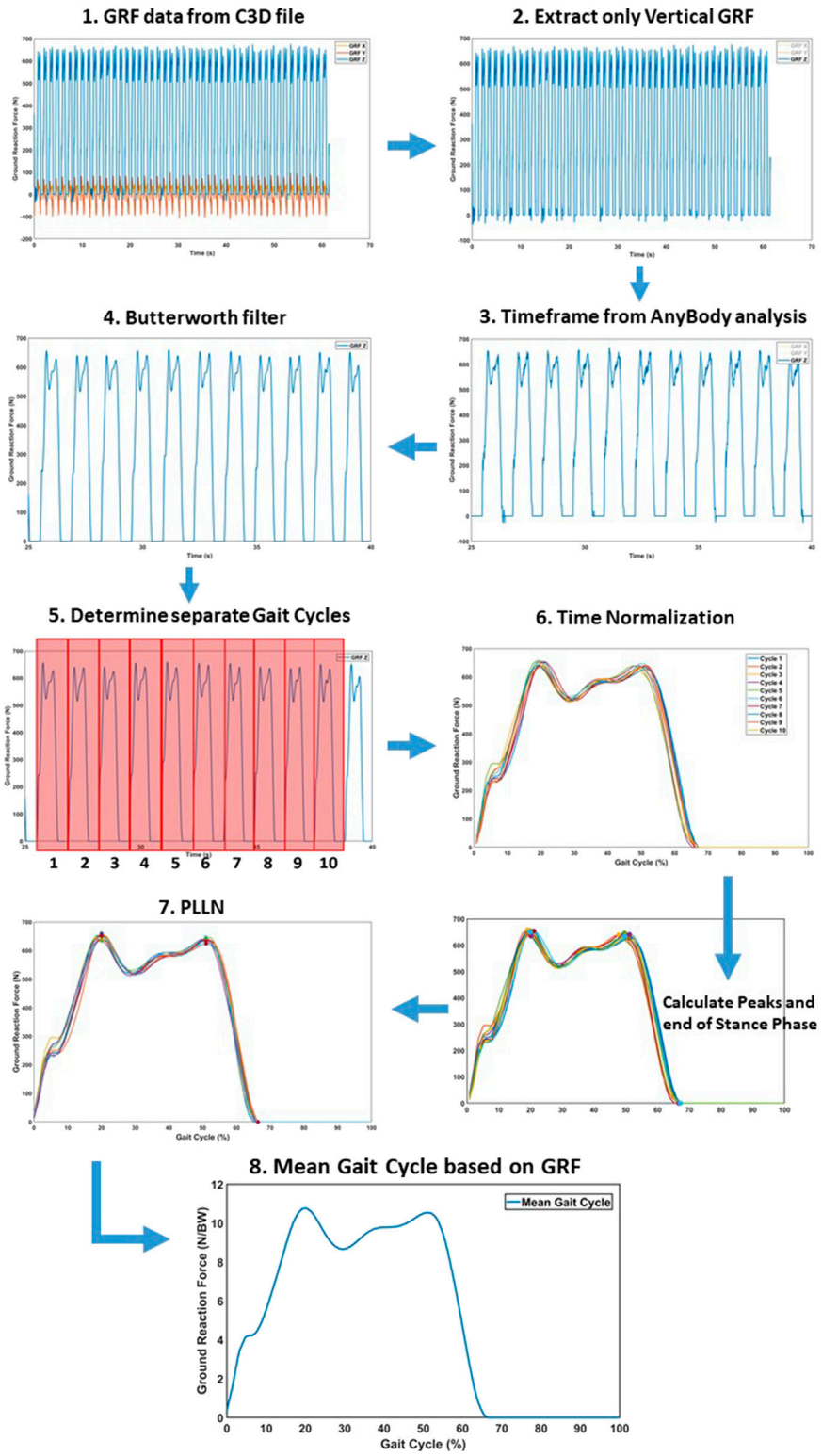

FIGURE 5
Time normalization protocol to convert the raw results into a separate mean gait cycle for statistical analysis. (1) Raw GRF data for the respective time frame. (2) Extracting only vertical GRF for alignment. (3) Matching the subset of the GRF to Anybody timeframe. (4) Butterworth filter to remove data noise. (5) Determine separate gate cycles by identifying the heel strike. (6) The different cycles were preliminary aligned, based on heel strike. (7) Piecewise Linear Length Normalization (PLLN) was performed, based on the end of the stance phase and two consistent GRF peaks. (8) The mean gait cycle, after PLLN.

external forces using the quadratic muscle recruitment criterion, as described more in depth in previous studies (Rasmussen et al., 2002; Damsgaard, 2006).

2.4 Data processing and statistical analysis

2.4.1 Time normalization

Kinematic and kinetic data were transferred to a custom-made Matlab® (Mathworks, Natick, MA, USA) script for further processing. Muscle forces and JRF's were normalized to bodyweight (BW), while moments were normalized by the mass (kg). To remove noise, data were filtered using a sixth lowpass digital Butterworth filter with a normalized cutoff frequency of 12 Hz. Subsequently, a mean single gait cycle was obtained for each pace by averaging all gait cycles in a 25 s timeframe. The separate gait cycles contained within the 25s continuous recordings were separated and subsequently temporally aligned, upon heel strike detection. Next, a Piecewise Linear Length Normalization (PLLN) was performed to further align and normalize the separate gait cycles, similar to the previous study by Helwig et al. (2011). PLLN was automatically performed by computational identification of three consistent landmarks: the two consistent prominent peaks of the GRF curve (i.e., 'maximum weight acceptance' and 'push-off', respectively) and toe-off. After aligning all separate gait cycles, the mean gait cycle was achieved by averaging these separate cycles. All variables were aligned based on the GRF, after which the mean gait cycle curve for each variable was attained. This time normalization protocol is presented in Figure 5.

2.4.2 Statistical parametric mapping

In order to investigate the time-continuous difference between the different paces, rather than a discrete analysis, Statistical Parametric Mapping (SPM) was performed for each variable by use of the Matlab 'spm1d' package (Pataky, 2010). SPM allowed to calculate statistically significant differences at each time point between different curves, taking into account the rest of the curve to calculate a statistically significant cutoff (Honert and Pataky, 2021). SPM has been most commonly used in functional magnetic resonance imaging as neuroimaging, but recent studies have successfully explored SPM also in gait analysis (Nieuwenhuys et al., 2017; Honert and Pataky, 2021; Alhossary et al., 2023). A 2-tailed SPM paired t-test compared the subject-averaged curves for each gait between two walking speeds (0.8 vs. 1.1 m/s). An alignment in time was performed to investigate the differences in magnitude, while a magnitude normalization (based on scaling the most prominent peak of the curves) was created to investigate spatiotemporal variations (Hu et al., 2005; Nieuwenhuys et al., 2017; Honert and Pataky, 2021).

3 Results

3.1 Ankle kinematics

3.1.1 Ankle flexion

A significant spatiotemporal difference of the ankle flexion curve between 0.8 m/s and 1.1 m/s was found for the whole gait cycle ($p < 0.001$), with the ankle plantar flexion occurring sooner at 0%–60% of the gait phase and ankle dorsiflexion occurring later at 75%–100% of the gait phase at 1.1 m/s. For magnitude, a significant difference was found between 0% and 10% representing greater plantarflexion at higher speed and 45%–65% representing greater dorsiflexion at higher speed of the gait cycle (Figure 6). A maximum ankle dorsiflexion of 15.01° was found for 0.8 m/s, in contrast to 13.91° for 1.1 m/s. At a pace of 1.1 m/s, the maximum angle of plantar flexion reached 8.35°, in contrast to 6.69° at 0.8 m/s (Table 2). With increasing velocity, a decrease in dorsiflexion angle was found, while the plantar flexion angle increased.

3.1.2 Subtalar version

Spatiotemporally, a significant difference between 40% and 65% was found for subtalar version; the transition from subtalar eversion to inversion occurred sooner when walking at 1.1 m/s. For magnitude, no difference was found for eversion, while a significant increase of 1.17° inversion was found for walking at 0.8 m/s (Figure 6).

3.2 Ankle kinetics

3.2.1 External joint moments

The ankle joint moment showed a significant difference at 0%–20%, 55%–60%, 63%–73% and 90%–95% of the gait cycle, with the changes in ankle joint moment occurring sooner within the gait cycle at higher speed. There was a significant increase of 0.03 Nm/kg when walking at 1.1 m/s (Figure 7; Table 3).

3.2.2 Muscle forces

When analyzing muscle forces involved in ankle and subtalar motion, changes in the required muscle force were observed. In the beginning of the gait cycle, the patterns were comparable across different walking speeds. However, starting from 45% of the gait cycle, a significant increase in muscle force development was found at 1.1 m/s for all muscle groups. Higher pace resulted in significantly faster attainment of peak force. Specifically, for the plantar flexors, the Musculus (M.) gastrocnemius and M. soleus, an increase of 0.09 and 0.21 times BW was observed at 1.1 m/s compared to 0.8 m/s (Figure 8; Table 4).

3.2.3 Joint reaction forces

Spatiotemporally, a significant difference at 0%–10%, 45%–60% and 95%–100% of the gait cycle was found for the ankle JRF, with the peak JRF occurring sooner within the gait cycle at higher speed. For magnitude, a significant increase of 0.5 times BW was observed when walking at 1.1 m/s, compared to 0.8 m/s. Furthermore, a significant lower ankle JRF was found during 0%–16%, 40%–50% and 95%–100% of the gait cycle (Figure 7).

4 Discussion

The objective of this study was to analyze the kinematics and kinetics of the ankle and subtalar joint in a group of healthy

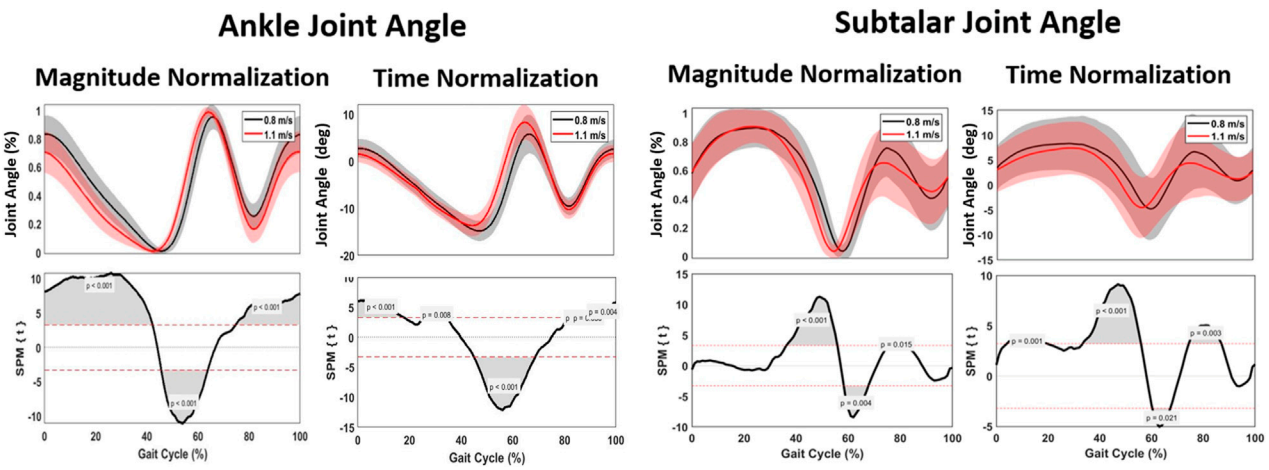

FIGURE 6
Mean gait cycles for ankle kinematics, regarding ankle joint angle and subtalar joint angle, comparing 0.8 m/s against 1.1 m/s pace.

TABLE 2 Kinematic parameters. Statistically noted the maximum parameters for 0.8 m/s and 1.1 m/s and the significant magnitude or timing difference during the gait cycle.

Kinematic parameters	0.8 m/s (SD)	1.1 m/s (SD)	Significant magnitude difference (% of gait cycle, $p < 0.05$)	Significant timing difference (% of gait cycle, $p < 0.05$)
Maximum ankle plantar flexion (°)	6.69 (3.31)	8.58 (3.67)	0–15/85–100	0–40/70–100
Maximum ankle dorsiflexion (°)	15.01 (2.06)	13.91 (2.11)	45–70	45–65
Maximum subtalar inversion (°)	10.18 (6.92)	9.01 (6.75)	5–15/75–85	76–82
Maximum subtalar eversion (°)	5.39 (5.96)	5.07 (5.79)	35–60	37–57/60–65

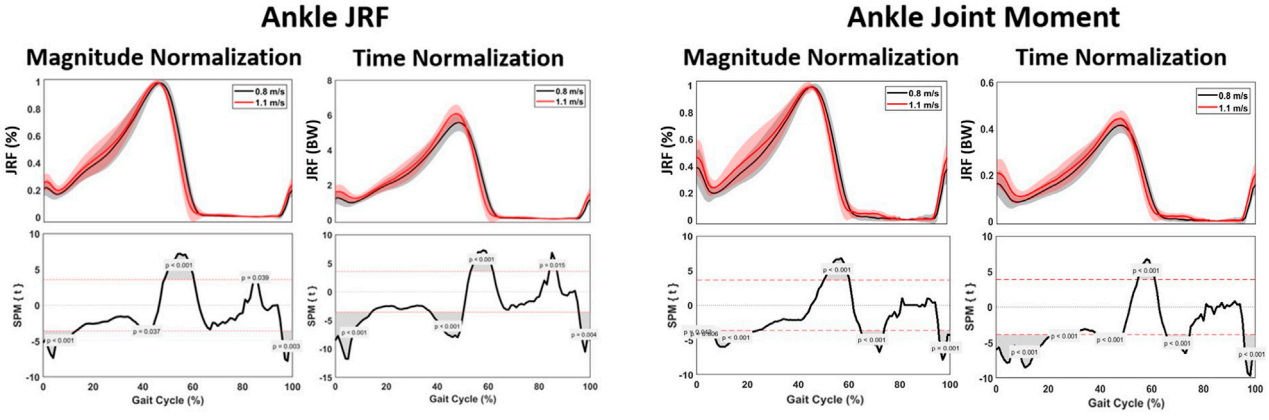

FIGURE 7
Mean gait cycles for muscle forces, including the M. soleus, M. gastrocnemius, M. tibialis posterior, M. tibialis anterior, M. peroneus longus and the M. peroneus brevis, comparing 0.8 m/s against 1.1 m/s pace.

participants. Specifically, treadmill-assisted gait analysis was conducted using the GRAIL system at two different walking speeds of 0.8 m/s and 1.1 m/s. Joint angles, muscle forces, and joint reaction forces were calculated and compared across the different speeds. As hypothesized, the variations in walking speed had a significant impact on these parameters.

TABLE 3 Kinetic parameters. Statistically noted the maximum parameters for 0.8 m/s and 1.1 m/s and the significant magnitude or timing difference during the gait cycle.

Kinetic parameters	0.8 m/s (SD)	1.1 m/s (SD)	Significant magnitude difference (% of gait cycle, $p < 0.05$)	Significant timing difference (% of gait cycle, $p < 0.05$)
Maximum ankle JRF (BW)	5.63 (0.45)	6.13 (0.53)	0–15/37–52/55–62/95–100	0–15/40–43/55–62/83–86/95–100
Maximum ankle JRF Moment (Nm/kg)	0.42 (0.03)	0.45 (0.04)	0–20/40–48/55–62/64–73/90–95	0–20/55–60/63–73/90–95

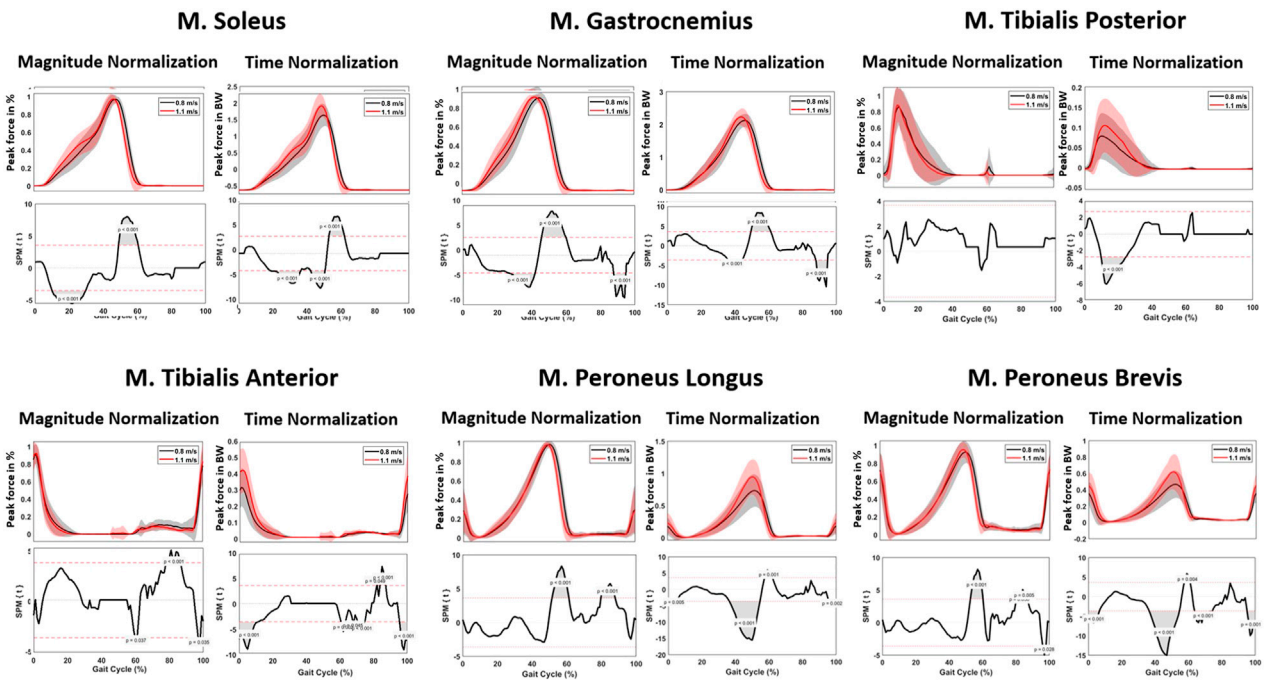

FIGURE 8
Kinetic parameters. Graphs comparing the ankle joint reaction force (left) and ankle joint moment (right) during the gait cycle between 0.8 m/s and 1.1 m/s.

TABLE 4 Muscle parameters. Statistically noted the maximum parameters for 0.8 m/s and 1.1 m/s and the significant magnitude or timing difference during the gait cycle.

Muscle parameters (peak force in BW)	0.8 m/s (SD)	1.1 m/s (SD)	Significant magnitude difference (% of gait cycle, $p < 0.05$)	Significant timing difference (% of gait cycle, $p < 0.05$)
M. gastrocnemius	2.23 (0.20)	2.32 (0.27)	38–42/50–60/85–95	30–40/42–60/85–95
M. soleus	1.74 (0.22)	1.95 (0.21)	20–30/38–47/50–57	10–30/50–62
M. tibialis anterior	0.34 (0.12)	0.46 (0.13)	0–10/55–60/70–80	40–42/58–65/80–81
M. tibialis posterior	0.09 (0.06)	0.12 (0.07)	10–25	/
M. peroneus brevis	0.49 (0.15)	0.64 (0.21)	0–8/40–57/62–71	57–62/80–85
M. peroneus longus	0.75 (0.25)	0.96 (0.28)	40–60	52–62/80–87

When investigating kinematics, an increase in plantarflexion and decrease in dorsiflexion was found when walking at 1.1 m/s compared to 0.8 m/s. Furthermore, a decrease in inversion was seen, while eversion remained constant. Plantarflexion occurred sooner in the gait cycle, corresponding to a faster attainment of terminal stance and pre-swing phase.

The analysis of kinetics revealed several differences, particularly in joint forces. Notably, a higher peak ankle JRF was found during

midstance (i.e., the phase between heel strike and toe-off) at faster walking pace. More specifically, a mean peak force of 5.6 times BW was calculated at 0.8 m/s, compared to 6.1 times BW at 1.1 m/s. While this difference has not been shown in previous literature, the magnitude of these values are in agreement with previous studies (Brockett and Chapman, 2016; Prinold et al., 2016; Kim et al., 2018; Benemerito et al., 2020). These findings are consistent with previous studies by Dubbeldam et al. for the kinematic results and Riley et al. regarding the kinetic results (Riley et al., 2001; Dubbeldam et al., 2010). Alexander et al. have also found higher joint reaction forces for the ankle at 1.3 m/s than at 0.9 m/s, with corresponding values reported (approximately 6 times BW at 0.9 m/s and 6.3 times BW at 1.3 m/s) (Alexander et al., 2021). Additionally, our study showed that the peak joint reaction force occurred sooner in the gait cycle when walking at higher pace, presumably as a result of the peak plantarflexion occurring sooner in the gait cycle.

Regarding muscle forces, an increase in peak force of all muscle groups was found when walking at 1.1 m/s. This increase was most pronounced for the M. soleus (0.21 times BW) and M. peroneus longus (0.21 times BW). A similar trend was found in the literature, exhibiting greater muscle forces in faster walking speeds (Liu et al., 2006). Furthermore, Liu et al. found similar results for the muscles of the upper leg; namely, higher speed resulting in greater muscle forces (Liu et al., 2006). The findings of this study highlight the distinct muscle activation patterns associated with different gait phases. During the support phase, characterized by the initial heel strike, the M. tibialis anterior demonstrated significant activity, signifying its role in foot dorsiflexion. In the midstance phase, the M. tibialis posterior showed predominant activation, indicating its involvement in foot inversion. As the gait transitioned from midstance to propulsion, the M. gastrocnemius exhibited early activation, followed by pronounced engagement during the propulsion phase, jointly with the M. soleus, which played a crucial role in plantar flexion. In the transition from propulsion to the swing phase, the M. peroneus longus displayed notable activity, contributing to toe-off. Toward the end of the swing phase, both the dorsiflexors and eversion muscles demonstrated coordinated activation in preparation for the subsequent heel strike. These findings confirm the results of previous studies in this domain (Riley et al., 2001; Liu et al., 2006; Dubbeldam et al., 2010; Fukuchi et al., 2019).

The principal findings of our study, which revealed greater joint reaction forces and muscle forces acting on the ankle during higher walking pace, hold significant clinical implications that can enhance our understanding of human gait mechanics and have practical applications in clinical practice. For example, in patients with osteochondral lesions of the ankle, limiting the amount of joint reaction force causes less stress on the articular cartilage, and potentially less risk for additional mechanically-induced cartilage breakdown (Peiffer et al., 2023). Furthermore, knowledge of which muscles are most active during the specific gait phases allow clinicians and physiotherapists to target rehabilitation interventions to strengthen and stabilize the specific muscles at the appropriate time points within the gait cycle.

The foot and ankle are susceptible to age-related pathologies, such as ankle osteoarthritis, ankle instability and deformities (Barg et al., 2013; Peiffer et al., 2018; Burssens et al., 2022). These conditions induce alterations in ankle biomechanics, prompting a growing emphasis on exploring foot kinematics and gait analysis. The investigation of an individual's biomechanics, specifically through a comprehensive gait analysis, holds substantial promise for these patients. Recognizing the nuanced variations in gait patterns among affected individuals can offer valuable insights into the progression and manifestation of these conditions (Valderrabano et al., 2007). The GRAIL system emerges as a possible optimal apparatus for the in-depth examination of such physiological dynamics. The utilization of GRAIL in clinical settings presents a promising avenue for advancing our understanding of these age-related diseases. Moreover, the implementation of the GRAIL system in clinical contexts could pave the way for the development of targeted therapeutic interventions. Since it can formulate precise and personalized treatment strategies, it holds the potential to enhance the overall quality of care for individuals grappling with these age-related afflictions.

The strengths of this study lie in the utilization of advanced technology such as the GRAIL system, assisted by treadmill, allowing for a continuous gait examination. Additionally, the AnyBody system was employed to estimate kinetics. The extensive use of markers on the foot and ankle allowed for a detailed examination of foot kinematics. Moreover, PLLN and SPM during statistical analysis made it possible to investigate both timing as magnitude significant differences during the whole gait cycle.

Several limitations of this study should be noted. First, as in all marked-based gait-analysis, errors in marker positioning can introduce errors in the described joint kinematics and subsequent calculation kinetics. By use of a multiple markers on the foot and ankle, this error was expected to be minimal. Furthermore, models were scaled using the length-mass-fat law, which is not as accurate as subject specific modelling (derived from medical imaging). Second, only young healthy participants in the age range of 18–50 years were included, without orthopedic or neurological conditions affecting gait. These do not represent the aging population. While this ensures reference values to be compared with further research in a pathological study group, it may not fully represent the aging population. Third, we have used a two-segment foot model, allowing for motion at the ankle and subtalar joint. Several previous studies have experimented with six-segment or even twenty-six-segment foot models, allowing for analysis of the different joints in the foot (Leardini et al., 1999; Forlani et al., 2015; Montefiori et al., 2022). An additional constraint necessitating consideration pertains to the sample size, which currently comprises only 20 subjects.

5 Conclusion

The findings of this study show that a higher walking pace significantly increases the peak joint reaction force and muscle force of the ankle. Furthermore, kinematic, and kinetic parameters exhibit timing differences between 0.8 m/s and 1.1 m/s walking pace. These results within young, healthy subjects may hold clinical implications for patients with foot and ankle conditions, such as rehabilitation choices to limit the forces exerted on the ankle joint. In research, it is vital to utilize standardized protocols that include predetermined

walking speeds, enabling a reliable comparison of patients with average normative values.

Data availability statement

The data that support the findings of this study are not openly available due to reasons of sensitivity and are available from the corresponding author upon reasonable request.

Ethics statement

The studies involving humans were approved by the studies involving humans were approved by Commissie voor Medische Ethiek Uz Gent IRB B6702021000905. The studies were conducted in accordance with the local legislation and institutional requirements. The participants provided their written informed consent to participate in this study.

Author contributions

MP: Conceptualization, Formal Analysis, Investigation, Methodology, Project administration, Writing–original draft, Writing–review and editing, Data curation, Funding acquisition, Software, Validation, Visualization. KD: Conceptualization, Data curation, Formal Analysis, Funding acquisition, Investigation, Methodology, Software, Validation, Writing–original draft. MD: Conceptualization, Data curation, Investigation, Methodology, Software, Writing–original draft. AVO: Conceptualization, Data curation, Formal Analysis, Investigation, Methodology, Software, Writing–original draft. SDM: Conceptualization, Data curation, Formal Analysis, Investigation, Methodology, Project administration, Software, Supervision, Validation, Writing–original draft. EA: Conceptualization, Data curation, Formal Analysis, Funding acquisition, Investigation, Methodology, Project administration, Resources, Software, Supervision, Writing–original draft. AB: Conceptualization, Formal Analysis, Investigation, Methodology, Project administration, Supervision, Writing–original draft, Writing–review and editing.

Funding

The author(s) declare that financial support was received for the research, authorship, and/or publication of this article. MP was financially supported by a Ph.D. grant (1120220N) from the Research Foundation Flanders (FWO). KD was financially supported by a Ph.D. grant (1137723N) from FWO. AVO was financially supported by a Ph.D. grant (1122821N) from FWO. EA was financially supported by a Senior Clinical Fellowship (1842619N) from FWO.

Conflict of interest

The authors declare that the research was conducted in the absence of any commercial or financial relationships that could be construed as a potential conflict of interest.

Publisher's note

References

Alexander, N., Schwameder, H., Baker, R., and Trinler, U. (2021). Effect of different walking speeds on joint and muscle force estimation using AnyBody and OpenSim. *Gait Posture* 90, 197–203. doi:10.1016/j.gaitpost.2021.08.026

Alhossary, A., Pataky, T., Ang, W. T., Chua, K. S. G., Kwong, W. H., and Donnelly, C. J. (2023). Versatile clinical movement analysis using statistical parametric mapping in MovementRx. *Sci. Rep.* 13 (1), 2414. doi:10.1038/s41598-023-29635-4

Althoff, T., Sosič, R., Hicks, J. L., King, A. C., Delp, S. L., and Leskovec, J. (2017). Large-scale physical activity data reveal worldwide activity inequality. *Nature* 547 (7663), 336–339. doi:10.1038/nature23018

Barg, A., Pagenstert, G. I., Hugle, T., Gloyer, M., Wiewiorski, M., Henninger, H. B., et al. (2013). Ankle osteoarthritis: etiology, diagnostics, and classification. *Foot Ankle Clin.* 18 (3), 411–426. doi:10.1016/j.fcl.2013.06.001

Benemerito, I., Modenese, L., Montefiori, E., Mazzà, C., Viceconti, M., Lacroix, D., et al. (2020). An extended discrete element method for the estimation of contact pressure at the ankle joint during stance phase. *Proc. Inst. Mech. Eng.* 234 (5), 507–516. doi:10.1177/0954411920905434

Bohannon, R. W. (1997). Comfortable and maximum walking speed of adults aged 20-79 years: reference values and determinants. *Age Ageing* 26 (1), 15–19. doi:10.1093/ageing/26.1.15

Booij, M. J., Meinders, E., Sierevelt, I. N., Nolte, P. A., Harlaar, J., and van den Noort, J. C. (2021). Matching walking speed of controls affects identification of gait deviations in patients with a total knee replacement. *Clin. Biomech.* 82, 105278. doi:10.1016/j.clinbiomech.2021.105278

Brockett, C. L., and Chapman, G. J. (2016). Biomechanics of the ankle. *Orthop. Trauma* 30 (3), 232–238. doi:10.1016/j.mporth.2016.04.015

Burssens, A., Krähenbühl, N., Lenz, A. L., Howell, K., Zhang, C., Sripanich, Y., et al. (2022). Interaction of loading and ligament injuries in subtalar joint instability quantified by 3D weightbearing computed tomography. *J. Orthop. Res. Off. Publ. Orthop. Res. Soc.* 40 (4), 933–944. doi:10.1002/jor.25126

Damsgaard, M. (2006). *Analysis of musculoskeletal systems in the AnyBody modeling system*. Amsterdam, Netherlands: Elsevier.

Delp, S. L., Anderson, F. C., Arnold, A. S., Loan, P., Habib, A., John, C. T., et al. (2007). OpenSim: open-source software to create and analyze dynamic simulations of movement. *IEEE Trans. Biomed. Eng.* 54 (11), 1940–1950. doi:10.1109/tbme.2007.901024

de Rooij, I. J. M., van de Port, I. G. L., Punt, M., Abbink-van Moorsel, P. J. M., Kortsmit, M., van Eijk, R. P. A., et al. (2021). Effect of virtual reality gait training on participation in survivors of subacute stroke: a randomized controlled trial. *Phys. Ther.* 101 (5), pzab051. doi:10.1093/ptj/pzab051

Dubbeldam, R., Buurke, J. H., Simons, C., Groothuis-Oudshoorn, C. G., Baan, H., Nene, A. V., et al. (2010). The effects of walking speed on forefoot, hindfoot and ankle joint motion. *Clin. Biomech. Bristol Avon* 25 (8), 796–801. doi:10.1016/j.clinbiomech.2010.06.007

Fineberg, D. B., Asselin, P., Harel, N. Y., Agranova-Breyter, I., Kornfeld, S. D., Bauman, W. A., et al. (2013). Vertical ground reaction force-based analysis of powered exoskeleton-assisted walking in persons with motor-complete paraplegia. *J. Spinal Cord. Med.* 36 (4), 313–321. doi:10.1179/2045772313y.0000000126

Forlani, M., Sancisi, N., and Parenti-Castelli, V. (2015). A three-dimensional ankle kinetostatic model to simulate loaded and unloaded joint motion. *J. Biomech. Eng.* 137, 061005. doi:10.1115/1.4029978

Fukuchi, C. A., Fukuchi, R. K., and Duarte, M. (2019). Effects of walking speed on gait biomechanics in healthy participants: a systematic review and meta-analysis. *Syst. Rev.* 8 (1), 153. doi:10.1186/s13643-019-1063-z

Gagliardi, C., Turconi, A. C., Biffi, E., Maghini, C., Marelli, A., Cesareo, A., et al. (2018). Immersive virtual reality to improve walking abilities in cerebral palsy: a pilot study. *Ann. Biomed. Eng.* 46 (9), 1376–1384. doi:10.1007/s10439-018-2039-1

Helwig, N. E., Hong, S., Hsiao-Wecksler, E. T., and Polk, J. D. (2011). Methods to temporally align gait cycle data. *J. Biomech.* 44 (3), 561–566. doi:10.1016/j.jbiomech.2010.09.015

Honert, E. C., and Pataky, T. C. (2021). Timing of gait events affects whole trajectory analyses: a statistical parametric mapping sensitivity analysis of lower limb biomechanics. *J. Biomech.* 119, 110329. doi:10.1016/j.jbiomech.2021.110329

Horst, F., Slijepcevic, D., Simak, M., and Schöllhorn, W. I. (2021). Gutenberg Gait Database, a ground reaction force database of level overground walking in healthy individuals. *Sci. Data* 8 (1), 232. doi:10.1038/s41597-021-01014-6

Hu, D., Yan, L., Liu, Y., Zhou, Z., Friston, K. J., Tan, C., et al. (2005). Unified SPM-ICA for fMRI analysis. *NeuroImage* 25 (3), 746–755. doi:10.1016/j.neuroimage.2004.12.031

Ingrosso, S., Benedetti, M., Leardini, A., Casanelli, S., and Giannini, S. (2008). Gait analysis of a novel design of ankle replacement. *J. Foot Ankle Res.* 1 (Suppl. 1), P1. doi:10.1186/1757-1146-1-s1-p1

Jarchi, D., Pope, J., Lee, T. K. M., Tamjidi, L., Mirzaei, A., and Sanei, S. (2018). A review on accelerometry-based gait analysis and emerging clinical applications. *IEEE Rev. Biomed. Eng.* 11, 177–194. doi:10.1109/rbme.2018.2807182

Kadaba, M. P., Ramakrishnan, H. K., Wootten, M. E., Gainey, J., Gorton, G., and Cochran, G. V. (1989). Repeatability of kinematic, kinetic, and electromyographic data in normal adult gait. *J. Orthop. Res. Off. Publ. Orthop. Res. Soc.* 7 (6), 849–860. doi:10.1002/jor.1100070611

Karcioglu, O., Topacoglu, H., Dikme, O., and Dikme, O. (2018). A systematic review of the pain scales in adults: which to use? *Am. J. Emerg. Med.* 36 (4), 707–714. doi:10.1016/j.ajem.2018.01.008

Kim, Y., Lee, K. M., and Koo, S. (2018). Joint moments and contact forces in the foot during walking. *J. Biomech.* 74, 79–85. doi:10.1016/j.jbiomech.2018.04.022

Klöpfer-Krämer, I., Brand, A., Wackerle, H., Müßig, J., Kröger, I., and Augat, P. (2020). Gait analysis – available platforms for outcome assessment. *Injury* 51 (Suppl. 2), S90–s96. doi:10.1016/j.injury.2019.11.011

Krumpoch, S., Lindemann, U., Rappl, A., Becker, C., Sieber, C. C., and Freiberger, E. (2021). The effect of different test protocols and walking distances on gait speed in older persons. *Aging Clin. Exp. Res.* 33 (1), 141–146. doi:10.1007/s40520-020-01703-z

Leardini, A., O'Connor, J. J., Catani, F., and Giannini, S. (1999). A geometric model of the human ankle joint. *J. Biomech.* 32 (6), 585–591. doi:10.1016/s0021-9290(99)00022-6

Liu, M. Q., Anderson, F. C., Pandy, M. G., and Delp, S. L. (2006). Muscles that support the body also modulate forward progression during walking. *J. Biomech.* 39 (14), 2623–2630. doi:10.1016/j.jbiomech.2005.08.017

Liu, W. Y., Meijer, K., Delbressine, J. M., Willems, P. J., Franssen, F. M., Wouters, E. F., et al. (2016). Reproducibility and validity of the 6-minute walk test using the gait real-time analysis interactive lab in patients with COPD and healthy elderly. *PloS One* 11 (9), e0162444. doi:10.1371/journal.pone.0162444

Montefiori, E., Fiifi Hayford, C., and Mazzà, C. (2022). Variations of lower-limb joint kinematics associated with the use of different ankle joint models. *J. Biomech.* 136, 111072. doi:10.1016/j.jbiomech.2022.111072

Motek (2023). Grail-The ultimate gate-lab solution. Available from: https://www.motekmedical.com/solution/grail/.

Nieuwenhuys, A., Papageorgiou, E., Desloovere, K., Molenaers, G., and De Laet, T. (2017). Statistical parametric mapping to identify differences between consensus-based joint patterns during gait in children with cerebral palsy. *PloS One* 12 (1), e0169834. doi:10.1371/journal.pone.0169834

Paluch, A. E., Bajpai, S., Bassett, D. R., Carnethon, M. R., Ekelund, U., Evenson, K. R., et al. (2022). Daily steps and all-cause mortality: a meta-analysis of 15 international cohorts. *Lancet Public Health* 7 (3), e219–e228. doi:10.1016/s2468-2667(21)00302-9

Pataky, T. C. (2010). Generalized n-dimensional biomechanical field analysis using statistical parametric mapping. *J. Biomech.* 43 (10), 1976–1982. doi:10.1016/j.jbiomech.2010.03.008

Peiffer, M., Belvedere, C., Clockaerts, S., Leenders, T., Leardini, A., Audenaert, E., et al. (2018). Three-dimensional displacement after a medializing calcaneal osteotomy in relation to the osteotomy angle and hindfoot alignment. *Foot Ankle Surg.* 26, 78–84. doi:10.1016/j.fas.2018.11.015

Peiffer, M., Burssens, A., Duquesne, K., Last, M., De Mits, S., Victor, J., et al. (2022). Personalised statistical modelling of soft tissue structures in the ankle. *Comput. Methods Programs Biomed.* 218, 106701. doi:10.1016/j.cmpb.2022.106701

Peiffer, M., Duquesne, K., Van Oevelen, A., Burssens, A., De Mits, S., Maas, S. A., et al. (2023). Validation of a personalized ligament-constraining discrete element framework for computing ankle joint contact mechanics. *Comput. Methods Programs Biomed.* 231, 107366. doi:10.1016/j.cmpb.2023.107366

Peri, E., Panzeri, D., Beretta, E., Reni, G., Strazzer, S., and Biffi, E. (2019). Motor improvement in adolescents affected by ataxia secondary to acquired brain injury: a pilot study. *Biomed. Res. Int.* 2019, 1–8. doi:10.1155/2019/8967138

Prinold, J. A., Mazzà, C., Di Marco, R., Hannah, I., Malattia, C., Magni-Manzoni, S., et al. (2016). A patient-specific foot model for the estimate of ankle joint forces in patients with juvenile idiopathic arthritis. *Ann. Biomed. Eng.* 44 (1), 247–257. doi:10.1007/s10439-015-1451-z

Rasmussen, J., Damsgaard, M., Christensen, S. T., and Surma, E. (2002). Design optimization with respect to ergonomic properties. *Struct. Multidiscip. Optim.* 24 (2), 89–97. doi:10.1007/s00158-002-0219-x

Rasmussen, J., de Zee, M., Damsgaard, M., Tørholm, S., Marek, C., and Siebertz, K. (2005). *A general method for scaling musculo-skeletal models*. Denmark: Aalborg University.

Riley, P. O., DellaCroce, U., and Kerrigan, D. C. (2001). Effect of age on lower extremity joint moment contributions to gait speed. *Gait Posture* 14 (3), 264–270. doi:10.1016/s0966-6362(01)00133-3

Schreiber, C., and Moissenet, F. (2019). A multimodal dataset of human gait at different walking speeds established on injury-free adult participants. *Sci. Data* 6 (1), 111. doi:10.1038/s41597-019-0124-4

Seth, A., Hicks, J. L., Uchida, T. K., Habib, A., Dembia, C. L., Dunne, J. J., et al. (2018). OpenSim: simulating musculoskeletal dynamics and neuromuscular control to study human and animal movement. *PLoS Comput. Biol.* 14 (7), e1006223. doi:10.1371/journal.pcbi.1006223

Song, S., Choi, H., and Collins, S. H. (2020). Using force data to self-pace an instrumented treadmill and measure self-selected walking speed. *J. NeuroEngineering Rehabil.* 17, 68. doi:10.1186/s12984-020-00683-5

Stebbins, J., Harrington, M., Thompson, N., Zavatsky, A., and Theologis, T. (2006). Repeatability of a model for measuring multi-segment foot kinematics in children. *Gait Posture* 23 (4), 401–410. doi:10.1016/j.gaitpost.2005.03.002

Tison, G. H., Barrios, J., Avram, R., Kuhar, P., Bostjancic, B., Marcus, G. M., et al. (2022). Worldwide physical activity trends since COVID-19 onset. *Lancet Glob. Health* 10 (10), e1381–e1382. doi:10.1016/s2214-109x(22)00361-8

Valderrabano, V., Nigg, B. M., von Tscharner, V., Stefanyshyn, D. J., Goepfert, B., and Hintermann, B. (2007). Gait analysis in ankle osteoarthritis and total ankle replacement. *Clin. Biomech.* 22 (8), 894–904. doi:10.1016/j.clinbiomech.2007.05.003

Van Bladel, A., De Ridder, R., Palmans, T., Van der Looven, R., and Cambier, D. (2023). Comparing spatiotemporal gait parameters between overground walking and self-paced treadmill walking in persons after stroke. *Disabil. Rehabil.* 45 (6), 1016–1021. doi:10.1080/09638288.2022.2046875

van Dijsseldonk, R. B., de Jong, L. A. F., Groen, B. E., Vos-van der Hulst, M., Geurts, A. C. H., and Keijsers, N. L. W. (2018). Gait stability training in a virtual environment improves gait and dynamic balance capacity in incomplete spinal cord injury patients. *Front. Neurol.* 9, 963. doi:10.3389/fneur.2018.00963

van Hoeve, S., Leenstra, B., Willems, P., Poeze, M., and Meijer, K. (2017). The effect of age and speed on foot and ankle kinematics assessed using a 4-segment foot model. *Med. Baltim.* 96 (35), e7907. doi:10.1097/md.0000000000007907

Van Houcke, J., Galibarov, P. E., Van Acker, G., Fauconnier, S., Allaert, E., Van Hoof, T., et al. (2020). Personalized hip joint kinetics during deep squatting in young, athletic adults. *Comput. Methods Biomech. Biomed. Engin* 23 (1), 23–32. doi:10.1080/10255842.2019.1699539

frontiers | Frontiers in Bioengineering and Biotechnology

TYPE Original Research
PUBLISHED 02 April 2024
DOI 10.3389/fbioe.2024.1347939

OPEN ACCESS

EDITED BY
Andrea Malandrino,
Universitat Politecnica de Catalunya, Spain

REVIEWED BY
Paolo De Blasiis,
University of Campania Luigi Vanvitelli, Italy
Franco Simini,
Universidad de la República, Uruguay

*CORRESPONDENCE
Simone Tassani,
simone.tassani@upf.edu

RECEIVED 01 December 2023
ACCEPTED 14 March 2024
PUBLISHED 02 April 2024

CITATION
Tassani S, Chaves P, Beardsley M, Vujovic M, Ramírez J, Mendoza J, Portero-Tresserra M, González-Ballester MA and Hernández-Leo D (2024), Breathing, postural stability, and psychological health: a study to explore triangular links.
Front. Bioeng. Biotechnol. 12:1347939.
doi: 10.3389/fbioe.2024.1347939

Breathing, postural stability, and psychological health: a study to explore triangular links

Simone Tassani[1]*, Paula Chaves[1], Marc Beardsley[1], Milica Vujovic[2], Juan Ramírez[3], Jimena Mendoza[1,4], Marta Portero-Tresserra[5], Miguel Angel González-Ballester[1,6] and Davinia Hernández-Leo[1]

[1]Department of Information and Communication Technologies Universitat Pompeu Fabra, Barcelona, Spain, [2]Technische Universität Wien, Vienna, Austria, [3]Universidad Nacional de Colombia, Medellín, Colombia, [4]Universidad Iberoamericana, Mexico City, Mexico, [5]Universitat Autònoma de Barcelona, Barcelona, Spain, [6]Catalan Institution for Research and Advanced Studies (ICREA), Barcelona, Spain

Objective: This study aims to test the hypothesis that breathing can be directly linked to postural stability and psychological health. A protocol enabling the simultaneous analysis of breathing, posture, and emotional levels in university students is presented. This aims to verify the possibility of defining a triangular link and to test the adequacy of various measurement techniques.

Participants and Procedure: Twenty-three subjects (9 females and 14 males), aged between 18 and 23 years, were recruited. The experiment consisted of four conditions, each lasting 3 minutes: Standard quiet standing with open eyes 1), with closed eyes 2), and relaxed quiet standing while attempting deep abdominal breathing with open eyes 3) and with closed eyes 4). These latter two acquisitions were performed after subjects were instructed to maintain a relaxed state.

Main Outcome Measures: All subjects underwent postural and stability analysis in a motion capture laboratory. The presented protocol enabled the extraction of 4 sets of variables: Stabilometric data, based on the displacement of the center of pressure and acceleration, derived respectively from force plate and wearable sensors. Postural variables: angles of each joint of the body were measured using a stereophotogrammetric system, implementing the Helen Hayes protocol. Breathing compartment: optoelectronic plethysmography allowed the measurement of the percentage of use of each chest compartment. Emotional state was evaluated using both psychometric data and physiological signals. A multivariate analysis was proposed.

Results: A holistic protocol was presented and tested. Emotional levels were found to be related to posture and the varied use of breathing compartments. Abdominal breathing proved to be a challenging task for most subjects, especially females, who were unable to control their breathing patterns. In males, the abdominal breathing pattern was associated with increased stability and reduced anxiety.

Conclusion: In conclusion, difficulties in performing deep abdominal breathing were associated with elevated anxiety scores and decreased stability. This depicts a circular self-sustaining relationship that may reduce the quality of life, undermine learning, and contribute to muscular co-contraction and the

development of musculoskeletal disorders. The presented protocol can be utilized to quantitatively and holistically assess the healthy and/or pathological condition of subjects.

KEYWORDS

breathing, posture, stability, psychological health, emotion, Wellbeing

1 Introduction

Modern society is suffering from contemporary pathologies that healthcare institutions can only partially address. Conditions and diseases traditionally linked to aging, including back pain, neck pain, and even arthrosis, are now emerging earlier in life, even during youth and adolescence (Prins et al., 2008). The rising incidence of musculoskeletal pain among younger populations is alarming, not only due to its early onset but also because of the potential to evolve into chronic musculoskeletal pain syndromes that persist into adulthood (Brattberg, 2004; Prins et al., 2008). Emerging evidence from the literature underscores the causal role of emotional distress, already related to the development of mental disorders, in the development of musculoskeletal disorders (Brattberg, 2004; Diepenmaat et al., 2006; McFarlane, 2007). Throughout our lives, we inevitably encounter various stressful situations, some of which can be avoided or mitigated, while others are an inherent part of life. Nevertheless, learning to regulate our emotional response becomes crucial for our adaptation in the environment, health, and wellbeing. Particularly, young individuals, including students, often confront stressors without the appropriate self-regulation skills (Prins et al., 2008; Sawatzky et al., 2012). Moreover, they are prone to adopting sub-optimal musculoskeletal strategies, such as maintaining poor sitting postures (Yang et al., 2020). These psychological and physical aspects, in turn, can impact their learning process and performance (Swiecki et al., 2019). Therefore, there is a need for methods that empower students to enhance their stress management skills, mitigating the potential long-term effects on both their musculoskeletal health and learning outcomes.

However, the direct correction of postural or psychological problems presents challenges. From a physical standpoint, learning correct posture is problematic due to the numerous degrees of freedom that need to be controlled, making it difficult to self-learn good posture (Sheikhhoseini et al., 2018). Technology-based solutions aimed at identifying and helping to correct poor postures have been developed (Wong and Wong, 2008; Byeon et al., 2020). However, the widespread availability of these approaches to all students remains an important challenge. On the psychological side, problems can arise even in earlier phases, with students often avoiding asking for help (Abdollahi et al., 2017). Moreover, students with mental health problems report lower engagement in campus activities (Byrd and McKinney, 2012), and few students experiencing stress-related mental health problems receive treatment (Garlow et al., 2008).

Breathing techniques offer an accessible approach to address both postural and psychological challenges (Gilbert, 2003; Busch et al., 2012) acting as a mediator between the two spheres. Unlike most physiological functions, breathing can be modulated voluntarily and serves as an entry point for both physiological and psychological regulation. Accordingly, clinical trials implementing disciplines specifically focused on breathing, like Tai Chi, Qi Gong, and Yoga, are exponentially increasing (Tassani et al., 2019). Repetitive motor tasks and long-lasting training can cause beneficial or disadvantageous postural adaptation with long-term effects on the Postural Control System

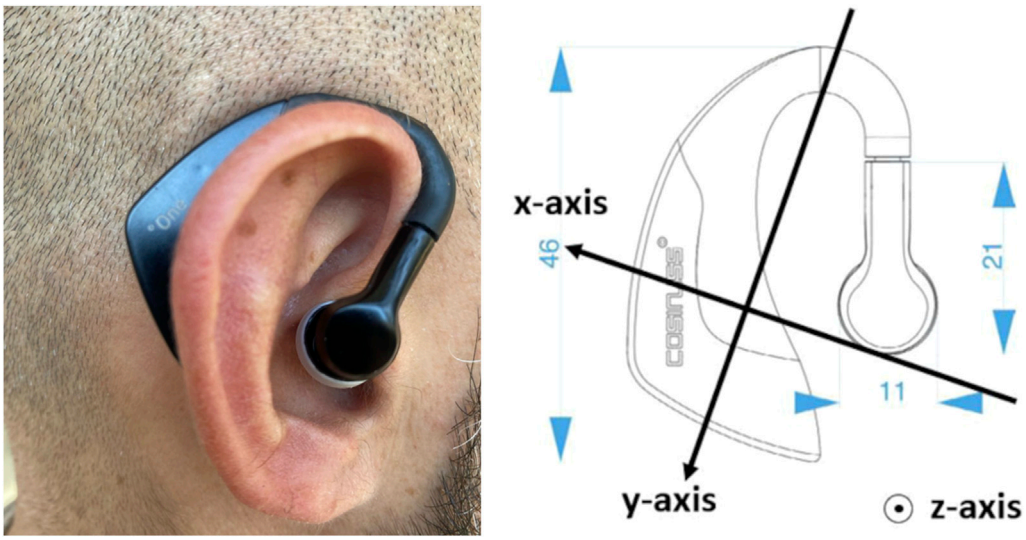

FIGURE 1
In-ear sensor "Cosinuss One." On the right are displayed the acceleration directions of the sensor.

TABLE 1 Complete list of variables analyzed for the stability analysis. Underlined items denote variables not used in the final analysis, after feature reduction.

Stability parameters
Time-domain: Center of Pressure (COP) stabilogram
Transversal COP displacement [mm] (mean and sd)
Longitudinal COP displacement [mm] (mean and sd)
Radius [mm] (mean and sd): COP distance from the barycenter
Maximum and minimum radius [mm]
Transversal and Longitudinal range [mm]
LFS1 [cm]: Length as a function of surface
Equivalent area [mm^2]: Area marked out by the COP
Equivalent radius [mm]: Radius of the circle with an area equal to the Equivalent Area
Speed [mm] (mean and sd): COP displacement velocity
Inertial axes [mm] X: X-axis of the 95% confidence ellipse area
Inertial axes [mm] Y: *Y*-axis of the 95% confidence ellipse area
Regression angle [°]: Inclination of the *X*-axis of inertia with respect to the *x*-axis of the reference system
Variable mean area [mm^2]
Variable sum area [mm^2]
Time-domain: Sway density curve
Peak number: number of peaks of the sway density curve
Peak amplitudes [s] (mean and sd): amplitude of the peaks of the sway density curve
Peak times [s] (mean and sd): time between peaks of the sway density curve
Peak distance [mm] (mean and sd): distance between peaks of the sway density curve
Frequency-domain
Px spectrum maximum peak: Max peak of the COP frequency spectrum in the *x* direction
Px spectrum MaxPeak frequency [Hz]: Frequency of the max peak of the spectrum in the x direction
Py spectrum maximum peak: Max peak of the COP frequency spectrum in the *y* direction
Py spectrum MaxPeak frequency [Hz]: Frequency of the max peak of the spectrum in the *y* direction
D spectrum maximum peak: Max peak of the spectrum of the distance from the barycenter
D spectrum Max Peak frequency Hz: Frequency of the max peak of the spectrum of the distance from the barycentre
Px spectrum mean values: Mean amplitude of the spectrum in the x direction
Px spectrum mean values Freq: Mean frequency of the spectrum in the *x* direction
Py spectrum mean values: Mean amplitude of the spectrum in the y direction
Py spectrum mean values Freq: Mean frequency of the spectrum in the *y* direction
D spectrum mean values: Mean amplitude of the spectrum of the distance from the barycenter
D spectrum mean values Freq: Mean frequency of the spectrum of the distance from the barycenter

(De Blasiis et al., 2022). The main advantages of these breathing practices are that they can be easily taught, are non-pharmacologic, self-administered, come at no cost, and can be performed at anytime and anywhere.

Scientific literature also suggests a clear relation between breathing and posture. Breathing and postural control are mechanically and neuromuscularly interdependent as the main muscles used during respiration (diaphragm and intercostal muscles) also contribute to postural control (Hodges and Gandevia, 2000). Poor posture (as an inclined position) impedes the proper function of the diaphragm resulting in increased activity of the upper respiratory duct (Kim et al., 2017). The effect of breathing on psychological stress is also increasingly studied (Perciavalle et al., 2017; Hopper et al., 2019) and specific

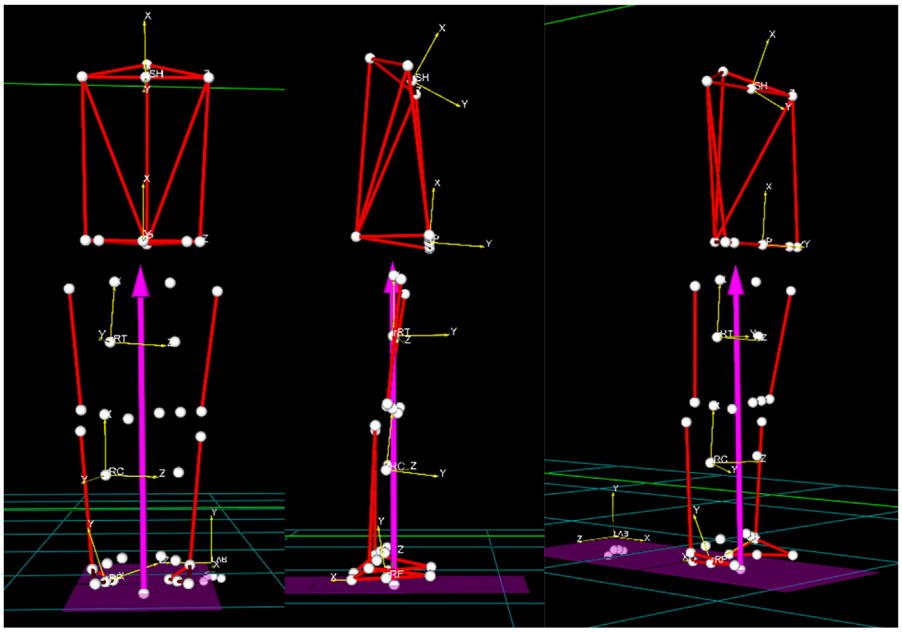

FIGURE 2
References systems of each body segment.

breathing patterns have been found to lower physiological arousal associated with emotional distress and measures of state anxiety (Balban et al., 2023).

These findings suggest a tight link between psychological health, breathing, and posture through self-regulation. However, the actual triangular relation between posture, breathing, and stress is still unclear. Understanding this relationship could shed more light on the efficiency of breathing therapies for both aiding young adults in controlling their mental distress and predicting/preventing the development of several musculoskeletal disorders for the population of any age. In this regard, instrumentation methods for the quantitative evaluation of posture, breathing, and stress could be useful to objectively demonstrate this triangular link. In particular, the gold standard for three-dimensional analysis of posture is 3D stereophotogrammetry, an optoelectronic system that allows for the evaluation of the whole-body in standing (Chiari et al., 2002; Rocchi et al., 2004) and while walking (Cappozzo et al., 2005) by using infrared cameras and reflective skin markers placed on specific landmarks. Moreover, 3D stereophotogrammetry is also used for optoelectronic plethysmography to assess thoracic and abdominal movements during breathing (Massaroni et al., 2017). For the analysis of body oscillations, force plate, and stabilometry are used to analyze postural stability parameters in open (De Blasiis et al., 2023) and closed eyes (Fullin et al., 2022), considering their reliability and variability too. Eventually, levels of psychological stress can be evaluated by wearable sensors. Examples include an "in-ear sensor" (Ellebrecht et al., 2022) which measures body temperature and heart rate as well as stabilometric parameters, and a "galvanic skin response (GRS) device" (Ellebrecht et al., 2022), which measures the conductivity of human skin through the activity of sweat glands stimulated by the sympathetic nervous system (SNS).

Currently, there seems to be an absence of studies considering the three effects at the same time. Therefore, the present study aims to test the relationship between breathing, postural stability, and psychological health under the hypothesis that deep abdominal breathing can reduce stress and increase stability in university students. For this reason, a protocol allowing simultaneous analysis of breathing, posture, and emotional levels is presented, to verify the possibility of defining a triangular link and to test the adequacy of different measurement techniques.

2 Materials and methods

2.1 Recruitment

Twenty-three subjects were recruited for this study, 9 females and 14 males, with ages ranging between 18 and 23 years old, 174 ± 9 cm height, 67.2 ± 9.5 kg weight, and 22.1 ± 2.3 kg/m^2 of BMI. Twenty-one subjects were within the normal BMI range (18.5–24.9) while two subjects were slightly overweight. No obese or underweight subjects were involved in the study. The inclusion criteria for the study were that the subjects were university students in the first to the third year of their undergraduate studies. Excluded from the study were frequent smokers (those who smoke more than 3 times a week), those with prior musculoskeletal disorders, those with reported cases of anxiety, and those who reported expert knowledge of breathing techniques. All subjects gave informed written consent before participating in the study.

2.2 Data collection

For all subjects, three sets of data collection were performed: breathing, postural/stability, and emotional.

TABLE 2 List of postural angles obtained and their acronyms. Underline items denote variables not used in the final analysis, after feature reduction.

Body posture parameters and their acronyms			
Postural angles		Acronyms	
		Right	Left
Spine	Lateral Bending	SPML	
	Rotation	SPIE	
	Flex-Extension	SPFE	
Trunk	Rotation	SHROT	
	Obliquity	SHOBLI	
	Tilt	SHTILT	
Pelvis	Tilt	PTILT	
	Rotation	PROT	
	Obliquity	POBLI	
Hip	Rotation	RHPIE	LHPIE
	Flex-Extension	RHPFE	LHPFE
	Ab-Adduction	RHPAA	LHPAA
Knee	Rotation	RKIE	LKIE
	Flex-Extension	RKFE	LKFE
	Valgus-Varo	RKAA	LKAA
Ankle	Rotation	RFIE	LFIE
	Dorsi-Plantar Flex	RAFE	LAFE
	Prone-supine	RFAA	LFAA
Foot	Foot Progression	RAIE	LAIE

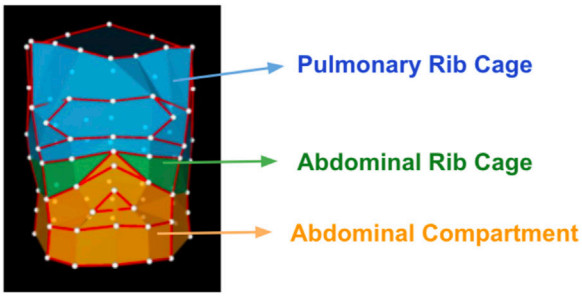

FIGURE 3
Compartmental 89-marker model of the chest wall in Optoelectronic Plethysmography.

2.2.1 Breathing and posture

Breathing and body postural/stability recordings were performed at the Motion Capture Laboratory using optoelectronic technology. Eight infrared cameras were used (BTS Smart-DX 700, 1.5Mpixels 250 fps). Four were placed on tripods close to the subject, with two in front of the subject and the other two behind. The remaining four cameras were fixed to the corners of the ceiling of the room. Two video cameras (BTS VIXTA 50HZ) were placed to record the frontal and the left side of subjects during all data acquisition as a reference for reflective marker positioning over subjects. Further, a force plate (BTS P-6000 50 Hz sampling) was used to acquire stability data. Synchronized data acquisition was guaranteed using the software SMART Capture, developed by BTS Bioengineering.

During posture and breathing analysis, a total of 105 reflective markers were attached to the subjects' skin of as two different marker protocols were combined. Firstly, breathing data was acquired using a validated protocol implemented by BTS in the software Smart Analyzer that was used for the data analysis (Aliverti and Pedotti, 2003; De Faria Júnior et al., 2013). The protocol consists of eighty-nine reflective markers placed over the chest of subjects and requires subjects to be bare chest. A minor modification to the protocol allowed women to wear any kind of upper undergarment during this study. Secondly, posture was measured using the Helen Hayes protocol with medial markers (Davis et al., 1991). This protocol makes use of 22 reflective markers. However, the placement of some markers coincides in the two protocols. Specifically, markers placed in the shoulders, C7 vertebrae, sacrum, and left and right anterior superior iliac spine were reused. Therefore, only sixteen additional markers were placed on the legs.

Stability estimations were performed by measuring the displacement of the center of pressure (COP) over the force plate. Subjects wore a single 3D commercial accelerometer in-ear sensor, called Cosinuss° One, Cosinuss GmbH, Munich, Germany (Burgos et al., 2020). The three axes of the in-ear sensor are

TABLE 3 Distribution of abdominal and pulmonary breathing of male and female subjects and their percentage over the total number of acquisitions.

Sex	Abdominal		Pulmonary		Total
Male	20	41%	29	59%	49
Female	8	25%	24	75%	32
Total	28	35%	53	65%	81

TABLE 4 *p*-values of the MANOVA analysis of Stability and Posture variables.

Factors	Stability		Posture
	Spatio-temporal	Frequency	
State	0.596	0.489	0.042
Eyes	0.342	0.293	0.506
Breathing	0.027	0.030	0.322
State * Eyes	0.528	0.640	0.978
State * Breathing	0.819	0.451	0.662
Eyes * Breathing	0.984	0.615	0.901
State * Eyes * Breathing	0.430	0.820	0.970

TABLE 5 Confusion matrix of breathing classification based on stability and posture variables. States of abdominal and pulmonary breathing were classified starting from, respectively, stability information based on the analysis of the COP displacement, and postural data obtained using stereophotogrammetric tools.

			Predicted stability			Predicted posture		
			Breathing		Percentage correct	Breathing		Percentage correct
			Abdominal	Pulmonary		Abdominal	Pulmonary	
Observed	Breathing	Abdominal	14	6	70.0	17	3	85
		Pulmonary	5	21	80.8	4	21	84
	Overall Percentage				76.1			84.4

identified in Figure 1. The three-axial accelerometric data were also used as estimators of subject stability.

2.2.2 Emotional data

Emotional data were collected following two different approaches. Firstly, psychometric data were used to acquire baseline information and collect subjects' feelings. Secondly, physiological signals were collected throughout to measure biometrics related to subjects' emotional responses.

2.2.2.1 Psychometric data

During recruitment, applicants to the study were asked to complete an online survey administered in the format of a Google form. The survey included the State-Trait Anxiety Inventory (STAI—link), Rosenberg Self-Esteem Scale (RSE), and Five Facet Mindfulness Questionnaire. Subjects were also asked some general questions about their knowledge of breathing techniques and questions related to the exclusion criteria.

2.2.2.2 Physiological signals

The same in-ear device used for measuring postural stability (Cosinuss° One, Cosinuss GmbH, Munich, Germany) also allowed for the measurement of body temperature and heart rate which were used as estimators of anxiety. Finally, galvanic skin response (GSR) was measured with a device (Shimmer3, Shimmer Sensing, Dublin, Ireland) placed on the arm with connected electrodes positioned close to the palm on the internal side of the wrist.

2.3 Procedure

The experiment consisted of four conditions with each recording having a duration of 3 minutes. 1) Standard quiet standing with open eyes and 2) standard quiet standing with closed eyes were the two first recordings. For these conditions, subjects were asked to stand on the force plate in a normal stance that they felt comfortable with and to avoid sudden movements. After the standard condition, subjects were given instructions on performing deep abdominal breathing. They were instructed to breathe in slowly and deeply into the abdomen and to breathe out in a relaxed manner. Subjects performed from six to ten deep breaths with the lab technician while using proprioceptive input in which subjects placed one hand on their chest and the other on their abdomen. Subjects were asked to practice this breathing technique for a few minutes and to perform some exercises to relax their joints (circular motions, flex-extension, ab-adduction, and rotation of each joint: neck, shoulders, hips, knees, and ankles) while maintaining their deep breathing as described in the literature (Tassani et al., 2019). At the end of the relaxation phase, 3) a recording with open eyes and then 4) with closed eyes was taken in which subjects were asked to be in a relaxed state while trying to perform deep breathing. This is what was referred to as the relaxed state.

2.4 Data processing

2.4.1 Stability data

Displacement of the center of pressure (COP) was analyzed using the software Sway (BTS Engineering, Milan, Italy). Analysis time was normalized to 180 s and all parameters described in the table below were computed (Table 1).

2.4.2 Body posture

Body posture analysis was performed using references identified by the Helen Hayes protocol as shown in Figure 2. As a general description, in the reference system of each body segment, X is the longitudinal axis of the segment and points up, Y is the sagittal axis of the segment and points forward, and Z is the transversal axis of the body and points to the left of the subject. The only exception to this definition is the reference system of the foot in which X points backward and therefore Y points up.

These definitions are general for all joints in the body. All measures are relative of the distal segment to the proximal one. In the case of the pelvis and trunk, Rotation refers to when there is rotation around the *X*-axis. Obliquity refers to when the rotation is around the *Y*-axis. Tilt refers to when the rotation is around the *Z*-axis. However, for these two segments, measures are defined with respect to the posture reference system (*X*-axis—vertical direction in the laboratory, *Z*-axis—axis passing through the two markers in the heels, *Y*-axis—vectorial product of X and Z). The complete list of body posture angles and their acronyms is presented in Table 2.

2.4.3 Breathing

The volumetric geometrical model of the chest wall was run through an OptoElectronic Plethysmography (OEP) protocol for quiet breathing, implemented by BTS Engineering. The protocol computes the chest's tidal volume and the three thoracic compartments (Pulmonary Rib Cage, Abdominal Rib Cage, and Abdominal) (Figure 3).

TABLE 6 Significant multiple linear regressions. The list of stability and postural predictors is reported along with the B coefficients and the adjusted R^2 of each of the regressions. Each set of predictors was related to the used percentage of the three chest compartments: Pulmonary, Abdominal rib cage and Abdomen. Regressions are shown separately for female and male subjects. For a complete description of the variables and their acronyms, refers to Tables 1, 2.

		Pulmonary			Abdominal rib cage			Abdomen		
		Predictors	B	Adj R^2	Predictors	B	Adj R^2	Predictors	B	Adj R^2
Female	Stability	-	-	-	(Constant)	22.968		-	-	-
					Peak amplitude (s) (m)	−1.551	0.355			
					Trasversal COP displacement(mm)(m)	0.088				
	Posture	(Constant)	60.944		(Constant)	18.924		(Constant)	14.086	
		RHPIE	−1.000	0.64	RKIE	0.509	0.865	RHPIE	1.546	0.772
		RAIE	0.701		RFAA	0.598		RAIE	−1.152	
		LKAA	1.117		SHTILT	0.160		LKAA	−2.108	
					SHROT	0.129				
	Emotion	-	-	-	-	-	-	-	-	-
Male	Stability	(Constant)	37.137	0.074	(Constant)	−37.645	0.528	(Constant)	131.157	0.337
		D spectrum, mean values Freq	18.819		Peak number	0.222		Peak number	−0.336	
					Peak amplitude (s) (m)	0.691		Peak amplitude (s) (m)	−1.011	
					Inertial axises(mm)(asseY)	0.398		Trasversal COP displacement (mm)(sd)	−0.845	
					Peak time (s) (sd)	26.986		Peak time (s) (sd)	−48.202	
	Posture	(Constant)	40.950	0.172	(Constant)	32.941	0.834	(Constant)	34.062	0.248
		RPROT	−0.438		LAFE	0.847		RHPAA	1.135	
					RAIE	−0.088				
					RKIE	0.294				
					SPFE	0.177				
					RFAA	−0.217				
					SPIE	−0.440				
					LHPAA	−0.913				
					RAFE	0.283				
					POBLI	−0.674				
	Emotion	-	-	-	(Constant)	12.157	0.506	(Constant)	56.219	0.468
					Score STAI	0.253		Score STAI	−0.466	

2.5 Data analysis

Data analysis was performed in consecutive steps that were repeated for each typology of data acquired to test possible relations between abdominal breathing, posture, and emotions. Analyses were performed using SPSS (version 23.0; IBM Corp., Armonk, NY, United States).

Firstly, stability data were normalized by the height of subjects as suggested in the literature (Chiari et al., 2002). Normalization was not applied to postural parameters, which are angles and not affected by subject height, nor to emotional data. Breathing data were not normalized either since the analysis focussed on the percentages of use of each thoracic compartment.

The use of each breathing compartment was computed as a percentage of the sum of the three. The breathing technique of each subject was defined as pulmonary if the pulmonary compartment covered a percentage of breathing volume greater than that of the abdominal compartment. Similarly, it was defined as abdominal if the abdominal compartment covered a percentage of breathing volume greater than the pulmonary compartment. The abdominal rib cage compartment was never found to be the compartment with a highest percentage.

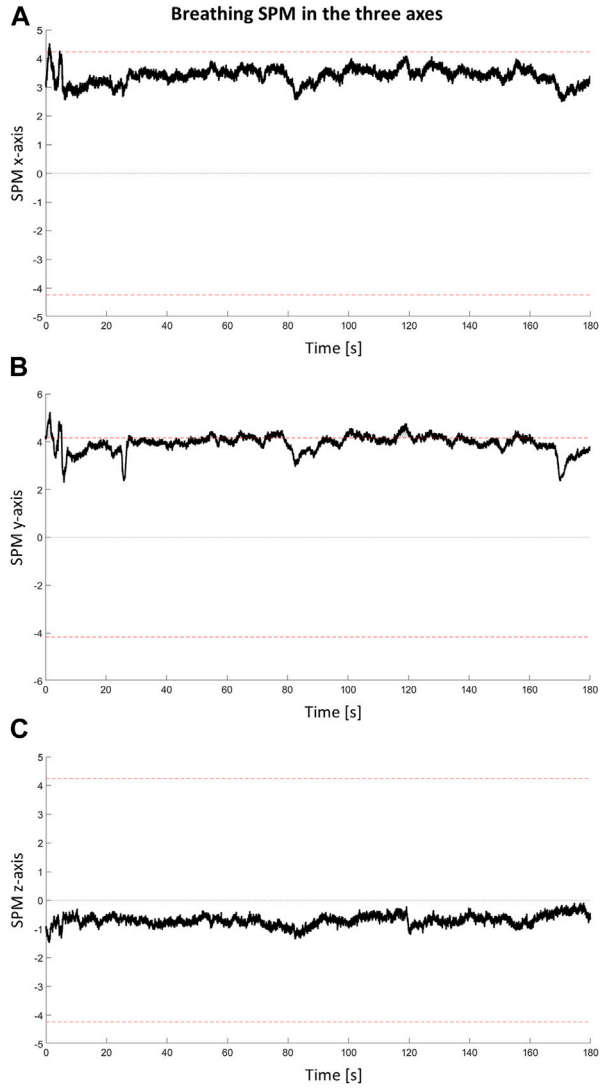

FIGURE 4
Statistical Parametric Mapping (SPM) of acceleration data. **(A)** X, **(B)** Y and **(C)** Z SPM accelerations are shown. Red dotted line identifies the significant level. When the SPM cross the red line a significant cluster is identified.

Secondly, a correlation analysis was performed to reduce the number of variables in the analysis. Every pair of variables presenting an absolute value of the Pearson correlation coefficient superior to 0.9 was identified as highly correlated and therefore, one of the two variables was excluded from the analysis.

2.5.1 Multivariate analysis of variance

The experiment was originally designed to perform repeated measurement tests among the four combinations of the *within factors*, **state** (standard and relaxed) and **eyes** (open and closed) and compare it with the *between factor* **sex** (male and female) (Tassani et al., 2019). However, a preliminary multivariate analysis of variance (MANOVA) for repeated measures showed no effect of the *within factors* over the breathing percentages of the pulmonary rib cage, abdominal rib cage, and abdominal compartment (p-value >0.40) nor their interactions (p-value >0.29). For this reason, in the presented analysis, results of the within variables were pooled, and the capability of each subject to breathe or not abdominally was analyzed as an independent factor, **breathing**.

On the other hand, the between-factor sex was significant, with females showing a higher percentage of pulmonary volume (Estimated marginal means: female 50.24 ± 2.1, male 41.18 ± 1.9), with only 8 abdominal acquisitions over 35.

Therefore, a MANOVA was performed to analyze the relationship between 3 factors and the three sets of dependent variables: stability, posture, and emotional data. The four factors under study were the state of the eyes (**eyes**: open or closed) posture stance (**stance**: standard or relaxed) and **breathing** (abdominal or pulmonary). Sex (male, female) where analyzed separately.

2.5.2 Classification

Binary logistic regression was applied to explore the possibility of classification of the breathing style of each subject starting from stability and postural data. Forward conditional feature selection was used.

2.5.3 Multiple linear regression

Both MANOVA and classification analysis assumed that it was possible to divide the breathing style into abdominal and pulmonary. Multiple linear regression analysis was performed to evaluate the possible continuous relationship between breathing, postural, stability, and emotional data.

2.5.4 Continuous time evaluation: statistical parametric mapping

Skin conductivity, temperature, heart rate, and acceleration of the head in three dimensions, were time-variant and therefore a time-continuous approach was proposed for their analysis. Statistical Parametric Mapping (SPM) refers to hypotheses testing of a spatially extended statistical procedure. SPM implements random field theory (Brett et al., 2003) and allows for the statistical identification of significant differences within time-variant variables.

Two-sample (independent) t-tests, performed using the MATLAB implementation “spm1d” (Pataky, 2012), were applied to examine the effects of breathing over each of the mentioned continual data.

3 Results

Abdominal breathing proved to be a difficult task for most subjects involved in the study. No significant difference in the use of breathing compartments was identified during the different phases of analysis (p-value = 0.404), showing an inability of subjects to breathe abdominally when instructed. Over a total of 81 valid breathing acquisitions, only 28 showed a dominant abdominal component (34%). Further, female subjects had greater difficulty breathing abdominally when instructed than male subjects as only 8 abdominal-dominant acquisitions (25%) were recorded from female subjects (Table 3).

Due to this disparity, male and female subject data were separated for subsequent analyses. Moreover, given the low number of female

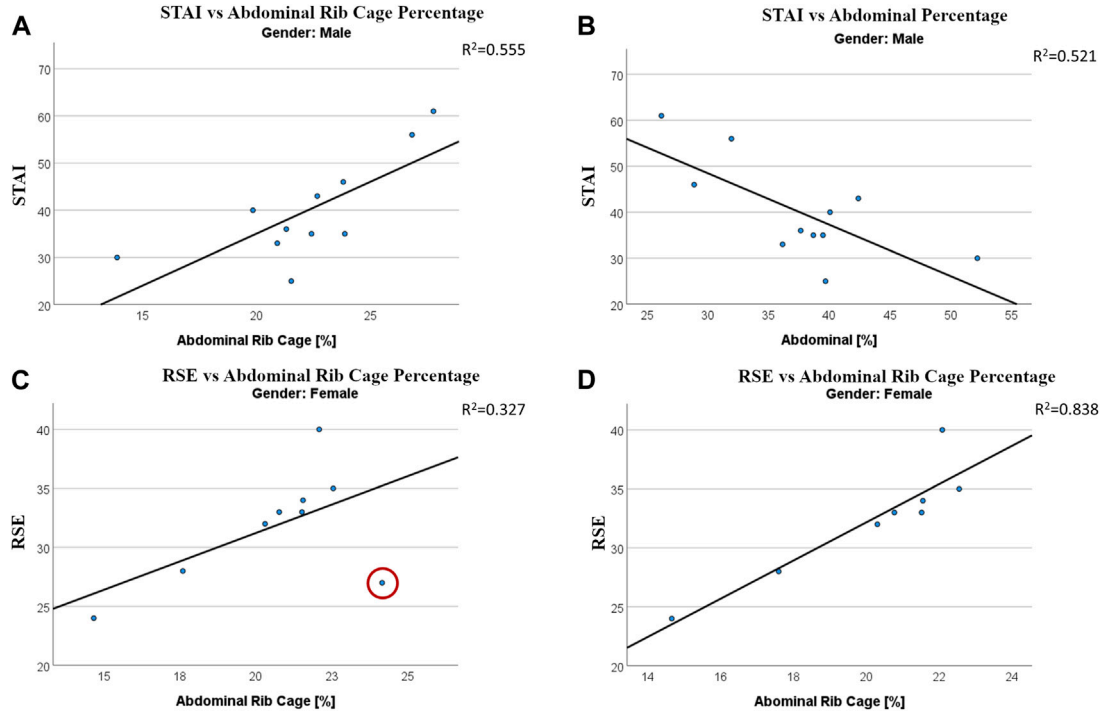

FIGURE 5
Regressions between emotional states and use of breathing compartments. Regression between State-Trait Anxiety Inventory (STAI) score and Abdominal Rib Cage **(A)** and Abdominal Compartment **(B)** in males. Regression between the Rosemberg Self-Esteem score and Abdominal Rib Cage in female, with **(C)** and without **(D)** the inclusion of a strong outlier.

TABLE 7 Significant multiple linear regressions. The list of stability and postural predictors is reported along with the B coefficients and the adjusted R^2 of each of the regressions. Each set of predictors was related to the three emotional scores: the State-Trait Anxiety Inventory (STAI), Rosenberg Self-Esteem Scale (RSE), and Five Facet Mindfulness Questionnaire (5Facet). Regressions are shown separately for female and male subjects. For a complete description of the variables and their acronyms, refers to Tables 1, 2.

		STAI			RSE			5Facet		
		Predictors	B	Adj R^2	Predictors	B	Adj R^2	Predictors	B	Adj R^2
Female	Stability	-	-	-	-	-	-	-	-	-
	Posture	(Constant)	−1.372	0.723	(Constant)	57.062	0.978	-	-	-
		SHTILT	1.247		SHTILT	−0.486				
					RAIE	1.242				
					RHPIE	−0.370				
Male	Stability	(Constant)	163.207	0.727	-	-	-	(Constant)	43.272	0.448
		Regression angle:()	0.188					D spectrum, maximum peak	0.006	
		Peak time (s) (sd)	−234.857							
		D spectrum, maximum peak	0.005							
	Posture	(Constant)	31.246	0.840	(Constant)	26.545	0.832	(Constant)	41.078	0.353
		RHPIE	−0.385		RKFE	1.599		SHOBLI	−3.872	
		LAIE	−1.018		LAFE	−1.484				
		RHPAA	−1.317		RKAA	−0.721				

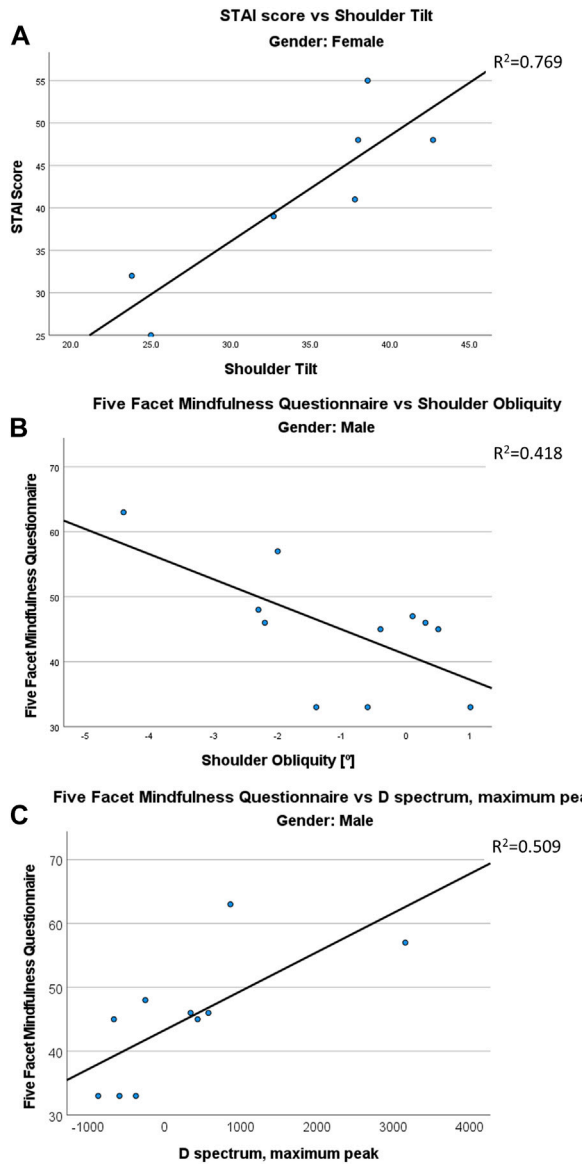

FIGURE 6
Regressions between emotional states and stability/postural parameters. Regression between State-Trait Anxiety Inventory (STAI) score with Shoulder Tilt in females **(A)**. Regression between the Five Facet score and the shoulder obliquity **(B)** and with Max peak of the spectrum of the distance from the barycenter **(C)** in males.

subjects able to perform abdominal breathing, MANOVA and classification analysis were only performed on data from males, while regression analysis was performed on both sets of data.

Twenty subjects filled out the survey collecting emotional data. Results showed the general emotional situation of subjects was critical. Seven subjects showed high anxiety (STAI>44—Ercan et al., 2015) of which, four also showed low levels of self-esteem (RSE<25—Isomaa et al., 2013). STAI and RSE were found to be negatively correlated (R^2 = 0.47, p-value<0.001). MANOVA and classification study were not performed with this data due to the small sample size once male and female data were separated and given the unbalanced distribution of breathing capabilities in females.

Finally, 3 MANOVA analyses were performed: for stability, divided between spatio-temporal and frequency parameters, and posture variables. To maintain the family-wise error at 5%, p-values were considered significant at a level of 0.017.

3.1 Breathing and stability

From the initial 37 stability parameters, 9 were found to be highly correlated with at least one other parameter—therefore, they were removed from the analysis. The remaining parameters in the analysis are shown in Table 1. Eighty-one acquisitions were finally valid for this analysis (46 for males and 35 for females).

MANOVA did not identify any factor or interaction related to stability for spatio-temporal or frequency parameters (Table 4). However, binary logistic regression was able to properly classify 76% of male acquisitions as belonging to abdominal or pulmonary breathing groups using only three stability variables: Standard deviation of the Transversal COP displacement, Peak number, and Peak Amplitude. Subjects showing abdominal breathing presented a reduced value of the three parameters therefore suggesting higher stability. All of them are related to the time-domain. The confusion matrix is shown in Table 5.

Multiple regression analysis showed a significant relation between the use of abdominal rib cage and stability parameters in women (adjR^2 = 0.36). For males, each chest compartment showed a relation with different stability parameters. In particular an opposite trend was identified between abdominal rib cage (adjR^2 = 0.528) and abdominal percentages (adjR^2 = 0.337). In males, an increased percentage of the abdomen was related to increased stability. Detailed results are shown in Table 6.

SPM of in-ear acceleration data showed statistical differences between subjects breathing abdominally or pulmonary in axes X and Y (Figure 4). Acquisitions identified as related to abdominal breathing showed reduced acceleration compared to those related to pulmonary breathing.

3.2 Breathing and posture

From the initial list of 29 postural parameters, 3 were found to be highly correlated with at least one other parameter—therefore, they were removed from the analysis leaving 26 parameters in the analysis (Table 2). In particular, both right and left hip flex-extension were found to be highly correlated (r > 0.9) to pelvis tilt, and spine flex-extension correlated to shoulder tilt. Seventy-three acquisitions were finally valid for this analysis (45 for males and 28 for females).

MANOVA did not identify any factor or interaction related to posture (Table 4). However, binary logistic regression was able to properly classify 84% of male acquisitions as belonging to abdominal or pulmonary breathing groups using only four postural variables: RKIE, POBLI, RHPAA, SHTILT. The confusion matrix is shown in Table 5.

Multiple regression analysis showed the relation between the use of any chest compartment and the posture of both male and female subjects. The compartment showing less relation to the posture was the pulmonary one (adjR^2 = 0.64 for females and 0.172 for males), while the abdominal rib cage compartment showed high adj R^2 for

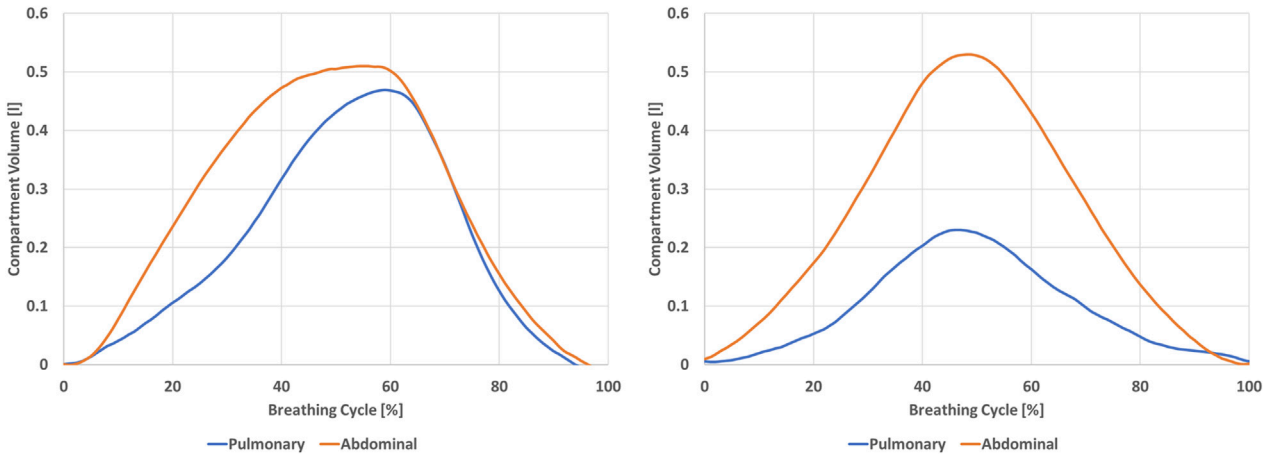

FIGURE 7
Two different breathing patterns are presented. On the left, Abdominal and Pulmonary patterns are similar with a small prevalence of abdominal breathing. On the right, the abdominal compartment is dominant over the whole breathing cycle. Both patterns were classified as Abdominal.

both male (adjR^2 = 0.834) and female (adjR^2 = 0.865) subjects. However, the two multiple regressions differ between sexes. In female subjects, a strong relation between the use of abdominal compartment and posture was also reported (adjR^2 = 0.772). Detailed results are shown in Table 6.

3.3 Breathing and emotion

The first part of the emotional evaluation was carried out using surveys, therefore it was not possible to relate these results to all four combinations of state and eyes used to acquire breathing patterns. Hence, the analysis was carried out by relating the emotional evaluation to breathing results from the condition of "standard open eyes." This forced a reduction in sample size to 20 acquisitions, only one for each subject (11 males and 9 females). Female subjects did not report any significant multiple regression with breathing compartments while males reported significant regressions with both Abdominal rib cage and Abdominal percentage (Table 6). STAI score was found to be positively related to the use of the abdominal rib cage and negatively related to the use of the abdominal compartment (Figure 5).

SPM of both the in-ear sensor and the GSR identified no statistical difference related to the use of different breathing compartments.

3.4 Stability and emotion

As for the connection to breathing, the linear relation between stability and emotional scores was studied only for the results related to the state of "standard—open eyes." Twenty acquisitions (11 males and 9 females) were available for this analysis. Women did not show any significant relation between stability predictors and any of the emotional scores used in this study. On the other side, males presented stability relations to both STAI score (adjR^2 = 0.727) and 5 Facet score (adjR^2 = 0.353). Results are summarized in Table 7. The mono-dimensional regression between D spectrum and 5 Facet score in males is presented in Figure 6.

3.5 Posture and emotion

As for the connection to breathing, the linear relation between posture and emotional scores was studied only for the results related to the state of "standard—open eyes." Eighteen acquisitions (11 males and 7 females) were available for this analysis.

Women showed significant correlations between postural parameters and both STAI (adjR^2 = 0.723) and RSE (adjR^2 = 0.978) scores while men showed significant correlations between postural parameters and all emotional ones (Table 7).

4 Discussions

The proposed protocol allowed for the simultaneous analysis of breathing, postural stability, and emotional indicators. Although the high number of reflective markers used for the analysis required a lengthy preparation time (around 30 min), the protocol allowed us to test the relations between breathing, postural stability, and psychological health, observing significant results and initiating the development of a relational map among the main sets of variables in the study.

Subjects showed general difficulties in performing abdominal breathing. The majority were not able to change their breathing pattern when requested, confirming previously reported findings (Tassani et al., 2019). A few minutes of training before acquisitions were not sufficient for subjects to learn to perform abdominal breathing intentionally. This result is consistent with the literature. Studies assessing the effects of abdominal breathing on a pathology found that deep breathing training phases vary from

3 weeks to 56 months in asthma (Santino et al., 2020). It is, therefore, reasonable to consider that subjects unable to perform deep breathing could not learn to do so during a brief session of a few minutes.

In this study, some subjects were constantly breathing abdominally or pulmonary and kept the same pattern for all four acquisitions. They only changed the total volume inhaled. In other cases, subjects were breathing abdominally at first but changed to pulmonary when asked to perform deep abdominal breathing. Subjects did not seem capable of controlling their breathing pattern intentionally. Only one subject was able to start deep abdominal breathing when requested. Furthermore, it must be considered that the threshold defined for the definition of abdominal breathing was arbitrary. In this study to define a breathing pattern as abdominal, the abdominal compartment must be used more than the pulmonary one. When a more conservative threshold for deep breathing classification is applied, in which the abdominal compartment is used for 60% of the abdominal and pulmonary volumes together, the number of acquisitions classified as abdominal would drop to only 5 (data in the Supplementary Material). This forced the use of a less strict threshold to classify rather different patterns as abdominal (Figure 7).

Given the importance that literature attributes to the ability to control breathing patterns for both physical (Hodges and Gandevia, 2000; Gilbert, 2003; Hodges et al., 2007) and emotional (Perciavalle et al., 2017; Hopper et al., 2019; Balban et al., 2023) management, this study presents a worrying scenario for young university students. Worries were confirmed by the number of subjects presenting high levels of anxiety in this study. The situation might be even more critical for female subjects who showed less capability of abdominal breathing (Table 3) and presented more cases of high anxiety (4 females and 3 males).

The reasons for this disparity between male and female subjects are not clear. The effect of sex on chest wall kinematics in literature is controversial. In agreement with our results, some authors have reported a relatively lower abdominal contribution to tidal volume and smaller abdominal dimensional changes in females compared to males during quiet breathing (Fugl Meyer, 1974; Gilbert et al., 1981; Romei et al., 2010). Others did not find any sex-related differences in thoraco-abdominal motion during quiet breathing in different postures (Sharp et al., 1975; Verschakelen and Demedts, 1995). However, the authors would like to stress the importance of not restricting the study of causes of this difference to biological ones. Sociological causes such as differences in gender beauty canons can lead to different perceptions of abdominal breathing and should also be explored.

Differences in behavior between sexes are another result of this study. In fact, while breathing was found to be related to both physical and emotional variables, these relations were found to be different between the two sexes. The analysis of individual indicators and their meaning was not the aim of this study; however, specific patterns can be identified and are for future research to be confirmed.

Postural characteristics were shown to be strongly related to breathing for both sexes (Table 6). The linear regression analysis showed a strong linear relation of abdominal rib cage and abdomen percentages to postural parameters. In males, postural parameters correctly classified 84% of acquisitions as abdominal or pulmonary (Table 5). This is an interesting result since posture parameters also showed the highest link to emotional scores, especially STAI and RSE, for both males and females (Table 7). These findings reinforce results obtained in the relation between breathing and emotional states and suggest the role of breathing as a mediator.

The results of the stability analysis presented weaker relations, especially in females. In males, MANOVA showed no significant results, however, the breathing factor was close to significance for both spatio-temporal (p = 0.027) and frequency (p = 0.03) parameters. In the regression analysis, both abdominal rib cage and abdomen percentages were related to stability parameters. Three out of four predictors selected by the stepwise procedure were the same, but the coefficients were inverted. This result suggests that, while an increase in the use of the abdominal rib cage compartment was related to the decrease in stability, the increased use of the abdominal compartment increased stability. SPM results of accelerometer data were found to be in the same direction. In several moments along the 3-min acquisition, subjects classified as using abdominal breathing showed a reduced acceleration of the head, suggesting higher stability (Figure 4). This supports the idea that a relaxed posture, decreasing co-contraction, can increase subject stability (Tassani et al., 2019). In males, stability was also found to be related to emotional states, whereas an increase in STAI score was related to a decrease in stability.

The main limitation of this study is in its aim of presenting a holistic protocol for the study of a breathing-physical-emotional relation. The physical sphere was analyzed in the form of stability and posture, and the emotional sphere in terms of anxiety and self-esteem, and for both measurement and analysis protocols had to be defined. For this reason, statistical analyses were presented as parts within a whole protocol. Results must be considered with caution and confirmed by future studies involving a bigger sample size. This limitation becomes clearer in the relation between breathing and emotional scores in females. In Figure 5 we can see how a single bivariate outlier can change the relation between RSE score and Abdominal Rib Cage percentage from not significant to R^2 = 0.838. Nonetheless, this study allows us to underline difficulties and criticisms that, based on this research and presented literature, might be common to many young university students.

In conclusion, this study shows how difficulties in performing deep abdominal breathing can be related to elevated anxiety scores and decreased stability, depicting a circular self-sustaining relationship that can decrease quality of life, undermine learning, produce muscular co-contraction and, in the long term, lead to the development of musculoskeletal disorders. While holistic techniques are more frequently appearing in literature to address these problems, the presented protocol can be used to quantify the effect of such techniques on subjects.

Data availability statement

The original contributions presented in the study are included in the article/Supplementary Material, further inquiries can be directed to the corresponding author.

Ethics statement

The studies involving humans were approved by the Institutional Committee for Ethical Review of Projects of Universitat Pompeu Fabra (CIREP-UPF). The studies were conducted in accordance with the local legislation and institutional requirements. The participants provided their written informed consent to participate in this study. Written informed consent was obtained from the individual(s) for the publication of any potentially identifiable images or data included in this article.

Author contributions

ST: Conceptualization, Investigation, Methodology, Supervision, Writing–original draft, Writing–review and editing, Project administration, Funding acquisition. PC: Data curation, Investigation, Methodology, Writing–original draft, Writing–review and editing. MB: Conceptualization, Investigation, Methodology, Writing–original draft, Writing–review and editing. MV: Methodology, Writing–review and editing. JR: Conceptualization, Investigation, Writing–review and editing. JM: Data curation, Investigation, Writing–review and editing. MP-T: Investigation, Writing–review and editing. MiG-B: Funding acquisition, Writing–review and editing. DH-L: Conceptualization, Funding acquisition, Writing–review and editing.

Funding

The author(s) declare that financial support was received for the research, authorship, and/or publication of this article. Funds from the Spanish Government (MDM-2015-0502) and from Center for the Studies on Planetary Wellbeing (BYMBOS-PLAWB00420) are acknowledged. This work has been also partially funded by MICIU/AEI/10.13039/501100011033 (PID2020-112584RB-C33). DHL (Serra Húnter) also acknowledges the support by ICREA under the ICREA Academia programme.

Acknowledgments

A special thanks to all the volunteers who participated in the study.

Conflict of interest

The authors declare that the research was conducted in the absence of any commercial or financial relationships that could be construed as a potential conflict of interest.

The author(s) declared that they were an editorial board member of Frontiers, at the time of submission. This had no impact on the peer review process and the final decision.

Publisher's note

Supplementary material

The Supplementary Material for this article can be found online at: https://www.frontiersin.org/articles/10.3389/fbioe.2024.1347939/full#supplementary-material

References

Abdollahi, A., Hosseinian, S., Beh-Pajooh, A., and Carlbring, P. (2017). Self-concealment mediates the relationship between perfectionism and attitudes toward seeking psychological help among adolescents. *Psychol. Rep.* 120, 1019–1036. doi:10.1177/0033294117713495

Aliverti, A., and Pedotti, A. (2003). Opto-Electronic plethysmography. *Monaldi Arch. Chest Dis.* 59, 12–16. doi:10.1007/978-88-470-2916-3_5

Balban, M. Y., Neri, E., Kogon, M. M., Weed, L., Nouriani, B., Jo, B., et al. (2023). Brief structured respiration practices enhance mood and reduce physiological arousal. *Cell Rep. Med.* 4, 100895. doi:10.1016/j.xcrm.2022.100895

Brattberg, G. (2004). Do pain problems in young school children persist into early adulthood? A 13-year follow-up. *Eur. J. Pain* 8, 187–199. doi:10.1016/j.ejpain.2003.08.001

Brett, M., Penny, W., and Kiebel, S. (2003). *Introduction to random field theory.* Human brain function. Second Edition. doi:10.1016/B978-012264841-0/50046-9

Burgos, C. P., Gartner, L., Ballester, M. A. G., Noailly, J., Stocker, F., Schonfelder, M., et al. (2020). In-ear accelerometer-based sensor for gait classification. *IEEE Sens. J.* 20, 12895–12902. doi:10.1109/JSEN.2020.3002589

Busch, V., Magerl, W., Kern, U., Haas, J., Hajak, G., and Eichhammer, P. (2012). The effect of deep and slow breathing on pain perception, autonomic activity, and mood processing — an experimental study. *Pain Med.* 13, 215–228. doi:10.1111/j.1526-4637.2011.01243.x

Byeon, Y. H., Lee, J. Y., Kim, D. H., and Kwak, K. C. (2020). Posture recognition using ensemble deep models under various home environments. *Appl. Sci. Switz.* 10, 1287. doi:10.3390/app10041287

Cappozzo, A., Della Croce, U., Leardini, A., and Chiari, L. (2005). Human movement analysis using stereophotogrammetry. Part 1: theoretical background. *Gait Posture* 21, 186–196. doi:10.1016/j.gaitpost.2004.01.010

Chiari, L., Rocchi, L., and Cappello, A. (2002). Stabilometric parameters are affected by anthropometry and foot placement. *Clin. Biomech.* 17, 666–677. doi:10.1016/S0268-0033(02)00107-9

Davis, R. B., Õunpuu, S., Tyburski, D., and Gage, J. R. (1991). A gait analysis data collection and reduction technique. *Hum. Mov. Sci.* 10, 575–587. doi:10.1016/0167-9457(91)90046-Z

De Blasiis, P., Caravaggi, P., Fullin, A., Leardini, A., Lucariello, A., Perna, A., et al. (2023). Postural stability and plantar pressure parameters in healthy subjects: variability, correlation analysis and differences under open and closed eye conditions. *Front. Bioeng. Biotechnol.* 11, 1198120. doi:10.3389/fbioe.2023.1198120

De Blasiis, P., Fullin, A., Caravaggi, P., Lus, G., Melone, M. A., Sampaolo, S., et al. (2022). Long-term effects of asymmetrical posture in boxing assessed by baropodometry. *J. Sports Med. Phys. Fit.* 62, 350–355. doi:10.23736/S0022-4707.21.12040-7

De Faria Júnior, N. S., Santos, I. R., Dias, I. S., Urbano, J. J., Da Palma, R. K., Fonsèca, N. T., et al. (2013). Opto-electronic plethysmography: noninvasive and accurate measurement of the volume of the chest wall and its different thoraco-abdominal compartments. *Clin. Exp. Med. Lett.* 54, 147–150. doi:10.12659/mst.889664

Diepenmaat, A. C. M., Van Der Wal, M. F., De Vet, H. C. W., and Hirasing, R. A. (2006). Neck/shoulder, low back, and arm pain in relation to computer use, physical activity, stress, and depression among Dutch adolescents. *Pediatrics* 117, 412–416. doi:10.1542/peds.2004-2766

Ellebrecht, D. B., Gola, D., and Kaschwich, M. (2022). Evaluation of a wearable in-ear sensor for temperature and heart rate monitoring: a pilot study. *J. Med. Syst.* 46, 91. doi:10.1007/s10916-022-01872-6

Ercan, I., Hafizoglu, S., Ozkaya, G., Kirli, S., Yalcintas, E., and Akaya, C. (2015). Examinando los puntajes de corte para el inventario de ansiedad estado-rasgo. *Rev. Argent. Clinica Psicol.* 24.

Fugl Meyer, A. R. (1974). Relative respiratory contribution of the rib cage and the abdomen in males and females with special regard to posture. *Respiration* 31, 240–251. doi:10.1159/000193113

Fullin, A., Caravaggi, P., Picerno, P., Mosca, M., Caravelli, S., De Luca, A., et al. (2022). Variability of postural stability and plantar pressure parameters in healthy subjects evaluated by a novel pressure plate. *Int. J. Environ. Res. Public Health* 19, 2913. doi:10.3390/ijerph19052913

Gilbert, C. (2003). Clinical applications of breathing regulation: beyond anxiety management. *Behav. Modif.* 27, 692–709. doi:10.1177/0145445503256322

Gilbert, R., Auschincloss, J. H., and Peppi, D. (1981). Relationship of rib cage and abdomen motion to diaphragm function during quiet breathing. *Chest* 80, 607–612. doi:10.1378/chest.80.5.607

Hodges, P. W., and Gandevia, S. C. (2000). Changes in intra-abdominal pressure during postural and respiratory activation of the human diaphragm. *J. Appl. Physiol.* 89, 967–976. doi:10.1152/jappl.2000.89.3.967

Hodges, P. W., Sapsford, R., and Pengel, L. H. M. (2007). Postural and respiratory functions of the pelvic floor muscles. *Neurourol. Urodyn.* 26, 362–371. doi:10.1002/nau.20232

Hopper, S. I., Murray, S. L., Ferrara, L. R., and Singleton, J. K. (2019). Effectiveness of diaphragmatic breathing for reducing physiological and psychological stress in adults: a quantitative systematic review. *JBI Database Syst. Rev. Implement Rep.* 17, 1855–1876. doi:10.11124/JBISRIR-2017-003848

Isomaa, R., Väänänen, J. M., Fröjd, S., Kaltiala-Heino, R., and Marttunen, M. (2013). How low is low? Low self-esteem as an indicator of internalizing psychopathology in adolescence. *Health Educ. Behav.* 40, 392–399. doi:10.1177/1090198112445481

Kim, M. S., Cha, Y. J., and Choi, J. D. (2017). Correlation between forward head posture, respiratory functions, and respiratory accessory muscles in young adults. *J. Back Musculoskelet. Rehabil.* 30, 711–715. doi:10.3233/BMR-140253

Massaroni, C., Carraro, E., Vianello, A., Miccinilli, S., Morrone, M., Levai, I. K., et al. (2017). Optoelectronic plethysmography in clinical practice and research: a review. *Respiration* 93, 339–354. doi:10.1159/000462916

McFarlane, A. C. (2007). Stress-related musculoskeletal pain. *Best. Pract. Res. Clin. Rheumatol.* 21, 549–565. doi:10.1016/j.berh.2007.03.008

Pataky, T. C. (2012). One-dimensional statistical parametric mapping in Python. *Comput. Methods Biomech. Biomed. Engin* 15, 295–301. doi:10.1080/10255842.2010.527837

Perciavalle, V., Blandini, M., Fecarotta, P., Buscemi, A., Di Corrado, D., Bertolo, L., et al. (2017). The role of deep breathing on stress. *Neurol. Sci.* 38, 451–458. doi:10.1007/s10072-016-2790-8

Prins, Y., Crous, L., and Louw, Q. (2008). A systematic review of posture and psychosocial factors as contributors to upper quadrant musculoskeletal pain in children and adolescents. *Physiother. Theory Pract.* 24, 221–242. doi:10.1080/09593980701704089

Rocchi, L., Chiari, L., and Cappello, A (2004). Feature selection of stabilometric parameters based on principal component analysis. *Med. Biol. Eng. Comput.* 42, 71–79. doi:10.1007/BF02351013

Romei, M., Mauro, A.L, D'Angelo, M. G., Turconi, A. C., Bresolin, N., Pedotti, A., et al. (2010). Effects of gender and posture on thoraco-abdominal kinematics during quiet breathing in healthy adults. *Respir. Physiol. Neurobiol.* 172, 184–191. doi:10.1016/j.resp.2010.05.018

Santino, T. A., Chaves, G. S. S., Freitas, D. A., Fregonezi, G. A. F., and Mendonça, K. M. P. P. (2020). Breathing exercises for adults with asthma. *Cochrane Database Syst. Rev.* 2020, CD001277. doi:10.1002/14651858.CD001277.pub4

Sawatzky, R. G., Ratner, P. A., Richardson, C. G., Washburn, C., Sudmant, W., and Mirwaldt, P. (2012). Stress and depression in students: the mediating role of stress management self-efficacy. *Nurs. Res.* 61, 13–21. doi:10.1097/NNR.0b013e31823b1440

Sharp, J. T., Goldberg, N. B., Druz, W. S., and Danon, J. (1975). Relative contributions of rib cage and abdomen to breathing in normal subjects. *J. Appl. Physiol.* 39, 608–618. doi:10.1152/jappl.1975.39.4.608

Sheikhhoseini, R., Shahrbanian, S., Sayyadi, P., and O'Sullivan, K. (2018). Effectiveness of therapeutic exercise on forward head posture: a systematic review and meta-analysis. *J. Manip. Physiol. Ther.* 41, 530–539. doi:10.1016/j.jmpt.2018.02.002

Swiecki, Z., Ruis, A. R., Farrell, C., and Shaffer, D. W. (2019). Assessing individual contributions to Collaborative Problem Solving: a network analysis approach. *Comput. Hum. Behav.* 104, 105876. doi:10.1016/j.chb.2019.01.009

Tassani, S., Font-Llagunes, J. M., González Ballester, M. Á., and Noailly, J. (2019). Muscular tension significantly affects stability in standing posture. *Gait Posture* 68, 220–226. doi:10.1016/j.gaitpost.2018.11.034

Verschakelen, J. A., and Demedts, M. G. (1995). Normal thoracoabdominal motions: influence of sex, age, posture, and breath size. *Am. J. Respir. Crit. Care Med.* 151, 399–405. doi:10.1164/ajrccm.151.2.7842198

Wong, W. Y., and Wong, M. S. (2008). Smart garment for trunk posture monitoring: a preliminary study. *Scoliosis* 3, 7. doi:10.1186/1748-7161-3-7

Yang, L., Lu, X., Yan, B., and Huang, Y. (2020). Prevalence of incorrect posture among children and adolescents: finding from a large population-based study in China. *iScience* 23, 101043. doi:10.1016/j.isci.2020.101043

Frontiers in
Bioengineering and Biotechnology

Accelerates the development of therapies, devices, and technologies to improve our lives

A multidisciplinary journal that accelerates the development of biological therapies, devices, processes and technologies to improve our lives by bridging the gap between discoveries and their application.

Discover the latest Research Topics

See more →

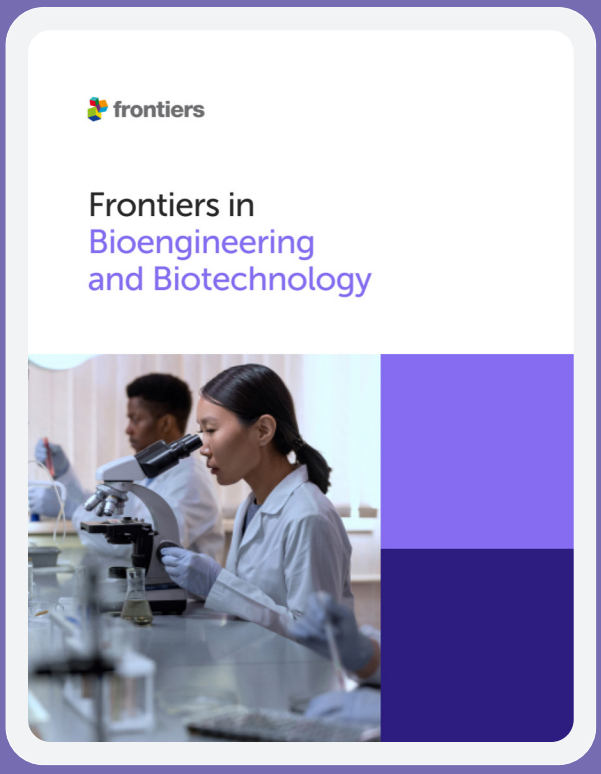

Frontiers

Avenue du Tribunal-Fédéral 34
1005 Lausanne, Switzerland
frontiersin.org

Contact us

+41 (0)21 510 17 00
frontiersin.org/about/contact